MEMO 12-10-58E

NASA MEMO 12-10-58E

NASA

MEMORANDUM

NASA REACTOR FACILITY HAZARDS SUMMARY

VOLUME II

By Lewis Research Center Staff

Lewis Research Center
Cleveland, Ohio

NATIONAL AERONAUTICS AND SPACE ADMINISTRATION
WASHINGTON
February 1959

NASA MEMO 12-10-58E

E-103

NASA REACTOR FACILITY HAZARDS SUMMARY

VOLUME II

By Lewis Research Center Staff
Cleveland, Ohio

Foreword

The papers presented herein were originally prepared as supplements to the "NASA Reactor Facility Hazards Summary" (vol. I) in 1956-1958. Supplement II is an evaluation of the proposed facility made by the Armour Research Foundation of Illinois Institute of Technology at the request of the NACA (now the NASA). Supplements IV, V, and VI were compiled in answer to questions raised by the Atomic Energy Commission. Additional information unavailable when volume I was submitted to the Atomic Energy Commission is contained in supplements I and III.

TABLE OF CONTENTS

Volume II

E-103

CO-1

I. SOME PRELIMINARY ANALYSES OF REACTOR KINETICS AND CONTROL

By Aaron S. Boksenbom

November 1, 1956

1. - LONG TERM Xe AND Sm TRANSIENTS

The operational flexibility and reactivity requirements of a high flux thermal reactor are greatly affected by the large cross section fission products, Xe^{135} and Sm^{149}. They are responsible for reactivities of approximately -4 and -1 percent, respectively, in equilibrium operation at high flux. Following a cut-back in flux level, these poisoning effects increase considerably, possibly shutting down the reactor and even prohibiting operation for as much as several days. An analysis of the transient build-up and decay of Xe and Sm for various cut-backs in flux level and for various start-ups follows.

1.1 Xe - LONG TERM TRANSIENTS

The decay and burnout chain for Xe^{135}, at any point in the core, can be described as follows (ref. 1):

$$\left.\begin{aligned} \frac{1}{\lambda_1}\frac{d}{dt}\left(\frac{Te}{Te_e}\right) + \left(\frac{Te}{Te_e}\right) &= \frac{F}{F_e} \\ \frac{1}{\lambda_2}\frac{d}{dt}\left(\frac{I}{I_e}\right) + \left(\frac{I}{I_e}\right) &= \frac{Te}{Te_e} \\ \frac{d}{dt}\left(\frac{Xe}{Xe_e}\right) + (\lambda_3 + \sigma\varphi_{th})\frac{Xe}{Xe_e} &= (\lambda_3 + \sigma\varphi_{th_e})\left(\frac{\frac{I}{I_e} + a\frac{F}{F_e}}{1+a}\right) \end{aligned}\right\} \qquad (1.1)$$

where conditions are taken with reference to any equilibrium condition, "e," and

F	fission rate
$\lambda_1, \lambda_2, \lambda_3$	decay constants of Te, I, and Xe, respectively
σ	cross section of Xe $\doteq 3\times10^6$ barns
a	ratio of direct yield of Xe to direct yield of Te $\doteq \frac{3}{56}$ to $\frac{3}{68}$

Equations (1.1) were solved for the following conditions:

(1) Te (having a 2 min. half-life) in equilibrium, $\frac{Te}{Te_e} = \frac{F}{F_e}$.

(2) During the transient, at a point in the reactor, fission rate proportional to thermal flux, $\frac{F}{F_e} = \frac{\varphi_{th}}{\varphi_{th_e}}$.

(3) Direct yield of Xe neglected, a = 0.

The solutions for a step change in φ_{th} from φ_0 to φ_1, are

$$\left.\begin{aligned} \frac{I(t)}{I_e} &= \frac{\varphi_1}{\varphi_e} + \left[\frac{I_0}{I_e} - \frac{\varphi_1}{\varphi_e}\right]\varepsilon^{-\lambda_2 t} \\ \frac{Xe(t)}{Xe_e} - 1 &= \left(\frac{Xe_0}{Xe_e} - 1\right)\varepsilon^{-(\sigma\varphi_1+\lambda_3)t} + \frac{\lambda_3(\varphi_1 - \varphi_e)}{(\sigma\varphi_1 + \lambda_3)\varphi_e}\left(1 - \varepsilon^{-(\sigma\varphi_1+\lambda_3)t}\right) + \\ &\quad \frac{(\sigma\varphi_e + \lambda_3)}{(\sigma\varphi_1 + \lambda_3 - \lambda_2)}\left(\frac{I_0}{I_e} - \frac{\varphi_1}{\varphi_e}\right)\left(\varepsilon^{-\lambda_2 t} - \varepsilon^{-(\sigma\varphi_1+\lambda_3)t}\right) \end{aligned}\right\} \quad (1.2)$$

As $t \to \infty$,

$$\frac{Xe(\infty)}{Xe_e} = \left(\frac{\lambda_3 + \sigma\varphi_e}{\lambda_3 + \sigma\varphi_1}\right)\frac{\varphi_1}{\varphi_e}$$

These solutions are plotted in figure 1, for 5 cases.

Case I. For cut-back to zero from $\varphi_{th} = 4\times10^{14}$, peak Xe build-up is 18.4 times, occurring at 11 hours. Initial Xe reached at 60+ hours.

Case II. For cut-back to zero from $\varphi_{th} = 2\times10^{14}$, peak build-up is 9.7 times, occurring at 11 hours. Initial Xe reached at 55 hours.

Case III. For cut-back from $\varphi_{th} = 4\times10^{14}$ to 4×10^{13}, $\frac{\varphi_1}{\varphi_0} = \frac{1}{10}$, peak build-up is 6 times, occurring at 4 hours. Initial Xe reached at 40 hours.

Case IV. For cut-back from $\varphi_{th} = 4\times10^{14}$ to 2×10^{14}, $\frac{\varphi_1}{\varphi_0} = \frac{1}{2}$, peak build-up is 1.8 times, occurring at 1 to 2 hours. Initial Xe essentially reached at 24 hours.

Case V. For Xe build-up on start-up at $\varphi_{th} = 4\times10^{14}$, at 7 hours get half the build-up, and at 24 hours equilibrium Xe is essentially obtained.

1.2. Sm - LONG TERM TRANSIENTS

The decay and burnout chain for Sm^{149}, at any point in the core, can be described as follows (ref. 1):

$$\left.\begin{aligned} \frac{1}{\lambda_4}\frac{d}{dt}\left(\frac{Nd}{Nd_e}\right) + \left(\frac{Nd}{Nd_e}\right) &= \frac{F}{F_e} \\ \frac{1}{\lambda_5}\frac{d}{dt}\left(\frac{Pm}{Pm_e}\right) + \left(\frac{Pm}{Pm_e}\right) &= \frac{\frac{Nd}{Nd_e} + c\,\frac{F}{F_e}}{1+c} \\ \frac{d}{dt}\left(\frac{Sm}{Sm_e}\right) + \sigma\varphi_{th}\left(\frac{Sm}{Sm_e}\right) &= \sigma\varphi_{th_e}\left(\frac{Pm}{Pm_e}\right) \end{aligned}\right\} \qquad (1.3)$$

where conditions are taken with reference to any equilibrium condition, "e," and

F fission rate

λ_4, λ_5 decay constants of Nd and Pm, respectively

σ cross section of Sm $\doteq 5\times10^4$ barns

c ratio of direct yield of Pm to direct yield of Nd

Equations (1.3) were solved for the following conditions:

(1) Nd (having a 1.7 hr half-life) in equilibrium,

$$\frac{Nd}{Nd_e} = \frac{F}{F_e}$$

(2) During the transient, at a point in the reactor, fission rate proportional to thermal flux,

$$\frac{F}{F_e} = \frac{\varphi_{th}}{\varphi_{th_e}}$$

The solutions for a step change in φ_{th}, from φ_0 to φ_1, are

$$\left.\begin{aligned}\frac{Pm(t)}{Pm_e} &= \frac{\varphi_1}{\varphi_{th_e}} + \left[\frac{Pm_0}{Pm_e} - \frac{\varphi_1}{\varphi_e}\right]\varepsilon^{-\lambda_5 t} \\ \frac{Sm(t)}{Sm_e} - 1 &= \left[\frac{Sm_0}{Sm_e} - 1\right]\varepsilon^{-\sigma\varphi_1 t} + \left(\frac{\sigma\varphi_e}{\sigma\varphi_1 - \lambda_5}\right)\left(\frac{Pm_0}{Pm_e} - \frac{\varphi_1}{\varphi_e}\right)\left(\varepsilon^{-\lambda_5 t} - \varepsilon^{-\sigma\varphi_1 t}\right)\end{aligned}\right\} \quad (1.4)$$

As $t \to \infty$, if $\varphi_1 \neq 0$, then $Sm(\infty) = Sm_e$.

As $t \to \infty$, if $\varphi_1 \doteq 0$, then $\frac{Sm(\infty)}{Sm_e} = \left(\frac{Sm_0}{Sm_e}\right) + \left(\frac{Pm_0}{Pm_e}\right)\frac{\sigma\varphi_e}{\lambda_5}$.

The solutions are plotted in figure 2 for 6 cases:

Case I. For cut-back to zero from $\varphi_{th} = 4\times10^{14}$, Sm reaches a quasi-equilibrium increase at 10 days of $1 + \frac{\sigma\varphi_0}{\lambda_5} = 5.88$ times.

Case II. For a cut-back to zero from $\varphi_{th} = 2\times10^{14}$, Sm reaches a quasi-equilibrium increase at 10 days of 3.4 times.

Case III. For a cut-back from $\varphi_{th} = 4\times10^{14}$ to 4×10^{13}, $\frac{\varphi_1}{\varphi_0} = \frac{1}{10}$, peak Sm build-up is 3.2 occurring at 4 days. Even at 10 days, build-up is 2.3 times.

Case IV. For a cut-back from $\varphi_{th} = 4\times10^{14}$ to 2×10^{14}, $\frac{\varphi_1}{\varphi_0} = \frac{1}{2}$, peak Sm build-up is 1.55 times occurring at 1.7 days. Takes about 10 days to return to initial value.

Case V. For Sm build-up on start-up at $\varphi_{th} = 4\times10^{14}$, at 2.5 days get half-build-up, and at 9 days equilibrium Sm is essentially reached.

Case VI. For Sm build-up on start-up at $\varphi_{th} = 4\times10^{13}$, at 7 days get half build-up.

1.3 REACTIVITY EFFECTS OF Xe AND Sm

1.3.1 Equilibrium Effects

The concentration of Xe, in equilibrium, at any point in the core, is $\frac{(\text{Xe total yield})F_e}{\lambda_3 + \sigma\varphi_{th_e}}$. For high thermal flux, $\sigma\varphi_{th_e} >> \lambda_3$ and equilibrium Xe is almost uniform in the core. The concentration of Sm, in equilibrium, at any point in the core is $\frac{(\text{Sm total yield})F_e}{\sigma\varphi_{th_e}}$ and, thus, is almost uniform in the core. The reactivity effects of equilibrium Xe and Sm were found in reference 2.

1.3.2 Transient Effects

The build-up of both Xe and Sm after a cut-back was shown to be flux dependent. If the assumption is made that the reactivity effect of the poison is proportional to its concentration at the point in the core of average thermal flux, then using $\varphi_{th} = \varphi_{th,av}$ in equations (1.1) to (1.4), and on figures 1 and 2, allows us to set

$$\frac{Xe}{Xe_e} \doteq \frac{\left(\frac{\Delta K}{K}\right)_{Xe}}{\left(\frac{\Delta K}{K}\right)_{\text{equil. Xe}}}$$

and

$$\frac{Sm}{Sm_e} \doteq \frac{\left(\frac{\Delta K}{K}\right)_{Sm}}{\left(\frac{\Delta K}{K}\right)_{\text{equil. Sm}}}$$

1.4 SUM OF Xe AND Sm LONG TERM EFFECTS

For the case of a cut-back to zero from $\varphi_{th} = 4\times10^{14}$, the total reactivity effect of Xe and Sm is shown on figure 3. The above assumptions for the transient poison effects on reactivity were used with $\left(\frac{\Delta K}{K}\right)_{\text{equil. Xe}} = 4$ percent and $\left(\frac{\Delta K}{K}\right)_{\text{equil. Sm}} = 1$ percent, which assumes equilibrium Sm before shut-down. The figure shows the Sm build-up to

compensate for the Xe decay giving a slight minimum at 105 hours of 5.05 percent, slightly greater than the initial effect of 5 percent. If cut-back occurs before equilibrium Sm is reached, its build-up is less. An appropriate formula for its final value, valid if operating at high flux at least one or two days before shut-down, is $\frac{Sm(\infty)}{Sm_0} = 1 + \frac{\sigma\varphi_0}{\lambda_5}$. If shut-down occurs after operating at $\varphi_0 = 4\times10^{14}$ for 5 days, the reactivity effect of Sm will approach 4.7 percent.

2. - RESTART TIMES

The Xe build-up after a shut-down has serious consequences in the operation of a high flux thermal reactor if continuity of operation is desired. Inadvertant scrams or ones due to a temporary difficulty must be expected. The Xe build-up after a scram will be linear in time and proportional to the operating flux before the scram. The minimum time in which to stop the Xe rise is taken up by (1) a waiting period to ascertain and correct the difficulty and to insert the rod drive, (2) the time to withdraw the rods to near criticality, and (3) the time to increase flux high enough to stop the Xe rise. The Xe build-up during rod withdrawal is so large that, in order to restart, rod withdrawal speeds much greater than that required or desired for normal start-ups or normal operation are necessary. An analysis of restart ability and its dependence on rod velocity and excess reactivity available is presented below.

2.1 SHORT-TERM Xe TRANSIENTS

Over times of one-half hour to one hour, the change in I decay is very small and the change in Xe decay is small relative to the change in Xe burnout. In this case, a simplified equation for Xe is

$$\frac{dXe}{dt} = \left(\frac{dXe}{dt}\right)_r + \sigma Xe_r \varphi_{th_r} - \sigma Xe \varphi_{th} + 0.003\ (F - F_r)$$

where "r" is any convenient nearby (in time) reference condition.

If we assume that $\Delta K/K$ due to Xe is proportional to the Xe concentration at the point of average φ_{th}, then, letting $P = -\left(\frac{\Delta K}{K}\right)$ due to Xe, we get

$$\frac{1}{\sigma}\frac{dP}{dt} = \frac{1}{\sigma}\left(\frac{dP}{dt}\right)_r + P_r\bar{\varphi}_{th_r} - P\bar{\varphi}_{th} + \frac{aP_e}{1+a}\left(\bar{\varphi}_{th} - \bar{\varphi}_{th_r}\right) \qquad (2.1)$$

where

P_e equilibrium effect at high flux

a ratio of direct yield of Xe to direct yield of Te

If reference condition is the equilibrium condition before scram, and $\bar{\varphi}_{th} \to 0$, then

$$\left(\frac{dP}{dt}\right)_{\substack{\text{after}\\ \text{scram}}} = \frac{\sigma P_e \bar{\varphi}_{th_e}}{1+a} \qquad (2.2)$$

where P_e and $\bar{\varphi}_{th_e}$ are conditions before scram.

After restart, in order to stop Xe rise,

$$\frac{\bar{\varphi}_{th}(\text{at max. P})}{\bar{\varphi}_{th_e}(\text{before scram})} = \frac{P_e}{(1+a)P_{max.} - aP_e} \doteq \frac{P_e}{P_{max.}} \qquad (2.3)$$

2.2 RESTART ANALYSIS

A qualitative picture of a restart is shown on figure 4. The excessive reactivity required to restart is

$$\delta k_{max.} - \delta k_{\substack{\text{before} \\ \text{scram}}} = \left(\frac{dP}{dt}\right)_0 \left[t_{wait} + \frac{x_1}{v} + T \log \left(\frac{\varphi_e}{\varphi_{restart}}\right)\left(\frac{\varphi_{restart}}{\varphi_1}\right)\right] \qquad (2.4)$$

where

t_{wait} — from scram to starting rod withdrawal

x_1 — rod position where period T is first reached

v — rod velocity

T — constant period of restart

$\varphi_{restart}$ — obtained from typical decay on 80 sec period to source level of $10^{-5}\varphi_e$.

φ_1 — obtained from typical restart transients

$$\frac{\varphi_1}{\varphi_{restart}} \doteq 30 \text{ to } 50$$

The assumption noted on figure 4 around peak Xe introduces a negligible error.

In a typical start-up at constant rod speed, the allowable period T is reached subcritically, about T seconds before criticality would be reached if rods continued at constant speed. This assumption locates the position, x_1, where rods must be slowed down to maintain the allowable period, T. The position of the rods at x_1 is thus obtained as

$$\delta k_{max.} - \delta k(x_1) = \left(\frac{dP}{dt}\right)_0 T \log \frac{\varphi_e}{\varphi_1} + v\tilde{s}_1 T \qquad (2.5)$$

where $\delta k(x)$ is rod calibration used, figure 5. Figure 6 is the idealized rod calibration for reference use. $\tilde{s}_1$ is control rod effectiveness at x_1.

The two-week cycle characteristic used of $\bar{\varphi}_{th_e}$ and P_e and $\left(\frac{dP}{dt}\right)_0$, calculated from equation (2.2), is

Time in cycle, days	$\bar{\varphi}_{th_e}$	P_e, percent	$\left(\frac{dP}{dt}\right)_0$, percent/min
0	3.21×10^{14}	4	0.22
2	3.33	3.96	.226
4	3.46	3.94	.233
6	3.61	3.9	.241
8	3.76	3.87	.25
10	3.93	3.82	.257

For assumed T, t_{wait}, v, and day of scram, the excess reactitivity, before scram, required to restart was calculated using equation (2.4) and (2.5), figure 5, and the above table. The results are shown in figures 7 to 11 for a range of down times from 1 to 20 minutes and rod velocities from 1.5 to 6 inch/minute.

Superposed on these curves are the reactivities available at each day with various assumed $\frac{\Delta K}{K}$ in experiments. The maximum of experiments would give zero excess $\frac{\Delta K}{K}$ at 10 days. The change in excess reactivity available was assumed at 0.625 percent/day.

Figure 12 gives maximum down time at each day of operation and for various $\frac{\Delta K}{K}$ in experiments, for a rod velocity of 3 inch/minute. Each percent sacrificed in experiments is worth about $1\frac{1}{2}$ days extra operation or 3 to 3.5 minutes extra down time. Three percent sacrificed in experiments would give 2 minutes at 9.5 days and 13.5 minutes at 5 days.

3. - MAXIMUM Xe BURNOUT RATE AFTER RESTART

A large concentration of Xe in the core represents a hazard as its removal is a positive effect on reactivity. There are two mechanisms for such removal; (1) Xe decay, and (2) Xe burnout. The decay of Xe is always a slow process, but could be a hazard in the case of the reactor going critical on Xe decay even with control rods inserted.

The burnout of Xe is an unstable phenomenon. The rate of Xe burnout is proportional to the product of the concentration of Xe and the thermal flux. For normal values of both parameters, burnout effects are manifested as an inherent reactor instability, as discussed in section 6. On a nuclear excursion, burnout of Xe can augment the accident, as discussed in section 10. After a restart, with Xe build-up, the possible burnout, even at normal flux levels, is a factor in setting control rod speeds. If the control rods cannot keep up with burnout, a nuclear excursion will be started, and the only protection to the reactor is the scram. This incident would not give large power overshoots if the reactor scrams. An analysis for the maximum Xe burnout rates after a restart at normal flux levels is presented below.

3.1 CASE I, RESTART ON Xe RISE

Using short-term Xe equation (2.1) with reference condition the equilibrium condition before scram, and restarting at constant $\bar{\varphi}_{th} = \varphi_{re}$, we get

$$P = \frac{P_e \bar{\varphi}_{th_e}}{\varphi_{re}} + \frac{aP_e}{1+a}\left(1 - \frac{\bar{\varphi}_{th_e}}{\varphi_{re}}\right) + \left[P_0 - \frac{P_e \bar{\varphi}_{th_e}}{\varphi_{re}} - \frac{aP_e}{1+a}\left(1 - \frac{\bar{\varphi}_{th_e}}{\varphi_{re}}\right)\right]\varepsilon^{-\sigma\varphi_{re}t}$$

$$P(\text{large } t) \to \frac{P_e \bar{\varphi}_{th_e}}{\varphi_{re}} + \frac{aP_e}{1+a}\left(1 - \frac{\bar{\varphi}_{th_e}}{\varphi_{re}}\right)$$

$$\left(\frac{dP}{dt}\right)_{max.} = \sigma P_0 \varphi_{re}\left[-1 + \frac{P_e \bar{\varphi}_{th_e}}{P_0 \varphi_{re}} + \left(\frac{1}{1+a}\right)\frac{P_e}{P_0}\left(1 - \frac{\bar{\varphi}_{th_e}}{\varphi_{re}}\right)\right] \qquad (3.1)$$

A rough plot of this burnout is shown below:

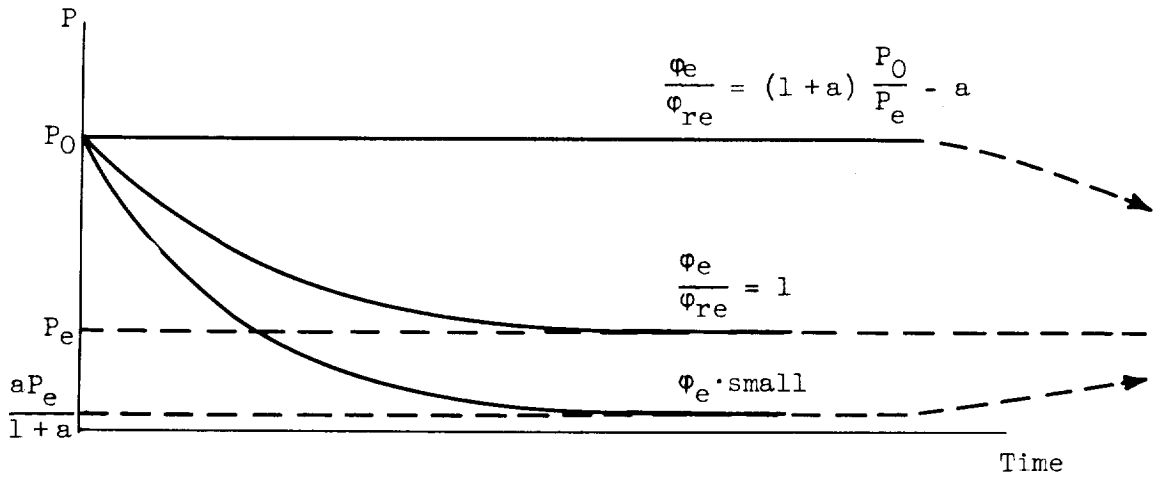

The time constant of these exponentials is $\frac{1}{\sigma\varphi_{re}} \doteq 14$ minutes (for $\varphi_{re} = 4\times10^{14}$), giving a settling time of about one hour for $\varphi_{re} = 4\times10^{14}$. After one hour or so, the I and Xe decay effects will cause (if $P \neq P_e$) $P \rightarrow P_e$ over a period of one day or so.

The maximum rates of Xe burnout for case I are shown below:

MAXIMUM BURNOUT RATE, PERCENT $\frac{\Delta K}{K}$/MINUTE

CASE I. P_e = 4 PERCENT, $\varphi_{re} = 4\times10^{14}$

P_0, percent	$\varphi_e = \varphi_{re} = 4\times10^{14}$	φ_e small
8	0.288 %/min.	0.56 %/min.
20	1.15	1.43 *

*Pessimistic.

Restarting at large Xe build-ups is always hazardous. Another hazardous case is when scram occurs after running at low φ (say $\frac{1}{4}\varphi_{max.}$, where almost normal Xe is present but I is decreased) and restarting at $\varphi_{max.}$. The greater the excess $\Delta K/K$ before scram, the greater the possible Xe burnout.

3.2 CASE II, RESTART ON Xe DECAY

Using short-term Xe equation (2.1), with reference condition, $\varphi_r = 0$, and restarting at constant $\bar{\varphi}_{th} = \varphi_{re}$, we get

$$P = \frac{1}{\sigma\varphi_{re}}\left(\frac{dP}{dt}\right)_r + \frac{aP_e}{1+a} + \left[P_0 - \frac{1}{\sigma\varphi_{re}}\left(\frac{dI}{dt}\right)_r - \frac{aP_e}{1+a}\right]\varepsilon^{-\sigma\varphi_{re}t}$$

$$P(\text{large } t) \rightarrow \frac{1}{\sigma\varphi_{re}}\left(\frac{dP}{dt}\right)_r + \frac{aP_e}{1+a} \doteq 0$$

$$\left(\frac{dP}{dt}\right)_{max.} = \sigma P_0 \varphi_{re}\left[-1 + \frac{1}{\sigma\varphi_{re}P_0}\left(\frac{dP}{dt}\right)_r + \left(\frac{a}{1+a}\right)\frac{P_e}{P_0}\right] \doteq -\sigma P_0 \varphi_{re} \qquad (3.2)$$

A rough plot of this burnout is shown below:

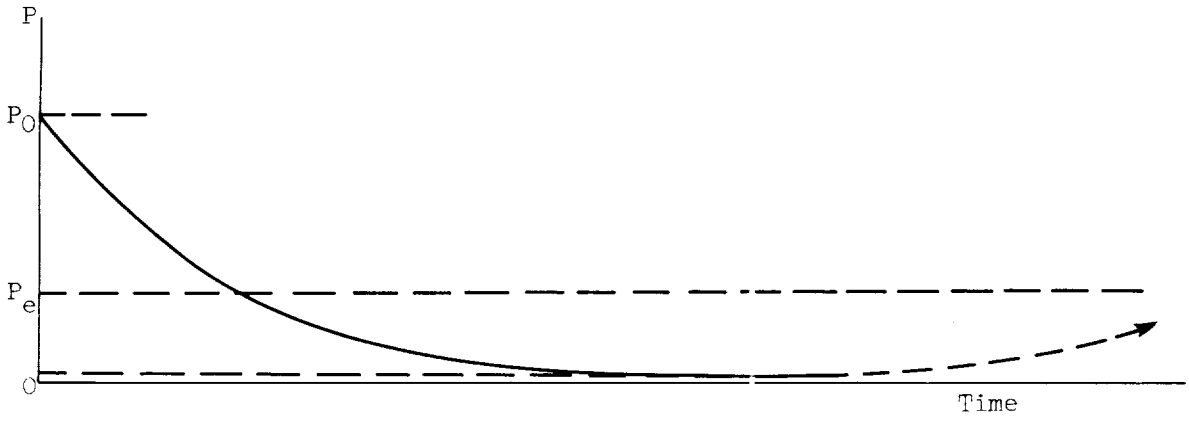

The time constant is $\frac{1}{\sigma\varphi_{re}} \doteq 14$ minutes for $\varphi_{re} = 4\times10^{14}$ and the settling time $\doteq$ 1 hour for $\varphi_{re} = 4\times10^{14}$. After 1 hour, or so, $P \rightarrow P_e$ over one to two days.

Maximum rates of Xe burnout for case II are shown below:

MAXIMUM BURNOUT RATE, PERCENT $\frac{\Delta K}{K}$ / MINUTE

CASE II. $\varphi_{re} = 4\times10^{14}$

P_0, percent	Percent/minute
8	0.576
20	1.44

This case actually includes restarts around peak Xe build-up. The worst case, possibly, is operation, before scram, at about $\bar{\varphi}_{th_e} = 10^{14}$, and restarting about 10 hours later at maximum Xe build-up.

3.3 ROD RATES REQUIRED

An optimistic estimate of minimum rod $\frac{\Delta K}{K}$ withdrawal rate (4:1 decrease in effectiveness) is 1.5 percent $\frac{\Delta K}{K}$/ minute (for $v = 3$ in./min). This is on the ragged edge of insuring control of Xe burnout at all times. A higher speed insertion rate of at least 3 times the withdrawal rate seems indicated.

4. - BASIC REACTOR KINETICS

4.1 KINETIC PARAMETERS

The prompt neutron lifetime, temperature coefficient, and void coefficient were discussed in reference 2. For the effective delayed neutron fraction, references 3 and 4, the following formula, consistent with the group diffusion approximation, was used.

$$\frac{\bar{\beta}_i}{\beta_i} = \frac{1 + L_{fp}^2 B^2}{1 + L_{fi}^2 B^2} \qquad (4.1)$$

where

$\bar{\beta}_i$ effective delayed neutron fraction

β_i yield of i^{th} delayed neutron group

L_{fp}^2 age of prompt neutrons averaged over fission spectrum

L_{fi}^2 age of i^{th} delayed neutrons

B^2 total buckling of reactor

This effect is tabulated below for two bucklings, with $L_{fp}^2 = 64\ cm^2$

i	L_{fi}^2, cm^2	$B^2 = 0.005405$		$B^2 = 0.00807$	
		$\bar{\beta}_i/\beta_i$	$\bar{\beta}_i$	$\bar{\beta}_i/\beta_i$	$\bar{\beta}_i$
1	32.5	1.145	0.00099	1.2	0.001036
2	37.2	1.12	.00276	1.166	.00288
3	32.8	1.144	.00247	1.198	.00259
4	35.5	1.13	.00197	1.18	.00206
5	29.5	1.16	.000304	1.223	.000321
			$\bar{\beta} = 0.008494$		$\bar{\beta} = 0.008887$

4.2 DIFFERENTIAL ANALYZER SETUP

For those studies, in this report, for which all the delayed neutron groups were considered, a differential analyzer was used. The equations that were solved, reference 3, can be written:

$$\left.\begin{aligned} \frac{d\varphi}{dt} &= (\delta k - \bar{\beta})\,\frac{\varphi}{l} + \sum_i \lambda_i C_i \\ \frac{dC_i}{dt} &+ \lambda_i C_i = \bar{\beta}_i\,\frac{\varphi}{l} \end{aligned}\right\} \quad i = 1,2,\ldots 5 \qquad (4.2)$$

where

φ time dependence of flux

δk reactivity

$\bar{\beta}_i$ effective delayed neutron fraction, $\bar{\beta} = \sum_i \bar{\beta}_i$

l prompt neutron lifetime

The parameters of the above equations are $\frac{\delta k}{l}$ and $\frac{\bar{\beta}_i}{l}$, or $\frac{\delta k}{\bar{\beta}}$ and $\frac{l}{\bar{\beta}_i}$. The equations were solved for $\frac{\bar{\beta}_i}{\bar{\beta}}$ equal to ratio of actual yields. Two sets of cases were run: (1) One set for $l = 15\times10^{-5}$ seconds and $\bar{\beta} = 0.0085$, (2) Second set for $l = 10.2\times10^{-5}$ seconds and $\bar{\beta} = 0.0085$. All the results can be generalized in terms of $\delta k/\bar{\beta}$ for the corresponding $l/\bar{\beta}$. For instance, the first set of runs can be applied to $l = 13.2\times10^{-5}$ seconds and $\bar{\beta} = 0.0075$. The second set of runs can be applied to $l = 9\times10^{-5}$ seconds and $\bar{\beta} = 0.0075$.

The stable reactor periods, based on equation (4.2), are shown on figure 13 as a function of $\delta k/\bar{\beta}$ for two values of $l/\bar{\beta}$, for reference use.

5. - CUT-BACKS

The effect of various cut-backs on flux level is shown on figure 14, for scrams, reverses, and set-back. These results were obtained on a differential analyzer including the effects of five delayed neutron groups. For scrams, the prompt drop is obtained in 0.25 to 0.5 second. For a total of -30.0 percent $\Delta K/K$, a cut-back to 2 percent is obtained in 1.16 seconds. If only a total of -10 percent $\Delta K/K$ is inserted, it takes 11 seconds to reduce flux level to 2 percent.

Cut-backs by reverses are very sensitive to reverse speeds. For a reverse of 0.7 percent $\Delta K/K$/second, a one decade drop is obtained in 5 seconds at which time -3.5 percent $\Delta K/K$ has been inserted. Immediate recovery from this level is always possible if there were about 0.7 percent $\Delta K/K$ excess before the reverse. The slower reverse, at 0.04 percent $\Delta K/K$/second, is only slightly more effective than a 20 second period set-back.

6. - REACTOR STABILITY

In normal operation, the inherent stability characteristics of the reactor determine the ease or difficulty of operation in manual control and the dependence on and requirements of the servo under automatic control. Xenon effects are always unstabilizing. The delayed neutrons and the negative temperature coefficient are stabilizing influences. To investigate over-all stability, the combined system of basic reactor kinetics, temperature effects on reactivity, and Xe effects on reactivity were studied analytically and presented below.

6.1 REACTOR KINETICS, 5 DELAY GROUPS

The linearized form of the reactor kinetic equations for the response of flux to net reactivity (δk), using operational notation, is

$$\frac{\Delta\varphi}{\varphi_0} = \frac{1}{(i\omega)\left[1 + \sum_{i=1}^{5} \frac{\bar{\beta}_i}{\lambda_i + i\omega}\right]} \cdot \delta k = \frac{\prod_{1}^{5} (1 + \tau_i i\omega) \cdot \delta k}{\left(\sum_{i=1}^{5} \tau_i \bar{\beta}_i + l\right)(i\omega) \prod_{1}^{5} (1 + \sigma_i i\omega)} \tag{6.1}$$

The equations were linearized around a "zero" critical condition, and $\tau_i = 1/\lambda_i$ is mean life of i^{th} delayed neutron group of effective fractional yield $\bar{\beta}_i$, and l is prompt neutron lifetime. Also,

$$\frac{\prod_{1}^{5} \tau_i}{\prod_{1}^{4} \sigma_i} \doteq \frac{\sum_{i=1}^{5} \tau_i \bar{\beta}_i + l}{\bar{\beta}} \doteq \frac{\sum \tau_i \bar{\beta}_i}{\bar{\beta}} = \tau_{average} = 12.474 \text{ seconds}$$

the σ_i are all real and lie alternately between the τ_i; the smallest one, $\sigma_5 \doteq l/\bar{\beta}$.

6.2 REACTOR KINETICS, 1 DELAY GROUP

The response equation is

$$\frac{\Delta\varphi}{\varphi_0} = \frac{1 + \tau i\omega}{(\tau\bar{\beta} + l)(i\omega)\left(1 + \frac{l\tau}{l + \tau\bar{\beta}}\, i\omega\right)} \cdot \delta k \tag{6.2}$$

Equation (6.1) and (6.2) agree at high frequencies ($\omega \geqq \bar{\beta}/l$). For agreement at low frequencies ($\omega < 1/\tau_i$) we need $\tau\bar{\beta} = \sum_i \tau_i \bar{\beta}_i$, and $\tau = \tau_{av} = 12.474$ seconds.

The time constants involved are 12.47 seconds and $\frac{l\tau}{l + \tau\bar{\beta}} \doteq \frac{l}{\bar{\beta}}$ = 12 to 17 milliseconds. Detailed study of equation (6.1) shows that the one delayed group approximation is not too valid in the intermediate frequency range, except for crude approximations.

6.3 KINETICS DUE TO Xe

The linearized form of the short-term Xe equation is

$$\Delta P = \frac{\frac{1}{\sigma\varphi_0} \cdot \left(\frac{dP}{dt}\right)_0 - (P_0 - 0.002) \cdot \frac{\Delta\varphi}{\varphi_0}}{1 + \frac{i\omega}{\sigma\varphi_0}}, \text{ for } \frac{aP_e}{1 + a} \doteq 0.002 \qquad (6.3)$$

where P is $-\Delta K/K$ effect due to Xe. The time constant is $\frac{1}{\sigma\varphi_0} > 14$ minutes.

6.4 KINETICS DUE TO TEMPERATURE

Equation (12.13) which neglects time constants < 10 milliseconds can be put in form

$$\Delta T_w = \frac{(T_{w_0} - T_{in_0})}{\left(1 + \frac{u}{v} i\omega\right)\left(1 + \frac{\rho_m c_m L_1 + \rho_c c_c L_2}{h_1} i\omega\right)} \cdot \frac{\Delta\varphi}{\varphi_0} + \left[\frac{1 + \frac{h_2}{L_3 \rho_w c_w} \frac{u}{v}}{1 + \frac{h_2}{L_3 \rho_w c_w} \frac{u}{v} + \frac{u}{v} i\omega}\right] \cdot \Delta T_{in} \qquad (6.4)$$

The time constants involved are about 33.3 and 46.7 milliseconds.

6.5 BLOCK DIAGRAM

A block diagram showing the transfer functions for the linearized responses of flux to reactivity (using one delayed neutron group), reactivity effect of Xe to flux and to gross burnout, and reactivity

effect of temperature to flux and to inlet water temperature is shown on figure 15. The Xe responses are valid for 1/2 to 1 hour, temperature responses have neglected time constants < 10 milliseconds, and $-\alpha$ is the temperature coefficient of reactivity.

6.6 UNCONTROLLED REACTOR

Neglecting time constant < 46.7 milliseconds, the response of flux to δk_{rods}, ΔT_{in}, and gross burnout ($\dot{P}_0$) is

$$\frac{\frac{\Delta\varphi}{\varphi_0}}{} = \frac{(1+\tau_{i\omega})\left(1+\frac{i\omega}{\sigma\varphi_0}\right)\cdot\left[\delta k_{rods} - \alpha\Delta T_{in}\right] - (1+\tau_{i\omega})\cdot\frac{\dot{P}_0}{\sigma\varphi_0}}{\left[\alpha(T_{w0}-T_{in0}) + 0.002 - P_0\right] + \left[\beta + 0.002 - P_0 + \alpha(T_{w0}-T_{in0})\left(1+\frac{1}{\tau\sigma\varphi_0}\right)\right]\tau i\omega + \left[\beta+\alpha(T_{w0}-T_{in0})\right]\frac{\tau(i\omega)^2}{\sigma\varphi_0}} \qquad (6.5)$$

The stability criterion is $\alpha(T_{w0} - T_{in0}) > P_0 - 0.002$. In our case, $\alpha(T_{w0} - T_{in0}) \leqq 0.15$ percent, while $P_0 \geqq 4$ percent. Therefore the reactor is definitely unstable. There are also odd long term reversal effects where increase of flux requires rod insertion, at least for one hour or so until Xe and I decay effects come in. For example, a 10 percent increase in flux requires, after initial transient, $\delta k_{rods} \doteq -0.37$ percent (for $P_0 = 4$ percent).

6.7 REACTOR INSTABILITY

The stability parameters are (1) $\sigma\varphi_0$, (2) P_0, and (3) $\alpha(T_{w0} - T_{in0})$. The two normal modes of response (roots of denominator of eq. (6.5)) are shown in the following tables. These modes are damped and undamped exponentials (nonoscillatory).

Case I. $\varphi_0 = 4\times10^{14}$, $P_0 = 4\%$, $\beta = 0.85\%$, $\tau_{av} = 12.47$ sec		
$\alpha(T_{w0} - T_{in0})$, percent	Unstable mode, sec	Stable mode, sec
0	43.5	-53.2
.0435	49.8	-49.8
[a].15	67	-42.5
.3	96.6	-35.1

[a]Approximate condition at rated power.

E-103

CO-3 back

Case II. $\Phi_0 = 4\times10^{14}$, $P_0 = 20\%$, $\beta = 0.85\%$, $\tau_{av} = 12.47$ sec (as during restart with maximum Xe)		
$\alpha(T_{w_0} - T_{in_0})$, percent	Unstable mode, sec	Stable mode, sec
0	16	-28
[a].15	20.4	-26

[a]Approximate condition at rated power.

This Xe power instability is manifested as a slow, positive exponential drift in flux level, increasing or decreasing. The temperature coefficient of reactivity only increases the unstable period from 43 to 55 - 60 seconds in normal operation. The unstable period could be as low as 16 seconds after a restart with maximum Xe build-up. On a restart, this period is also that which would develop, at first, if the control rods do not keep up with Xe burnout.

It can be shown that the stable and unstable modes are perturbed almost equally by any reactivity disturbance. For a pulse reactivity disturbance, and $P_0 = 4$ percent, $\Phi_0 = 4\times10^{14}$, and $\alpha(T_{w_0} - T_{in_0}) = 0.0435$ percent, the unstable transient, after the initial pulse, is

$$\frac{\Delta\varphi}{\varphi_0} \doteq 5.85 \left[\int \delta k_{dist.} \frac{dt}{sec}\right] \epsilon^{+t/50 \text{ sec}}$$

For example, a 0.5 percent pulse lasting 1 second would give a 50 percent overshoot in about 2.4 minutes.

7. - CONTROLLED REACTOR

A complete investigation of the servocontrolled reactor requires an analogue study simulating the reactor kinetics and servocharacteristics in detail. Some of the general requirements on regulating rod speed and range and limitations in controllability because the regulating rod speed and range must be limited, due to the hazard involved on servo failure, can be deduced from general considerations. An analysis for stability, control on constant period set-backs, and control of reactivity disturbances follows.

7.1 CONSTANT PERIOD SET-BACK

The behavior of the setting is $\varphi_0 \varepsilon^{-t/T}$ where T is period of set-back. Neglecting the time constants in control, or assuming perfect control, the rod transient to obtain this set-back, over a few minutes, is

$$\left.\begin{aligned} \delta k_{rods} &= \frac{-\beta\tau}{T-\tau}\left(\varepsilon^{-t/T} - \varepsilon^{-t/\tau}\right) \\ (\delta k_{rods})_{max.} &= -\frac{\beta\tau}{T-\tau}\left[\left(\frac{T}{\tau}\right)^{-\frac{\tau}{T-\tau}} - \left(\frac{T}{\tau}\right)^{-\frac{T}{T-\tau}}\right] \end{aligned}\right\} \qquad (7.1)$$

which occurs at

$$\left.\begin{aligned} t_{max.} &= \frac{\tau T}{T-\tau}\log\frac{T}{\tau} \\ \left(\frac{d}{dt}\,\delta k_{rods}\right)_{max.} &= -\beta/T \end{aligned}\right\}$$

A typical transient is shown below:

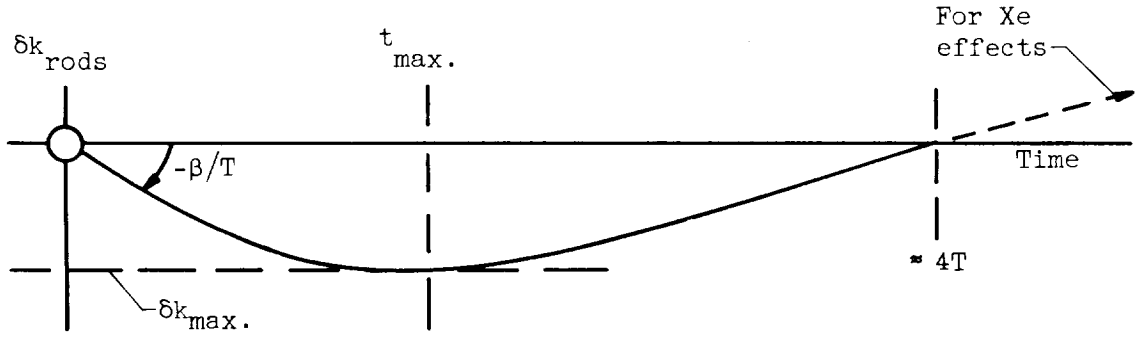

A table of regulating rod speed and range requirements, for constant period set-backs is given below. These are pessimistic values as the small Xe rise in this time interval would reduce these speed and range requirements.

Set-back period, sec	$t_{max.}$, sec	Required range $(\delta k_{rods})_{max.}$, percent	Required speed $\left(\frac{d}{dt}\ \delta k_{rods}\right)_{max.}$, percent/sec
20	15.6	-0.243	-0.04
90	28.5	-.086	-.01

Using one average delayed neutron group indicates that, to maintain a constant period set-back, there is a maximum insertion of the regulating rod after which the rod will withdraw and approach its original position. The table shows that the regulating rod speed is adequate for set-backs but that the range required for a 20 second period set-back may be critical.

7.2 STABILITY

If a pure integral controller is placed around the system (block diagram, fig. 15), that is

$$\delta k_{rods} = \frac{K}{i\omega}\left[\frac{\Delta\varphi_{set}}{\varphi_0} - \frac{\angle\varphi}{q_0}\right]$$

the stability criterion on controlled system is

$$K > \sigma P_0 \varphi_0 = \begin{matrix} 0.0048\ \%/\text{sec} & \text{for} & P_0 = 4\% \\ 0.024\ \%/\text{sec} & \text{for} & P_0 = 20\% \end{matrix}$$

If the gain is set so that a 17.5 percent error in φ will give maximum rod velocity, then stability requires

$$\left(\frac{d}{dt}\ \delta k_{rods}\right)_{max.} > \begin{matrix} 0.00084\ \%/\text{sec} & \text{for} & P_0 = 4\% \\ 0.0042\ \%/\text{sec} & \text{for} & P_0 = 20\% \end{matrix}$$

A regulating rod can easily meet this requirement. One shim rod would be marginal in this regard. A gain (K) of 3.4 percent/second, which is 140 times that required to stabilize Xe in the worst condition, seems reasonable for a regulating rod.

A rough estimate for the upper limit on gain for stability can be deduced from the following assumptions:

(1) Delayed neutrons act as a constant source at these relatively high frequencies.

(2) Pure integral control action; perfect servoaction at the frequencies of interest.

(3) Small reactivities involved ($\delta k \ll \bar{\beta}$).

(4) Xe and temperature neglected at these relatively high frequencies.

The response of flux to φ_s and δk disturbance is

$$\frac{\Delta\varphi}{\varphi_0} = \frac{K\left(\frac{\Delta\varphi}{\varphi_0}\right)_s + i\omega\,\delta k_{dist}}{K + \beta i\omega + l(i\omega)^2} \tag{7.2}$$

If critical damping is the effective stability limit then, the stability criterion is

$$K < \frac{\bar{\beta}^2}{4l} = 20\ \%/\text{sec}$$

If $K \ll 80$ percent/second, the denominator of the above responses (eq. (7.2)) factors into $K\left(1 + \frac{\beta}{K} i\omega\right)\left(1 + \frac{l}{\beta} i\omega\right)$; $\frac{\bar{\beta}}{K} = 0.25$ second (for $K = 3.4$ percent/sec); $\frac{l}{\bar{\beta}} = 10.6$ milliseconds.

7.3 CONTROLLED RESPONSES

For the pure integral controller, the controlled responses, valid for one minute or so before Xe effects come in, of flux and rod position to flux setting and reactivity disturbances are

$$\left.\begin{aligned} \delta k_{rods} &= \frac{\beta\tau i\omega \cdot \left(\frac{\Delta\varphi}{\varphi_0}\right)_s}{(1 + \tau i\omega)\left(1 + \frac{\beta}{K} i\omega\right)} - \frac{1 \cdot \delta k_{dist}}{\left(1 + \frac{\beta}{K} i\omega\right)\left(1 + \frac{l}{\beta} i\omega\right)} \\ \frac{\Delta\varphi}{\varphi_0} &= \frac{\left(\frac{\Delta\varphi}{\varphi_0}\right)_s + \frac{i\omega}{K}\,\delta k_{dist}}{\left(1 + \frac{\beta}{K} i\omega\right)\left(1 + \frac{l}{\beta} i\omega\right)} \end{aligned}\right\} \tag{7.3}$$

Where one average delayed neutron group was used and $K >> \beta/\tau \doteq 0.07$ percent/second. There are three time constants involved: (1) the mean life of delayed neutrons, $\tau = 12.47$ seconds, (2) the time constant of control, $\beta/K = 0.25$ second for $K = 3.4$ percent/second, and (3) the time constant of the prompt neutron effect, $l/\beta = 10.6$ milliseconds. The additional effect of the velocity limit of the regulating rod, approximately 0.6 percent/second, must be considered.

For a reactivity disturbance above a frequency of K/β there is little control action. Also, for a frequency above $\frac{\dot{\delta k}_{max.}}{|\delta k_{dist}|}$ there is little control action because of the velocity limit on regulating rod. For these limits to occur simultaneously, $\frac{K}{\beta} = \frac{\dot{\delta k}_{max.}}{|\delta k_{dist}|}$. Using $\dot{\delta k}_{max.} = 0.6$ percent/second, $|\delta k_{dist}| = 0.15$ percent gives $\frac{K}{\beta} = 4 \frac{\text{radians}}{\text{second}}$, as the essential upper frequency which can be controlled. For this set of parameters, a servofrequency response of 3 to 5 cps seems adequate. Such a servo would not control the prompt neutron effects.

For a step reactivity disturbance, the peak flux would be the irreducible (almost) prompt rise. The maximum rod velocity during the transient would be $\frac{K}{\beta} \delta k_{dist}$. The flux would return to its original value on an exponential with a time constant β/K. For a $\delta k_{dist} = 0.15$ percent, and $\frac{K}{\beta} = 4 \frac{\text{radians}}{\text{second}}$, the maximum rod velocity would be 0.6 percent/second and the settling time for the transient, about $4\beta/K$, would be about one second.

8. - START-UP ACCIDENT

It was shown in sections 2 and 3 that the Xe build-up and burnout rates sets minimum values of control rod speeds in order to restart after a recent shut-down and to insure control of Xe burnout at all times. The maximum allowable rod rates are set by reference to the start-up accident, where it is assumed that all control rods are being withdrawn at their maximum possible speeds and the reactor is protected only by a level scram. It is well known that the higher the rate of insertion of reactivity the shorter the period at any level and thus the larger the overshoot after the level scram. It is shown below that the peak flux, or peak specific power, is the major consideration for these accidents. An analysis for the start-up accident is given below.

8.1 CRITERION ON EXCURSION

As shown in section 12, in neglecting time constants of the order of 6.5 milliseconds there is a static correspondence between surface heat flux and surface temperature, both lagging the heat release with a time constant of 46 milliseconds at normal conditions. On nucleate boiling, this lag decreases considerably. If, for the start-up accident with periods greater than 40 milliseconds and overshoots which must be in nucleate boiling, this lag is neglected, the analysis would be slightly pessimistic as any additional heat stored would attenuate peak surface heat flux and surface temperature, raising the temperature at center of plate which would be (for mild overshoots) well below melting anyway.

Thus, the start-up accident excursions can be considered as following the static curve of surface heat flux versus surface temperature. A safe criterion for this accident is that the peak heat flux be below the burnout heat flux. From existing burnout data a value for burnout heat flux of 2.2×10^6 Btu/hour - square feet appears to be a conservative limit. This value would allow an overshoot to 2.5 times rated power. Pressure build-up on nucleate boiling, for the periods involved in the start-up accident, would not be harmful, reference 2.

8.2 KINETICS DURING SCRAM

If, previous to scram, flux has increased over a wide range fairly rapidly so that the relative contribution of neutrons from the delayed emitters is small, then reactor kinetics can be written

$$\frac{d\varphi}{\varphi dt} = \left(\frac{d\varphi}{\varphi dt}\right)_r + \frac{\delta k - \delta k_r}{l} \qquad (8.1)$$

where "r" is any convenient nearby (in time) reference condition.

For reference condition at dropping of rods (t = 0), and

$$\delta k - \delta k_{drop} = -\frac{s}{2} g t^2$$

then

$$\log \frac{\varphi}{\varphi_{drop}} = \frac{t}{T_{drop}} - \frac{s g t^3}{6 l}$$

$\varphi_{max.}$ occurs when

$$t^2 = \frac{2l}{sgT_{drop}}$$

and

$$\log \frac{\varphi_{max.}}{\varphi_{drop}} = \frac{2}{3T_{drop}} \left(\frac{2l}{sgT_{drop}} \right)^{\frac{1}{2}} \tag{8.2}$$

where T is period and s is rod effectiveness. This equation is plotted in figure 16, for $l = 9 \times 10^{-5}$ seconds and a range of "s."

8.3 KINETICS DURING DEAD TIME

Using equation (8.1), reference condition at scram signal (t = 0), and $\delta k - \delta k_{ss} = Rt$, we get

$$\left.\begin{aligned} \log \frac{\varphi_{drop}}{\varphi_{ss}} = \frac{\Delta t}{T_{ss}} + \frac{R}{2l} \Delta t^2 = \frac{\Delta t}{2} \left[\frac{1}{T_{ss}} + \frac{1}{T_{drop}} \right] \\ \frac{1}{T_{drop}} = \frac{1}{T_{ss}} + \frac{R}{l} \Delta t \end{aligned} \right\} \tag{8.3}$$

where

R accident rate (or rod rate)

Δt dead time

For any given l, s, R, and Δt we need only the period at the scram signal level to calculate the overshoot over that level, using equations (8.2) and (8.3).

E-103

CO-4 back

8.4 KINETICS BEFORE SCRAM SIGNAL

8.4.1 Newson Analysis (ref. 5)

The basic reactor kinetics is described by

$$l \frac{d\varphi}{dt} = (\delta k - \beta)\varphi + \sum_i \lambda_i C_i + S \tag{8.4}$$

If we let

$$\left[\frac{\sum_i \lambda_i C_i}{\beta\varphi} + \frac{S}{\beta\varphi}\right]\frac{\beta}{l} = \nu(t) > 0$$

then

$$\frac{d\varphi}{\varphi dt} = \frac{\delta k - \beta}{l} + \nu(t)$$

Starting the analysis when the accident has progressed to prompt critical, that is, at $t = 0$, $\varphi = \varphi_{pc}$, and $\delta k - \beta = Rt$. Then

$$\left.\begin{aligned} \log \frac{\varphi_{ss}}{\varphi_{pc}} &= \frac{Rt_{ss}^2}{2l} + \int_0^{t_{ss}} \nu(t)dt \\ \frac{1}{T_{ss}} &= \frac{Rt_{ss}}{l} + \nu(t_{ss}) \end{aligned}\right\} \tag{8.5}$$

Eliminating t_{ss} in above equations gives

$$\log \frac{\varphi_{ss}}{\varphi_{pc}} = \frac{l}{2R}\left[\frac{1}{T_{ss}} - \nu(t_{ss})\right]^2 + \int_0^{t_{ss}} \nu(t)dt \tag{8.6}$$

The approximate behavior of $\nu(t)$ is given below:

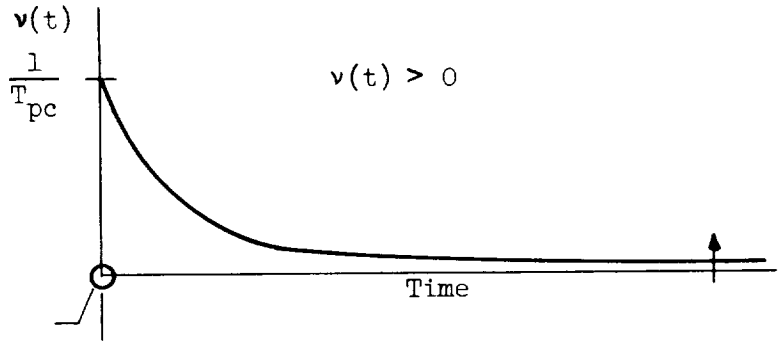

The detailed nature of this function allows us to write equation (8.6) as

$$\log \frac{\varphi_{ss}}{\varphi_{pc}} > \frac{l}{2RT_{ss}^2}$$

and since

$$\log \frac{\varphi_{pc}}{\varphi_{initial}} > 0$$

$$\text{Minimum possible period at scram signal} = \left[\frac{l}{2R \log \frac{\varphi_{ss}}{\varphi_{initial}}}\right]^{\frac{1}{2}} \tag{8.7}$$

This minimum possible period will give the maximum possible overshoot over the scram signal level. The above equation is plotted in figure 17 for $l = 9\times10^{-5}$ seconds over a range of R.

8.4.2 Initial Level Close to Scram Level

The reactor kinetic equations with 5 delayed neutron groups were solved on a differential analyzer for two cases: (1) Constant rod withdrawal at 0.1 percent/second, and (2) 0.5 percent step plus a constant rod rate of 0.1 percent/second. This simulates the worst that the rods can do, starting, for example, in the power range.

The results are plotted in figure 17 and also on figure 22. It is seen that for $\frac{\varphi_{ss}}{\varphi_{initial}}$ of, for example, 100, the Newson-type analysis is far too pessimistic, giving a period at scram of 100 milliseconds when the actual period is about 400 milliseconds.

8.5 TOTAL OVERSHOOTS

Combining equations (8.2) and (8.3), the total overshoot over the scram signal level can be written

$$\log \frac{\varphi_{max.}}{\varphi_{ss}} = \frac{2}{3T_{ss}}\left(\frac{2l}{sgT_{ss}}\right)^{\frac{1}{2}} + \frac{\Delta t}{T_{ss}} + \frac{R\Delta t^2}{2l} + \frac{2}{3T_{ss}}\left(\frac{2l}{sgT_{ss}}\right)^{\frac{1}{2}}\left[\left(1 + \frac{R\Delta t T_{ss}}{l}\right)^{\frac{3}{2}} - 1\right] \tag{8.8}$$

The first and second terms on the right hand side of the previous equation give the total overshoot under the assumption that the period does not change during the dead time. The error involved using this assumption, is the magnitude of the third and fourth terms of equation (8.8). For the start-up accident, this error is less than 15 percent in $\varphi_{max.}$. The overshoots given below were calculated using the assumption that the period changes very little during the dead time duration. Periods at scram are obtained from figure 17. The first term of equation (8.8) is plotted in figure 16.

The total overshoots over the scram signal level is plotted in figure 18, as a function of dead time, for various $\frac{\varphi_{ss}}{\varphi_{initial}}$ values, using the Newson-type analysis for the large range accidents and the actual transients for the small range accidents. Figure 17 showed the boundary $\frac{\varphi_{ss}}{\varphi_{initial}}$ value between the two approaches to be about 10^4. A table of some specific start-up accidents is given below.

STARTUP ACCIDENTS

[Rod velocity, 3 in./min; rod effectiveness, 2 percent Δk/in.]

Accident conditions				Period at scram signal level	Ratio of peak level to scram signal level	Peak level
Initial level	Scram signal level	Ratio of scram signal to initial level	Dead time in scram			
$10^{-14}\ \varphi_f$	$10^{-3}\ \varphi_f$	10^{11}	80 Millisec	42 Millisec	9.7	$10^{-2}\ \varphi_f$
$10^{-14}\ \varphi_f$	$10^{-1}\ \varphi_f$	10^{13}	80	39	12	$1.2\ \varphi_f$
*$10^{-14}\ \varphi_f$	$1.5\ \varphi_f$	1.5×10^{14}	40	37	4.6	$6.9\ \varphi_f$
		2.25	80 Millisec	1.8 Sec		
	$1.5\ \varphi_f$	1000	80	170 Millisec	1.66	$2.5\ \varphi_f$
*	$1.5\ \varphi_f$	4000	40	100	1.66	$2.5\ \varphi_f$

*Slow scram inoperative, four simultaneous failures.

Note: If period scram operates with dead time < 3 sec then peak level always < $2.5\ \varphi_f$.

For the accident beginning at a very low source level and scramming at the lowest protection level of $10^{-3}\ \varphi_f$, where φ_f is the rated power level, the period at scram would be 42 milliseconds. Using a dead time of 80 milliseconds for this slow scram gives an overshoot of 9.7 times, which is very safe. If we consider the protection level not acting until 10^{-1} rated power, the period at scram would be 39 milliseconds and the overshoot 12 times which is still very safe. If the slow scram protection does not act at all, the minimum period at scram would be 37 milliseconds and, with a dead time in the fast scram of 40 milliseconds, the peak power would be 6.9 times rated. This accident involves four simultanious failures: uncontrolled rod withdrawal, failure of the slow scram system and its back-up, and failure of the period scram. Also, as discussed in reference 2, periods of 37 milliseconds are controllable by the self-regulating features of the reactor, which are not included in this analysis. Also, the conservative limit on peak power of 2.5 times rated is the static burn-out limit; allowable transient peaks being much higher.

In the power range, above 10^{-3} rated power, the protection will be very close whereby the scram level should not exceed the operating level by more than 2.25. The minimum period that could develop from a control rod withdrawal would be 1.8 sec. If this protection takes a level rise of as much as 1000 to act, instead of 2.25, the period at scram would be 170 milliseconds and the excursion would be safe. The fast level scram, set at 1.5 φ_f with a dead time less than 40 milliseconds, is always in effect. If the slow scram protection does not act at all, a level rise of as much as 4000 would give a period of 100 milliseconds, which, for the fast scram would give a safe peak power.

All cases discussed above were for the period scram inoperative. If only the period scram operates with a dead time less than 3 seconds, then the excursions for any startup accident would be safe.

The drive system providing the rod insertion speed of 9 in./min is designed to insure one-directional operation. Even if this speed should somehow become effective as a withdrawal, and uncontrolled withdrawal should occur, the scram system would keep the excursions safe. In addition, the minimum period that can develop from this higher rod speed, about 21 milliseconds, can be controlled by the self-regulation of the reactor as discussed in reference 2.

9. - CONTROLLABILITY OF LARGE ACCIDENTAL REACTIVITY INSERTIONS

In order to set the minimum requirements on the safety system and the allowable reactivity insertions that can be safely handled by this system, it is necessary to understand the behavior of the reactor in response to the accident and the corrective action of the control system. The basic reactor kinetic equations are of 6^{th} or 7^{th} order and are amenable to analysis for only a few special cases. An understanding of all the implications of such an equation is best obtained by solving for a wide variety of special cases using machine methods.

A differential analyzer was used to solve the equations describing a number of accidental reactivity insertions and the subsequent corrective action of the control safety system. Both step and ramp reactivity insertions were made and both scram and reverse actions were studied for a range of dead times, control rod effectiveness, rod speeds, accident rates and amounts, and levels of safety signal.

9.1 ONE PERCENT ACCIDENTS - WITH SCRAMS

Figure 19 gives peak flux for a 1 percent step $\Delta K/K$ accident, with scram signal set at $\varphi/\varphi_0 = 1.5$, as a function of dead time and rod effectiveness. The peaks are sensitive to both parameters. Only the very best conditions for scram contain this accident. But, if the accident progresses ramp-wise, then, for a rather poor scram condition, an accident ramp time of 0.2 second would reduce peak φ from 9.3 φ_0 to 3 φ_0. In this case, the entire 1 percent of accident was not involved. For such large accidents, the rate of $\Delta K/K$ insertion is of utmost importance and is more fully discussed later.

9.2 FIVE TENTHS PERCENT STEP ACCIDENTS

Figure 20 shows that scrams can easily contain this accident. Slow reverses, like 0.04 percent/second, are not effective. Peak flux is very sensitive to reverse rates up to about 0.15 percent/second; little improvement is obtained above this speed. The dead time is of secondary importance.

9.3 RAMP-WISE ACCIDENTS

Figure 21 shows peak flux plotted against the accident $\Delta K/K$ insertion rate, which continues indefinitely, for various scrams and reverses;

a poor scram condition assumed. Accident rates of 5 percent/second are contained. A reverse rate of 3 percent/second can handle accident rates of 2 percent/second. A reverse rate of 0.7 percent/second can handle accident rates of 0.5 percent/second.

9.4 CONTINUED REACTIVITY INSERTION AT CONSTANT RATE

All the previous accidents started at full power with a reverse signal at 1.2 φ_f or a scram signal at 1.5 φ_f. It is more dangerous, if the accident starts well below the correction signal level. For such accidents, cases were run of continued $\Delta K/K$ insertion at constant rates; the results are shown on figures 22, 23, and 24. Figure 22 was used for the start-up accident analysis.

The higher the accident rate, the lower the period at any level. For corrections tripped by a level signal, figure 23 gives the period at that signal. The overshoots can be found analytically from the period, for most cases, using equation (8.1) for both scrams and fast reverses. For corrections tripped by a period signal, figure 23 gives level at that signal. For accident rates greater than about 1 percent δk/second, the 1 second period signal is obtained immediately.

9.5 PERIOD AGAINST REACTIVITY - CONSTANT REACTIVITY INSERTION RATES

Figure 25 and 26 show period as a function of δk for various constant rates of δk insertion. Also shown, is the stable period, which would be obtained for very slow rates. The faster the reactivity rate, the smaller the period at any reactivity. All the curves approach the stable period curve as higher reactivities are reached. These figures also prove the accuracy of the differential analyzer calculations.

9.6 CONTROLLABLE ACCIDENTS

One of the basic criterions on the design of the reactor, experiment and control systems is that no possible accident can introduce changes in reactivity which cannot be safely handled by the reactor control system. The basic safety feature of the control system is the level fast scram which is set to trip at a level 50 percent or less above the maximum reactor operating level required for the particular reactor cycle. This saftey trip is backed up by the one second period fast scram, the intermediate level slow scrams, as well as reverses and set-backs which are triggered at the first indications of malfunction.

Figure 16 can be used to find the minimum allowable period at the scram signal power level. In order to relate these restrictions on reactor periods to allowable reactivity insertions, the transient reactor periods must be considered as well as the stable periods. For step or ramp-wise insertions of reactivity, the transient periods are always smaller than the ultimate stable period. To obtain these effects, the reactor kinetic equations, using 5 delayed neutron groups, were solved on a differential analyzer for cases of continued insertion of reactivity at constant rates. The results were shown on figures 23 to 26.

In general, the period at the scram signal is determined by the level at the start of the accident, the rate of reactivity insertion, and the total reactivity inserted. For any reactivity insertion rate, figure 25 shows that the period decreases continuously until the total reactivity is inserted. At this time the period is the minimum for the transient as, past this point, the period would increase toward the stable period corresponding to the total reactivity inserted. If the smallest allowable period during the transient is set according to figure 16, which only specifies minimum periods at scram, a definitely safe and pessimistic relation between reactivity insertion rate and total reactivity inserted can be obtained from figure 25. These limitations on reactivity, which are independent of the power level at which the accident starts, are shown on figure 27.

Ramp-wise accidents are assumed: Each such accident is represented by a point on figure 27 corresponding to the reactivity and time at the corner of the ramp. Accidents which so map into a point below the curve under consideration can be safely handled by the control system for that curve. The curves apply to the least favorable power levels at the start of the accident, up to the 60 mw power level, and for the least effective control rod position, and for the conservative criterion on any excursion that the peak power be less than 2.5 times rated.

If only the level fast scram system is operative, a step of 0.5 percent δk or a slow insertion up to 0.9 percent δk is always controllable. If only the set-point level scram system is operative, a reactivity insertion of 1.2 percent in 0.6 second is always controllable. If only the one second period scram system is operative, with a dead time less than 40 milliseconds, a reactivity insertion of 1.35 percent in 0.23 second is always controllable.

It is emphasized that these limits are for the least favorable power levels at the start of the accident. If, for example, considering the fact scram only is operative, a 2 percent δk per second accident starts at power levels greater than 20 mw, the reactor scrams before the limiting total reactivity of 0.74 percent is inserted. If the same accident starts at power levels less than 20 mw, then a somewhat larger total insertion of reactivity is controllable as the reactor scrams after the minimum period of the transient. If the accident starts at 60 mw, a reactivity insertion rate of 4 to 5 percent δk per second is controllable.

10. - Xe BURNOUT ON NUCLEAR EXCURSION

As noted in section 3, the Xe in the core is an ever-present hazard because it can be burned out in an unstable manner at appreciable rates. The possibility of burning out a large fraction of this Xe in a short time requires thorough study. An analysis of this Xe burnout on a nuclear excursion is given below.

10.1 GENERAL EXCURSION

Using the short-term Xe equation (2.1), with reference condition at start of run-away, t = 0, and assuming

$$P\bar{\varphi}_{th} >> P_0\bar{\varphi}_{th_0} + \frac{aP_e}{1+a}\left(\bar{\varphi}_{th} - \bar{\varphi}_{th_0}\right) + \frac{1}{\sigma}\left(\frac{dP}{dt}\right)_0$$

we get

$$\frac{dP}{dt} = -\sigma P\bar{\varphi}_{th} \tag{10.1}$$

whose solution is

$$\frac{P}{P_0} = \varepsilon^{-\sigma\int_0^t \bar{\varphi}_{th}(x)dx} \tag{10.2}$$

which gives the burnout as a function of nuclear energy release only. For any average energy per unit volume released, the worst burnout is when the corresponding $\bar{\varphi}_{th}$ is greatest - for our case, at the end of the 10-day cycle. Assuming $\bar{\varphi}_{th} = 4\times10^{14}$ corresponds to 60 megawatts for the full core, equation (10.2) becomes

$$\frac{P(t)}{P(0)} = \varepsilon^{-\frac{1}{5\times10^4}\left(\frac{E(t)}{MW\ sec}\right)} \tag{10.3}$$

where $E(t)$ is nuclear energy released on the excursion for the full core.

This equation is plotted in figure 28. If run-away starts with equilibrium Xe (P_0 = 4 percent), then it takes a 6700 megawatt seconds excursion to add 0.5 percent reactivity. In the worst case, if run-away starts after a restart, where P_0 may reach as high as 20 percent, then

a 1250 megawatt seconds excursion will add 0.5 percent reactivity. It is interesting to note that in general, the maximum burn-up rate (at $\ddot{P} = 0$) occurs when $\frac{1}{\bar{\varphi}_{th}} \frac{d\bar{\varphi}_{th}}{dt} = \sigma\bar{\varphi}_{th}$, but, as seen below, about 2/3 of the Xe would have already been burned out.

10.2 CONSTANT PERIOD EXCURSION (REF. 6)

In this case,

$$\bar{\varphi}_{th} = \bar{\varphi}_{th_0} \varepsilon^{t/T}$$

where T is constant period of excursion. Equation (10.2) becomes

$$\frac{P}{P_0} = \varepsilon^{-\sigma T\bar{\varphi}_{th_0}(\varepsilon^{t/T}-1)} = \varepsilon^{-\sigma T(\bar{\varphi}_{th}-\bar{\varphi}_{th_0})} \doteq \varepsilon^{-\sigma T\bar{\varphi}_{th}} \tag{10.4}$$

Let $t = t_1$ be time at maximum burnout rate ($\ddot{P} = 0$). Then,

$$\left.\begin{aligned} \frac{P}{P_0} &= \varepsilon^{-\varepsilon^{\frac{t-t_1}{T}} + \sigma T\bar{\varphi}_{th_0}} \doteq \varepsilon^{-\varepsilon^{\frac{t-t_1}{T}}} \\ \sigma T\bar{\varphi}_{th} &= \varepsilon^{\frac{t-t_1}{T}} \\ \sigma\int_0^t \bar{\varphi}_{th}(x)dx &= \varepsilon^{\frac{t-t_1}{T}} - \sigma T\bar{\varphi}_{th_0} \doteq \varepsilon^{\frac{t-t_1}{T}} \end{aligned}\right\} \tag{10.5}$$

where

$$\sigma T\bar{\varphi}_{th_0}\varepsilon^{\frac{t_1}{T}} = \sigma T\bar{\varphi}_{th_1} = 1$$

and

$$\left(\frac{dP}{dt}\right)_{max.} = \frac{-P_0}{T\varepsilon^{1-\sigma T\varphi_0}} \doteq \frac{-P_0}{T\varepsilon}$$

E-103

CO-5 back

and

$$\left(\frac{P}{P_0}\right)_{t_1} = \varepsilon^{\sigma T \varphi_0 - 1} \doteq \frac{1}{\varepsilon}$$

It is seen that $\bar{\varphi}_{th0}$, condition at start of run-away, is not important for these Xe burnout effects.

Equation (10.5) is plotted in figure 29. This transient is for a constant period. But, as burnout progresses, the period will decrease and the sharp rise in the curve at about 2 periods before the maximum burnout rate, indicates that the flux at this point,

$\bar{\varphi}_{th} \doteq \frac{1}{\sigma T \varepsilon^2} = \frac{4.52 \times 10^{16}}{(T/sec)}$ neutrons/cm^2 sec and

energy release = 6770 megawatt seconds, would be a trigger to burnout all the Xe in much less than 3 periods.

11. - HAZARDS DUE TO REGULATING ROD

The regulating rod will be calibrated to insure reactivity worth of less than 0.6 percent δk. The rod is velocity limited to give full travel in about one second. This would give for full travel at maximum speed a minimum transient period of 400 milliseconds, figure 25, and a stable period of 1.7 second, which is not at all hazardous. The hazard in the regulating rod is shown on figure 27 for full travel of 0.6 percent δk in one second. The regulating rod could be worth as much as 0.87 percent δk for only the level fast scram system operative or as much as 1.2 percent δk for only the set-point level scram system operative and still be safe.

12. - TRANSIENT HEAT TRANSFER ANALYSIS

The basic hazard in the operation of a reactor using MTR type fuel plates can be traced to the mechanism of transient heat transfer in the plates and to the coolant. This mechanism determines allowable excursions in terms of peak values or minimum periods to avoid damage or severe accidents caused by pressure surges, burnout, and melting.

In the analysis that follows, the equations describing transient heat conduction in the meat and clad were exactly solved in the frequency, or operational, domain. Expansion of the operators gives the more useful lumped parameter form for the responses. A fairly general model for the transient heat transfer to the coolant was then used and the two sets of equations then combined, operationally, give the net responses of surface heat flux, plate temperatures, and coolant temperatures to nuclear energy release rate and inlet coolant temperature.

12.1 HEAT CONDUCTION IN FUEL PLATE

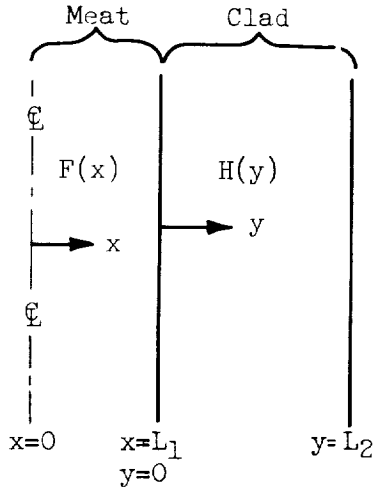

12.1.1 Meat

The partial differential equation for transient heat conduction is

$$\left.\begin{aligned} \frac{\partial T_m}{\partial t} &= \alpha_m \frac{\partial^2 T_m}{\partial x^2} + \frac{Q_m}{\rho_m c_m} \\ \alpha_m &= \left(\frac{k}{\rho c}\right)_m \end{aligned}\right\} \qquad (12.1)$$

where

Using a frequency response approach, let

$$\left.\begin{aligned} \frac{Q_m}{\rho_m c_m} &= G\varepsilon^{i\omega t} \\ \text{and} \qquad T_m &= F\varepsilon^{i\omega t} \end{aligned}\right\} \tag{12.2}$$

then equation (12.1) becomes

$$i\omega F = \alpha_m F_{xx} + G \tag{12.3}$$

whose solution with $F_x(0) = 0$ is

$$\left.\begin{aligned} F &= A(\varepsilon^{rx} + \varepsilon^{-rx}) + G/i\omega \\ \text{where} \qquad r^2 &= \frac{i\omega}{\alpha_m} \end{aligned}\right\} \tag{12.4}$$

12.1.2 Clad

The partial differential equation for transient heat conduction is

$$\left.\begin{aligned} \frac{\partial T_c}{\partial t} &= \alpha_c \frac{\partial^2 T_c}{\partial y^2} \\ \text{where} \qquad \alpha_c &= \left(\frac{k}{\rho c}\right)_c \end{aligned}\right\} \tag{12.5}$$

Let $T_c = H\varepsilon^{i\omega t}$, then equation (12.5) becomes

$$i\omega H = \alpha_c H_{yy} \tag{12.6}$$

whose solution is

$$\left.\begin{aligned} H &= B\varepsilon^{sy} + C\varepsilon^{-sy} \\ \text{where} \qquad s^2 &= \frac{i\omega}{\alpha_c} \end{aligned}\right\} \tag{12.7}$$

12.1.3 Boundary Conditions

The continuity of temperature and heat flux gives

$$\left.\begin{aligned} F(L_1) &= H(0) \\ k_m F_x(L_1) &= k_c H_y(0) \end{aligned}\right\}$$

and from equations (12.4) and (12.7) we get

$$B + C = A\left(\varepsilon^{rL_1} + \varepsilon^{-rL_1}\right) + G/i\omega$$

$$B - C = A\left(\varepsilon^{rL_1} - \varepsilon^{-rL_1}\right)\frac{k_m r}{k_c s}$$

As $\left(\frac{k_m r}{k_c s}\right) = \left(\frac{\rho_m c_m k_m}{\rho_c c_c k_c}\right)^{\frac{1}{2}} \doteq 1$ for our case, then

$$\left.\begin{aligned} 2B &= 2A\varepsilon^{rL_1} + G/i\omega \\ 2C &= 2A\varepsilon^{-rL_1} + G/i\omega \end{aligned}\right\} \qquad (12.8)$$

12.1.4 Fuel Plate Transient Heat Conduction

Transfer Functions

Using equation (12.7) and (12.8) to eliminate A, B, and C we get the general transient responses,

$$\left.\begin{aligned} T_{surface} &= \frac{\sinh(rL_1)}{\sinh(rL_1 + sL_2)}\left(\frac{1}{i\omega}\right)\frac{Q_m}{\rho_m c_m} + \left[\frac{\coth(rL_1 + sL_2)}{s}\right]\cdot\left(\frac{\partial T}{\partial y}\right)_{surface} \\ T(0) &= \left[1 - \frac{\sinh sL_2}{\sinh(sL_2 + rL_1)}\right]\cdot\left(\frac{1}{i\omega}\right)\frac{Q_m}{\rho_m c_m} + \frac{1}{s}\frac{1}{\sinh(sL_2 + rL_1)}\cdot\left(\frac{\partial T}{\partial y}\right)_{surface} \end{aligned}\right\} \qquad (12.9)$$

relating the temperatures at the surface and center of plate to the heat released and to the temperature gradient at the surface.

Expanding equation (12.9), we obtain the final lumped parameter form for the responses as follows:

$$(\rho_m c_m L_1 + \rho_c c_c L_2)\frac{d}{dt}T_{surface} = \left[\frac{1 + \tau_1\frac{i\omega}{6} + \frac{(\tau_1 i\omega)^2}{5!} + \cdots}{1 + \frac{\tau i\omega}{6} + \frac{(\tau i\omega)^2}{5!} + \cdots}\right]\cdot(L_1 Q_m) + \left[\frac{1 + \frac{\tau i\omega}{2} + \frac{(\tau i\omega)^2}{4!} + \cdots}{1 + \frac{\tau i\omega}{6} + \frac{(\tau i\omega)^2}{5!} + \cdots}\right] k_c\left(\frac{\partial T}{\partial y}\right)_{surface} \tag{12.10}$$

where

$$\tau_1 = \frac{L_1^2}{\alpha_m} = 0.00122 \text{ second}$$

$$\tau = \left(\frac{L_1}{\sqrt{\alpha_m}} + \frac{L_2}{\sqrt{\alpha_c}}\right)^2 = 0.00835 \text{ second}$$

The largest time constant involved $(\tau/2)$ is 4.18 milliseconds. The lumped parameter form for the response of the temperature at the center of the plate can be obtained in a similar manner.

12.2 HEAT TRANSFER TO COOLANT

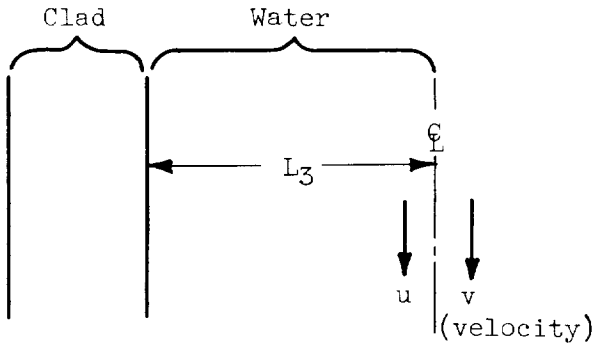

Assuming:

(1) Temperature rise of water is linear in direction of flow.

(2) Heat transfer to water is of form $(h_1 T_{surface} - h_2 T_{water})$.

The responses of the heat flux through the plate surface and the water temperature to the surface temperature of the plate and the inlet water temperature are

$$\left.\begin{aligned} -k_c\left(\frac{\partial T}{\partial y}\right)_{surface} &= \frac{\left(i\omega + \frac{v}{u}\right)h_1 T_{surface} - \frac{v}{u}\, h_2 T_{inlet}}{i\omega + \frac{v}{u} + \frac{h_2}{L_3\rho_w c_w}} \\ T_w &= \frac{\frac{h_1}{L_3\rho_w c_w}\, T_{surface} + \frac{v}{u}\, T_{inlet}}{i\omega + \frac{v}{u} + \frac{h_2}{L_3\rho_w c_w}} \end{aligned}\right\} \qquad (12.11)$$

$$\frac{h}{L_3\rho_w c_w} = \frac{7.3}{sec} \quad \text{for} \quad h = 8000 \text{ Btu/(hr)(ft}^2\text{)(}^\circ\text{F)(normal)}$$

$$\frac{v}{u} = \frac{30}{sec} \quad \text{for} \quad v = 30 \text{ ft/sec},\ u = 1 \text{ ft}$$

The largest time constant involved is 33.3 milliseconds, $\left(\frac{u}{v}\right)$, the transit time to the center of the core.

12.3 COMBINED TRANSFER FUNCTIONS

12.3.1 Surface Heat Flux and Temperature Responses

We will neglect 4 millisecond time constants in equation (12.10), and neglect time constants like $\left(\frac{\frac{h_2}{L_3\rho_w c_w}}{\frac{h_2}{L_3\rho_w c_w} + \frac{v}{u}}\right)\frac{1}{v} \leq$ 6.53 milliseconds in equation (12.11). The 6.53 millisecond time constant corresponds to $h_2 = 8000$, and h_2 (effect of water temperature on heat transfer) probably decreases on nucleate boiling. We then get, at constant T_{inlet},

$$h_1 T_{surface} = -K_c\left(\frac{\partial T}{\partial y}\right)_{surface} = \frac{L_1 Q_m}{1 + \left(\frac{\rho_m c_m L_1 + \rho_c c_c L_2}{h_1}\right)i\omega} \qquad (12.12)$$

Thus, neglecting time constants of order 6.53 milliseconds, there is a static correspondence between surface heat flux and temperature and both lag heat release with time constant,

$$\frac{\rho_m c_m L_1 + \rho_c c_c L_2}{h_1} = 46.7 \text{ milliseconds} \quad \text{for} \quad h_1 = 8000 \text{ (normal)}$$

On nucleate boiling this lag would decrease considerably

E-103

CO-6 back

12.3.2 Coolant Temperature Responses

Neglecting about 10 millisecond time constants, responses of water temperature are

$$T_w = \frac{\frac{u}{v}\frac{L_1}{L_3}\frac{Q_m}{\rho_w c_w}}{\left(1 + \frac{u}{v} i\omega\right)\left(1 + \frac{\rho_m c_m L_1 + \rho_c c_c L_2}{h_1} i\omega\right)} + \left(\frac{1 + \frac{h_2}{L_3 \rho_w c_w}\frac{u}{v}}{1 + \frac{h_2}{L_3 \rho_w c_w}\frac{u}{v} + \frac{u}{v} i\omega}\right) \cdot T_{in} \qquad (12.13)$$

The coolant temperature response to nuclear energy release rate is a double lag with time constants of 33 milliseconds and 47 milliseconds in normal operation. The coolant temperature response to its inlet temperature is a lag with a time constant of about 27 milliseconds in normal operation.

REFERENCES

1. Glasstone, S., and Edlund, M. C.: Elements of Nuclear Reactor Theory, (Van Nostrand.)

2. Lewis Research Center: NASA Reactor Facility Hazards Summary. Vol. I. NASA MEMO

3. Henry, A. F.: Computation of Parameters Appearing in the Reactor Kinetic Equations. WAPD-142 Navy.

4. Weinberg, A. M., and Noderer, L. C.: Theory of Neutron Chain Reactions. Vol. II, Part 1.

5. Newson, H. W.: MonP 271 (classified).

6. Mills, M. M.: NAA-SR-31, 1949 (classified).

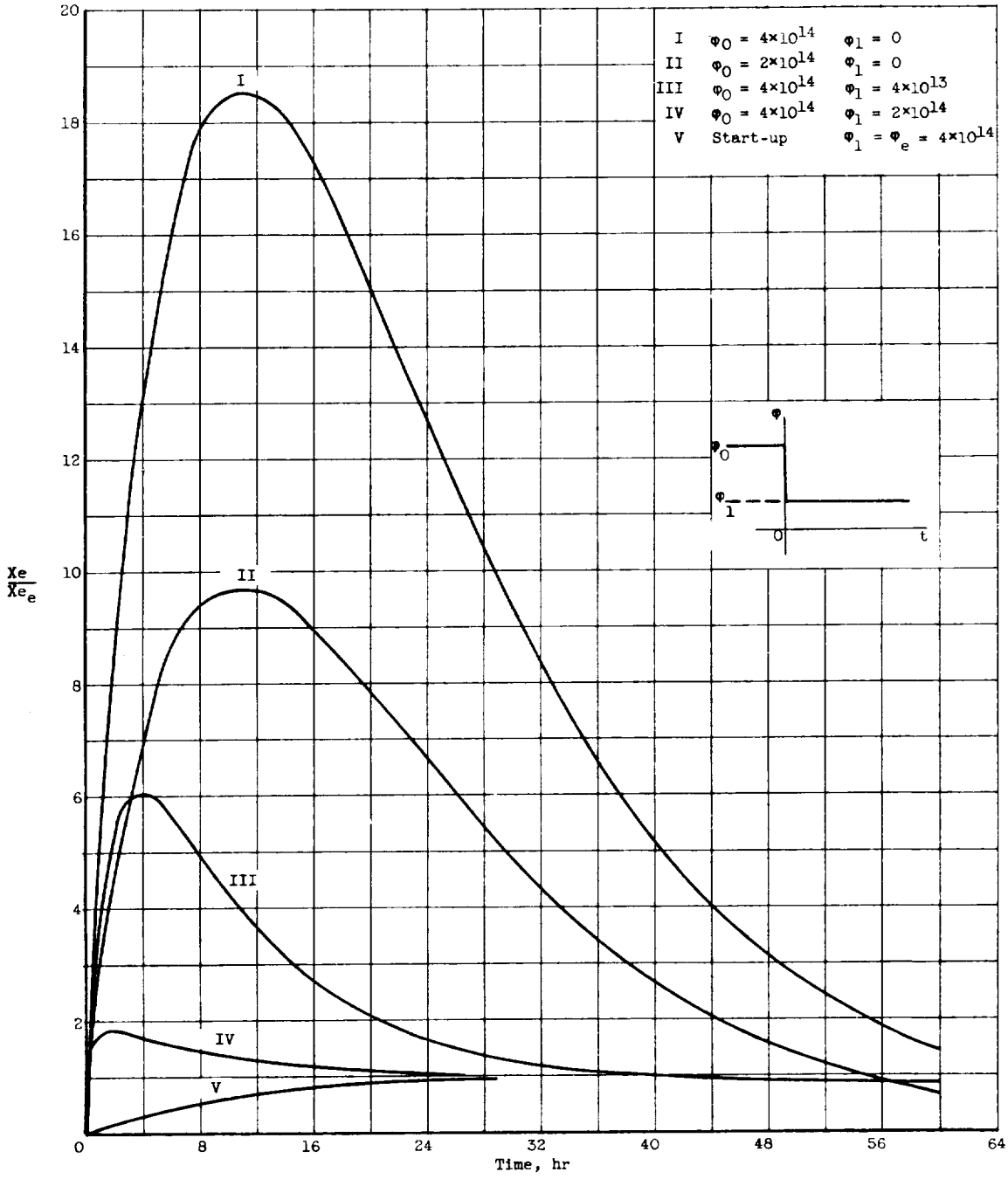

Figure 1. - Long term Xe transients.

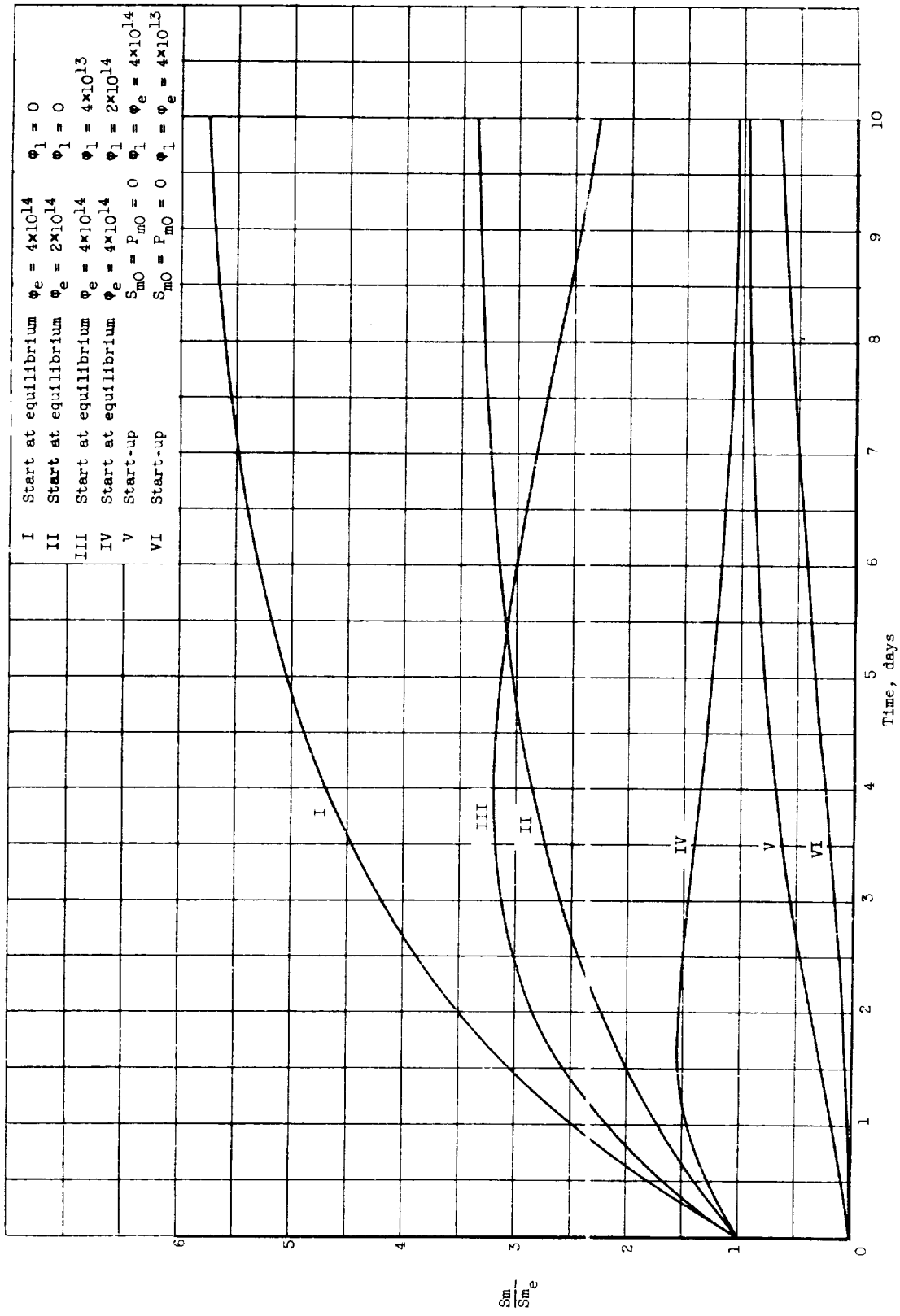

Figure 2. - Long term Sm transients.

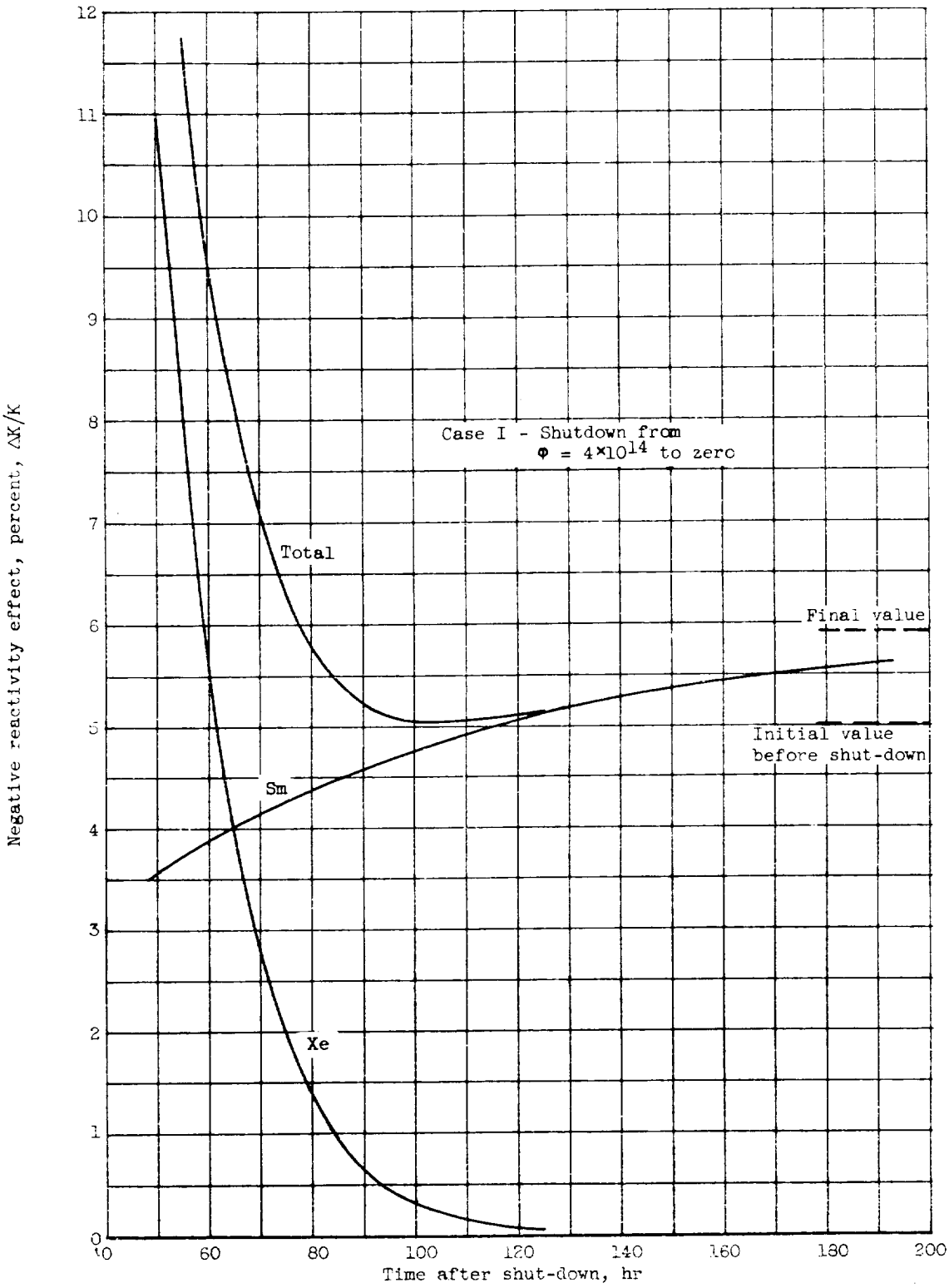

Figure 3. - Total of Xe and Sm long term transient.

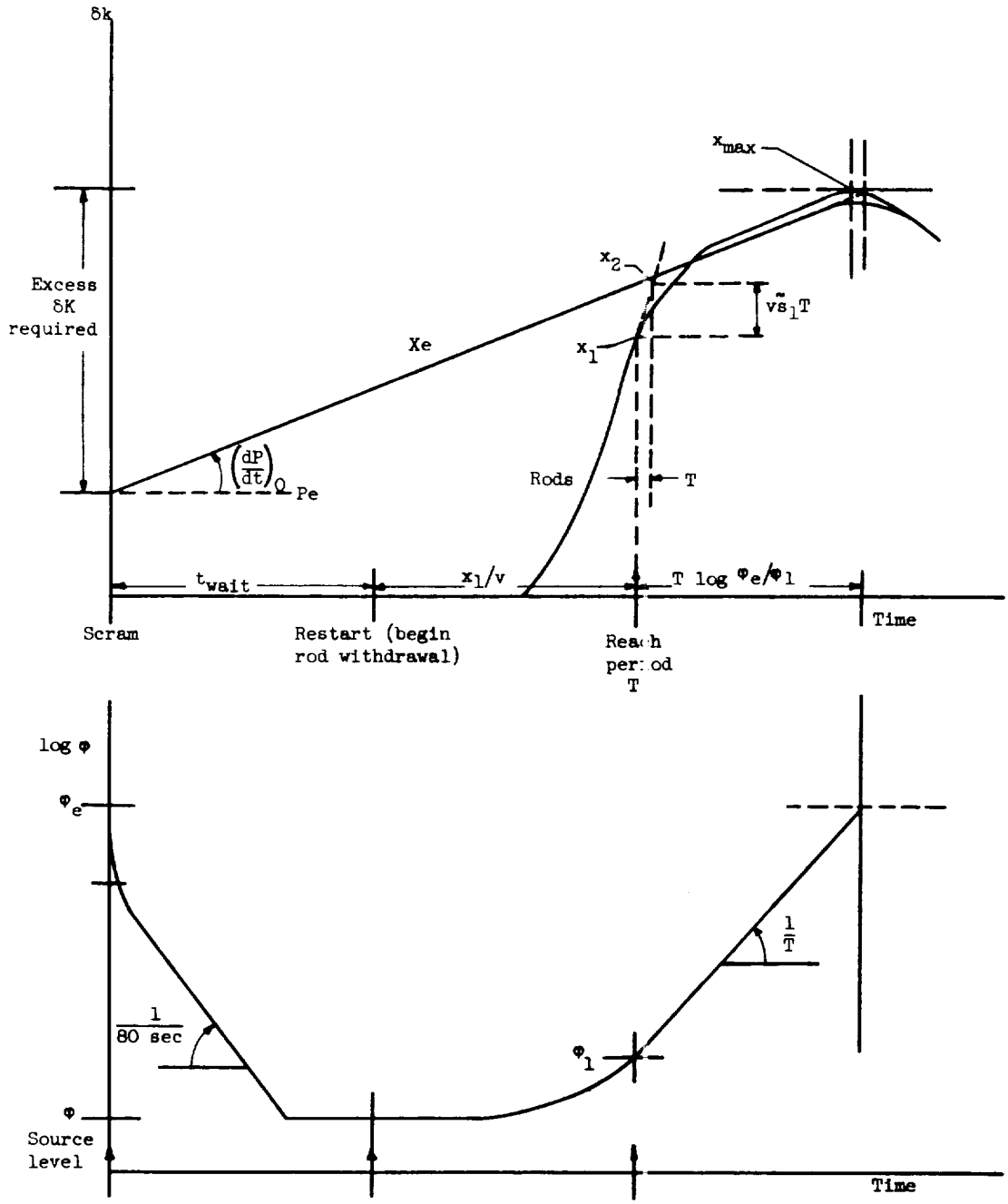

Figure 4. - Qualitative picture of restart with Xe buildup.

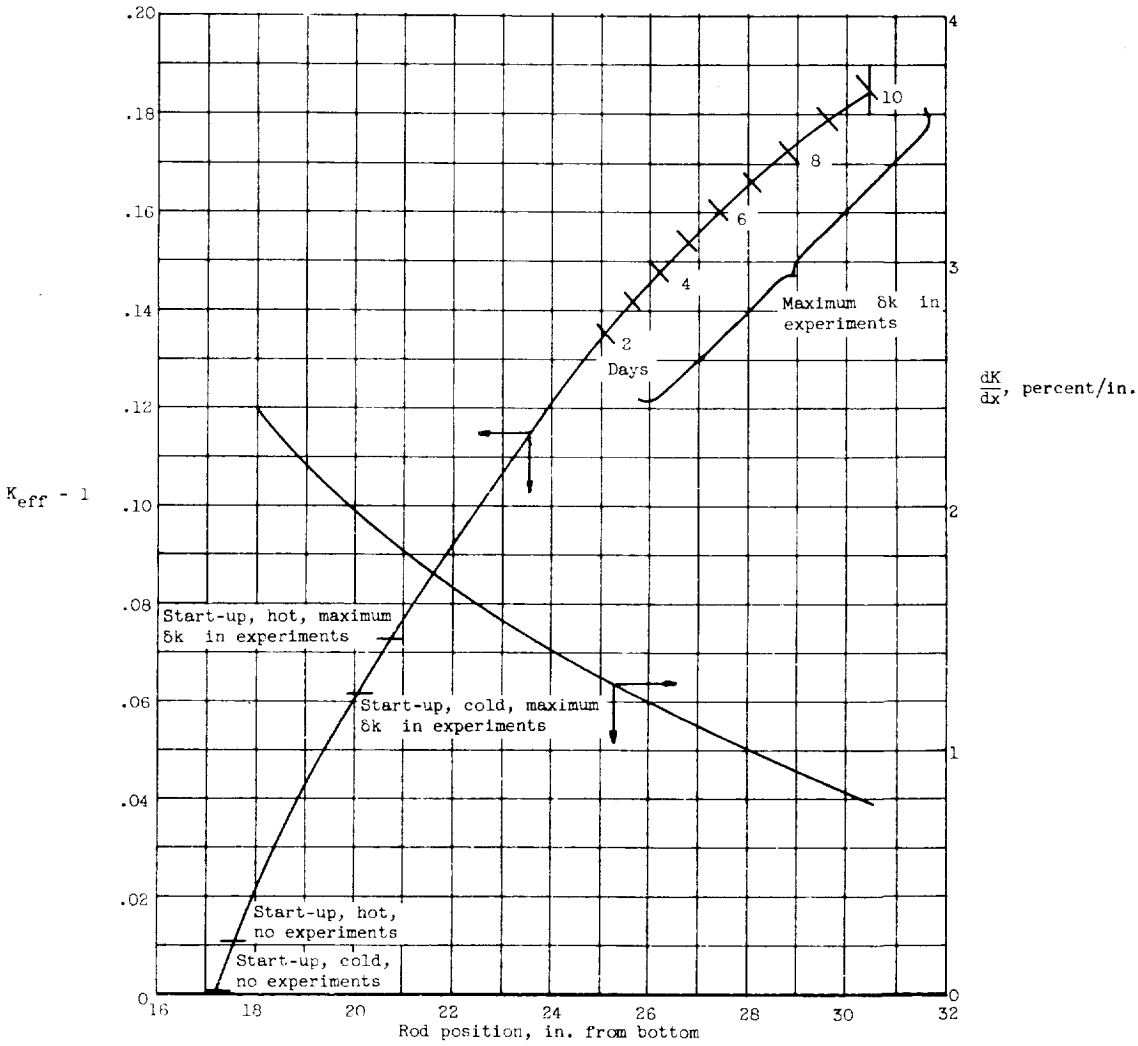

Figure 5. - Rod calibration - used in analysis of restart times.

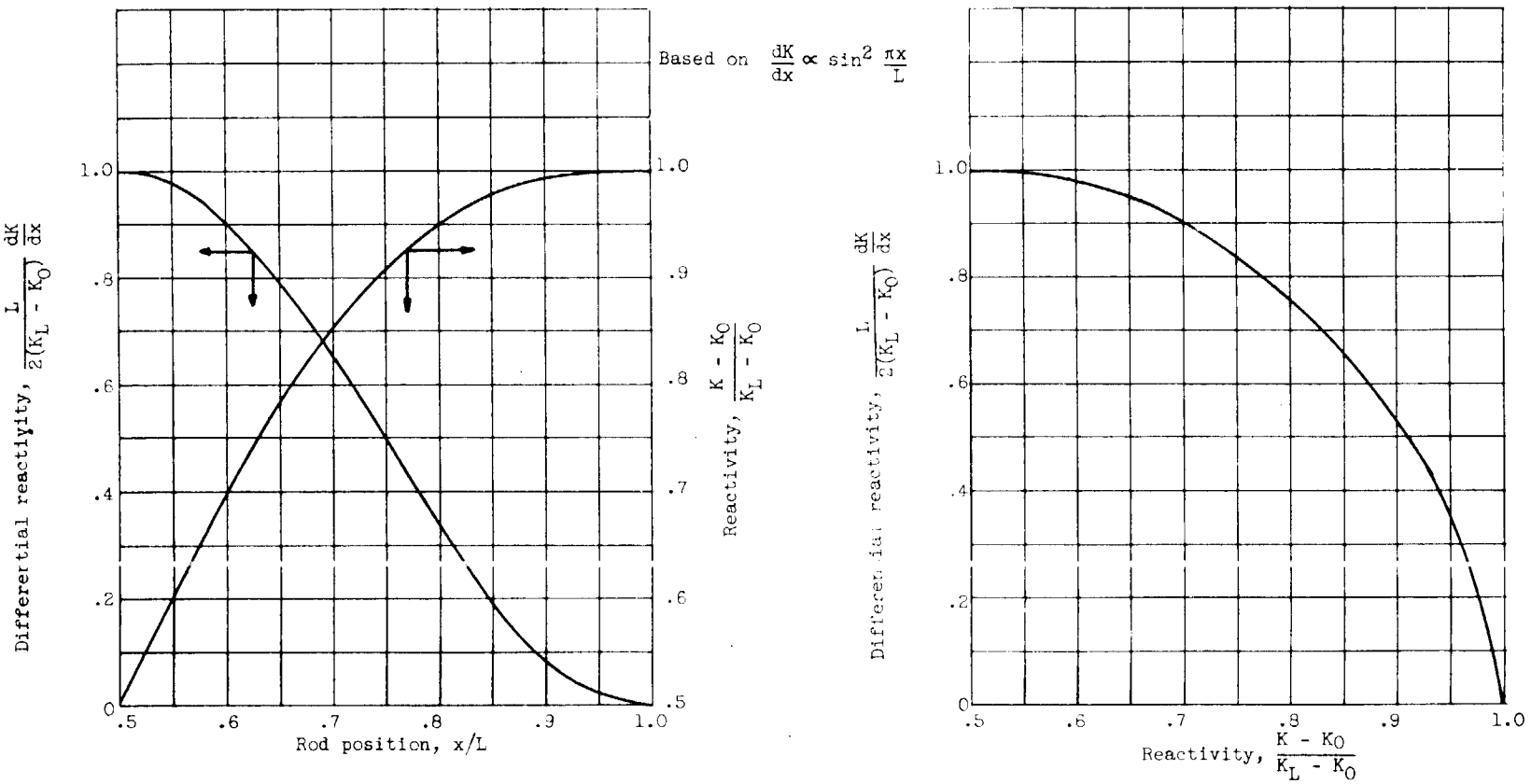

Figure 6. - Idealized rod calibration - for reference use.

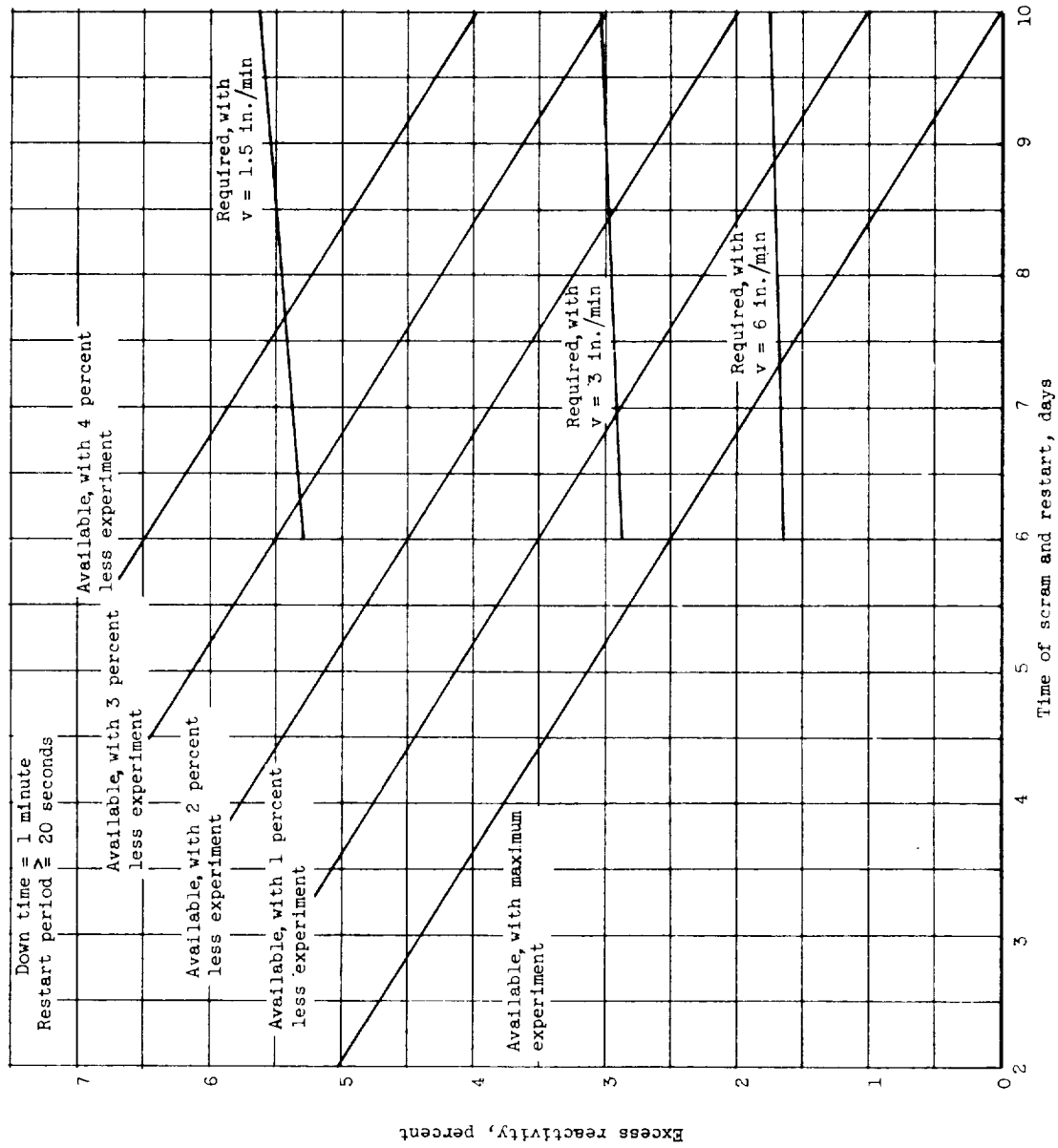

Figure 7. - Excess reactivity required for a one minute down time after a shutdown.

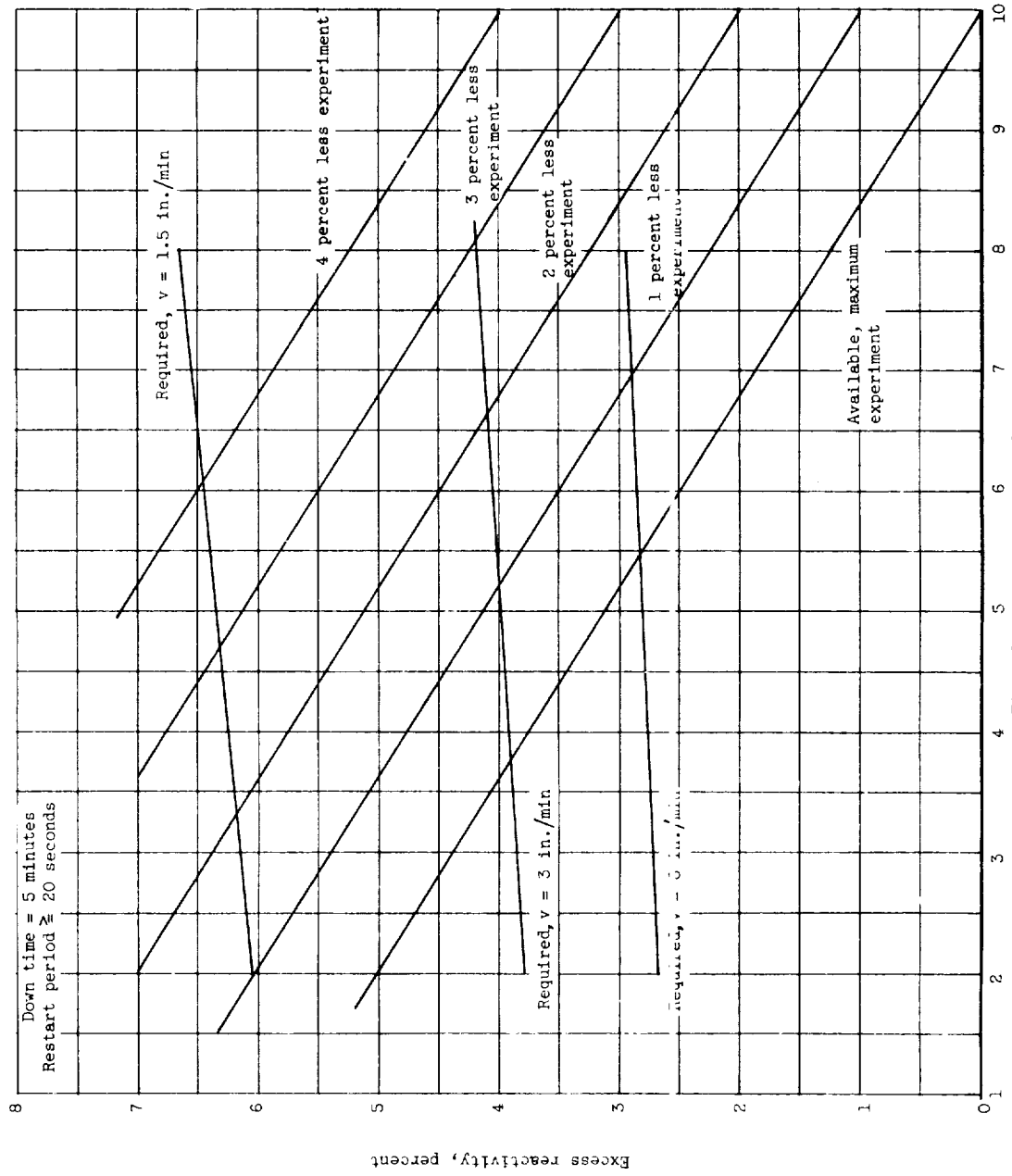

Figure 8. - Excess reactivity required for a five minute down time after a shutdown.

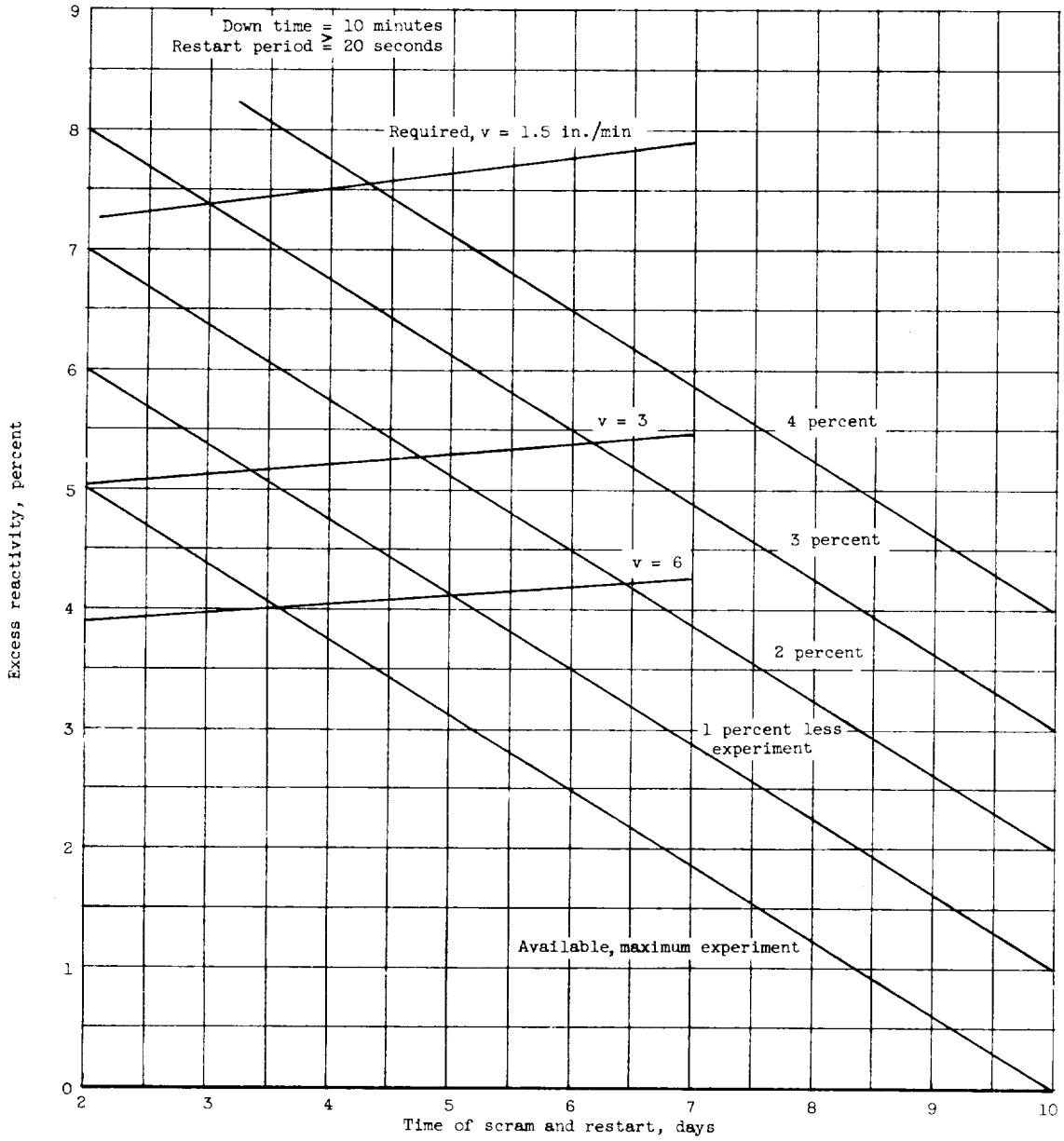

Figure 9. - Excess reactivity required for a ten minute down time after a shutdown.

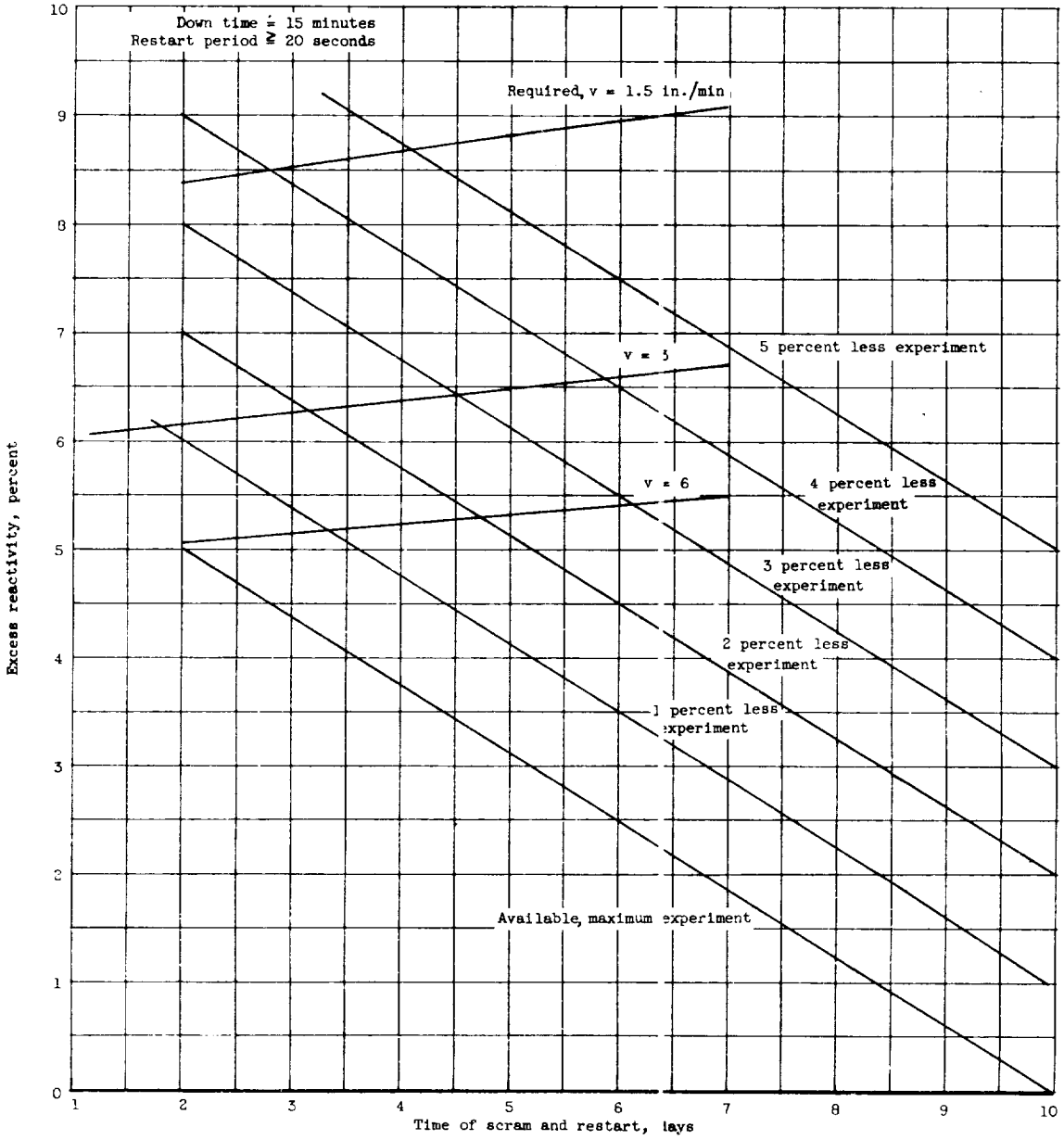

Figure 10. - Excess reactivity required for a fifteen minute down time after a shutdown.

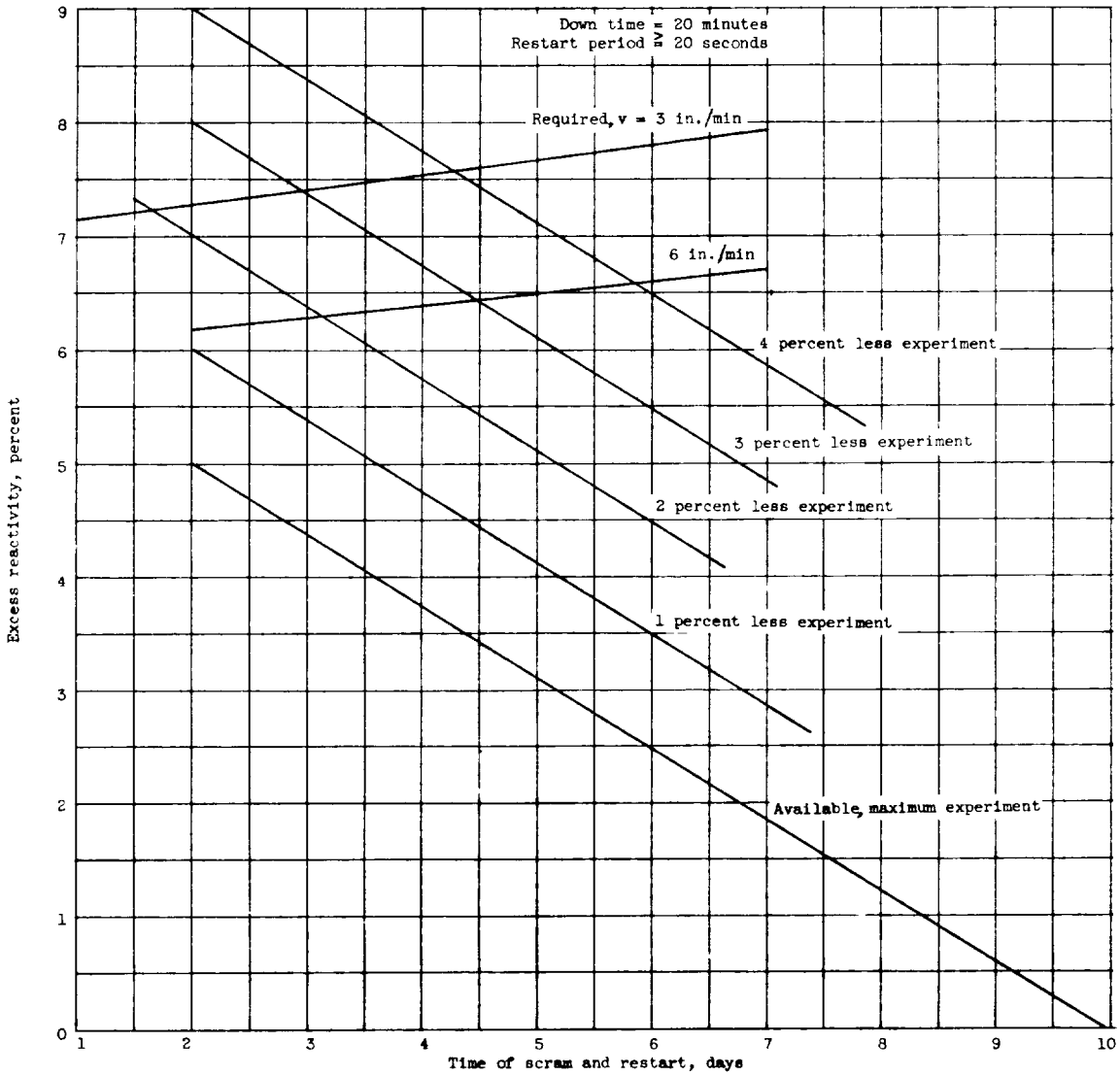

Figure 11. - Excess reactivity required for a twenty minute down time after a shutdown.

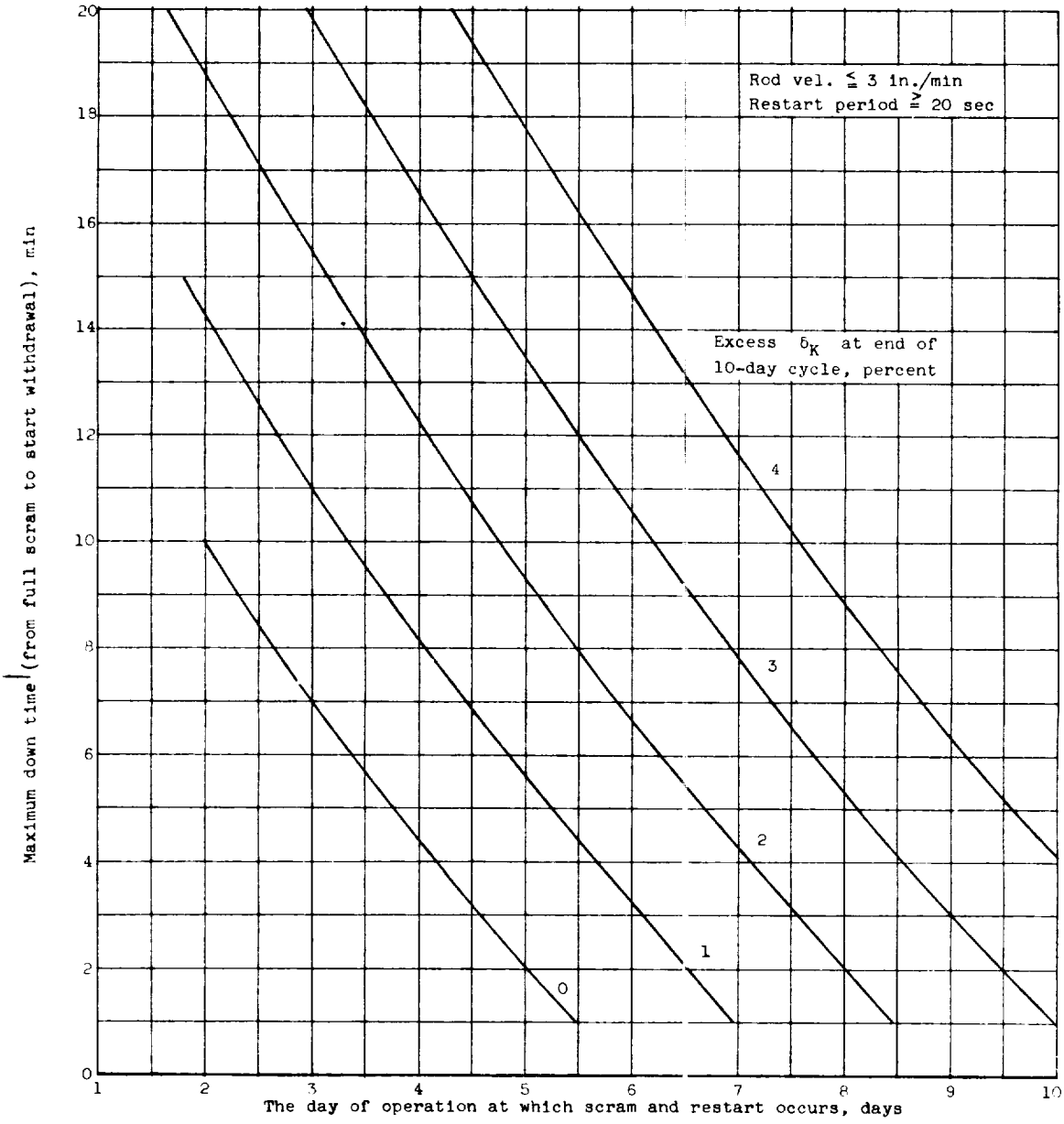

Figure 12. - Allowable times in which to restart after a recent shutdown.

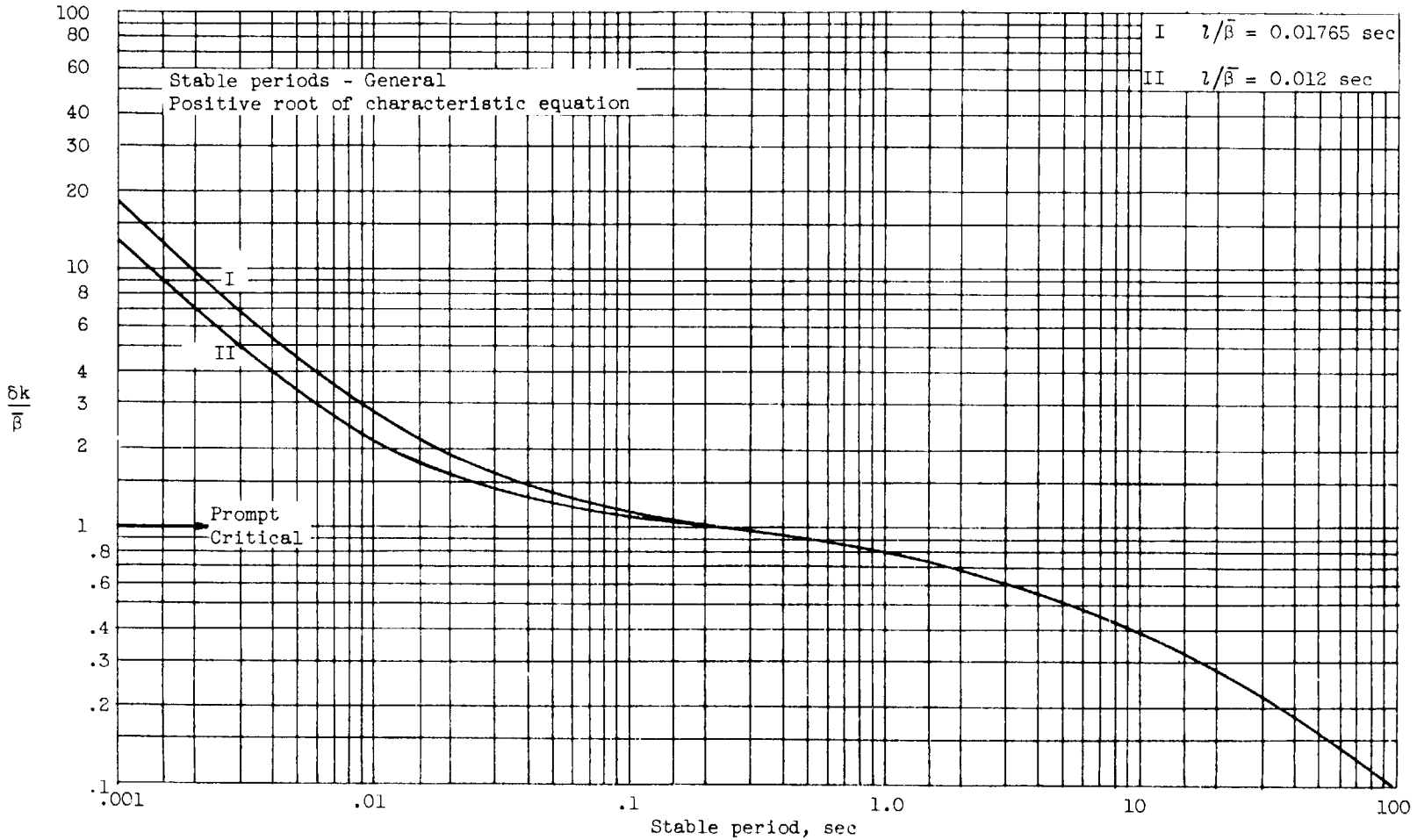

Figure 13. - Stable reactor periods.

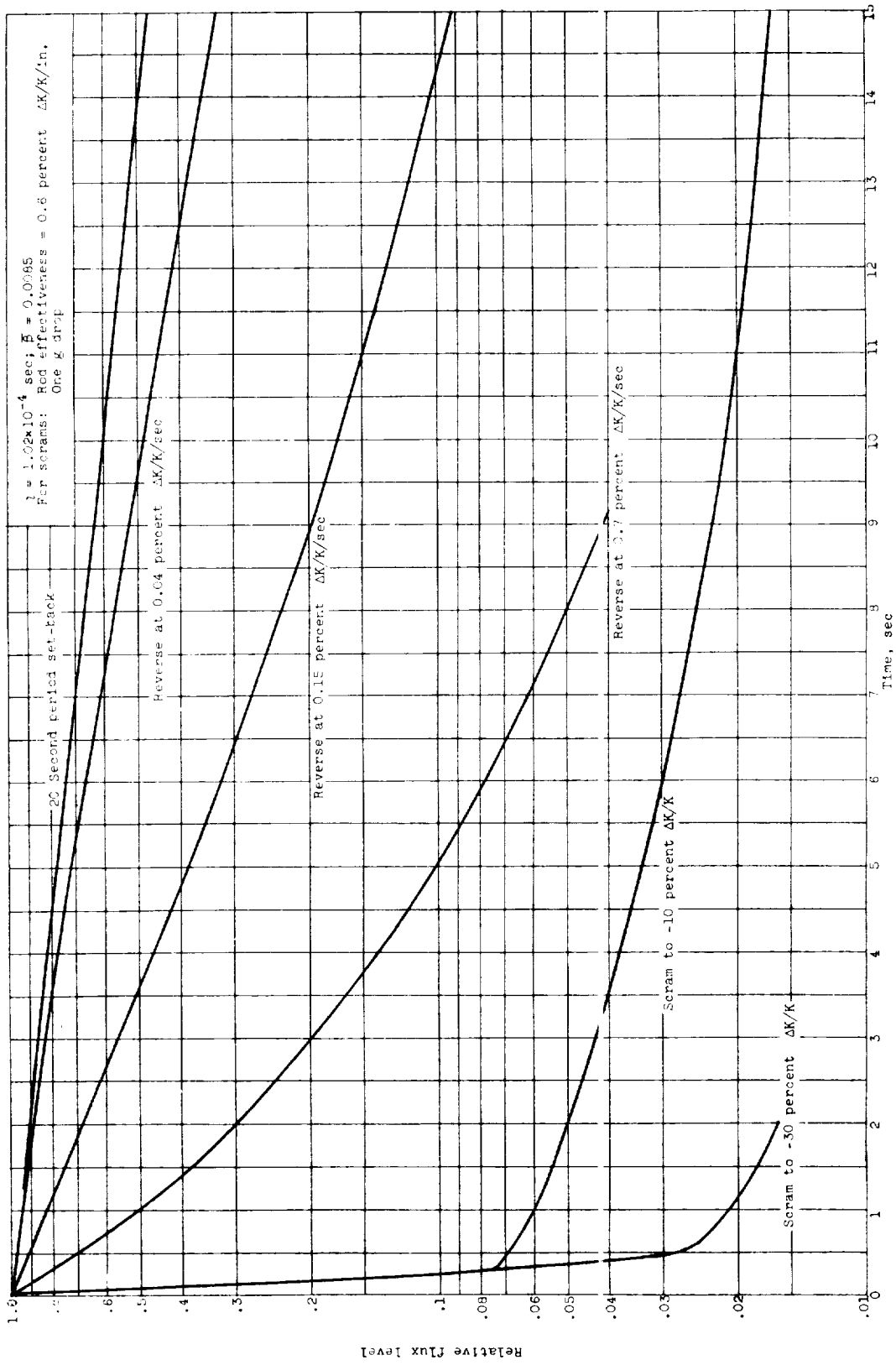

Figure 14. - Effect of cut-backs on flux level.

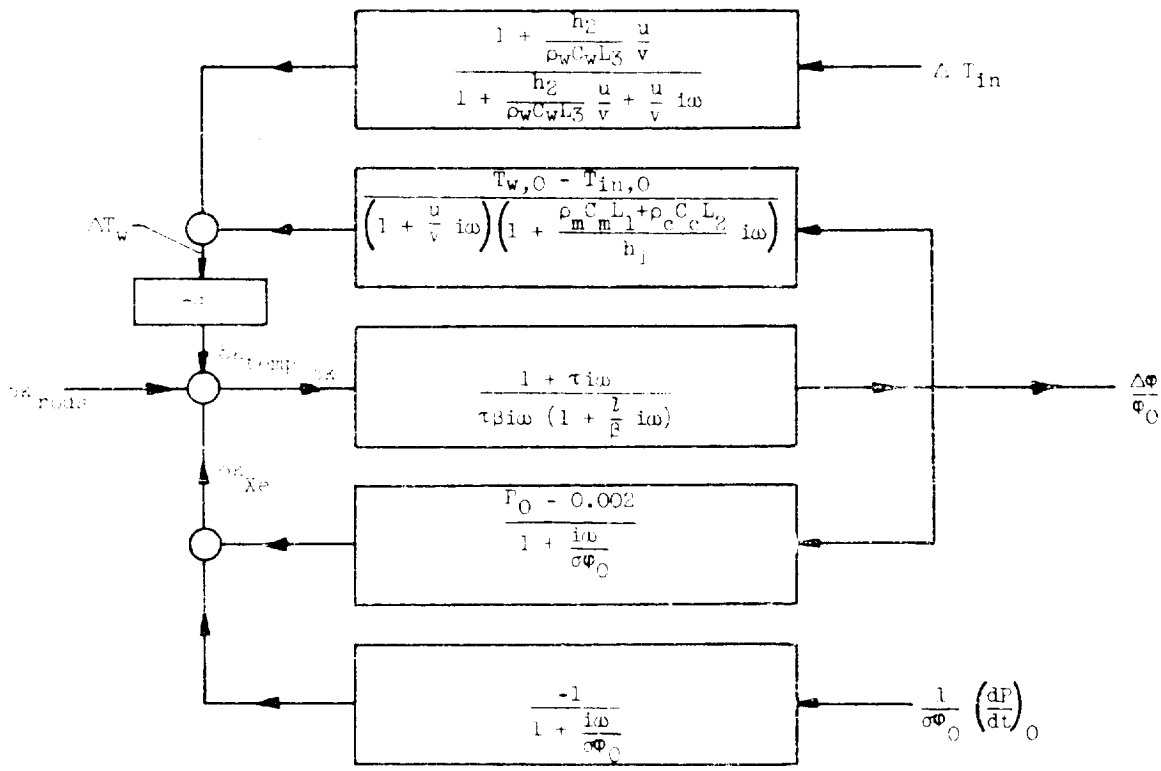

Figure 15. - Block diagram of simplified reactor kinetics with temperature and Xenon effects.

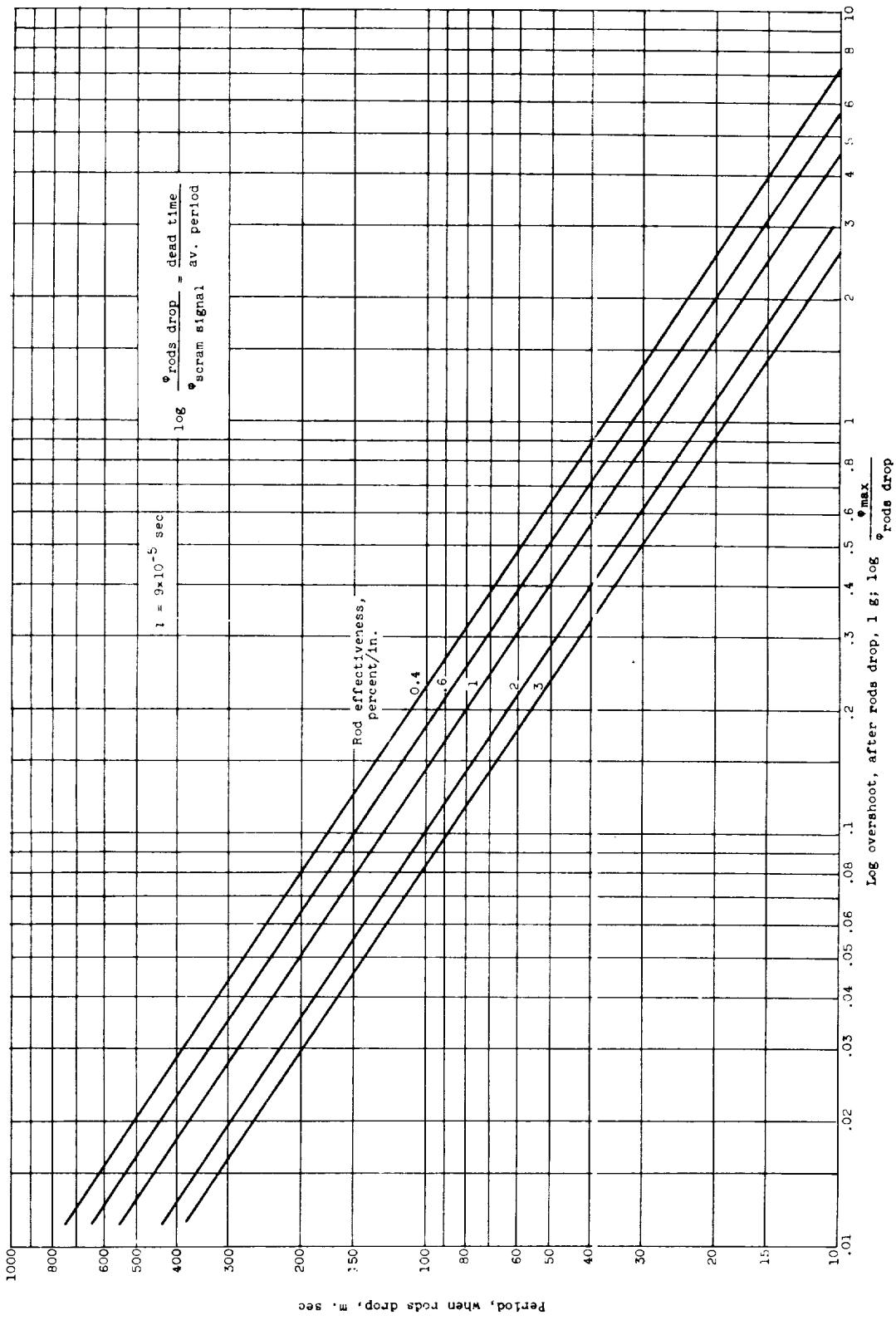

Figure 16. - Overshoot in power level during scram.

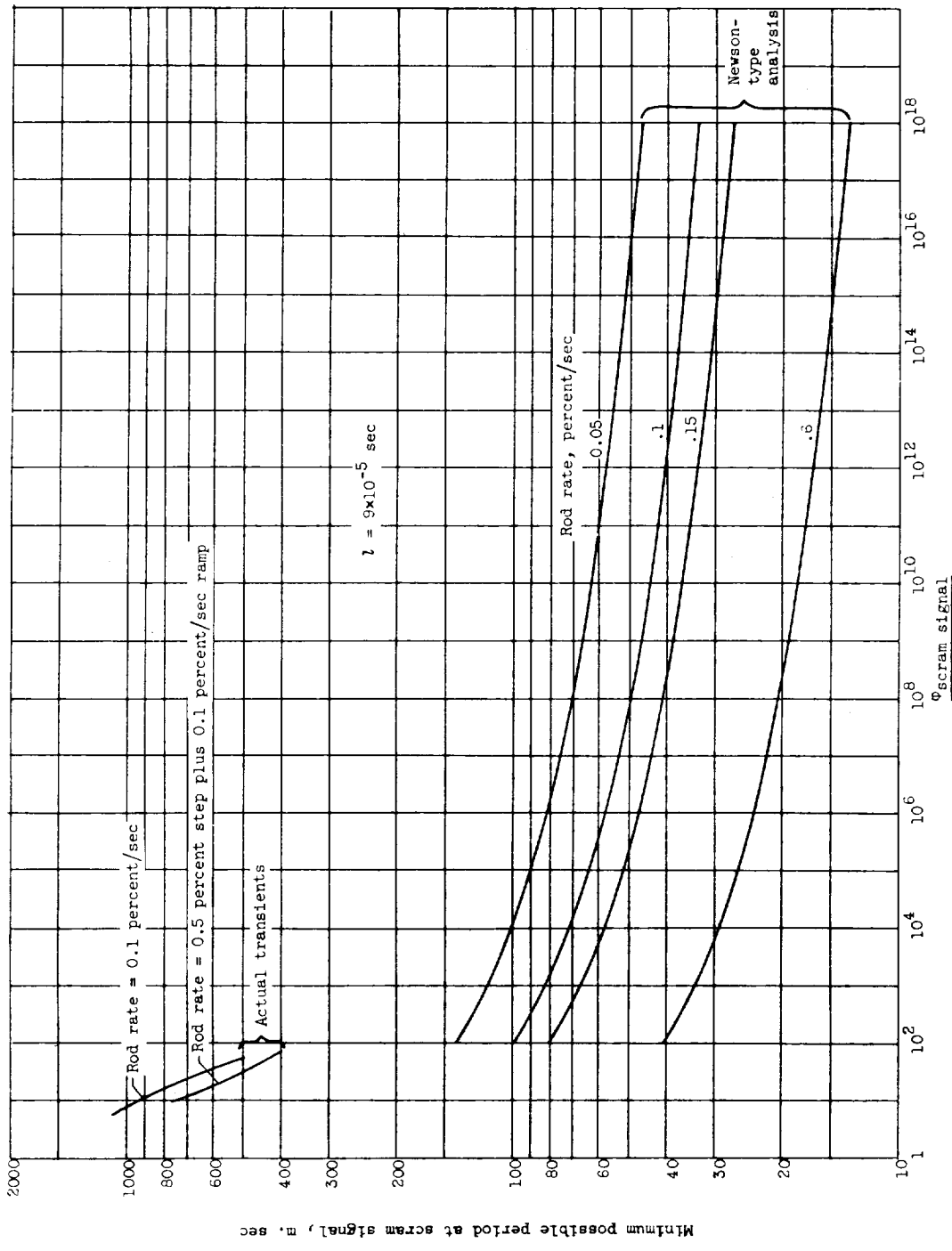

Figure 17. - Reactor periods at scram signal power levels during start-up accident.

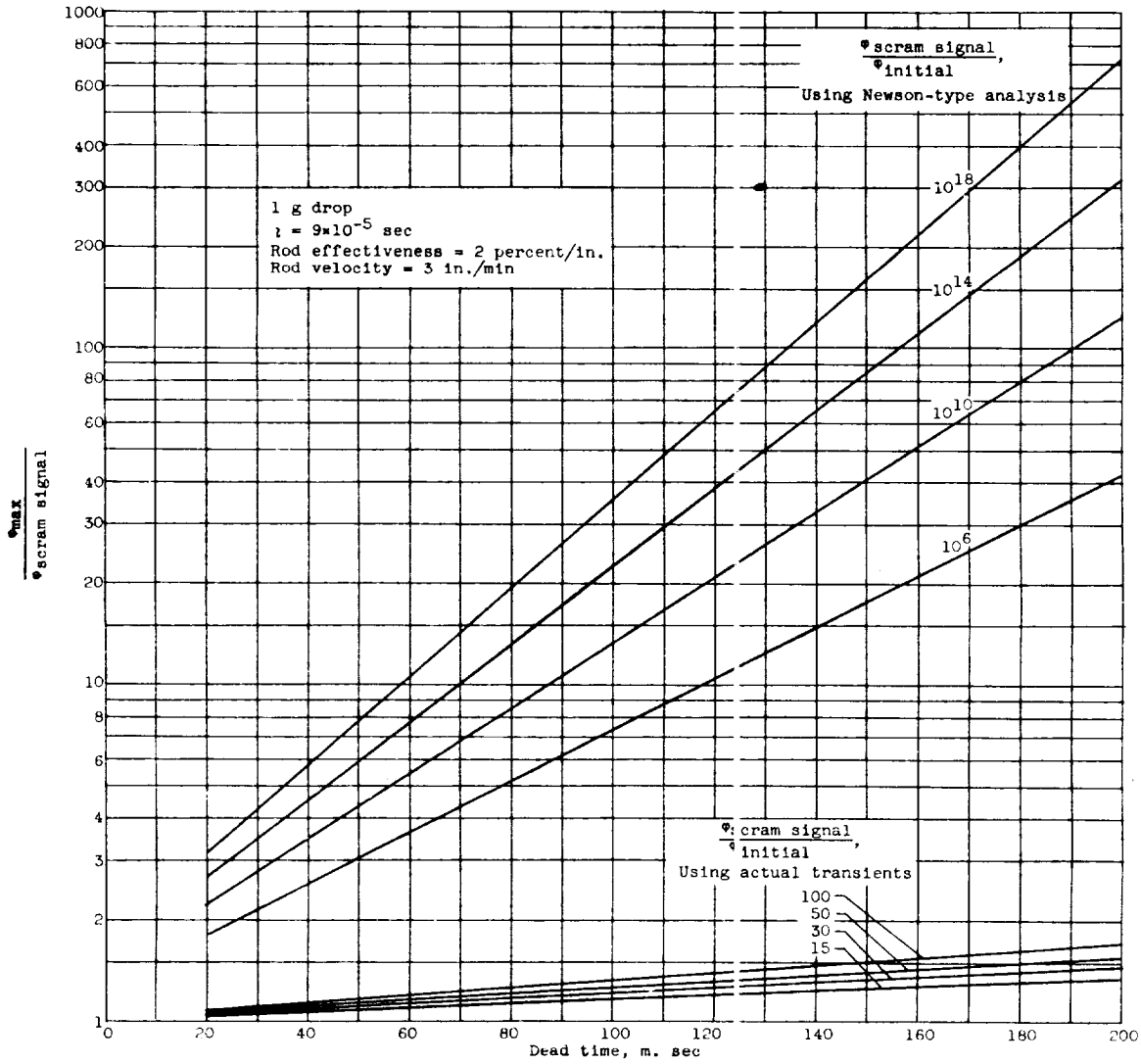

Figure 18. - Total overshoots above the scram signal power level for the start-up accident.

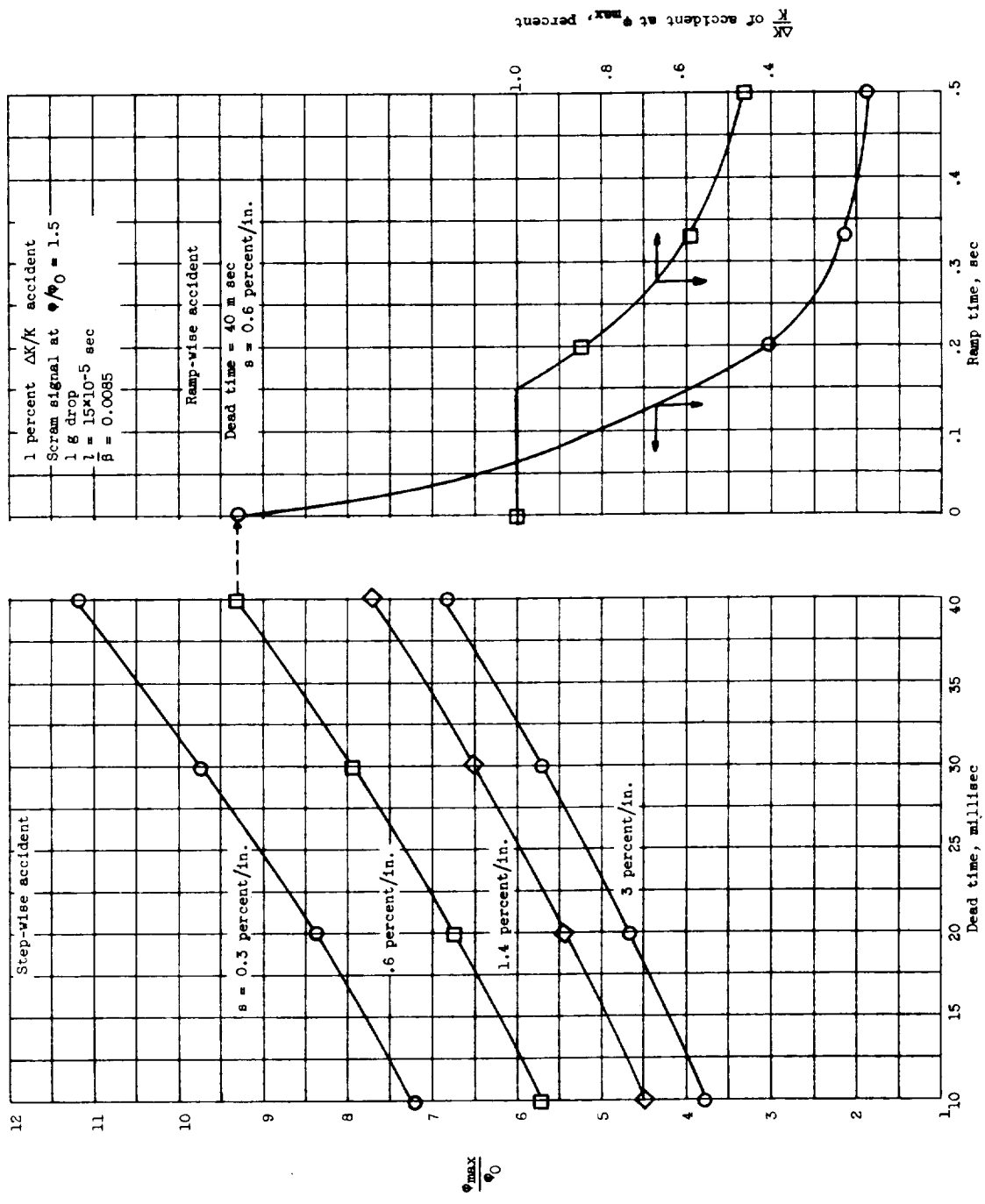

Figure 19. - Overshoots in power level for 1 percent ΔK/K accidents corrected by scrams.

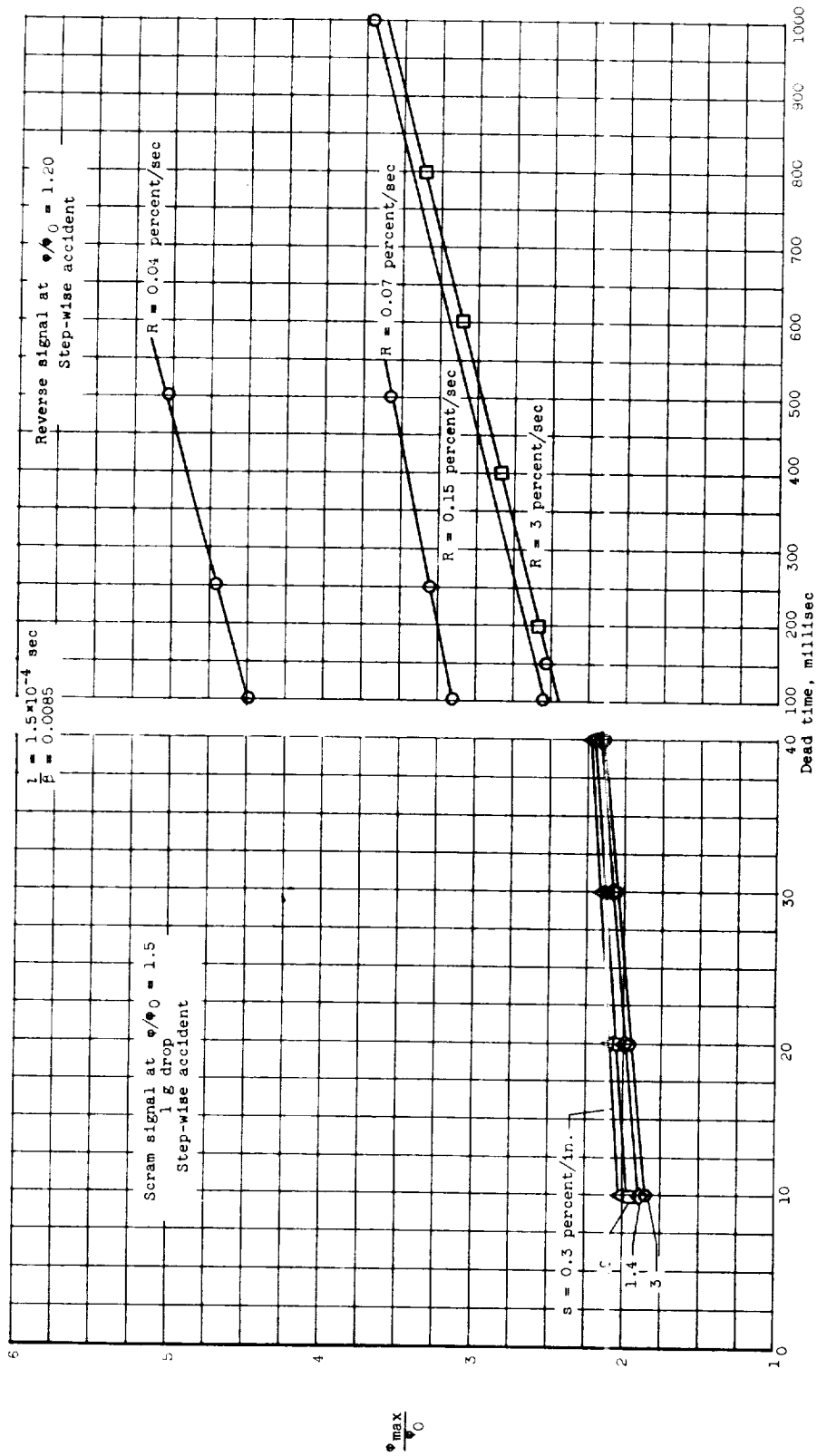

Figure 20. - Overshoots in power level for 0.5 percent ΔK/K accidents corrected by scrams and reverses.

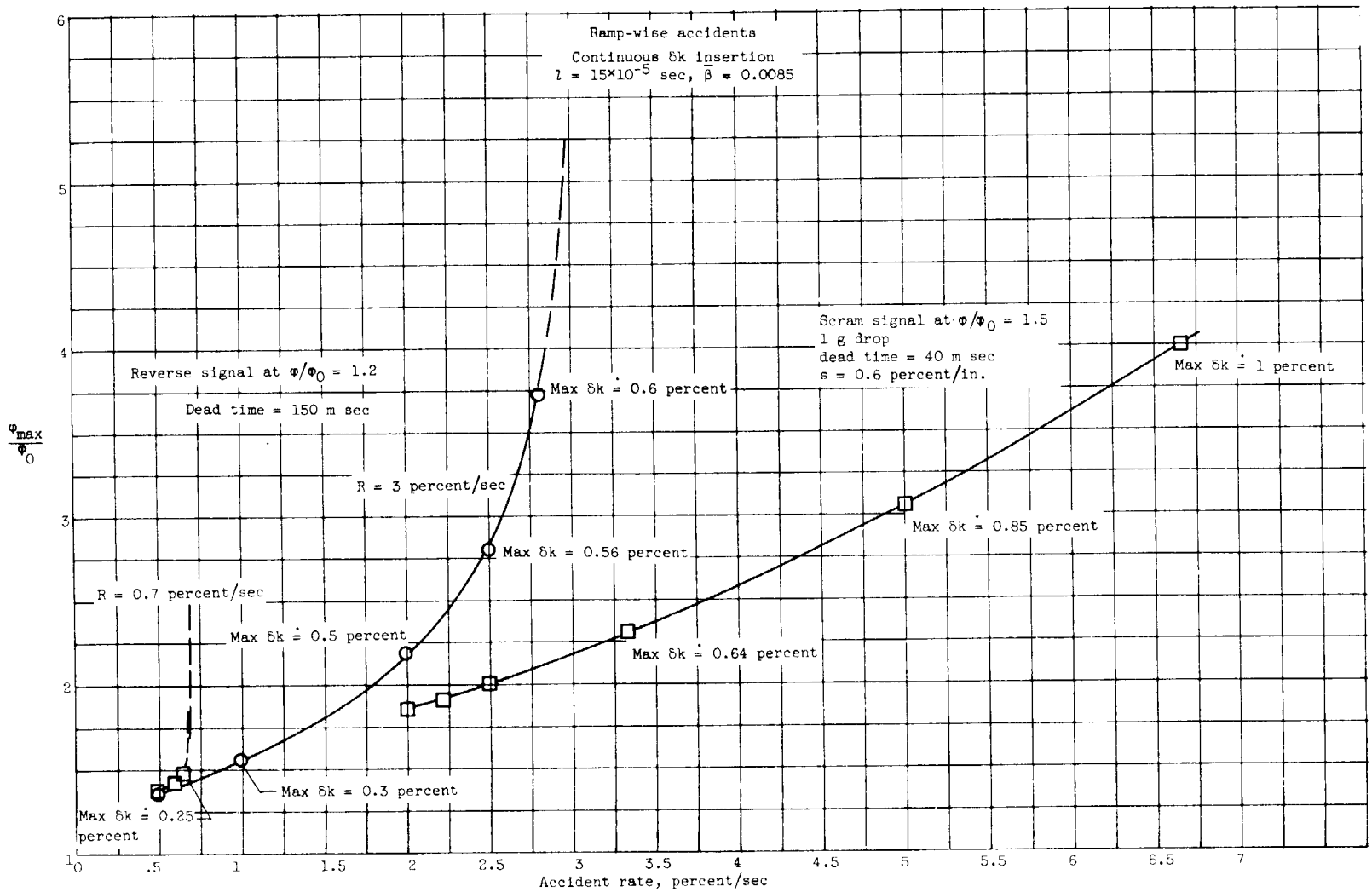

Figure 21. - Overshoots in power level for ramp-wise ΔK/K accidents corrected by scrams and reverses.

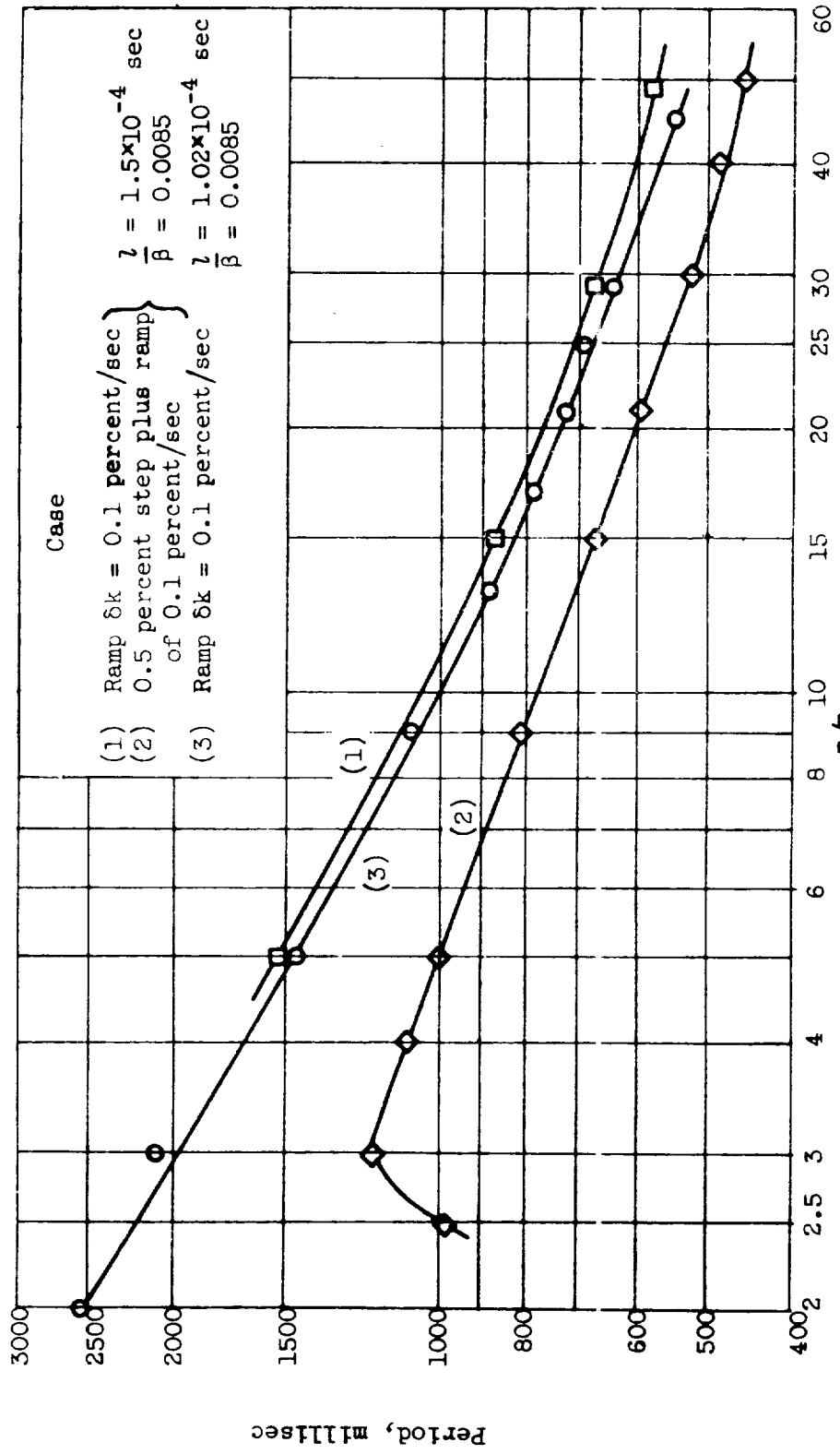

Figure 22. - Period against level for various rod motions for use in startup accident.

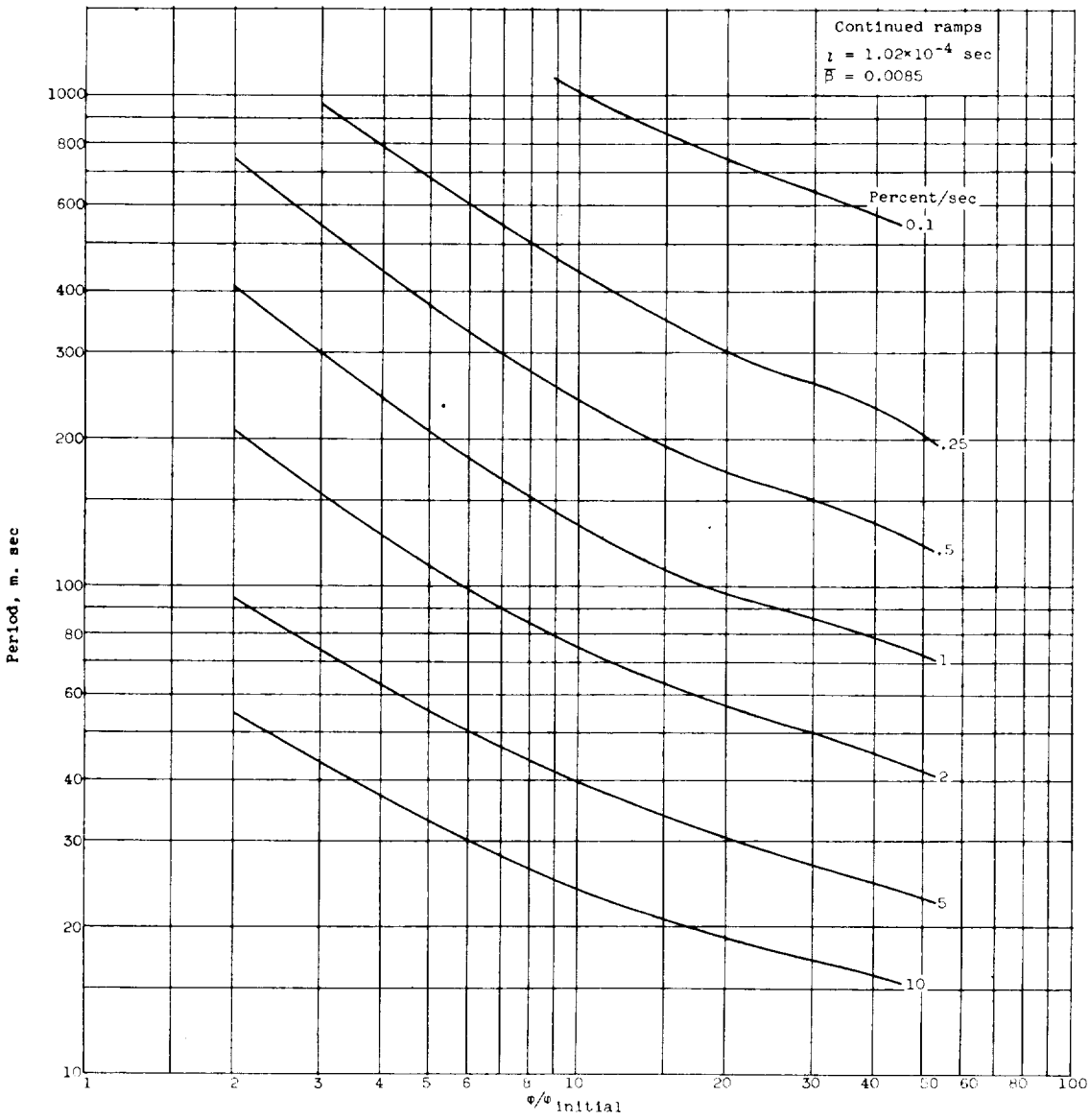

Figure 23. - Relation between reactor period and power level for continued insertion of reactivity at constant rates: ℓ = 1.02 10^{-4} sec.

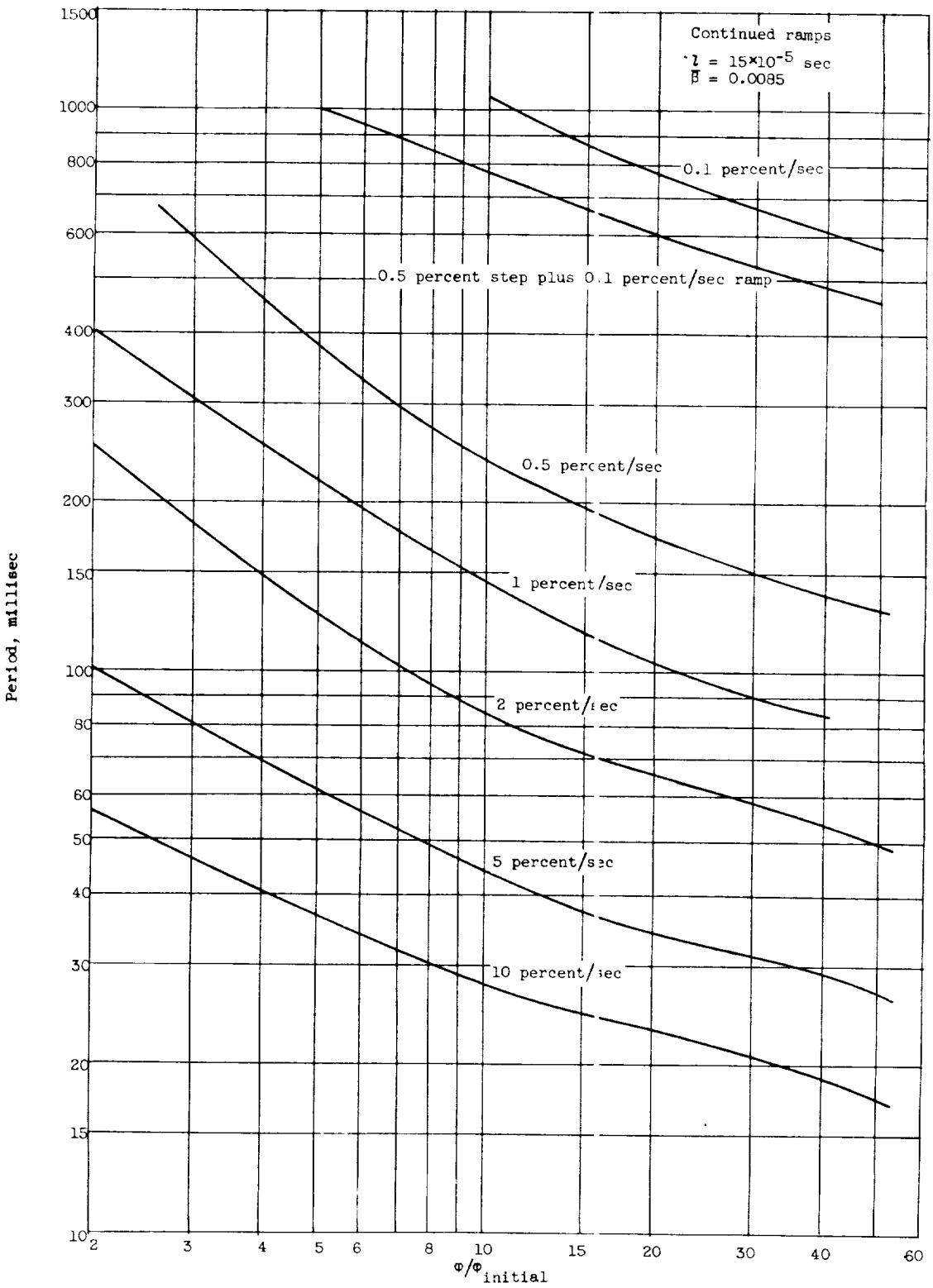

Figure 24. - Relation between reactor period and power level for continued insertion of reactivity at constant rates; $l = 1.5 \times 10^{-4}$ sec.

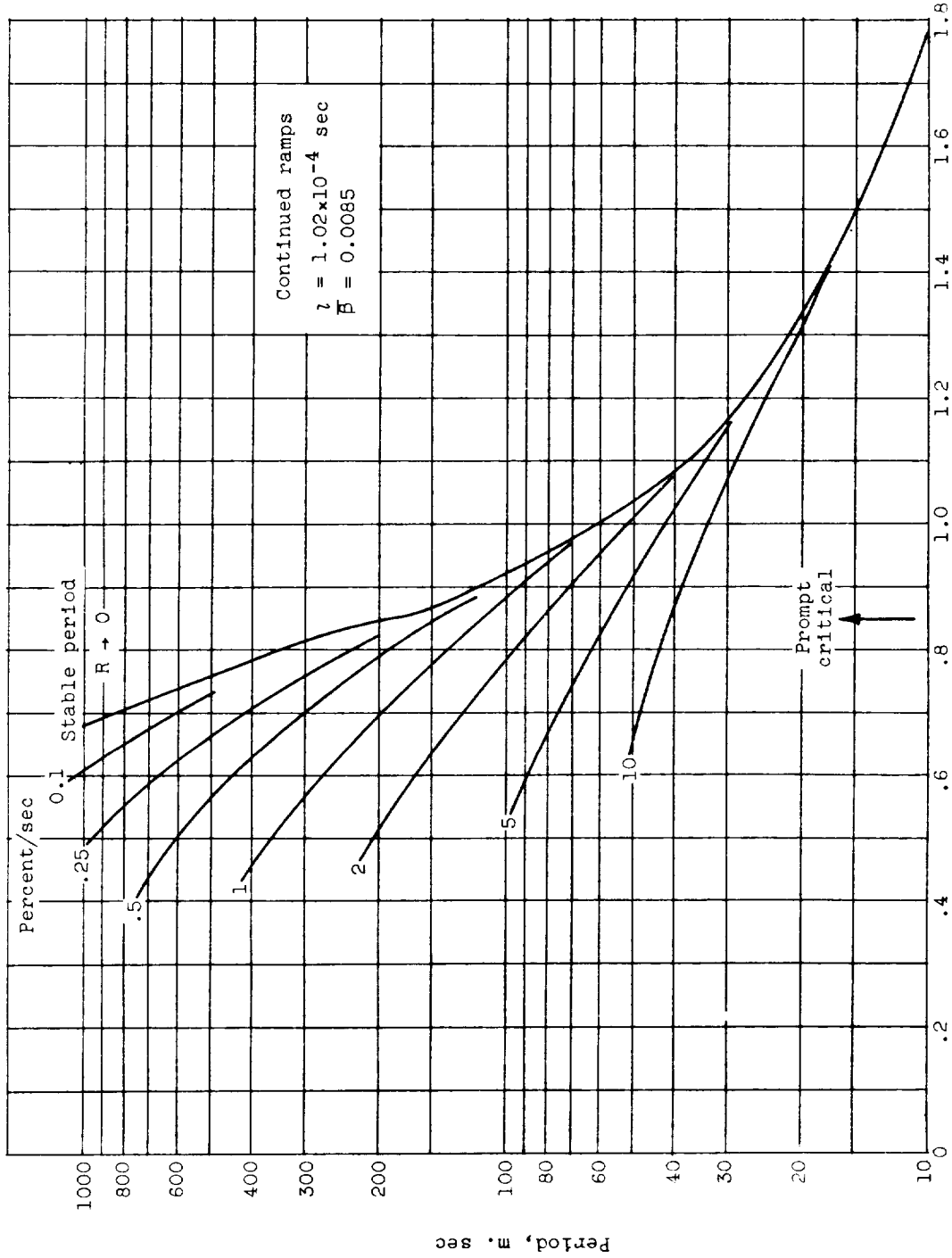

Figure 25. - Relation between reactor period and reactivity for continued insertion of reactivity at constant rates: $\ell = 1.02 \times 10^{-4}$ sec.

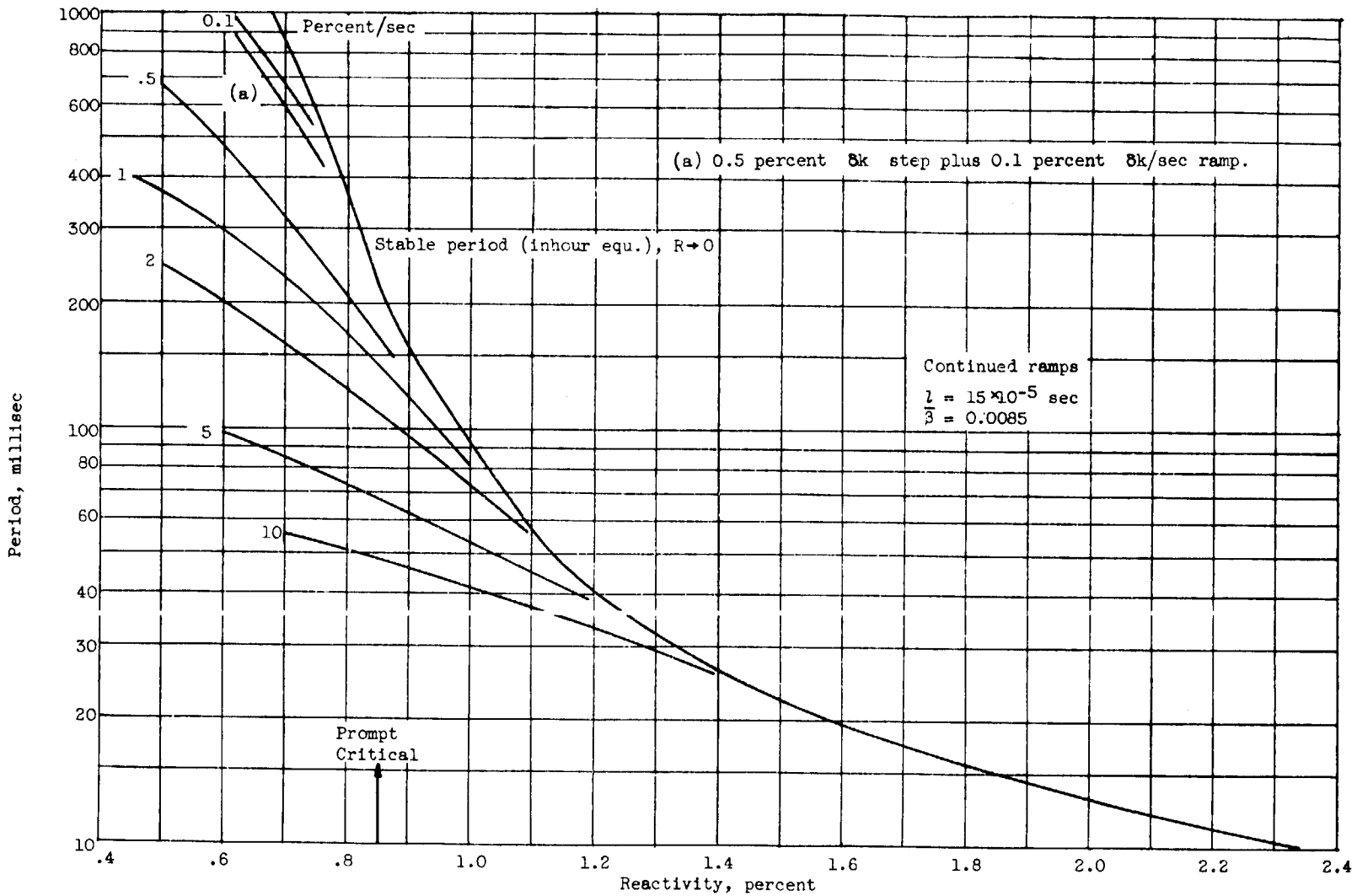

Figure 26. - Relation between reactor period and reactivity for continued insertion of reactivity at constant rates: $l = 1.5 \times 10^{-4}$ sec.

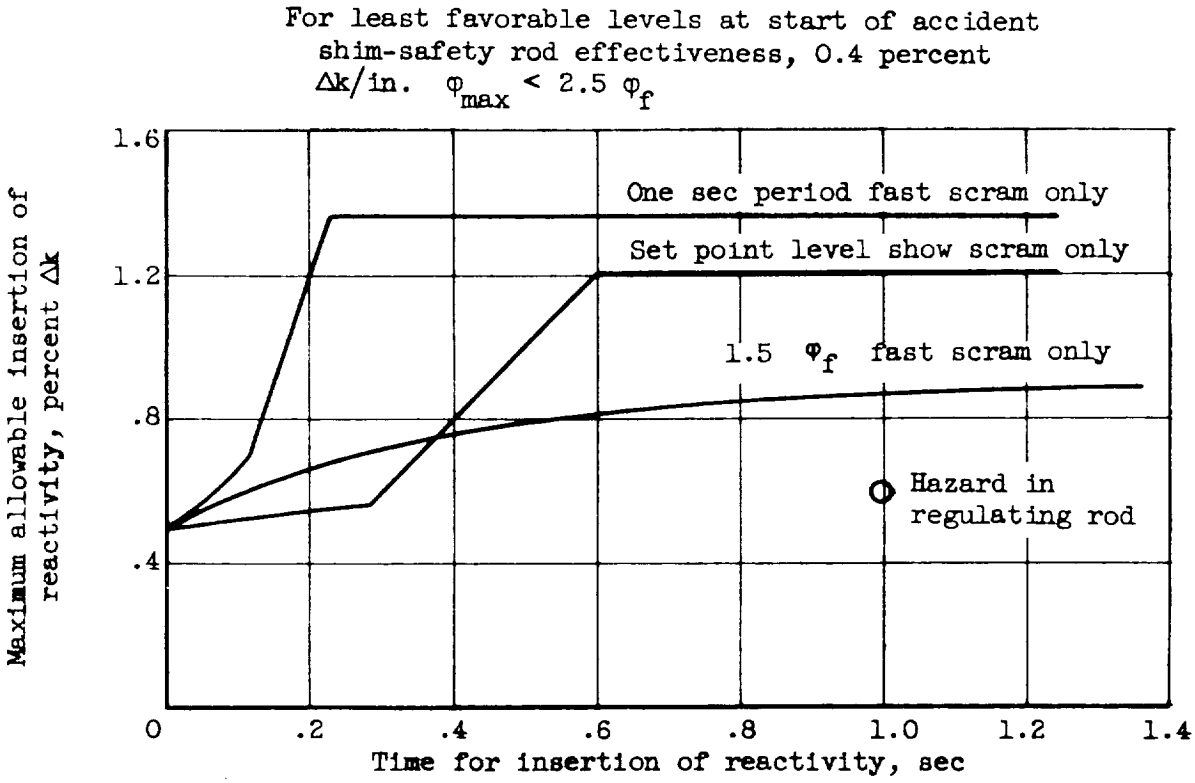

Figure 27. - Controllable accidential insertions of reactivity.

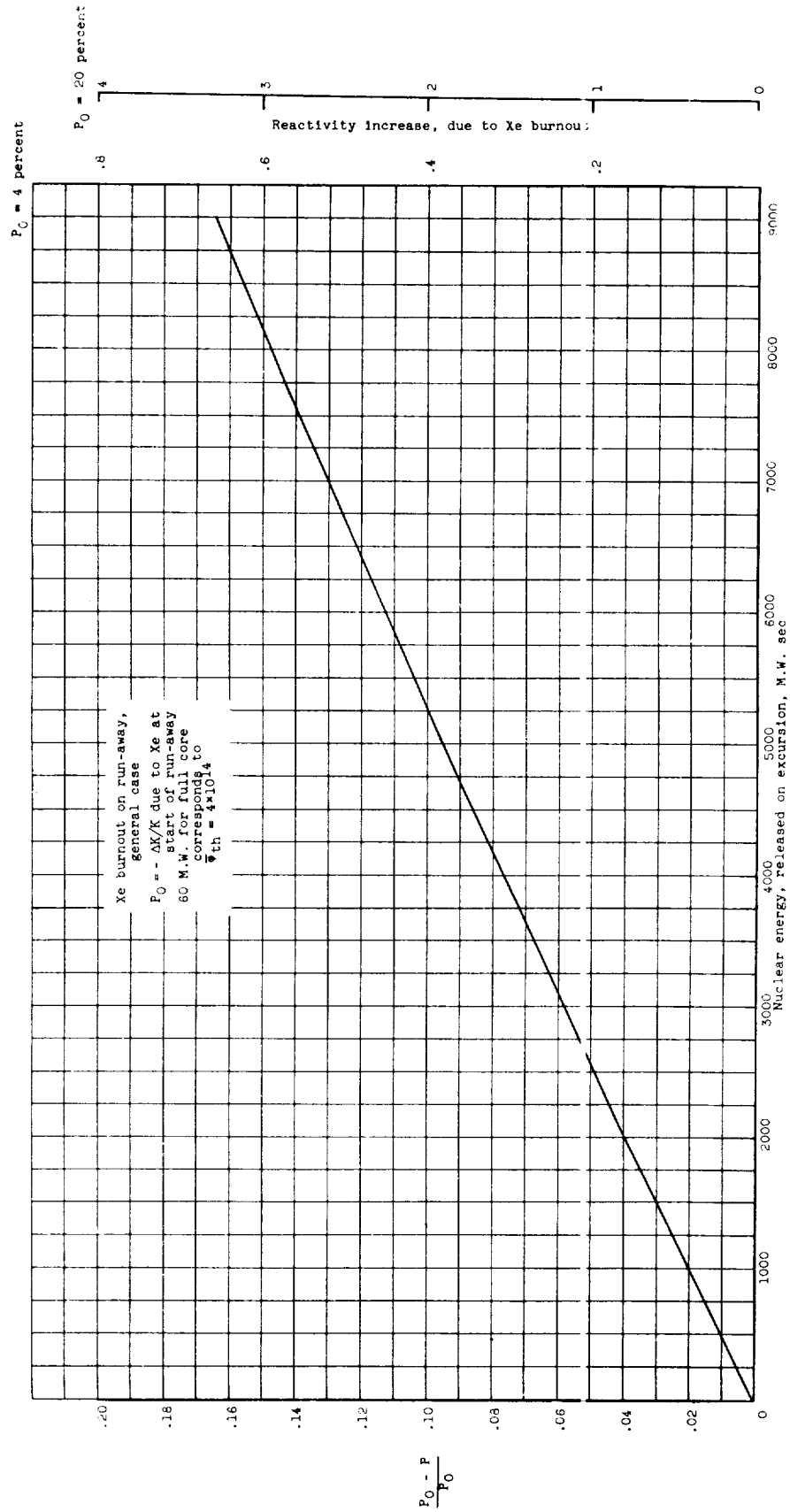

Figure 28. - Xe burnout on nuclear excursion, general case.

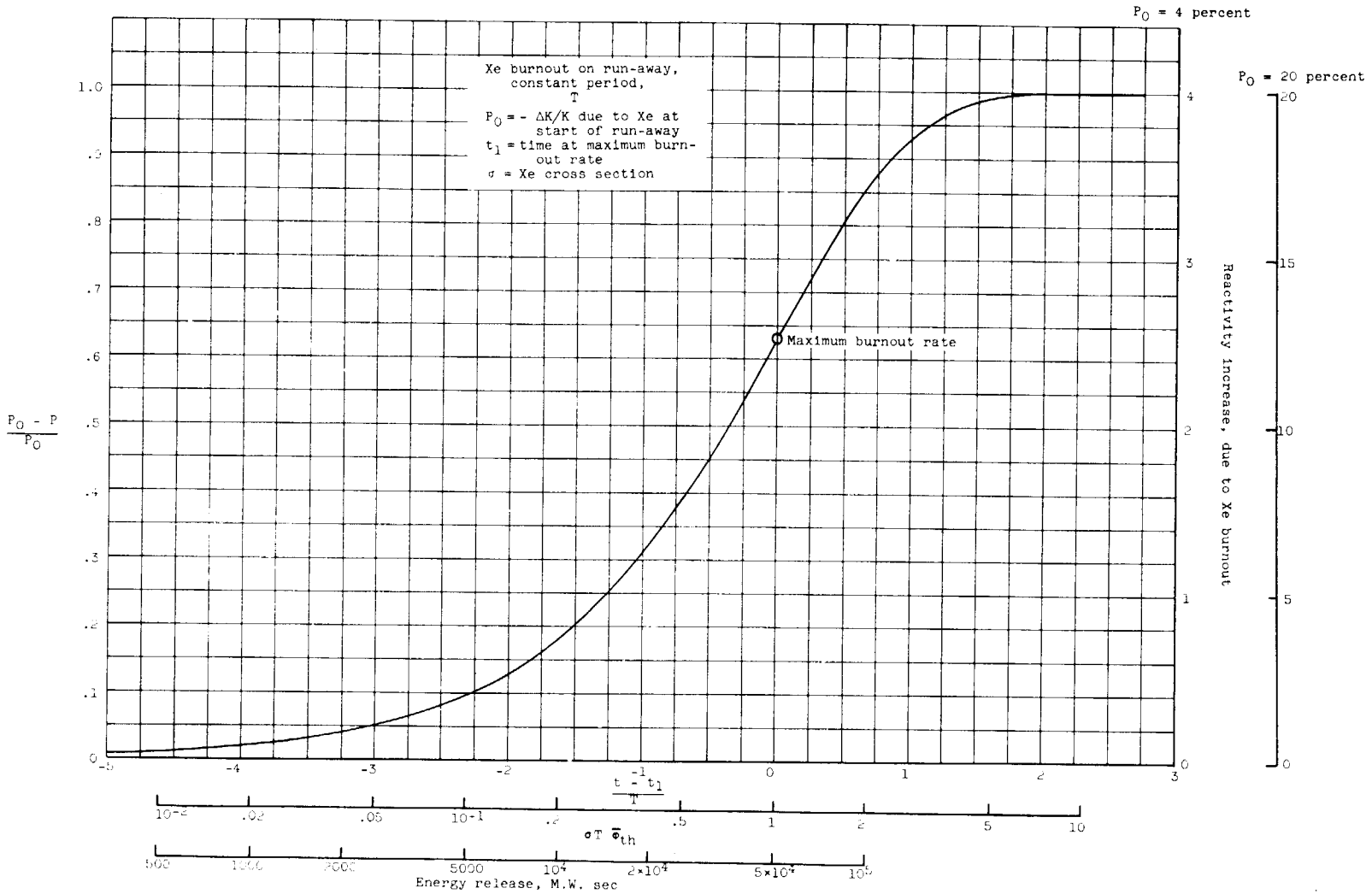

Figure 29. - Xe burnout on constant period nuclear excursion.

II. FINAL REPORT OF NATIONAL ADVISORY COMMITTEE FOR AERONAUTICS REACTOR SAFETY PROGRAM*

By S. Hoenig, E. Saleme, and F. B. Porzel

June 30, 1956

I. INTRODUCTION

This analysis was done in response to a request by the National Advisory Committee for Aeronautics for a safety analysis on a proposed nuclear reactor facility, to be constructed at Plum Brook Ordnance Works, Ohio. The major requirement was that the gas-tight shell must remain integral under an internal explosion without compromising the value of the reactor as a research tool.

The purpose of this study is to design the containment structure of the reactor so it remains integral and gas-tight under the explosion of 400 pounds of TNT (equivalent) at the center of the reactor.

Major recommendations were made to NACA for increasing the thickness of the reactor floor and the 70-foot wall. With these changes and other detailed modifications worked out in joint meetings between F. B. Porzel and S. A. Hoening of Armour Research Foundation, and J. Turk and S. Maslin of NACA, the reactor was adjudged reasonably safe.

Details of the analysis and drawings of the final design configuration are in the analysis section of the report. Section D, added at the request of NACA, gives approximate safety factors for the final design.

It must be recognized that in any design the actual safety can only be ascertained within certain limits. In any complex engineering structure there are possible sequences of design and construction modifications which could lead to unexpected failure. The attempt to completely analyze and prevent such failures would result in a delay of years and perhaps in impossible designs. In the authors' opinion the reactor is safe on the basis of the best reasonable analysis that can, at the present, be made.

In the analysis, 400 pounds of TNT was assumed to explode at a location on the centerline of the reactor, ten feet from the bottom. The effects of base surge, the shock wave, and final gas pressure on the top, bottom, and sides of the gas-tight shell were taken into account. The energy required to crush concrete and the equation of state for solids like concrete is developed in some detail.

---

*This report is reproduced herein as originally published by the Armour Research Foundation, Illinois Institute of Technology, with no changes.

II. ANALYSIS

A. Basic Formulas

Explosive energy, equivalent to 400 pounds of TNT, was assumed to have been released instantaneously in the reactor tank ten feet from the bottom. The explosive pressures in water were calculated from a widely-used equation given in Cole's "Underwater Explosions"[1] where

$$P = 2.16 \times 10^4 \left(\frac{W^{1/3}}{R}\right)^{1.13} \qquad (1)$$

P = peak pressure, psi

W = weight of charge, pounds of TNT

R = distance, feet

The other state variables behind the shock may be obtained from the solution of the continuity and momentum conservation laws as

$$U^2 = \frac{P_1 - P_o}{V_o - V_1} V_o^2 \qquad (2)$$

$$u^2 = (P_1 - P_o)(V_o - V_1) \qquad (3)$$

where

u = flow velocity behind shock wave, ft/sec

U = shock velocity, ft/sec

P_o = pressure ahead of shock wave, psf

P_1 = pressure behind shock wave, psf

V_o = specific volume ahead of shock wave, $\frac{ft^4}{lb \cdot sec^2}$

V_1 = specific volume behind shock wave, $\frac{ft^4}{lb\ sec^2}$

The general adiabat for liquids and solids was assumed to have the form (See Allis & Herlin

---

(1) R. H. Cole, Underwater Explosions, Princeton University Press, Princeton, New Jersey, 1948

(2) W. Allis & M. Herlin, Thermodynamics and Physics of Matter, McGraw Hill, Inc., New York, 1952

$$(a + bP)^{1/b} \; V = C \text{ (constant)} \qquad (4)$$

for water $a \cong 21{,}000$ for P in bars

$b \cong 7$

If the shock wave is reflected from a wall, the pressures behind it are obtained from

$$\left(\frac{P_2}{P_1} - 1\right)\left(1 - \frac{V_2}{V_1}\right) = \left(1 - \frac{P_o}{P_1}\right)\left(\frac{V_o}{V_1} - 1\right) \qquad (5)$$

P_2 = pressure behind reflected shock wave, psf

V_2 = specific volume behind reflected shock wave, $\frac{ft^4}{lb\text{-}sec^2}$

Now $P_1 >>> P_o$ for the cases under study and the right-hand side of the equation becomes $\approx \left(\frac{V_o}{V_1} - 1\right)$. The equation is then solved by an iteration procedure.

B. Bottom of Tank

The shock wave proceeding downward reflects at the bottom of the tank and the reflected pressures are about 30,000 psi. At this pressure the plug fails immediately and the crushed fragments are set into motion by the shock wave.

To obtain the flow velocity behind the shock wave in the concrete, we can write the equation of state for concrete, just as we did for water, as

$$(a + bP)^{1/b} \; V = C \quad \text{(Eq. 4)}$$

and dividing by $(a + bP_o)^{1/b} \; V_o = C$

$$\left(\frac{a + bP}{a + bP_o}\right)^{1/b} \frac{V}{V_o} = 1 \qquad \left(\frac{a + bP}{a + bP_o}\right)^{1/b} = \frac{V_o}{V}$$

$$\left(\frac{1 + \frac{b}{a} P_1}{1 + \frac{b}{a} P_o}\right)^{\frac{1}{b}} = \frac{V_o}{V} \qquad \frac{b}{a} P_o \approx o$$

leads to $$(1 + \frac{b}{a} P_1)^{1/b} = \frac{V_o}{V}$$

Expanding by the binomial theorem gives

$$1 + \frac{1}{b}\frac{b}{a} P_1 + \ldots = \frac{V_o}{V} \text{ or } \frac{P_1}{a} = \frac{V_o}{V} - 1 = \frac{V_o - V}{V}$$

Now $V \approx V_o$, so we replace V by V_o in the denominator, and obtain

$$\frac{P}{a} = \frac{V_o - V}{V_o} \qquad (6)$$

Previously we wrote that

$$u^2 = (P_1 - P_o)(V_o - V_1) \qquad \text{(Eq. 3)}$$

then by substitution from Eq. 6 we obtain for this case

$$u^2 = (P_1 - P_o)\frac{P_1 V_o}{a} \qquad (7)$$

$$u^2 = (P_1 - P_o)\frac{P_1 V_o}{a} \approx \frac{P_1^2 V_o}{a} \qquad (7a)$$

Differentiating Eq. 6 gives the result

$$\frac{1}{a} dP = -\frac{dV}{V_o} \qquad \frac{dP}{dV} = -\frac{a}{V_o}$$

Now $c^2 = \frac{dP}{d\rho}$ where c = speed of sound in concrete = 13,000 ft/sec

$$\rho = \frac{1}{V} \qquad d\rho = -\frac{1}{V^2} dV$$

$$c^2 = -V^2 \frac{dP}{dV} \text{ or } \frac{dP}{dV} = -\frac{c^2}{V^2} \approx -\frac{c^2}{V_o^2}$$

Then by substitution,

$$-\frac{a}{V_o} = -\frac{c^2}{V_o^2} \qquad V_o = \frac{c^2}{a}$$

and by substitution in Eq. 7a gives

$$u^2 = \frac{P_1^2 c^2}{a^2} \qquad u = P_1 \frac{c}{a}$$

$$u = P_1 \frac{c}{a} \tag{8}$$

$a = 435{,}000$ for P in bars, for concrete

$c = 13{,}000$ ft/sec

The shock wave in the concrete raises the pressure to 30,000 psi = 2040 bars,

$$u = \frac{2040 \cdot 13{,}000}{4.35 \cdot 10^5} = \frac{20.4 \cdot 13}{4.35} = 61 \text{ ft/sec}$$

When the shock wave reaches the air interface at the bottom of the plug it reflects in the concrete as an expansion wave, and this wave doubles the material velocity. Thus, the three-foot thick plug should clear in about 30 milliseconds. This is much too late to afford substantial pressure relief to the top and sides of the tank.

C. Damage to Floor Adjacent to Tank

On the basis of the solid angle intercepted by the area adjacent to the tank, it readily follows that this region receives 7.5 per cent of the $1.8 \cdot 10^8$ calories generated by the explosion. This is $1.35 \cdot 10^7$ calories. However, this energy is not completely delivered to the concrete because much of it is degraded in the water to irreversible thermal energy by the shock wave.

Calculation of this loss has shown that under the conditions in the tank, only 6.6 per cent of the initial $1.35 \cdot 10^7$ calories is available for hydrodynamic work. The transfer of energy from water to concrete is a rather inefficient process due to the different characteristics of the material and therefore only 40 per cent of the useful energy in the water is given up to the concrete. The result of these losses, due to irreversibility and poor energy transfer, is that only $3.18 \cdot 10^5$ calories are available to crush concrete.

If we consider the shock wave as a piston, the rate of work per unit area in a shock is given by

$$\frac{dW}{dt} = Pu$$

The energy required to crush concrete is then given by:

$$W = \int P\ u\ dt \qquad (9)$$

dt can be written as $dt = \frac{dR}{U_s}$ then

$$W = \int P\ u\ \frac{dR}{U_s} \qquad (10)$$

where, using conservative and convenient approximations,

P = pressure required to crush concrete $\approx$ 3500 psi

u = flow velocity behind the shock wave $\approx$ 14 ft/sec

U_s = shock wave velocity in concrete $\approx$ 13,000 ft/sec

dR = linear distance parameter in feet

With these values,

$$W = \int_0^{1\ ft} \frac{3500\ \text{lb-sec}\ 144\ \text{in.}^2}{13{,}000\ \text{ft in.}^2} \frac{14\ \text{ft}\ dR}{\text{ft}^2\ \text{sec}}$$

$$W = 542\ \text{lb-ft}\ \frac{32\ \text{ft}}{\text{sec}^2} = 17{,}300\ \frac{\text{lb-ft}^2}{\text{sec}^2}\ \text{for one cubic foot of}$$

concrete.

One calorie = $100\ \frac{\text{lb-ft}^2}{\text{sec}^2}$, so that 173 calories are required to crush one cubic foot of concrete. See author's note page 90.

The bottom section contains 1029 ft^3 of concrete according to the last set of plans submitted to Armour Research Foundation. To crush this amount of concrete, $1029 \cdot 173 = 178{,}000$ calories are required. Previously, it was determined that $3.18 \cdot 10^5$ calories were available for crushing the bottom, therefore, it appears that the bottom would be destroyed. This was mentioned to Mr. Turk at an ARF-NACA meeting, and the concrete was later substantially increased in thickness to approximately 17 feet. The bottom of the reactor was then adjudged safe with a factor of about four.

The question was also raised as to the effect crushed sand particles from the plug might have on striking the floor of the control room, possibly

cracking it. If the sand strikes the floor at 120 ft/sec, the velocity of the concrete after the blow is given by the formula:

$$u_2 = \frac{u_1}{1 + \frac{\rho_2 c_2}{\rho_1 c_1}} \qquad (11)$$

where u_1 is the crushed material velocity, 120 ft/sec; c_1 is the velocity of sound in loose sand, $c_1 \cong 2000$ ft/sec; the density of loose sand 60 $\frac{lb}{ft^3} = \rho_1$.

The factors u_2, c_2, ρ_2 represent the same parameters for concrete.

$$u_2 = \frac{120}{1 + \frac{14 \cdot 13}{6 \cdot 2}} = 7.4 \text{ ft/sec}$$

By our previous formula applied to the wave in concrete

$$u_2 = \frac{Pc}{a} \qquad a = 435{,}000 \text{ for P in bars}$$

yields, $P \cong 3600$ psi.

This pressure is barely enough to crush concrete and would not conceivably crush the floor of the control room.

Other than the 9-foot thick quadrant, the sides of the reactor were expected to fail immediately. The shock pressures were computed on the water retaining wall some 30 feet away after ignoring these walls. This will somewhat overestimate the forces on these walls and is therefore conservative.

A calculation of the pressures from Cole's equation gives 4300 psi on the 70-foot water retaining wall. If we assume that this wall fails immediately, then the water velocity behind the shock wave would be 60 ft/sec. When the wall breaks, an expansion wave passes into the water and increases its velocity to 120 ft/sec. The expansion wave then reflects from the remains of the reactor tank and returns to catch up with the water-concrete interface moving at 120 ft/sec. The distance this interface travels before the reflected wave catches up and causes cavitation is obtained from

$$\frac{d}{120} = \frac{d + 55}{4000}$$

$$4000\,d = 120\,d + 55 \cdot 120 \qquad 3880d = 55 \cdot 120 \qquad (12)$$

$$d = \frac{55 \cdot 120}{3880} = 1.7 \text{ feet}$$

Thus no solid wave of water reaches the outer wall of the canal and the only pressures will be due to "water seiche" effects until the water settles to a depth of about 9 feet in the canal. Therefore, the far wall of the canal should be safe as designed.

The question of sand from this wall hitting the 100-foot wall that is 15.5 feet further can be analyzed the same way. Here P = 4300 psi = 292 bars, so the sand velocity is

$$u = \frac{292 \cdot 13{,}000}{435{,}000} = 8.75 \text{ ft/sec} \qquad \text{(Eq. 8)}$$

When reduced by the previous formula to peak pressure, this analysis shows that no damage from sand need be anticipated. The latter wall is then safe if designed for the static pressures alone.

For the quadrant where the concrete is 9 feet thick, there is about 1230 ft^3 of concrete which would require $1230 \cdot 173 = 213{,}000$ calories to crush it. From a calculation of the energy available in this reactor, we see that 350,000 calories could be transmitted to the concrete, so the 9-foot sector is probably crushed, but barely so.

If we then calculate the pressures on the water retaining wall for an explosion of 350,000 - 213,000 = 137,000 calories or 137 grams of TNT (137 grams at 453 g/lb = 0.31 pounds of TNT),

$$P = 2.16 \cdot 10^4 \left(\frac{(0.31)}{31} \right)^{1/3} \quad ^{1.13}$$

$$P = 2.16 \cdot 10^4 \quad (0.0135) = 290 \text{ psi}$$

Reflected pressure = 600 psi

Thus the pressure on the water retaining wall is 600 psi but the available energy is only 1400 calories. Therefore, the duration of the pressure is so short that the wall may be considered to hold. This may be easily shown as follows: Only 1400 calories are available in the water. A calculation of the energy required to compress one cubic inch of water to 600 psi shows it to be 0.017 calories. Therefore, only 82,500 $in.^3$ or 47.7 ft^3 of water can be compressed. For a wall area of 8120 ft^2 in this sector, the layer is 0.006 foot thick, and can maintain such a pressure for only a few microseconds. A pressure of such short duration will not damage the wall.

D. Final Pressure in the Enclosure under the Dome

Using the equation

$$E = \frac{PV}{\gamma - 1} \tag{13}$$

with V, the volume under the dome = 292,000 ft^3

E, the total energy release = $1.8 \cdot 10^8$ calories

$$\left(\text{one calorie} = 100 \cdot \frac{\text{lb ft}^2}{\text{sec}^2}\right)$$

and choosing $\gamma = 1.4$, we obtain

$$P = \frac{1.8 \cdot 10^{10} \text{ lb ft}^2 \text{ sec}^2 \ (0.4)}{2.9 \cdot 10^5 \text{ sec}^2 \ \ 32 \text{ ft}}$$

$$P = 705 \text{ lb/ft}^2 = 4.9 \text{ psi}$$

Since the dome will be designed for static pressures of this order with an adequate safety factor, it appears that the dome will remain intact.

The possibility of pieces of concrete being driven through the dome may be eliminated by considering the behavior of the sides of the tank after the explosion. The speed of sound in concrete is much higher than the speed of the shock wave in water so a precursor will travel through the concrete and will begin to force the concrete sides of the tank inward at the top of the tank. Since these pieces will be under the lead top of the tank, they cannot be driven far by the water shock wave when it comes. This precrushing of the concrete top of the tank will allow further escape of the high pressure water from the top of the tank.

E. The Top of the Tank

The top of the tank consists of several plates with a total mass of 107,800 pounds. With allowances for waste heat in water, the top of the tank receives $11.4 \cdot 10^4$ calories. If all this energy is given to the plates, the plates can rise to a height given by

$$h = \frac{E}{mg} = \frac{11.4 \text{ lb ft}^2 \text{ sec}^2 \cdot 10^4}{1.078 \text{ sec}^2 \text{ lb } 32 \text{ ft}} = 3.3 \text{ feet} \tag{14}$$

So this set of plates can rise only 3.3 feet above the top of the reactor structure.

Mr. Turk of NACA made a more conservative analysis in which the pressure-time distribution for a fixed plate was used but the plates were considered unrestrained. The result of this analysis was that the plate rose to a height of 15 feet. So even on this basis, the top of the reactor is safe.

F. The Spray Dome

When the shock wave from the exploding reactor intersects the water surface, it reflects as an expansion wave and raises the water in a base surge. This spray dome will travel at about 120 ft/sec into the air and will strike the sides and the top of the dome. The force on the dome due to this spray is given by

$$\frac{1}{2}\frac{\rho u^2}{g} = \frac{1}{2}\frac{64 \cdot (120)^2}{32 \cdot 144}\frac{\text{ft}^2\ \text{sec}^2}{\text{ft}^3\ \text{sec}^2}\frac{\text{ft}^2}{\text{ft in.}^2} = \frac{100\ \text{lb}}{\text{in.}^2} \qquad (15)$$

This pressure will exist locally and for very short times. Since this is far below the yield strength of steel, no damage need by expected from the spray dome.

G. Analysis of the Design Safety Factors

1. The plug and bottom of the reactor

The incident pressure on the plug is

$$P_1 = \frac{20.5 \cdot 10^4}{(10)^{1.13}} = 1.5 \cdot 10^4 = 15{,}000\ \text{psi} = 1025\ \text{bars}$$

The shock wave velocity is 5180 ft/sec in the water; therefore by the time this wave strikes the plug it is essentially a plane wave and the plug fails as a unit. The water velocity behind the shock wave is 205.0 ft/sec. When the shock wave hits the plug it starts to move at a velocity of

$$\mu = P\frac{c}{a} = 1025\ \frac{13}{435} = 30.7\ \text{ft/sec}$$

if the plug yields right away. If the plug does not, then its velocity would go up to 60 ft/sec since the transmitted pressure would be higher by at most a factor of two. When the shock wave reaches the bottom of the plug it reflects as an expansion wave and doubles the material velocity. Thus we get a picture of the broken plug followed closely by the water, moving

down into the control room like a piston. We have shown previously that the damage from loose flying sand is negligible, but the moving water has a large amount of kinetic energy which could damage the control room floor if no energy extraction from the water took place.

If the door to the control room is of heavy construction and fails comparatively slowly, the trapped air in the room will absorb a large amount of energy from the moving water as it comes down. It is suggested that compression takes place so rapidly that the door does not fail until the walls of the control room do (at some 3500 psi).

The work required to compress an ideal gas isentropically, per unit mass is given by

$$W = \int PdV \tag{16}$$

For an ideal gas

$$V = \frac{C}{(P)^{1/\gamma}}$$

then

$$dV = -\frac{\frac{1}{\gamma}(P)^{\frac{1}{\gamma}-1} C}{(P)^{\frac{2}{\gamma}}}\, dP$$

$$W = \int PdV = -C\int \frac{1}{\gamma}(P)^{\frac{1}{\gamma}-\frac{2}{\gamma}} dP = \frac{C}{\gamma}\int (P)^{-\frac{1}{\gamma}} dP \tag{17}$$

$$W = \frac{1}{\gamma}\, C \left[\frac{\gamma}{\gamma - 1} (P)^{\frac{\gamma-1}{\gamma}} \right]_{P_1}^{P_2}$$

$$W = -\frac{C}{\gamma - 1} \left[(P)^{\frac{\gamma-1}{\gamma}} \right]_{P_1}^{P_2} \tag{18}$$

can be written as

$$W = -\frac{1}{\gamma - 1} \int_{P_1}^{P_2} (P) \left(\frac{P}{\gamma}\right)^{\frac{1}{\gamma}} \qquad (19)$$

but since

$$V = \frac{C}{(\rho)^{\frac{1}{\gamma}}}$$

We can write it as

$$-\frac{1}{\gamma - 1} \int_{P_1}^{P_2} PV \qquad (20)$$

So that the work done is

$$-\frac{P_1 V_1 - P_2 V_2}{\gamma - 1} = W \qquad (21)$$

$$\frac{c_p}{c_v} = \gamma = 1.4 \text{ for air}$$

If the final pressure $P_2 = 3500$ psi and $P_1 = 14.7$ psi, $\frac{P_2}{P_1} = 238$. Since for an isentropic compression $\frac{V_1}{V_2} = \left(\frac{P_2}{P_1}\right)^{\frac{1}{\gamma}}$ $\frac{V_1}{V_2} = 19$

$$V_1 = \frac{1}{0.072} \frac{ft^3}{lb} = 13.9 \frac{ft^3}{lb} \qquad V_2 = 0.276 \frac{ft^3}{lb}$$

$$W = \frac{(13.9)(14.7)(144) - (0.276)(3500)(144)}{0.4} \frac{lb\text{-}in.^2 ft^3}{in.^2\text{-}ft^2 lb}$$

$$= 269{,}000 \text{ ft} \frac{(32 \text{ ft})}{sec^2} = 86 \cdot 10^5 \frac{ft^2}{sec^2} \text{ per lb of air}$$

The control room contains 64.2 pounds of air so the energy required to compress this air is

$$5400 \cdot 10^5 \frac{lb\text{-}ft^2}{sec^2} = 54 \cdot 10^5 \text{ calories}$$

The fraction of the energy which is sent toward the plug by the shock wave is

$\frac{20.2}{100} = 0.202 = 20.2$ per cent of the initial amount.

Since spreading of the plug will give most of the energy to the walls, we can calculate the percentage of energy delivered to the floor of the control room.

$$\frac{20.2}{(27)^2} = 0.0277 = 2.77 \text{ per cent}$$

Since 400 pounds of TNT will give up $1.8 \cdot 10^8$ calories, we see that $1.8 \cdot 10^6$ x (2.77) = $4.98 \cdot 10^6$ calories are sent toward the plug. All but 6.5 per cent of this is lost due to irreversible heating, leaving $4.98 \cdot 10^4$ (6.5) = $32.4 \cdot 10^4$ calories. But this is about 10 times less than the energy required to compress the air in the control room to the point where the walls might fail. On this basis, the fragments do not damage the floor and we have a safety factor of about 10 for crushing of the control room walls. After the door ruptures, a shock wave will propagate through the passageway from the control room and exhaust into the room outside the gas-tight enclosure.

The strength of this shock wave may be roughly computed from standard shock tube theory if the door is presumed to burst like a diaphragm. (Note that any fragments from the door will be stopped by the stairways.)

The incident pressure behind this shock wave will be about 308 psi initially and the reflected pressure will be about 2000 psi. Due to shock wave attenuation, the actual pressures on the door that closes off the stairway to the control room passage, from the room outside to the 100-foot shell, will be about 290 psi. The duration of this pressure will be about 3 milliseconds. If the door is designed to sustain this pressure, no further damage from the shock wave need be expected.

The 70-foot wall was shown to be safe for the explosion of 400 pounds of TNT, since its failure would not injure the 100-foot wall, or the gas-tight shell. Just what factor of safety this provides is difficult to say since the expansion waves which cavitate the residual fragments of the 70-foot wall, will perform the same function for much larger quantities of explosive.

H. The Cap of the Reactor Tank

The calculation by Mr. Turk of NACA showed that on the most conservative assumptions, the cap would rise only 15 feet above its position on the reactor. If we assume the effects of the explosion to scale according

to the standard $W^{1/3}$ scaling, the cap would rise only 19 feet for 800 pounds of TNT. Since the distance from the cap to the top of the dome is 48 feet, it would seem that there is an adequate factor of safety for even 1000 pounds of TNT.

Recently a decision was made to construct the 70-foot wall so that it would hold under the blast from 400 pounds of TNT. The incident pressure would be about 4300 psi and the reflected pressure about 9450 psi (643 bars). In the worst case this pressure would have the longest duration at the bottom of the tank, about 6.65 milliseconds, while at the top of the tank the pressures would be relieved immediately. A first estimate of the pressure-time curve is given below.

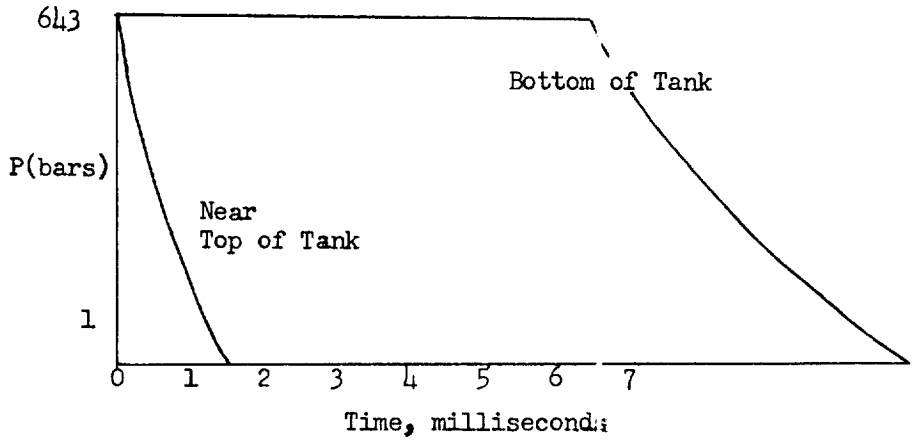

A more realistic assumption can be obtained from a consideration of the energy available at the 70-foot wall. For a wall 25 feet high, 30 feet from the explosion, and extending around three-fourths of the tank perimeter, we have

$$\frac{3}{4}(2\pi)\,30(25) = 3670 \text{ ft}^2$$

A sphere 30 feet in diameter would have a surface area

$$4\pi(30)^2 = 11{,}300 \text{ ft}^2$$

Thus the wall receives 31.8 per cent of the original energy of the explosion, less waste heat losses. At a pressure of 643 bars only 5.5 per cent of the available energy remains once waste heat losses are calculated.

Thus of the original $1.8 \cdot 10^8$ calories only $3.69 \cdot 10^6$ calories remain after the losses due to waste heat and the factor due to the geometry, have been subtracted. Dividing this net energy available by the wall area in this reactor we obtain 327 calories/ft^2. To compress one cubic foot of water to 9450 psi requires 7000 calories. Since only 327 calories/ft^2 are available a layer only 0.046-foot thick can be compressed. This thin layer of water could sustain the pressure for less than a few milliseconds. It seems therefore that the impulse delivered to this wall will be almost negligible, even at the bottom of the wall.

A final estimate of impulse function was made using a pressure-time law of the form of a square wave

$$P = P_c \qquad P_c = 9450 \ \frac{lb}{in.^2}$$

This formula was used for the pressure-time curve with a cut-off sharply at 5 milliseconds, because at that time the relieving expansion wave would have traveled back through the wall to the water-concrete interface. The analysis of the wall on this basis is given at the end of this report.

I. Calculation of Energy Required to Compress Water

$$W = \int_{V_1}^{V_2} PdV \qquad \text{(Eq. 16)}$$

Then from our earlier work,

$$\frac{dP}{dV} = -\frac{c^2}{V_o^2} \qquad dV = \frac{V_o^2}{c^2}\, dP$$

$$W = -\frac{V_o^2}{c^2} \int_{P_1}^{P_2} PdP = \frac{V_o^2}{2c^2} \left[P_2^2 - P_1^2 \right] \qquad (21)$$

For one case $P_1 = 14.7$ psi $\qquad P_2 = 600$ psi

$$V_o = 0.016 \ \frac{ft^3}{lbs} \qquad c = 4500 \text{ ft/sec}$$

$$W = \left(\frac{256 \cdot 10^{-6} \ ft^6\text{-sec}^2}{2(20.2 \cdot 10^6) \ lbs^2\text{-ft}^2} \right) \left[600 \ \frac{lbs \ 144 \ in.^2}{in.^2 - ft^2} \right]^2 \left(1020 \ \frac{ft^2}{sec^4} \right)$$

$W = 46 \ \frac{ft^2}{sec^2}$ per pound; then one cubic foot weighs 62.4 pounds

Therefore,

$$W = 62.4(46) \text{ lbs } \frac{ft^2}{sec^2} = 2870 \ \frac{lbs\text{-}ft^2}{sec^2} \quad \text{for one cubic foot}$$

that is,

$$\frac{2870}{1730} = 1.66 \ \frac{lbs\text{-}ft^2}{sec^2} = 0.0166 \text{ cal/in.}^3$$

For the other case where the pressure goes to 9500 psi,

$$W = \frac{(256 \cdot 10^{-6}) \ ft^6\text{-sec}^2 \ 1020 \ ft^2}{2(20.2 \cdot 10^6) \ sec^4} \left[(9.5) \ (1.44) \right]^2 \ 10^{10}$$

$= 11{,}200 \ \frac{ft^2}{sec^2}$; so for one cubic foot, it is

$$(1.12 \cdot 10^4) \ (62.4) = 70 \cdot 10^4 \ \frac{lbs\text{-}ft^2}{sec^2} = 7000 \text{ calories per ft}^3$$

Author's Note

In evaluating Eq. 8 for a particular case it was assumed that the shock wave could raise the pressure in the concrete to 30,000 psi. In evaluating Eq. 10, however, it was assumed that the material was crushed at 3500 psi. The obvious contradiction of these two assumptions requires some explanation.

To the best of the author's knowledge no data exists for the equation of state for concrete under shock loading. However it is known that the yield properties of concrete are a function of the rate of application of stress, see Watstein[3].

[3] Watstein D. Properties of Concrete at High Rates of Loading; ASTM Preprint #936, 1955

Under these circumstances a decision was made to be as conservative as possible without prejudice to the overall reactor design. Therefore in Eq. 8 when the crushed material velocity is determined as a function of shock overpressure, the highest pressure is used. While in Eq. 10 the standard cylinder strength of 3500 psi is used to determine the energy required to crush concrete.

The Foundation has proposed to the AEC a general reactor safety program with particular emphasis on safe design practices and equation of state for parameters for materials like concrete. Since no data of this sort will be available until too late to influence the NACA reactor, it is thought that the above assumptions are necessary to assure an adequate factor of safety regardless of the final equation of state data obtained as a result of the general study mentioned above.

J. Motion of Containment Wall Due to Shock Loading*

Nomenclature

e_ϕ = strain in the tangential direction, in./in.

u = displacement, in.

r = inside radius of wall, in.

γ = density of wall, $lb/in.^3$

σ_y = yield stress of steel, psi

p_o = characteristic pressure, psi

h = thickness of wall, in.

h_1 = equivalent thickness of steel reinforcement, in.

t_o = duration of loading, sec

t^* = time of maximum deflection, sec

The analysis of the containment wall due to shock loading will be carried on by considering a thin-walled cylinder of circular cross section loaded uniformly with a load per unit area of $p = p_o f(t)$, Fig. 4. Due to symmetry the displacements will be radial and the strains will be given by

$$e_\phi = \frac{u}{r} \tag{22}$$

u, positive outward, is the radial displacement.

---

* by E. Saleme

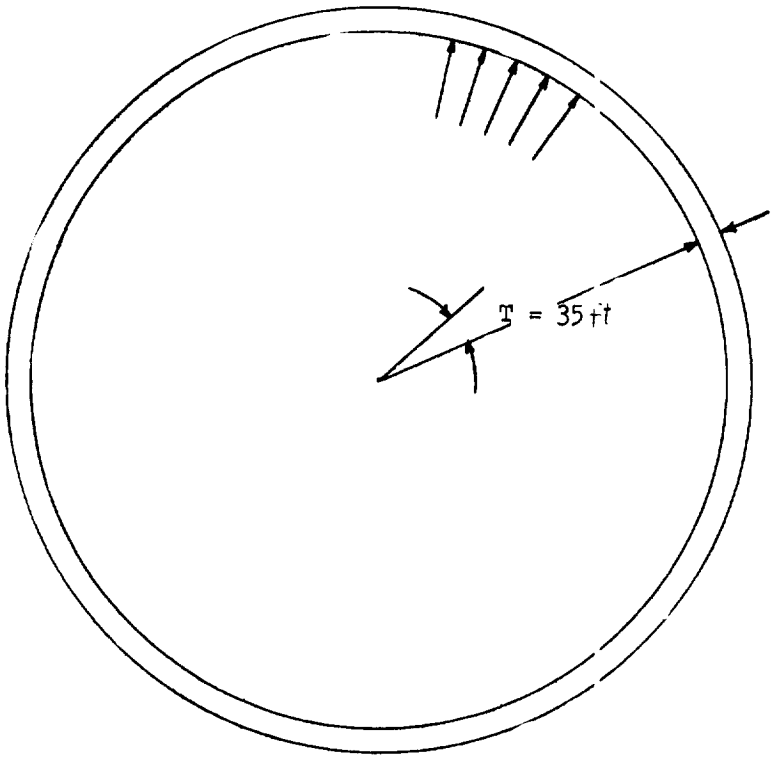

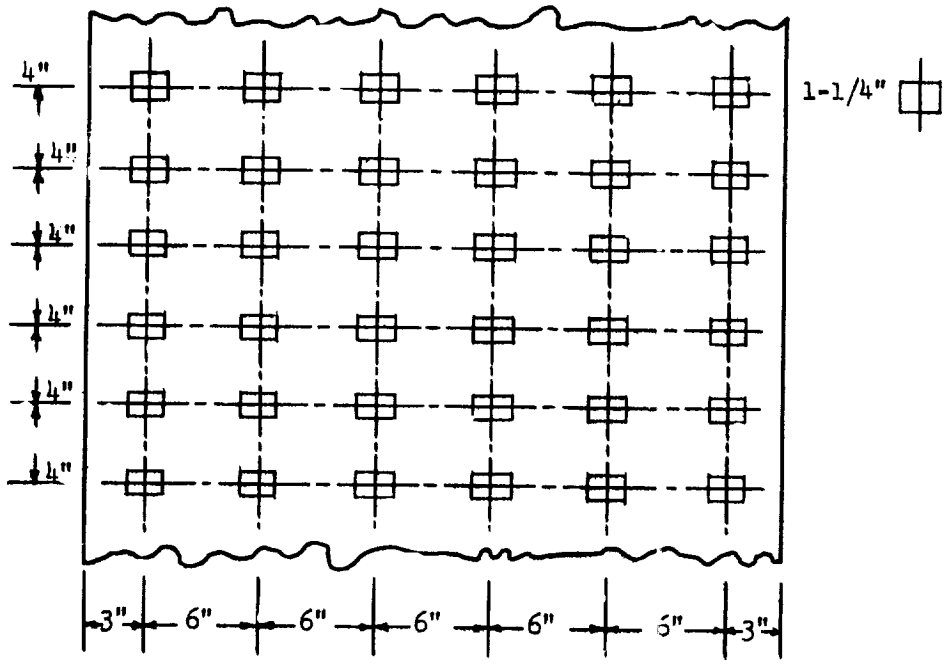

Fig. 1 LONGITUDINAL SECTION THROUGH 70-FOOT WALL

The inertia force of an element of mass $\frac{\gamma}{g} r h d\theta$ will be

$$\frac{\gamma}{g} r h \ddot{u} d\theta \tag{23}$$

Neglecting the elastic portion of the deformation, the restraining force will be $\sigma_y h_1$ which gives a component in the radial direction.

$$\sigma_y h_1 d\theta \tag{24}$$

The forcing function can be written as

$$p_o r d\theta f(t) \tag{25}$$

The equation of motion is then

$$\frac{\gamma}{g} r h u d\theta + \sigma_y h_1 d\theta = p_o r d\theta f(t) \tag{26}$$

or

$$\ddot{u} = \frac{g}{\gamma} \frac{p_o}{h} \left[f(t) - \frac{\sigma_y}{p_o} \frac{h_1}{r} \right]$$

$$\gamma = \frac{(4 \times 36 - 6 \times 1.25^2) \times 0.0868 + 6 \times 1.25^2 \times 0.283}{4 \times 36} = 0.0996 \text{ lb/in.}^3$$

$$p_o = 600 \times 15 = 9000 \text{ lb/in.}^2$$

$$h = 36 \text{ in.}$$

$$r = 35 \times 12 = 420 \text{ in.}$$

$$\sigma_y = 30{,}000 \text{ lb/in.}^2$$

$$h_1 = \frac{6 \times 1.25^2}{4} = 2.344 \text{ in.}$$

Then

$$\frac{g}{\gamma} \frac{p_o}{h} = \frac{386}{0.0996} \quad \frac{9000}{36} = 0.994 \times 10^6 \text{ in./sec}^2$$

$$\frac{\sigma_y}{p_o} \frac{h_1}{r} = \frac{30{,}000}{9000} \quad \frac{2.344}{420} = 0.0186$$

$f(t) = 1 \qquad 0 \leq t \leq t_o$

$f(t) = 0 \qquad t_o \leq t$

$F'(t) = t \qquad 0 \leq t \leq t_o$

$F'(t) = t_o \qquad t_o \leq t$

$F(t) = \frac{t^2}{2} \qquad 0 \leq t \leq t_o$

$$F(t) = \frac{t_o}{2}\ (2t - t_o) \qquad t_o \leq t$$

$$\ddot{u} = 0.994 \cdot 10^6 \quad f(t) - 0.0186$$

$$\dot{u} = 0.994 \cdot 10^6 \quad F'(t) - 0.0186t$$

$$u = 0.994 \cdot 10^6 \quad F(t) - 0.0186 \frac{t^2}{2}$$

$$t^* = \frac{t_o}{0.0186}$$

$$U_{mx} = 0.994 \cdot 10^6 \ \frac{t_o}{2}\ (2t^* - t_o) - 0.0186 \frac{t^{*2}}{2} = 0.994 \cdot 10^6$$

$$\frac{0.9814}{0.0186}\ \frac{t_o^2}{2} = 26.223\ (t_o \cdot 10^3)^2$$

$$t_o = 0.0005 \text{ sec}$$

$$U_{mx} = 6.56 \text{ in.}$$

$$\epsilon_{mx} = \frac{U_{mx}}{r} = \frac{6.56}{420} = 0.0156$$

which is acceptable for steel.

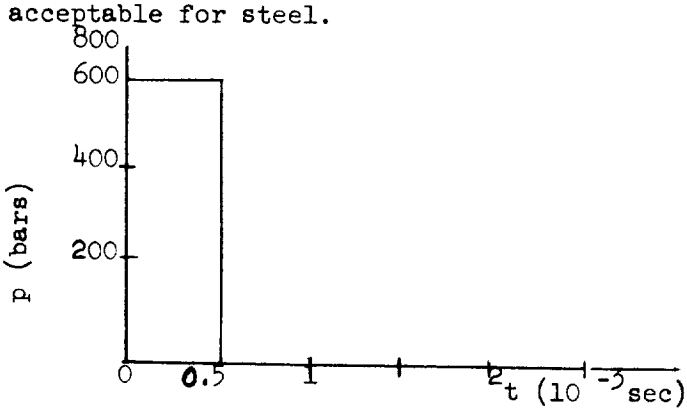

Fig. 2 PRESSURE TIME CURVE ON 70-FOOT WALL

The foregoing analysis shows that under the condition of the problem, the strain in the steel bars will reach a value of 1.56 per cent or some fifteen times the strain corresponding to the yield point of the material. This means that the damage to the wall due to the blast will reduce to some permanent deformation of the reinforcing bars and a partial cracking of the concrete.

K. Motion of the Outer Reactor Shell Due to Internal Explosion*

The outer reactor shell has the shape of an ellipsoid of revolution, see Fig. 3.

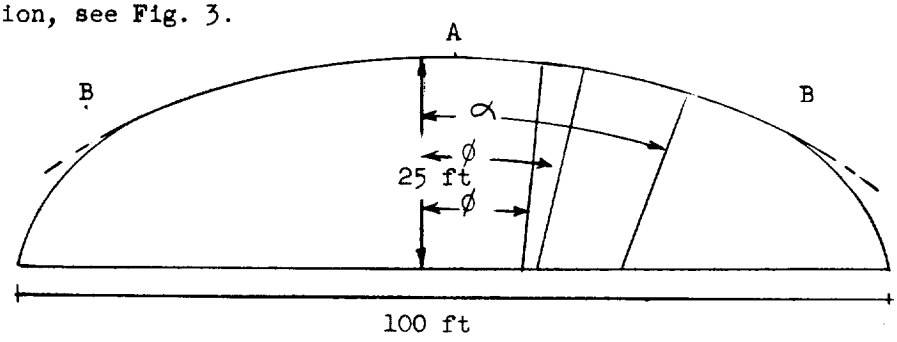

Fig. 3 MERIDIAN SECTION OF SHELL

The meridian ellipse is defined by

$$\frac{x^2}{50^2} + \frac{y^2}{25^2} = 1 \qquad (27)$$

In what follows, an approximate analysis of the shell under a dynamic loading acting over a portion of its surface is carried out by means of the following simplifying assumptions.

(1) The ellipsoidal shell is substituted by a spherical shell whose meridian passes through the Points A and B (40,15) with radius

$$r = \frac{x^2 + (b - y)^2}{2\ (b - y)} = \frac{40^2 + (25 - 15)^2}{2(25 - 15)} = 85 \text{ feet} \qquad (28)$$

(2) The displacements of the points of the shell are given by radial displacement

$$w(\phi) = w_o \cos \phi \qquad (29)$$

meridional displacement

$$v = 0 \qquad (30)$$

where w_o is the displacement of Point A.

(3) The shell deforms plastically above the parallel of radius $r_\alpha = r \sin\alpha$ for which the meridional stress is equal to σ_y.

---

* By E. Saleme

The loading consists of a uniformly distributed pressure, $p = p_o f(t)$, as a function of time, Fig. 4, applied on the surface bound by the parallel of radius $r_o = r \sin \phi_o$. Then, the resultant external force will be

$$F(t) = \pi r_o^2 p_o f(t) = \pi p_o r^2 \sin^2 \phi_o f(t) \tag{31}$$

where p_o is the peak pressure.

The total inertia force is, by Assumption 2,

$$I = 2\pi \frac{\gamma}{g} h r^2 \ddot{w}_o \int_0^{\alpha} \cos^2 \phi \sin \phi \, d\phi = \frac{2}{3} \pi \frac{\gamma}{g} h r^2 \ddot{w}_o (1 - \cos^3 \alpha) \tag{32}$$

The resisting force is by Assumption 3,

$$R = 2\pi h r \sigma_y \sin^2 \alpha \tag{33}$$

The equation of motion is then

$$\frac{2}{3} \pi \frac{\gamma}{g} h r^2 (1 - \cos^3 \alpha) \ddot{w}_o + 2\pi h r \sigma_y \sin^2 \alpha = \pi p_o r^2 \sin^2 \phi_o f(t) \tag{34}$$

or

$$\ddot{w}_o = \frac{3}{2} \frac{g}{\gamma} \frac{p_o}{h} \frac{\sin^2 \phi_o}{1 - \cos^3 \alpha} \left[f(t) - 2 \frac{\sigma_y}{p_o} \frac{h}{r} \frac{\sin^2 \alpha}{\sin^2 \phi_o} \right] \tag{35}$$

Upon integrating

$$\dot{w}_o = \frac{3}{2} \frac{g}{\gamma} \frac{p_o}{h} \frac{\sin \phi_o}{1 - \cos^3 \alpha} \left[\int_0^t f(\tau) d\tau - 2 \frac{\sigma_y}{p_o} \frac{h}{r} \frac{\sin^2 \alpha}{\sin^2 \phi_o} t \right] \tag{36}$$

The time of maximum is given by

$$\int_0^{t^*} f(\tau) \, d\tau - \frac{2\sigma_y}{p_o} \frac{h}{r} \frac{\sin^2 \alpha}{\sin^2 \phi_o} t^* = 0 \tag{37}$$

Figure 5 shows the graphical solution of Eq. 37 for various values of α.

The maximum displacement is

$$w_{o\,mx} = \frac{3}{2} \frac{g}{\gamma} \frac{p_o}{h} \frac{\sin^2 \phi_o}{1 - \cos^3 \alpha} \left[\int_0^{t^*} \int_0^t f(\tau) \, d\tau \, dt - \frac{\sigma_y}{p_o} \frac{\sin^2 \alpha}{\sin^2 \phi_o} t^{*2} \right] \tag{38}$$

In Eq. 12 let

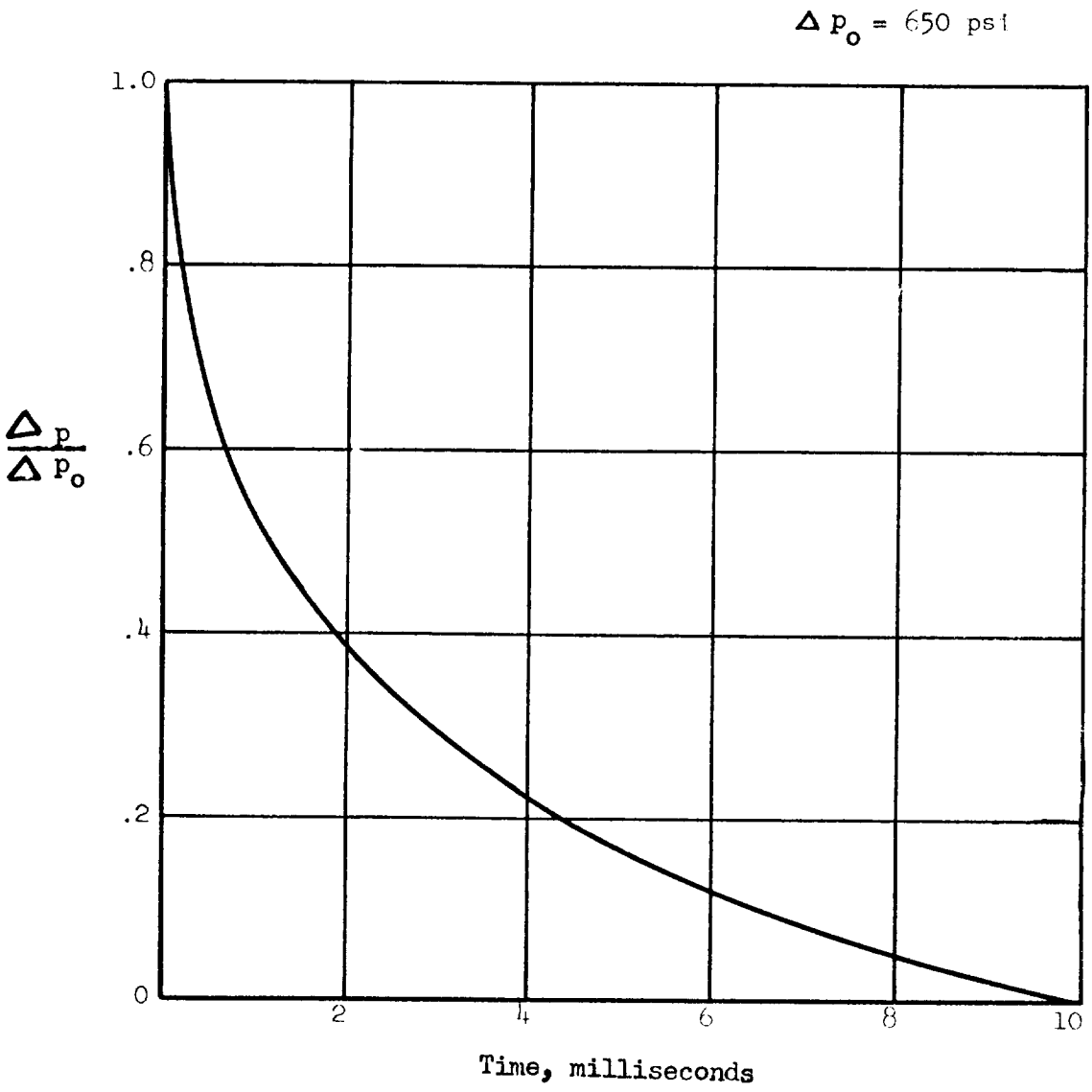

Fig. 4 PRESSURE-TIME CURVE FOR HYDROGEN-OXYGEN EXPLOSION UNDER SHELL

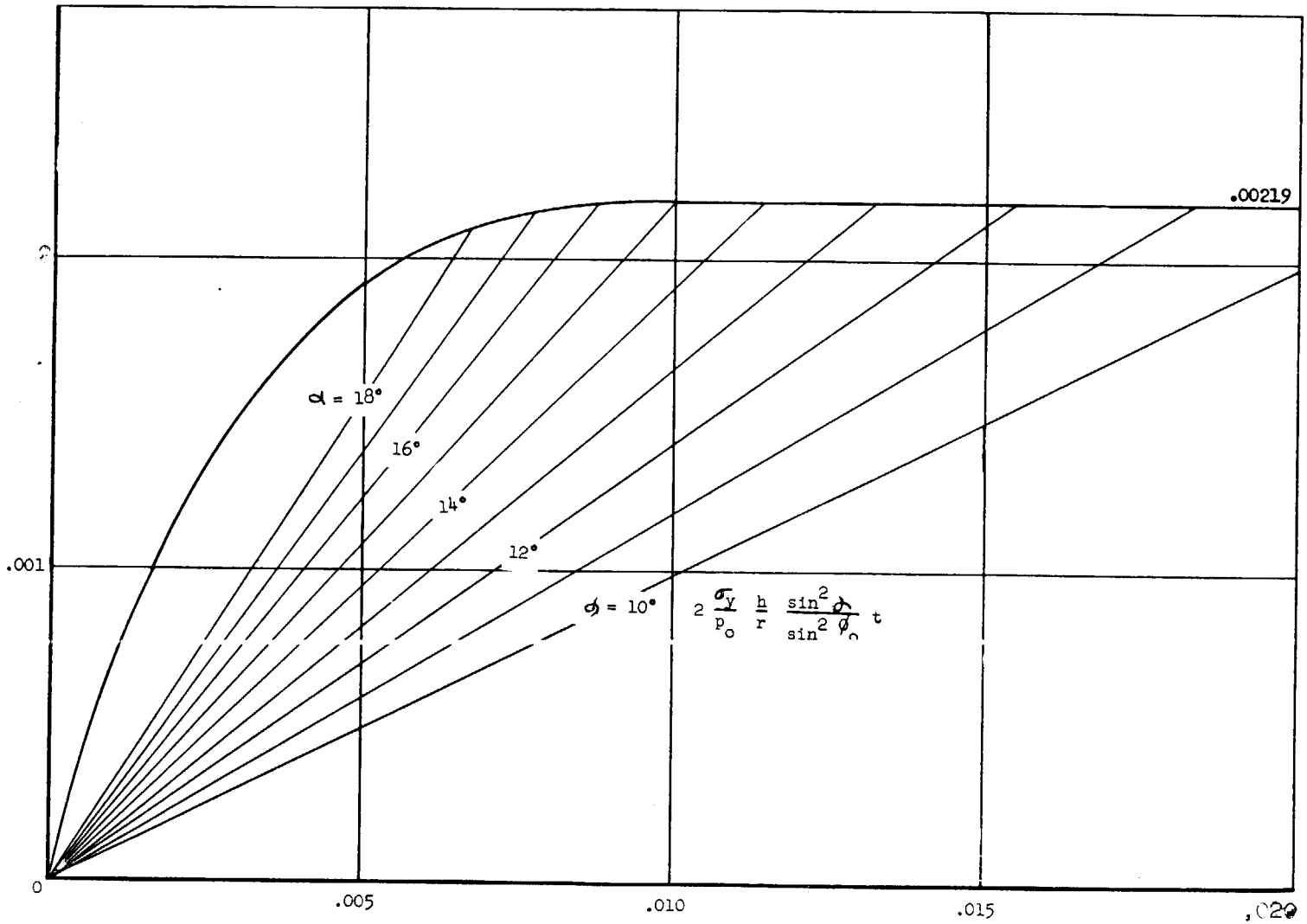

Fig. 5 GRAPHICAL SOLUTION OF EQUATION 37

$$A = \frac{3}{2} \frac{g}{\gamma} \frac{p_o}{h} \tag{39}$$

$$B = 2 \frac{\sigma_y}{p_o} \frac{h}{r}$$

$$A_1^* = \int_0^{t^*} \left[\int_0^t f(\tau) \, d\tau \right] dt = \int_0^{t^*} F(t) \, dt$$

$$A_2^* = B \frac{t^{*2}}{2}$$

Then

$$w_o mx = A \frac{\sin^2 \phi_o}{1 - \cos^3 \alpha} \left[A_1^* - A_2^* \right] = A \frac{\sin^2 \phi_o}{1 - \cos^3 \alpha} A^* \tag{40}$$

By Assumption 2 we have

$$w(\alpha) = w_o \cos\alpha \tag{41}$$

By Assumption 3, the meridional strain at $\phi = \alpha$ must be equal to the yield strain, that is,

$$\frac{w(\alpha)}{r} = \frac{1 - \nu}{E} \sigma_y \tag{42}$$

From Eqs. 40, 41 and 42 it follows

$$\frac{1 - \nu}{E} \sigma_y = A \frac{\sin^2 \phi_o}{1 - \cos^3 \alpha} A^* \cos \alpha \tag{43}$$

Data

$g = 386$ in./sec^2

$\gamma = 0.283$ lb/in.^{3}

$h = 0.5$ in.

$p_o = 650$ psi

$\sigma_y = 30{,}000$ psi

$r = 85$ ft $= 1020$ in.

$\sin\phi_o = \frac{10}{85} = 0.11756$; $\phi_o = 6° \; 45.38'$

then

$$A = \frac{3}{2} \frac{g}{\gamma} \frac{p_o}{h} = \frac{3}{2} \frac{386}{0.283} \frac{650}{0.5} = 2.66 \cdot 10^6 \text{ in./sec}^2$$

$$B = 2 \frac{\sigma_y}{p_o} \frac{h}{r} = 2 \frac{30,000}{650} \frac{0.5}{1020} = 0.04525$$

$$w\ (\alpha) = \frac{(1 - \gamma)\sigma_v}{E} r = \frac{0.7 \cdot 30,000}{30 \cdot 10} \cdot 1020 = 0.714 \text{ in.}$$

The values of $w\ (\alpha)$ for values of α ranging from 11° to 18° are tabulated on Table I. Figure 6 shows that, for $\alpha = 17°.6$ $w\ (\alpha)$ has the value of 0.714 inches and $w_{o\ max}$ is equal to 0.749 inches.

Therefore the maximum displacement of Point A is 0.749 inches which is well within safe design limits.

E-103

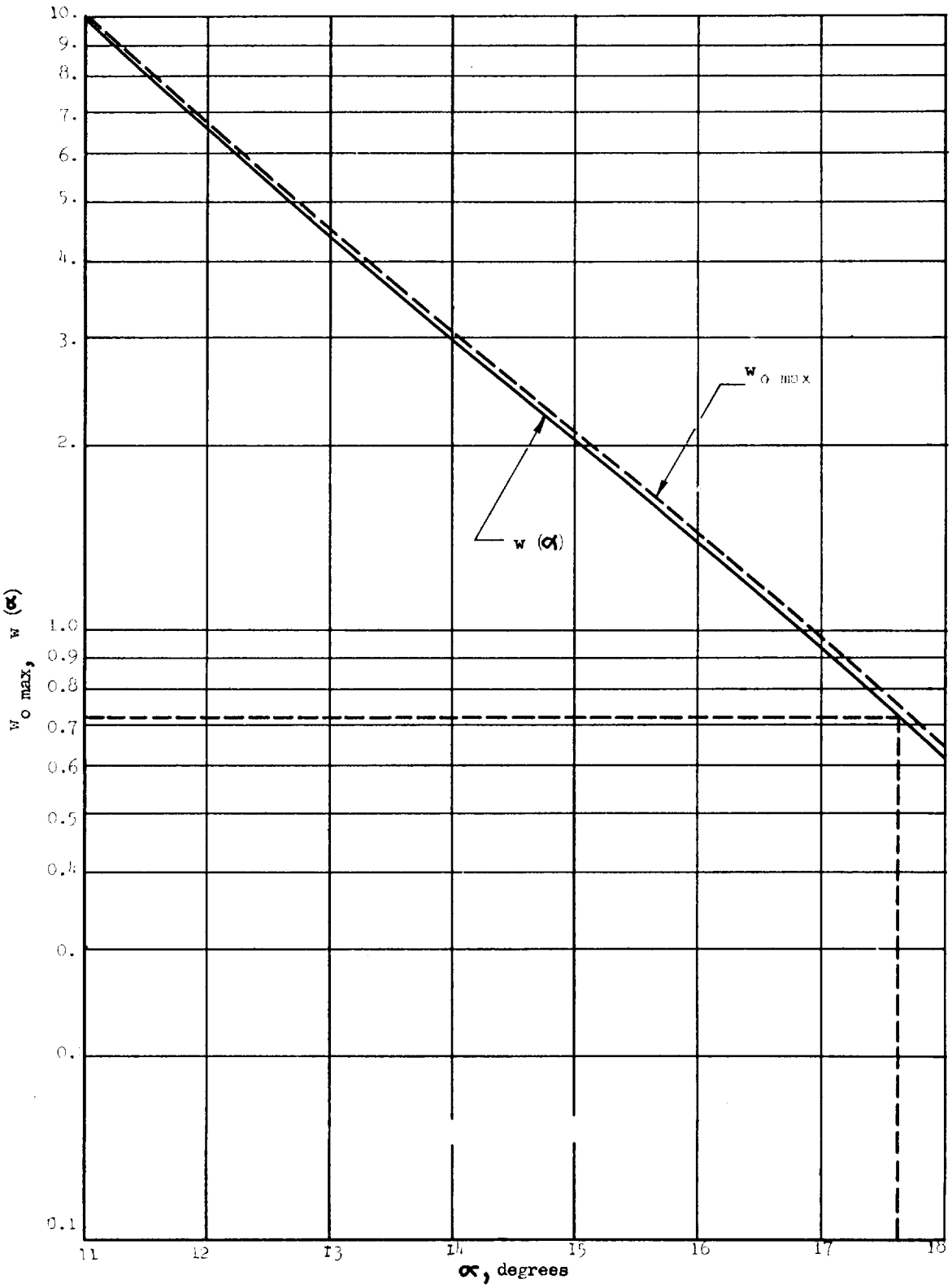
10.
9.
8.
7.
6.
5.
4.
3.
2.
1.0
0.9
0.8
0.7
0.6
0.5
0.4
0.
0.
0.1
$w_{o\ max}$
$w\ (\alpha)$
$w_{o\ max},\ w\ (\alpha)$
11
12
13
14
15
16
17
18
α, degrees

Table I

CALCULATIONS OF THE DEFLECTIONS AND STRESSES IN THE TOP OF THE CONTAINMENT SHELL

α (degrees)	$\sin\alpha$	$\cos\alpha$	$\frac{\sin\alpha}{\sin\phi_o}$	$B(\frac{\sin\alpha}{\sin\phi_o})^2$	t^* (sec)	$A_1^* \times 10^8$ †	$A_2^* \times 10^8$ †	$A_2^* \times 10^8$ †	$1-\cos^3\alpha$	$A\frac{\sin^2\phi_o}{1-\cos^3\alpha} \times 10^6$	w_o	$w(\alpha)=w_o\cos\alpha$
10	.17365	.98481	1.47598	.09858	.02222	4335.41	2433.09	1902.32	.04488	.82038	15.606	15.369
11	.19081	.98163	1.62184	.11902	.01840	3498.83	2014.80	1484.03	.05410	.68056	10.100	9.914
12	.20791	.97815	1.76719	.14131	.01550	2863.73	1697.25	1166.48	.06413	.57412	6.697	6.551
13	.22495	.97437	1.91203	.16543	.01324	2368.79	1449.78	919.01	.07493	.49137	4.516	4.400
14	.24192	.97030	2.05627	.19133	.01145	1976.78	1253.78	723.00	.08648	.42574	3.078	2.987
15	.25882	.96593	2.19992	.21899	.01000	1659.23	1095.00	564.23	.09877	.37277	2.103	2.031
16	.27564	.96126	2.34288	.24838	.00874	1384.18	952.66	431.52	.11178	.32938	1.421	1.366
17	.29237	.95630	2.48508	.27945	.00768	1154.64	823.30	331.34	.12545	.29349	.972	.930
18	.30902	.95106	2.62660	.31218	.00670	946.69	703.50	243.19	.13975	.26346	.641	.610

† Defined in Eqs. 39 and 40

Values of $w_{o\ max}$ and w

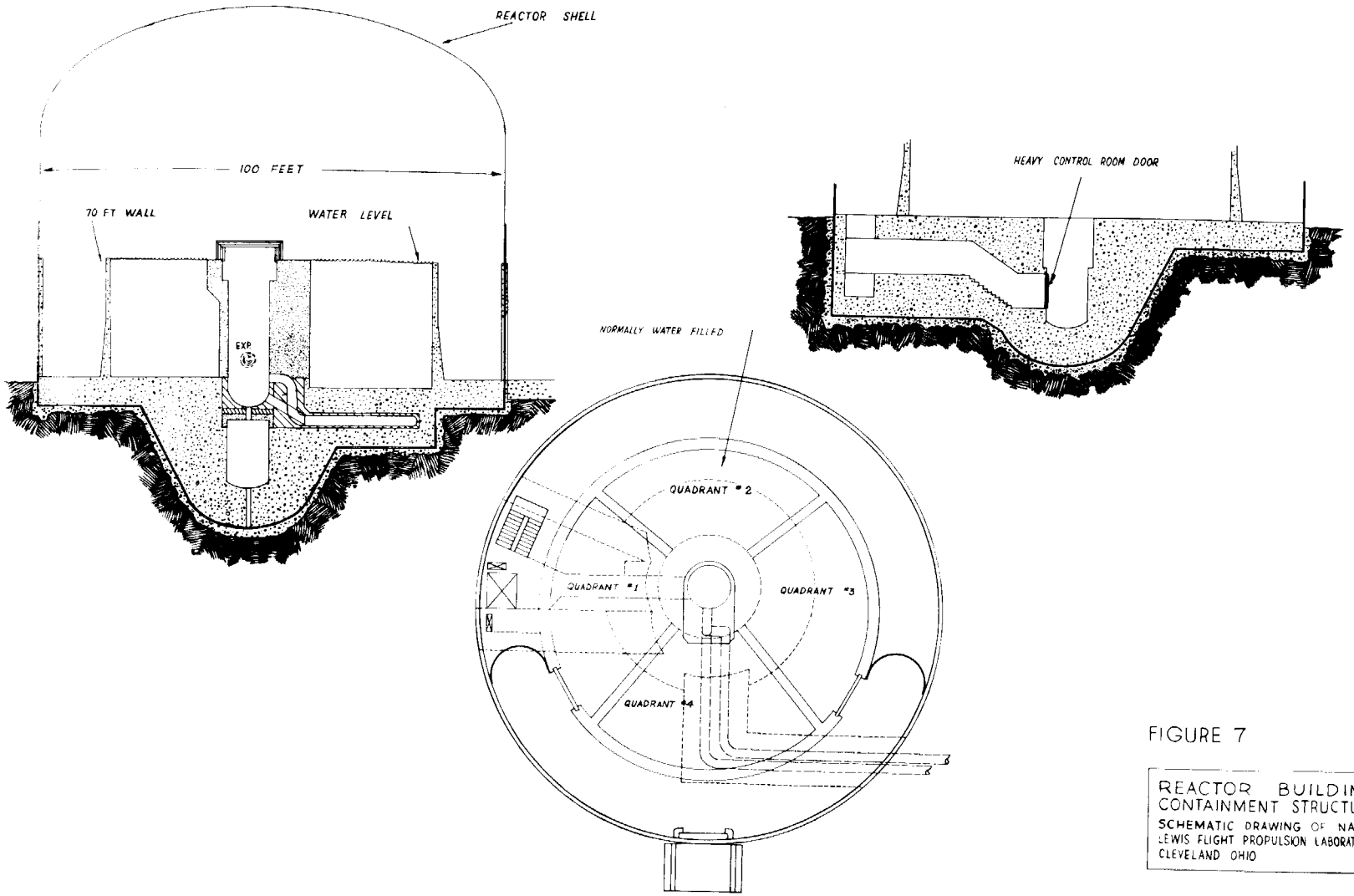

FIGURE 7

REACTOR BUILDING
CONTAINMENT STRUCTURE
SCHEMATIC DRAWING OF NACA
LEWIS FLIGHT PROPULSION LABORATORY
CLEVELAND OHIO

III. REACTIVITY MEASUREMENTS WITH THE BULK SHIELDING REACTOR: WORTH OF VOIDS WITHIN CORE; WORTH OF FUEL ELEMENT WATER PASSAGES AND FUEL ELEMENT PLATES

By Donald Bogart and Theodore M. Hallman

November 15, 1956

SUMMARY

Reactivity effects of voids, water passages, and fuel plates in a fuel element at the center of a 7 element by 3 element core loading have been measured at the Bulk Shielding Reactor. This loading was intended to simulate the first core loading of the NACA Research Reactor. It was found that displacement of water from unfueled regions at the center of the core by air introduced positive reactivity. The worth of voided fuel element water passages extending the full height of the core was negative, however. Removal of fuel plates also introduced negative reactivity.

These results indicate that for some reactor designs, displacement of water by air or steam in regions of high statistical importance can introduce significant positive reactivities. Although continued displacement of water will finally introduce strong negative reactivities, a negative void coefficient may not always exist.

In regard to the NACA Research Reactor it is concluded that negative reactivity changes are introduced on accidental flooding by water of gas-cooled unfueled experiments at the center of the reactor core.

INTRODUCTION

An important space for experiments in the NACA Research Reactor is the volume made available by removing the shim-rod fuel element at the center of the 9 element by 3 element active lattice comprising the proposed initial loading. Experimental assemblies designed for suitable containment in this 3-inch square by 24-inch long high flux space may contain gas or liquid cooled fueled or unfueled test specimens.

The reactivity effects for fueled and unfueled experiments in this vertical center test hole as calculated by group diffusion theory are been presented in the Hazards Summary report (ref. 1). To augment these reactivity calculations and to permit estimation of reactivity effects of compositional changes to the center test space, an experimental program with the Bulk Shielding Reactor at Oak Ridge National Laboratory was jointly planned and executed by BSR and NACA personnel. In these experiments the NACA core loading was mocked up within the limits of excess

reactivity and materials available to BSR. A 7 element by 3 element loading of 140 gram fuel elements was assembled which was reflected by rows of canned beryllium oxide followed by water and which provided 2.5 percent excess reactivity. This loading permitted the measurement of reactivity effects of voids within the core and the worth of fuel element water passages and fuel element plates. The Bulk Shielding Reactor is fully discussed in reference 2. Reactivity measurements with this reactor have been reported in references 3, 4, and 5.

It is a pleasure to acknowledge the cooperation of the staff of the Bulk Shielding Reactor; in particular the efforts of F. C. Maienschein, K. M. Henry, and E. B. Johnson who were resporsible for completing the lengthy experimental program in the brief period allotted.

REACTOR

The BSR is an assembly of MTR-type fuel elements which may be arranged into various critical configurations. The fuel is fully enriched uranium contained in aluminum-clad fuel plates. A complete fuel element is made up of eighteen fuel plates and contains a total of about 140 grams of uranium-235.

The reactor is controlled by two guillotine-type safety "rods," one conventional safety rod, and one regulating rod. The elements through which the conventional safety rod and the regulating rod move contain half the normal number of fuel plates and, therefore, about 70 grams of uranium-235 each. The primary reflector elements are hot-pressed beryllium oxide blocks encased in water tight aluminum cans of the same outer dimensions as the fuel elements. The reactor is moderated and cooled by water which also serves as the secondary reflector and reactor shield.

The reactor configuration used in the present reactivity experiments is schematically shown in figure 1. This loading, designated loading 53 at BSR, consisted of 21 fuel elements in a 7 by 3 array with one row of BeO reflector pieces on the north and two rows of BeO reflector pieces on the south. The east and west faces of the core were reflected by water and permitted complete insertion or complete withdrawal of the two guillotine safeties shown. Each guillotine safety was made of a thin cadmium sheet between two aluminum plates approximately 12 inches wide and 24 inches high. The guillotine safeties were guided and positioned relative to the core by vertical grooved aluminum pieces and supported by the electromagnets actuated by the scram circuits. A regulating rod and a core safety rod were provided in the control-rod fuel elements in grid positions 23 and 27 respectively.

Experimental fuel assemblies occupied the number 25 grid position and were of three kinds:

1. A standard control-rod fuel element into which aluminum chambers of various sizes and contents were inserted in the control-rod space. This element with a typical aluminum chamber partially inserted is shown in figure 2.

2. A standard fuel element specially modified by manifolds at both top and bottom so that the seventeen individual water passages between fuel plates could be selectively voided in any combination. The water passages were voided by blowing air through any of 34 plastic air tubes.

3. A standard fuel element in which twelve of the eighteen convex fuel plates were not brazed into the grooved straight end plates. A photograph of this removable fuel plate assembly is shown in figure 3. With the exception of the end fuel plates and four fuel plates blocked by the fuel element handle, the remaining fuel plates are removable.

REGULATING-ROD CALIBRATIONS

From safeguards considerations, core loadings at BSR are specifically prohibited from containing excess reactivities greater than 2.5 percent. It is desirable to have as much excess reactivity as possible in order to cover a wide range of compositional changes in the experimental fuel assemblies; it will be shown that the core loading selected (see fig. 1) had the legal maximum $\Delta K/K$ of 2.5 percent.

The regulating rod calibration was obtained by the method of distributed poisons (ref. 2) for three configurations of the guillotine safeties: both guillotines out, no. 1 guillotine out - no. 2 guillotine in, and both guillotines in. As the regulating rod in the 23 grid position was inserted, the safety rod in the 27 grid position was withdrawn to maintain criticality for each guillotine configuration. This procedure was repeated for the clean core and for the core as uniformly poisoned as possible by 224 quarter - gram pieces of gold foil. Seven gold foils were taped to each of 32 thin strips of Lucite 26-inches long. The foils were equally spaced on the strips and located in fuel-element water passages so as to poison the core vertically and laterally as uniformly as possible. In all 56.25 grams of gold were used with a cross section of 0.299 cm^2/gm for a total poison cross section of 16.82 cm^2. The reactor core was estimated to have a total cross section of 6281 cm^2. During these calibrations, a standard fuel element assembly occupied the 25 grid position.

The addition of the gold thermal absorber has a negligible effect on the epithermal and thermal neutron diffusion properties of the core and the Lucite foil holders are sufficiently similar in composition to water to introduce no additional heterogeneity. Therefore, from elementary reactor theory, the change in reactivity is given by the fractional change in total absorption cross section for the core resulting from the addition of the gold foils or

$$\frac{\Delta K}{K} = \frac{\Delta \Sigma}{\Sigma} = \frac{16.82}{6281} = 0.00268$$

The number 1 safety rod position as a function of the regulating rod position for the core configuration with both guillotine safeties out is shown in figure 4. Two curves are shown for the core without gold foils and for the core with gold foils. The horizontal difference between these curves is the regulating rod travel corresponding to the $\Delta K/K$ of the gold foils. This change in reactivity due to the gold foils and the smoothed curves of the regulating rod position as a function of the number 1 safety rod position necessary to maintain criticality permit the graphical construction of the integral regulating rod calibration curves shown in figure 5. Three curves, each for a configuration of the guillotine safeties, are presented which have been normalized to a point at the approximate center of the regulating rod travel. These curves are constructed from the faired data and no extrapolations are employed. It may be seen that the curves for the configurations in which both guillotines were out and the no. 1 guillotine out and no. 2 guillotine in practically superimpose for most of the regulating rod travel. However, the curve for the configuration in which both guillotines were in indicates a reduction in rod effectiveness resulting from the depression of neutron flux around the regulating rod due to the proximity of the no. 1 guillotine. The regulating rod at 23 grid position is sufficiently removed from the no. 1 safety rod in the 27 grid position to minimize interaction of these rods in the calibration procedure. It is noted that the calibration curves are not symmetrical about the center of regulating rod travel. Furthermore, the effectiveness of the regulating rod given by the slope of the curve is not zero when fully inserted or fully withdrawn relative to the active portion of the core.

An alternative method for calibrating the regulating rod is to place the reactor on various asymptotic periods by withdrawal of the regulating rod various amounts. The inhour relation may then be used to translate the asymptotic period into reactivity corresponding to the total regulating rod movement. This method cannot be used with the present core because of the photoneutron source arising from the $Be^4(\gamma,n)\ He^4$ reaction in the BeO primary reflector which acts to augment the delayed neutron fraction and perturb the usual inhour relation.

To obtain an indication of the magnitude of the photoneutron contributions to reactivity in the present core loading, the reactor was placed on various asymptotic periods by sudden withdrawal of the regulating rod. The reactivity inserted was obtained from the integral regulating rod calibration curves presented in figure 5. The asymptotic periods were obtained from a logarithmic count rate recorder and from a period indicator. These data, which were obtained for the reactor with all three configurations of the guillotine safeties, are presented in figure 6. Included on figure 6 is the variation of reactivity with asymptotic period

for an equivalent unreflected reactor as calculated by the inhour equation considering five delayed neutron groups (this curve was taken from ref. 3). Differences in neutron lifetime for the various reactor loadings at BSR have a negligible effect on the long periods presented in figure 6.

It may be seen that all of the data lie above the usual inhour values indicating the presence of extraneous neutron sources which may be attributed to the interaction of fission product gammas with the beryllium in the primary reflector.

REACTIVITY EFFECTS OF VOIDS

A standard control-rod fuel element was placed in the number 25 grid position into which aluminum chambers of various sizes and contents were inserted in the water filled control-rod space as shown in figure 2. The construction of these hollow 2S aluminum chambers is shown in figure 7. A reinforcing web and relatively thick end plates were required to prevent distortion of the 0.064-inch thick walls under the external pressure of 20 feet of water in the reactor pool. Chambers of inside height of 4, 12, 20, and 24 inches were used; a photograph of several of these assembled with the bolted cover and aluminum positioning rod are shown in figure 8.

These chambers were positioned in the aperture of the control-rod fuel element in the empty condition and when full of water and the individual reactivity effects measured. The difference in ΔK should estimate the reactivity effects of the air spaces or void volumes in the chamber at various vertical positions in the reactor core. A 24-inch chamber was also filled with graphite powder in one case and with a silica aerogel compound in another case to ascertain the reactivity effects of low-density scattering media in the aluminum chambers.

An additional experiment was performed to determine the reactivity effects of water displacement by material above and below the chamber in the control-rod aperture. Special 2S aluminum plate pieces, which were of the same aluminum-water ratio as the core, were added to the top and bottom of two chambers. These assembled chambers are shown in the photograph in figure 9; the inset shows the cross section of one of the top pieces.

The reactivity effects of the 4-inch and 12-inch aluminum chambers for various vertical locations in the 25 grid position are shown in figures 10 and 11 respectively. The chamber locations relative to the core horizontal midplane are schematically illustrated. The observed reactivities are plotted at the geometric center of the chambers for both the air-filled and water-filled cases. The difference between these cases is then an estimate of the reactivity effect of the air or void volume only, and these are plotted as the dashed lines.

The data indicate that displacement of water in the aperture of the control-rod fuel element either by the aluminum of the water-filled chambers or by the total volume of the air-filled chambers introduces positive reactivity. The positive reactivity due to introduction of voids is greatest at the geometric center of the core; reactivity falls off and changes sign at the top and the bottom regions of the core.

A qualitative explanation of these data must lie in the relative spatial importance of absorptivity and moderating ability of the various materials. Inasmuch as the macroscopic absorption cross section for thermal neutrons is 0.0133 cm^{-1} for aluminum and 0.0220 cm^{-1} for water, a positive reactivity due to displacement of water by aluminum should be expected. Similarly, the displacement of water by air should result in positive reactivity. These absorptivity effects seem to dominate in central core regions of high statistical importance. However, at the top and bottom regions of the core, where absorber importance becomes relatively small, it appears that displacement of water is more an effect of loss of moderator than loss of absorber. The net result in core regions of low statistical importance is a negative reactivity due to displacement of water by either aluminum or void.

Results for the 4-inch and 12-inch chambers with the aluminum-plate end pieces (shown in fig. 9) are also presented in figures 10 and 11 as the flagged points near the core midplane. The aluminum end-plate assembly weights are tabulated below:

Chamber	Weight, gm	
	Top plates	Bottom plates
4-Inch	503.4	593.1
12-Inch	305.5	422.6

The data of figures 10 and 11 indicate that the increased displacement of water by the aluminum-plate end pieces for the water-filled chambers resulted in smaller net positive reactivities. This is probably due to negative reactivity contributions resulting from water displacement at the top and bottom of the core. On the other hand, the increased displacement of water by the aluminum-plate end pieces for the air-filled chambers resulted in a greater $+\Delta K/K$ for the 4-inch chamber and a smaller $+\Delta K/K$ for the 12-inch chamber. The net void effects in both cases were slightly more positive.

Because the reactivity is changing so rapidly at the top and the bottom of the core, the curve of void effect due to the 4-inch chamber in figure 10 cannot be considered a measure of the differential void effect. A finer vertical traverse with the 4-inch chamber would have permitted graphing the differential void effect; unfortunately this was not done.

For the central regions of the core, however, the void effect curve of figure 10 does approximate a differential curve. Integration of the results for the 4-inch chamber gives very closely the reactivity effects of the 12-inch chamber at the center of the core. An attempt to improve the resolution of these data may be made by consideration of the results for the 4, 12, 20, and 24-inch chambers at the center of the core. The reactivity effects for these chambers relative to the water-filled control-rod aperture are tabulated below:

Chamber			ΔK/K, percent			ΔK/K Inch* chamber void
Nominal length, in.	Weight, gm	Volume, cc	Air filled	Water filled	Void effect	
4	168.6	143	0.087	0.034	0.053	0.0133
12	375.1	418	.156	.051	.105	.0088
20	520.7	723	.073	.029	.044	.0022
24	604.1	850	.032	.032	.000	.0000
24	603.2	859	.024	.033	-.009	-.0004

*One inch chamber length is equivalent to 35.5 cc of void.

The reactivity per inch of chamber void tabulated is plotted in figure 12 against chamber length (one-in. of chamber length is equivalent to 35.5 cc of void). The data indicate a reasonably smooth curve, which extrapolated to zero chamber length, indicates the differential void effect at the core midplane. In a similar manner, the void effect curves of figures 10 and 11 for the 4-inch and 12-inch chambers may be plotted and curves extrapolated to zero chamber length; several of these curves are shown.

The resulting differential void effect curve is shown in figure 13 as the variation of fractional void coefficient with core height. This fractional void coefficient $\Delta K/K/\Delta V/V_{H_2O}$ expresses the percent change in reactivity per percent displacement of water from the core. For purposes of deriving these void coefficients, it was assumed that the 7 by 3 fuel element loading consisted of standard fuel elements. The water volume was taken to be 47,030 cc and the aluminum volume of the core was taken to be 34,100 cc resulting in an aluminum-water volume ratio of 0.726. Therefore one inch of chamber length, which is equivalent to 35.5 cc of void, represents 0.0755 percent displacement of the water volume of the core.

The differential void effect curve, shown in figure 13, is most accurate near the core midplane; although the negative reactivity portions of the curve have been extrapolated, the measured void effects for the chambers used are reasonably well integrated from the curve. The positive void effect from -7 inches to +7 inches relative to the core midplane (a

void of 500 cc) is +0.135 ΔK/K percent; the void effect for the entire height of the core (a void of about 850 cc or 50 cu in.) is closely zero ΔK/K.

These results indicate that for some reactor designs, displacement of water by air or steam in regions of high statistical importance can introduce significant positive reactivities. Although continued displacement of water will finally introduce strong negative reactivities, a negative void coefficient may not always exist.

The reactivity effects of the 24-inch chamber filled with various materials relative to the water-filled control rod aperture are tabulated below:

Chamber			Material in chamber	ΔK/K, percent
Nominal length, in.	Weight, gm	Volume, cc		
24	604.1	850	Graphite powder (475.9 gms)	+0.158
			Water	+.032
			Air	+.032
24	603.2	859	Silica aerogel (76.9 gms)	+0.032
			Water	+.033
			Air	+.024

It may be seen that displacement of water by graphite powder (apparent density 0.56) introduced a net reactivity of +0.126 ΔK/K. Displacement of water by silica aerogel (apparent density 0.089) introduced a net reactivity of -0.001 ΔK/K. In both cases, the very low absorptivity but significant scattering properties of these materials, resulted in a positive reactivity over the cases in which the chambers were air filled and so effectively voided.

REACTIVITY EFFECTS OF VOIDING FUEL ELEMENT WATER PASSAGES

A standard fuel element was modified by welding aluminum manifolds to the top and bottom so that the seventeen individual water passages between fuel plates could be selectively voided in any combination. The water passages were voided by blowing air through any of 34 plastic air tubes extending from the top of the reactor pool to the modified fuel assembly in the core. This modified fuel assembly occupied successively

the number 25 grid position at the center of the core and the number 35 grid position at the interface of the core and the thick BeO reflector (the 35 grid position corresponds to the "hot-spot" region in the NACA Research Reactor core).

The water passages were voided in two sequences. One sequence was used in which the interactions of each voided water passage were minimized by keeping the voided passages as far apart as possible. A second sequence was used in which the interactions were maximized by successively voiding adjacent water passages and so enlarging the voided region at the center of the fuel element. These sequences are illustrated in figure 14 in which the 17 water passages are lettered. The successive order of voiding and water passages voided are indicated. In these sequences as many as twelve water passages were voided cummulatively. A leak between water passages i and j in sequence I necessitated voiding these two passages simultaneously.

The reactivity per incremental water passage voided in the maximum interaction sequence I for the 25 grid position is presented in figure 15(a). The reactivity per incremental water passage voided in the minimum interaction sequence II for the 25 and 35 grid positions are presented in figure 15(b). Voiding of water passages in all cases introduced negative reactivity.

It would have been interesting to have measured the worth of partially voided water passages; from the data presented for voids in the aperture of the control-rod fuel element, one would expect positive reactivity to be introduced by voiding parts of individual water passages near the center of the core.

The reactivity per incremental water passage voided is not very greatly effected by the sequence of voiding indicating that there is little interaction between the voided water passages. However, reactivity per passage is somewhat greater for sequence I than for sequence II for the fuel element in the 25 grid position. The lowered reactivity per passage for sequence II in the 35 grid position is an indication of the reduced statistical importance of this reflector region relative to the central core region.

The cumulative effects of these sequences is presented in figure 16 as the total reactivity introduced as a function of the number of water passages successively voided expressed as a percentage of the water volume in the core. The slopes of these curves represent the fractional void coefficient. For purposes of deriving these void coefficients, it was assumed that the 7 by 3 fuel element loading consisted of standard fuel elements. The water volume of the core was taken to be 47,030 cc and the aluminum volume of the core was taken to be 34,100 cc resulting in an aluminum-water volume ratio of 0.726. Each water passage contains 123.8 cc and represents 0.263 percent displacement of the water volume of the core. The fractional void coefficients $\Delta K/K/\Delta V/V_{H_2O}$ are tabulated on figure 16.

REACTIVITY EFFECTS OF REMOVING FUEL ELEMENT PLATES

A standard fuel element, in which twelve of the eighteen fuel plates were removable, occupied the 25 grid position at the center of the core loading. These fuel plates were removed in two sequences. One sequence was used in which the interactions of each plate were minimized by removing plates farthest apart from each other. A second sequence was used in which the interactions were maximized by successively removing adjacent fuel plates and so forming an increasingly large water region near the center of the loading. These sequences are illustrated in figure 17 in which the removable fuel plates are lettered (fuel plates near the center of the element were not removable due to obstruction by the fuel element handle). The successive order of removal is indicated.

The reactivity per incremental fuel plate removed in the maximum interaction sequence I is presented in figure 18(a). Similar data for the minimum interaction sequence II is presented in figure 18(b). Removal of fuel plates and consequent enlargement of water regions in all cases introduced negative reactivity. The reactivity per incremental fuel plate removed is very greatly effected by the sequence of removal. In sequence I, for example, worth of adjacent fuel plates, increases rapidly as the region devoid of fuel enlarges. On the other hand in sequence II, individual fuel plates from opposite sides of the element have equal worth; the worth of fuel plates from intermediate positions in the element increases slowly.

In these removable fuel plate sequences available core excess reactivity permitted eleven fuel plates to be removed; removal of the twelfth plate, number D, in the maximum interaction sequence I shut down the reactor when the plate was 45 percent withdrawn from the core. At this point the regulating rod was fully withdrawn from the core indicating this portion of the twelfth fuel plate to be worth 0.16 $\Delta K/K$ percent. The accumulated reactivity of the first eleven fuel plates was 2.36 percent. The total excess reactivity available in BSR core loading 53 is estimated therefore to be 2.52 percent. The complete twelfth fuel plate is estimated to be worth at least $0.16/0.45 = 0.36$ $\Delta K/K$ percent. This point is shown in figure 18(a) as a flagged data point.

The worth of the twelfth fuel plate in the minimum interaction sequence II is readily estimated by subtracting cummulative reactivity of sequence II - step 11 from the cummulative reactivity of sequence I - step 12. A reactivity of 0.48 $\Delta K/K$ percent for this fuel plate is shown in figure 18(b) as a flagged data point.

The cummulative effects of these sequences is presented in figure 19 as the total reactivity introduced as a function of mass of uranium removed (each fuel plate is assumed to contain 7.78 grams of fully enriched uranium). The data of each sequence have been extrapolated to estimate the reactivity of the entire 140 gram fuel element in the number 25 grid position; this fuel element is estimated to be worth approximately 6 $\Delta K/K$ percent.

CONCLUSIONS

From the results of these experiments at the Bulk Shielding Reactor certain conclusions may be drawn regarding hazards which might be encountered with a gas-cooled test at the center of the NACA Research Reactor core. The data show that no net reactivity is inserted if a voided chamber without fuel about 1 inch by 2 inches in section extending the full height of the core is completely flooded. This chamber contains a void volume of 50 cubic inches. If a gas-cooled fueled experiment with the same volume is flooded the data show that a reactivity of +0.65 percent is inserted. This result would apply for an experiment which contains 30 grams of uranium-235 distributed as it is in four adjacent BSR fuel plates.

E-103

Tests containing voids and no fuel which occupy less than the full height of the core and are centered on the horizontal midplane would introduce a negative reactivity upon accidental flooding and so tend to shut down the reactor. This is indicated by the data for the smaller chambers; for example, a chamber 1 inch by 2 inches by 12 inches located centrally in the core introduced -0.10 percent reactivity when flooded with water. No data were obtained for chambers containing fuel and voids.

CO-15 back

The data also indicate that removal of fuel from the center of the reactor is always safe. This effect amounted to about -0.011 percent reactivity per gram of uranium-235 for small amounts removed and corresponds to -0.085 percent reactivity for removal of a single BSR fuel plate in the central fuel element.

REFERENCES

1. Lewis Research Center: NASA Reactor Facility Hazards Summary. Vol. I. NASA MEMO

2. Research Reactors. TID 5275.

3. Cochran, R. G., et al.: Reactivity Measurements with the Bulk Shielding Reactor. ORNL 1682, November 19, 1954.

4. Johnson, E. B., et al.: Reactivity Measurements with the Bulk Shielding Reactor: Control Rod Calibrations; Beam Hole Coefficients; Partial Reflector Coefficients. ORNL 1871, September 16, 1955.

5. Johnson, E. B., and Henry, K. M.: Recent Void Experiments with the Bulk Shielding Reactor. American Nuclear Society Meeting, Chicago, Ill., June 8, 1956.

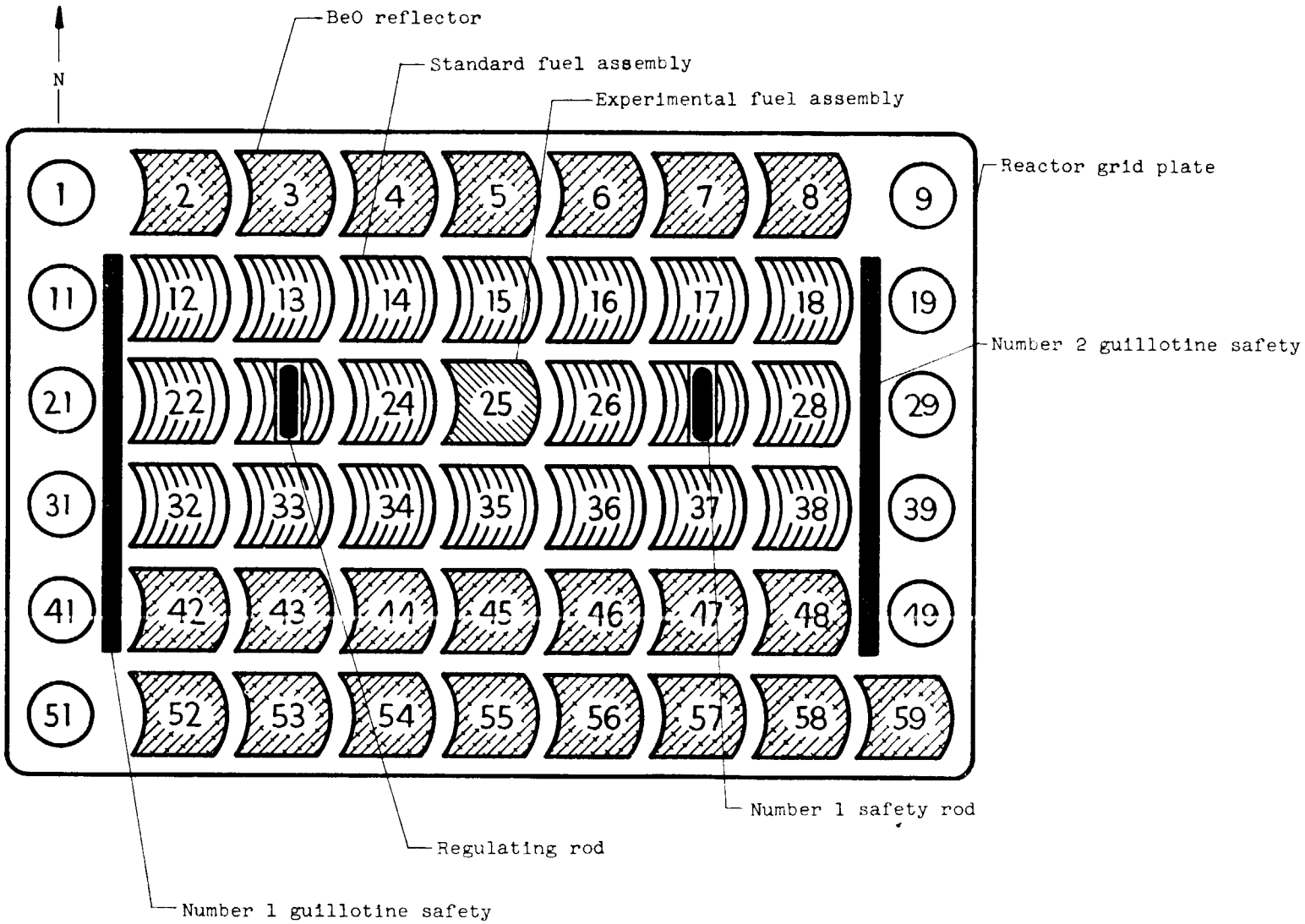

Figure 1. - Reactor loading for NACA reactivity experiments at Bulk Shielding Reactor.

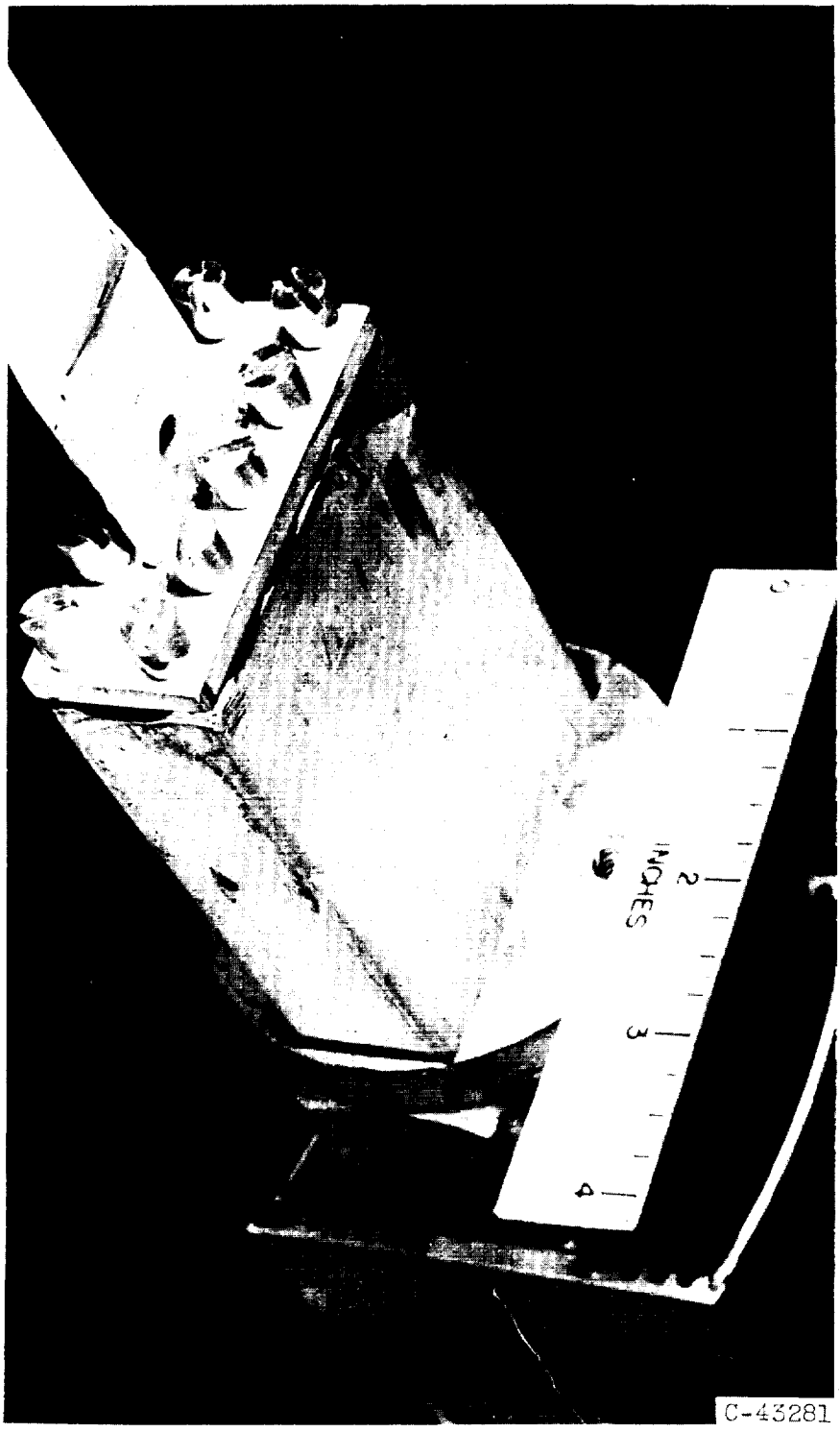

Figure 2. - Standard control rod fuel element with typical aluminum chamber partially inserted.

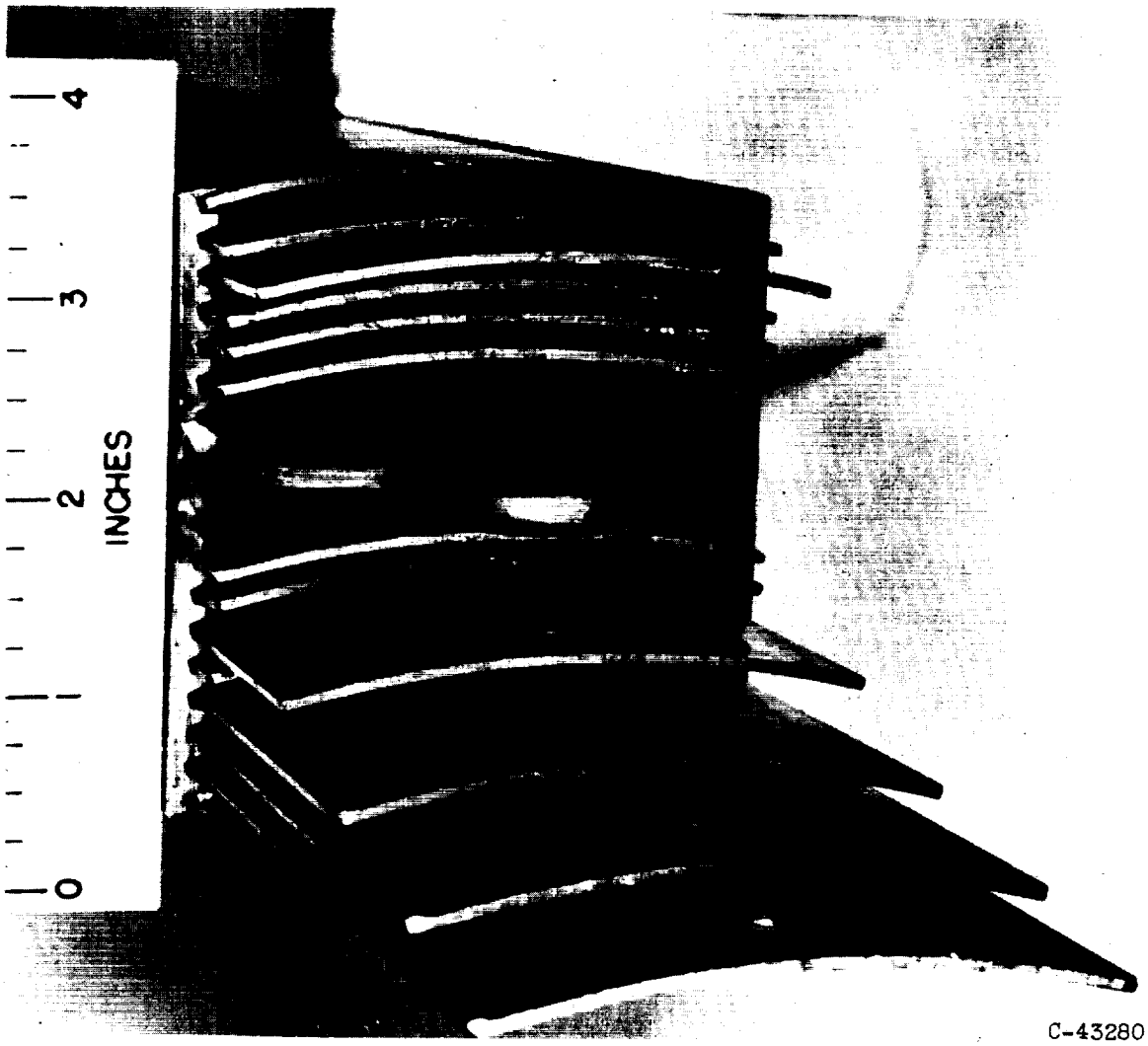

Figure 3. - Removable fuel plate assembly.

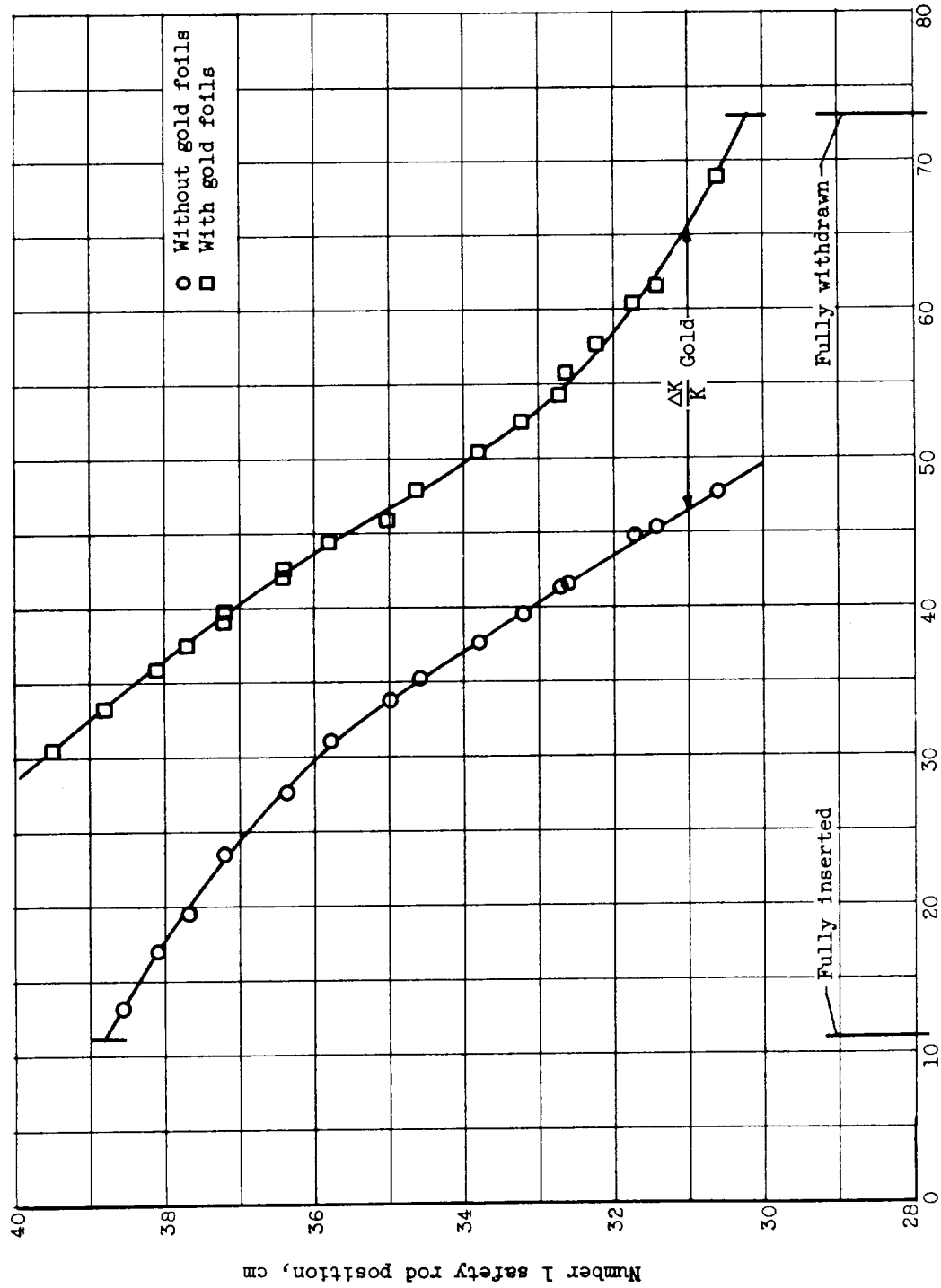

Figure 4. - Regulating rod calibration data for core configuration with both guillotine safeties out.

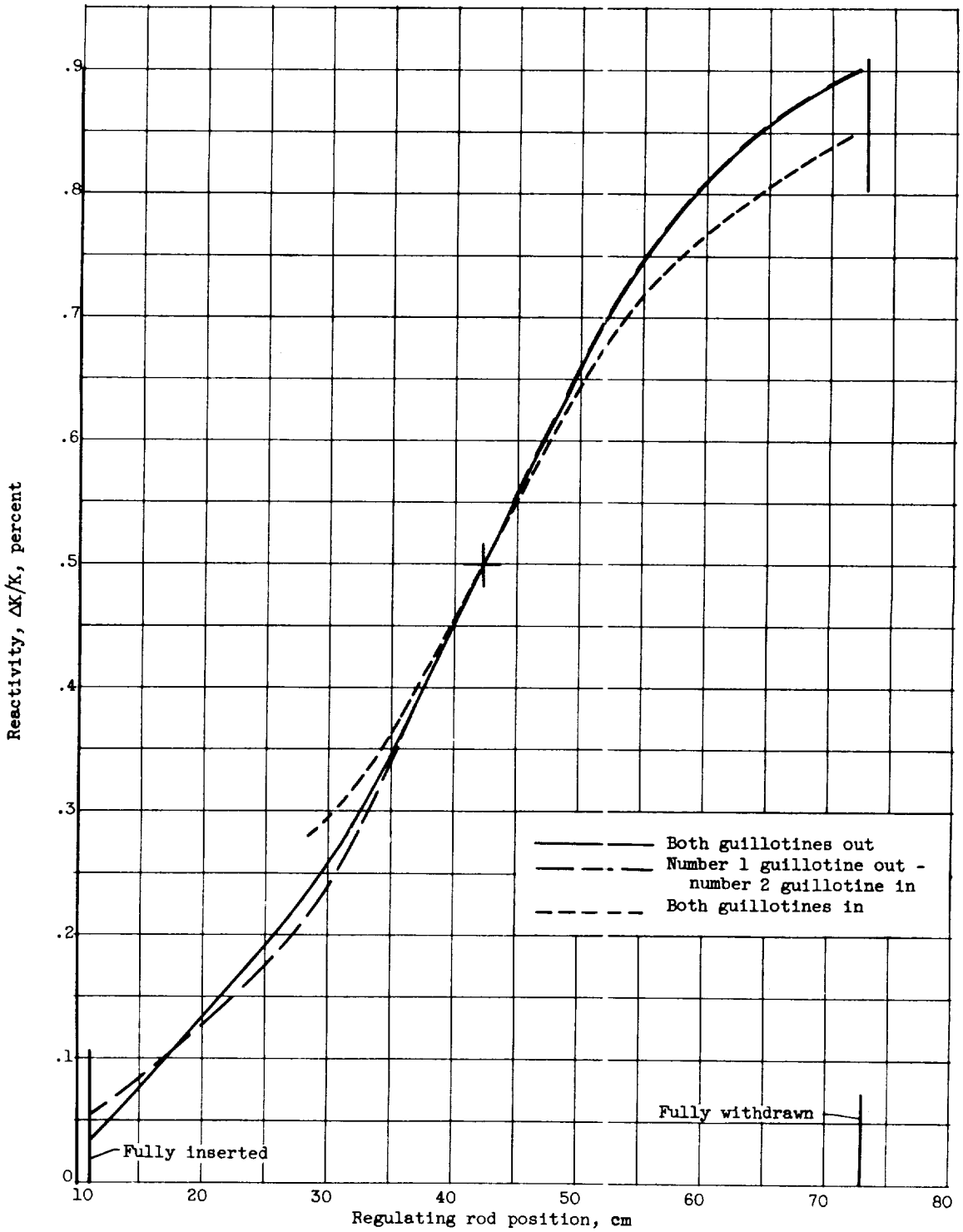

Figure 5. - Integral regulating rod calibration curves for BSR loading 53.

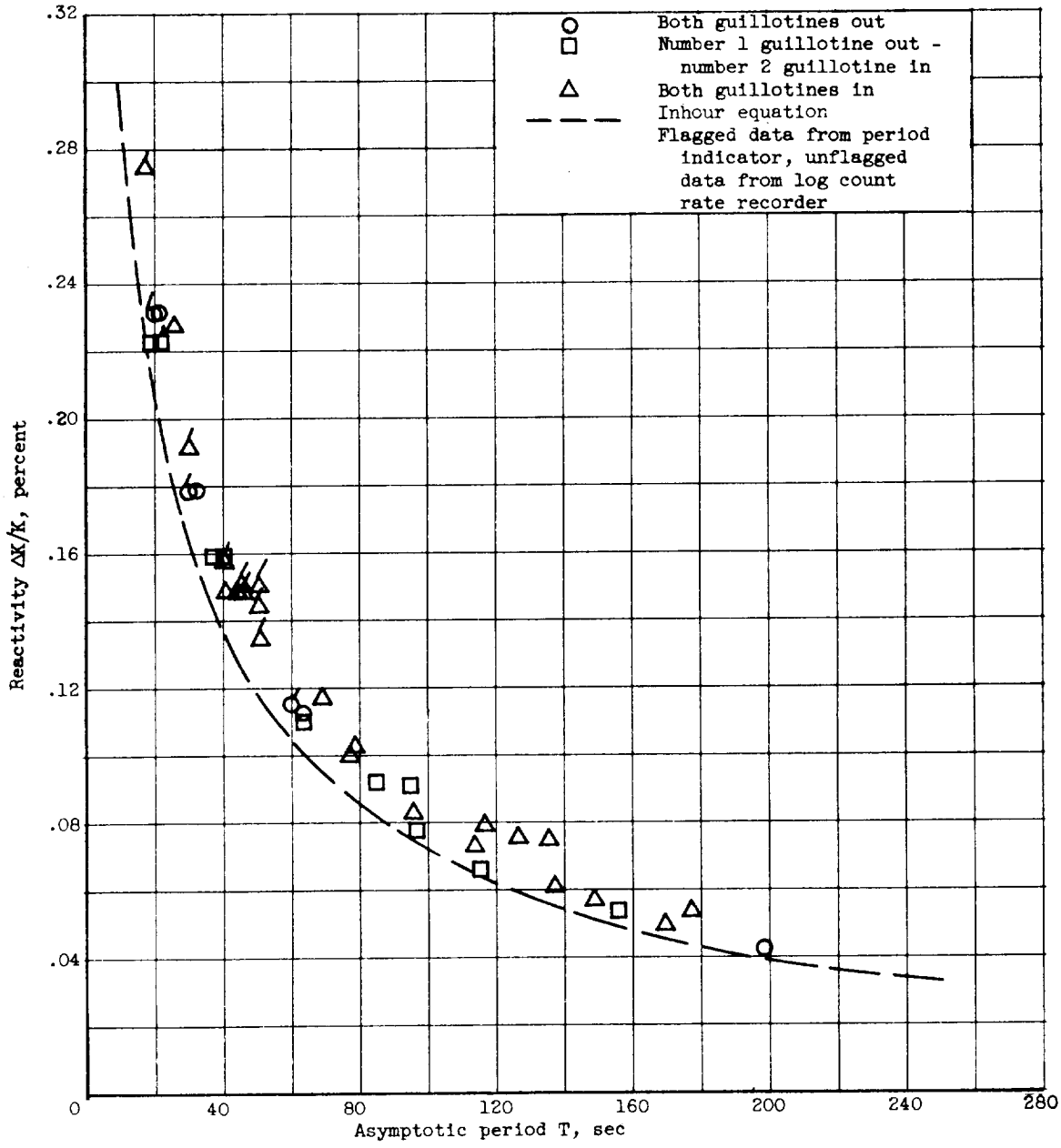

Figure 6. - Reactivity against reactor period for BSR loading 53.

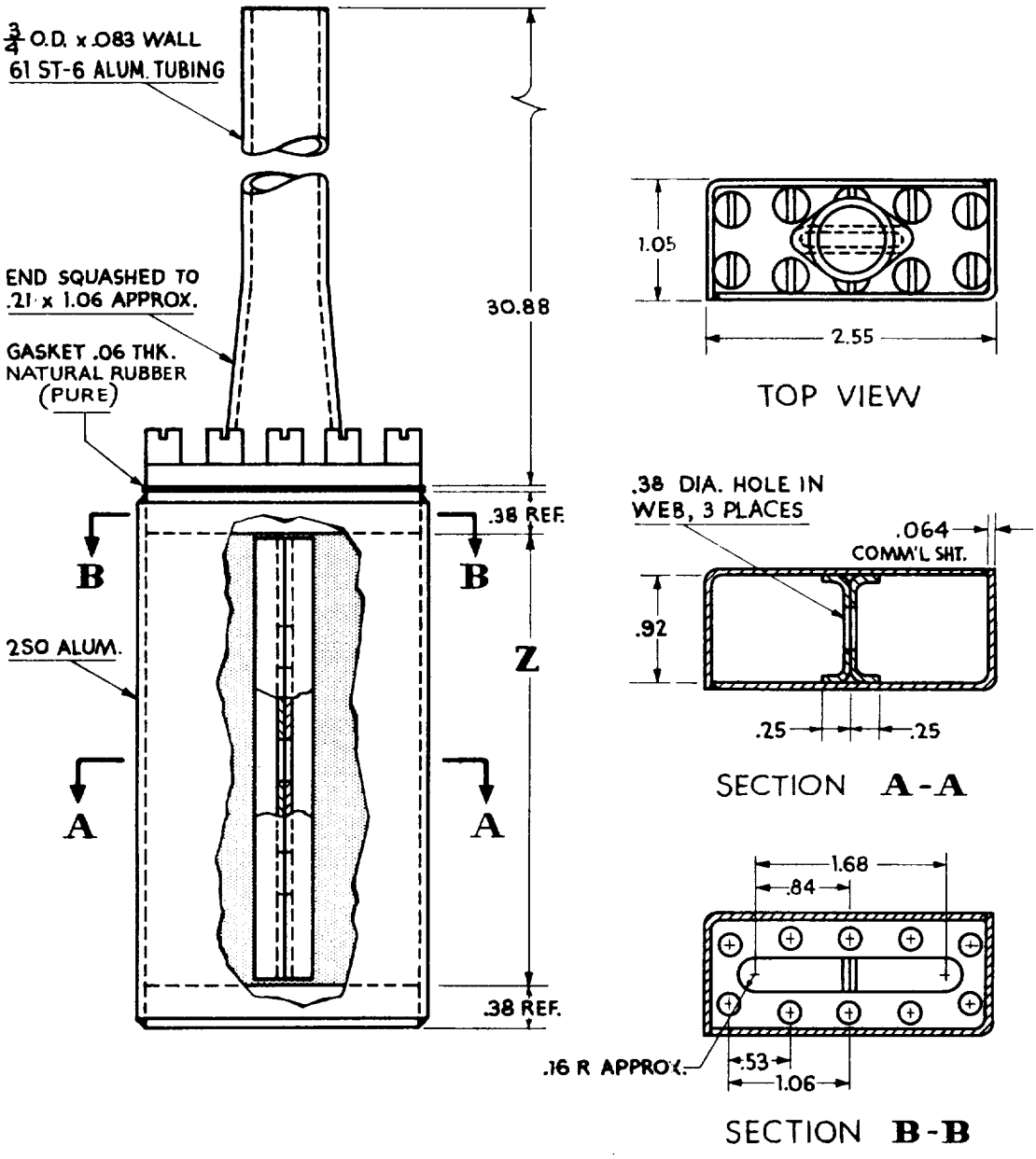

Z	VOID LENGTH, IN.			
	4	12	20	24

Figure 7. - Construction details of aluminum chambers inserted into core.

CO-16 back E-103

Figure 8. - Aluminum chambers with bolted covers and positioning rods.

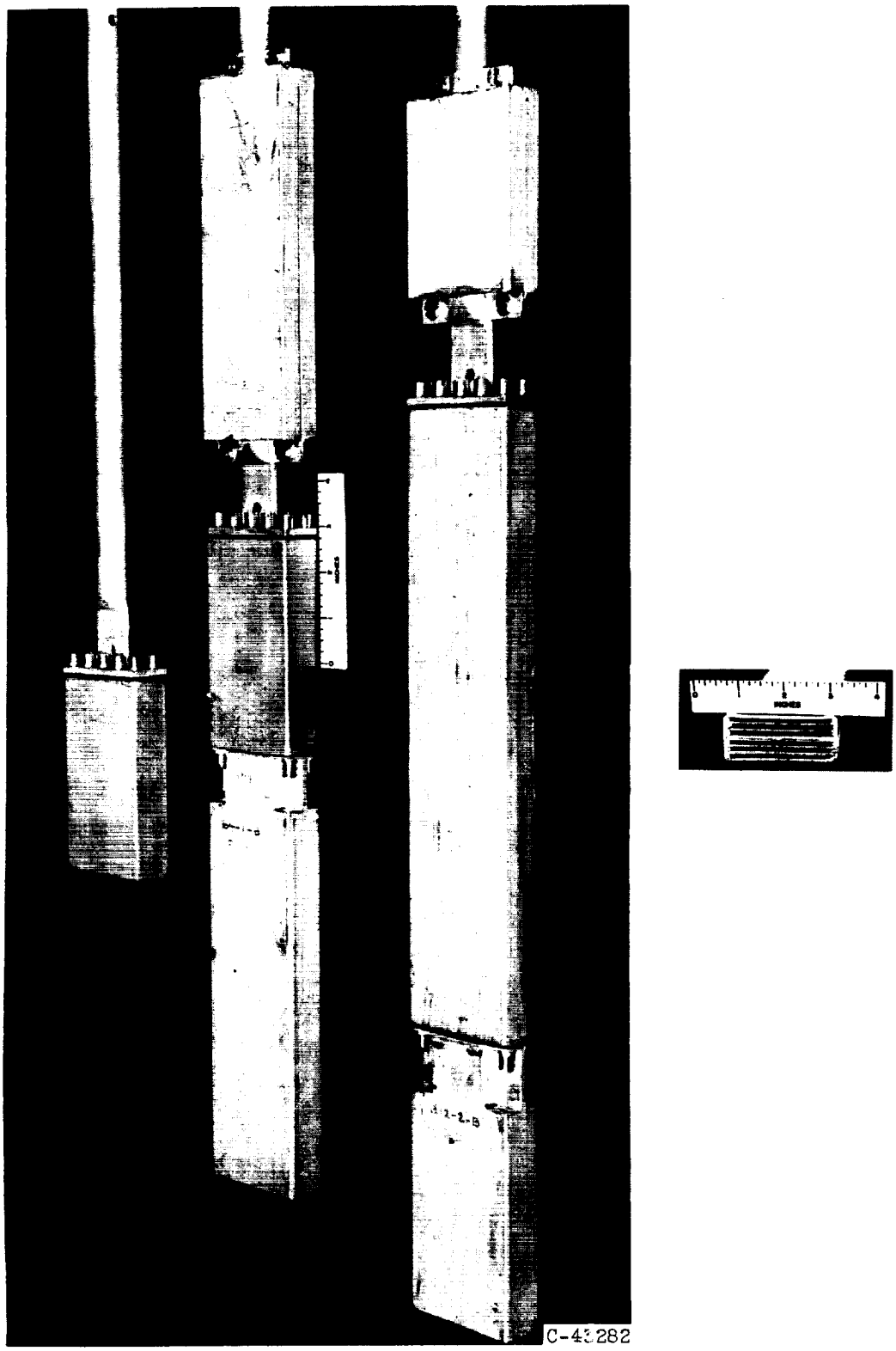

Figure 9. - Chambers with aluminum plate top and bottom pieces.

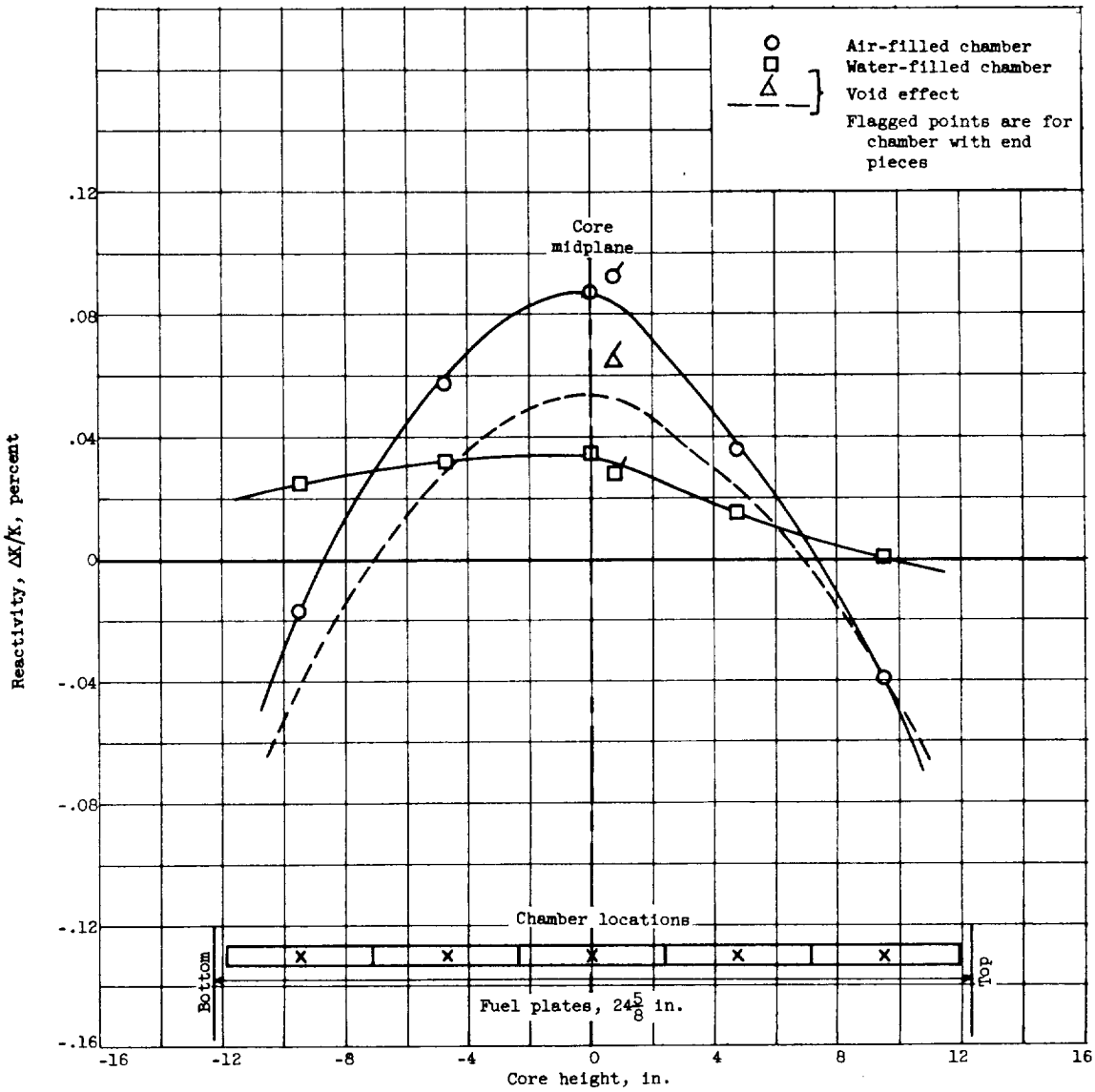

Figure 10. - Reactivity effects of 4-inch 2S aluminum chamber in 25 grid position; empty chamber weight 168.6 gm; inside chamber volume 143 cc.

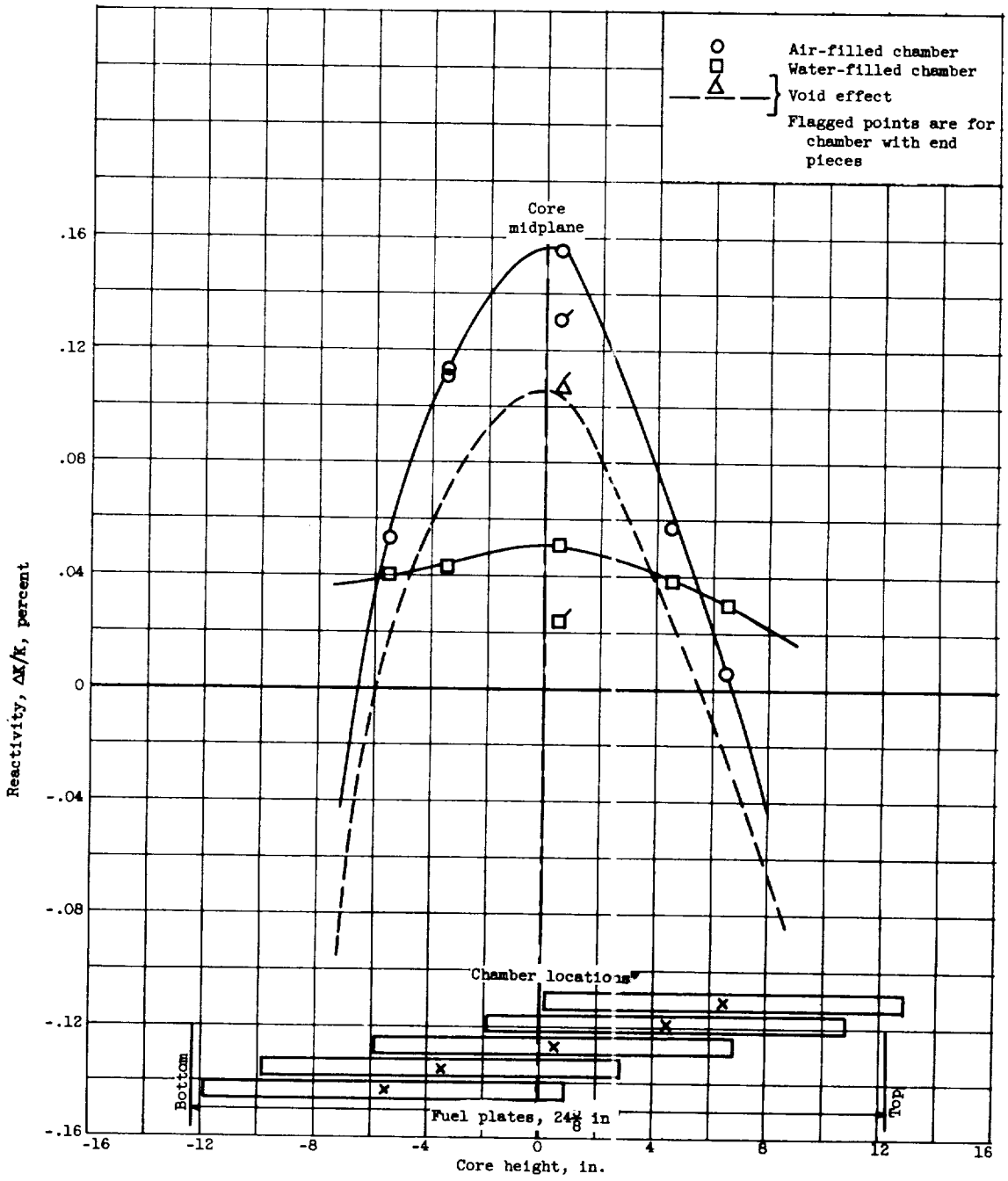

Figure 11. - Reactivity effects of 12-inch 2S aluminum chamber in 25 grid position; empty chamber weight 375.1 gm; inside chamber volume 418 cc.

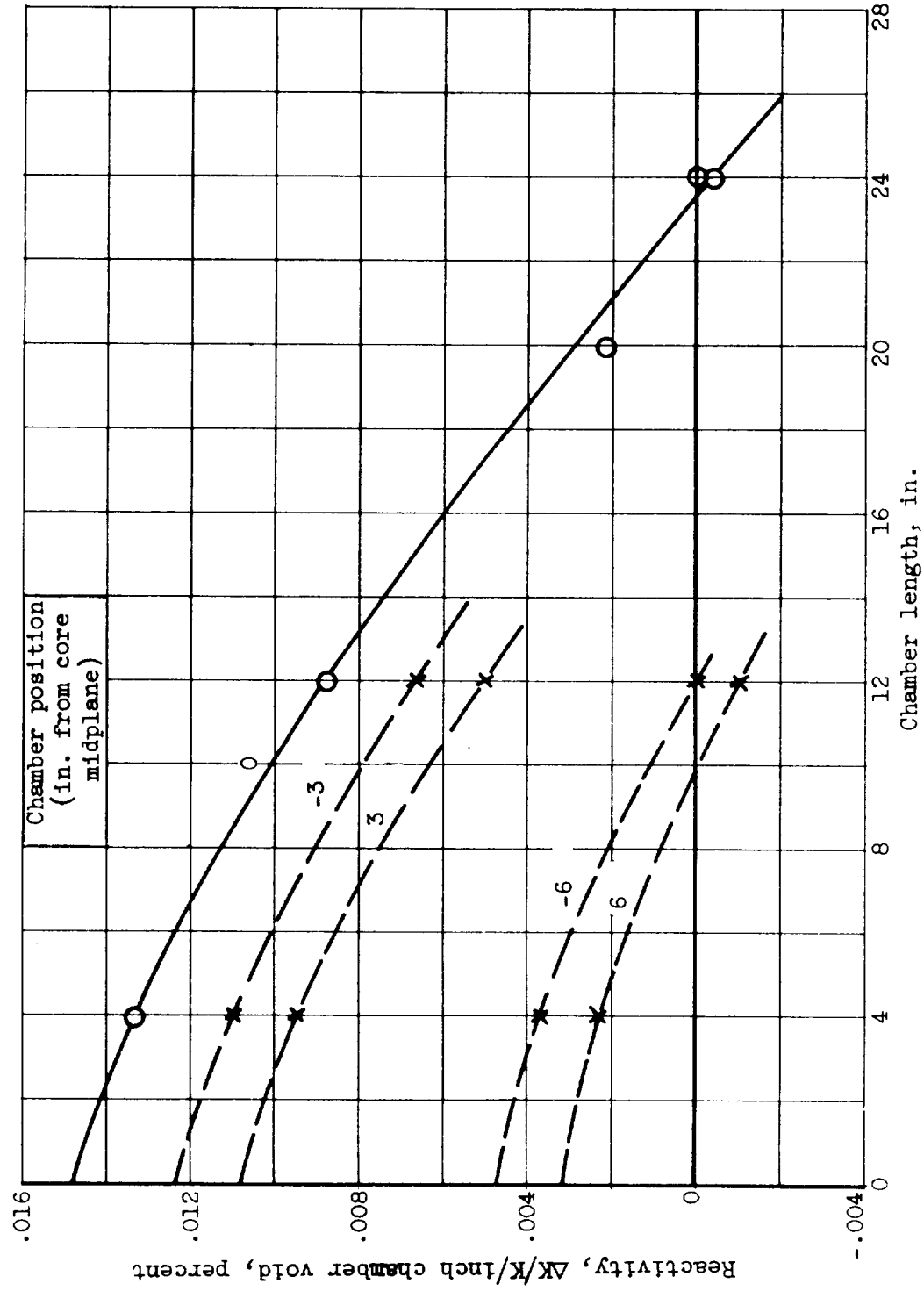

Figure 12. - Reactivity per inch of chamber void for various chambers. (One inch chamber length equivalent to 35.5 cc of void.)

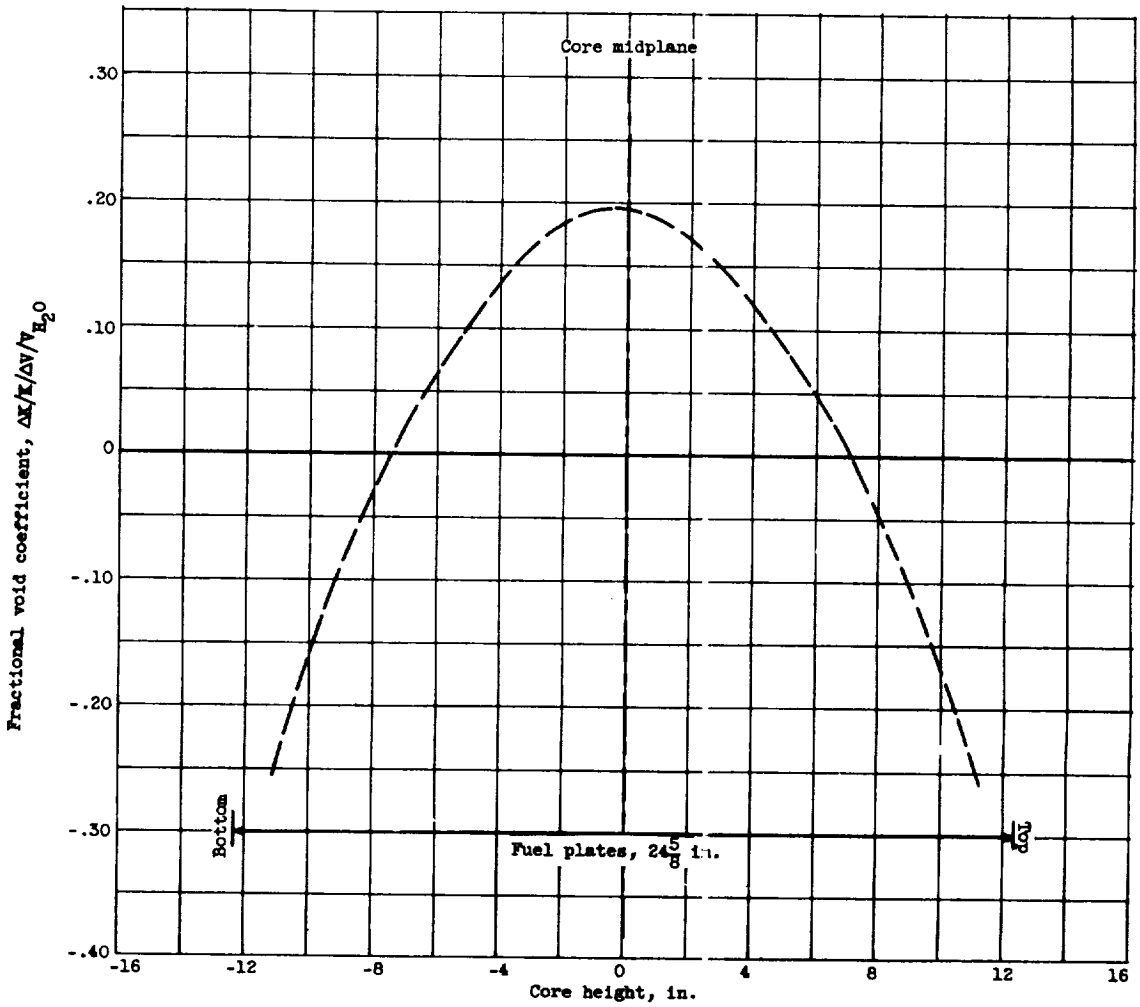

Figure 13. - Differential void effect in control-rod fuel-element at center of BSR loading 53.

BSR standard fuel element

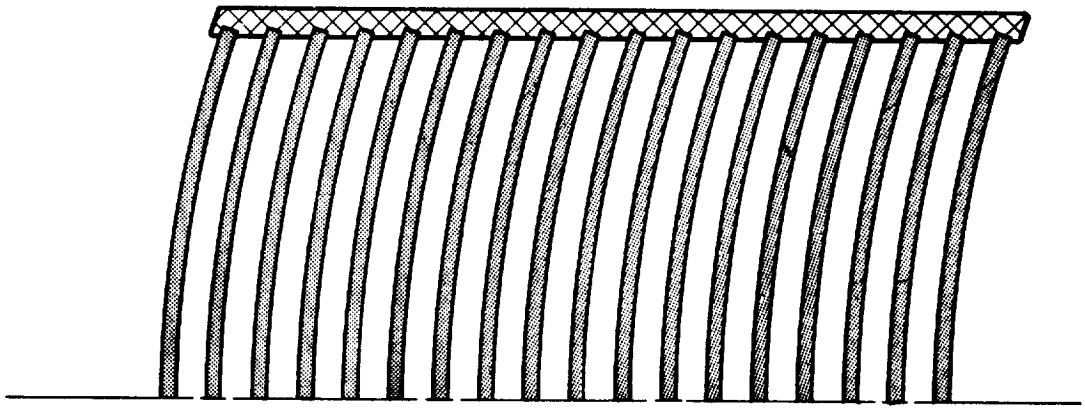

a b c d e f g h i j k l m n o p q

17 Voidable water passages

Maximum interaction Sequence I

1							h								
2								i	j						
3							h	i	j						
4							h	i	j	k					
5						g	h	i	j	k					
6						g	h	i	j	k	l				
7					f	g	h	i	j	k	l				
8					f	g	h	i	j	k	l	m			
9				e	f	g	h	i	j	k	l	m			
10				e	f	g	h	i	j	k	l	m	n		
11			d	e	f	g	h	i	j	k	l	m	n		
12			d	e	f	g	h	i	j	k	l	m	n	o	

Minimum interaction Sequence II

1	a														
2	a														q
3	a									k					q
4	a			e						k					q
5	a			e						k		m			q
6	a		c	e						k		m			q
7	a		c	e						k		m		o	q
8	a		c	e		g				k		m		o	q
9	a		c	e		g		i		k		m		o	q
10	a		c	e		g		i	j	k		m		o	q

Figure 14. - Sequences of voiding water passages in manifolded fuel element.

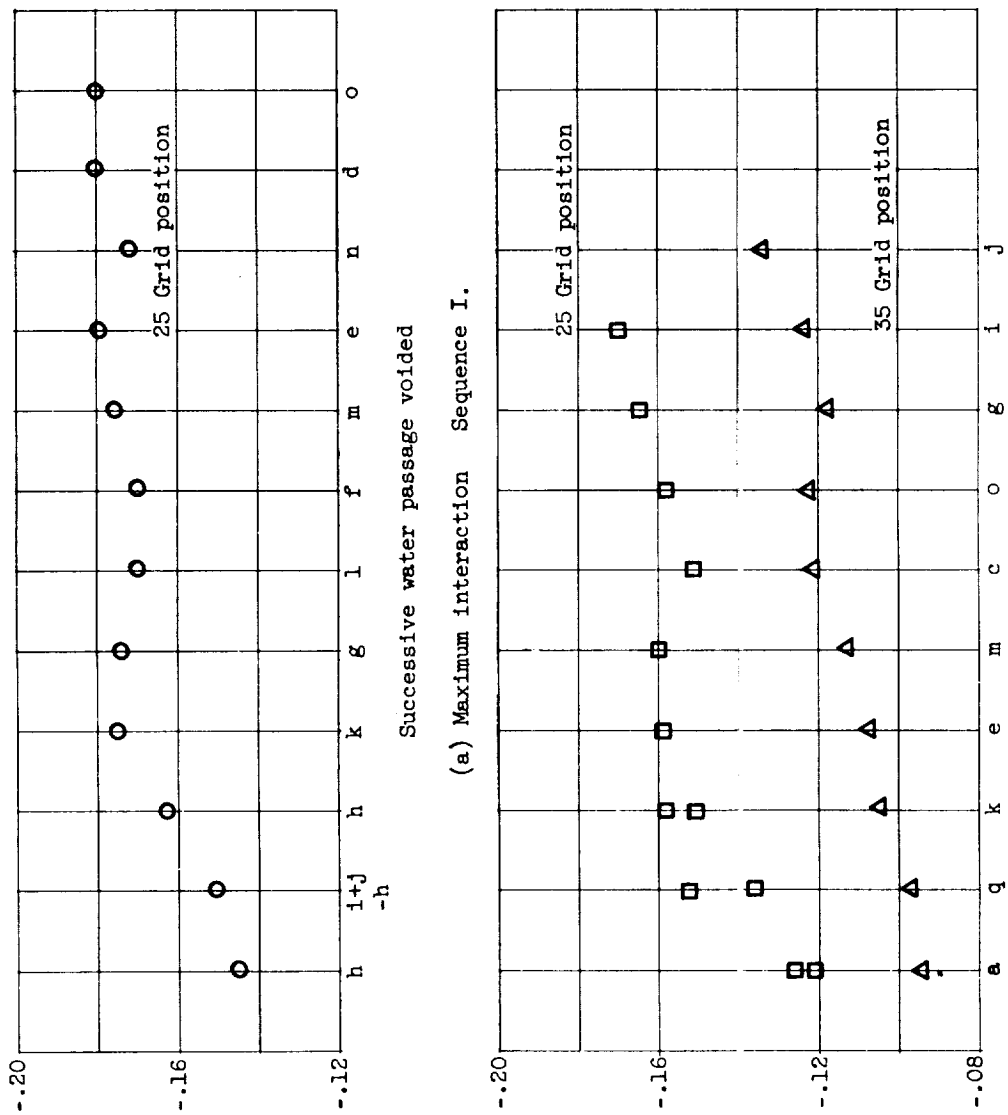

Figure 15. - Reactivity per incremental voided fuel element water passage.

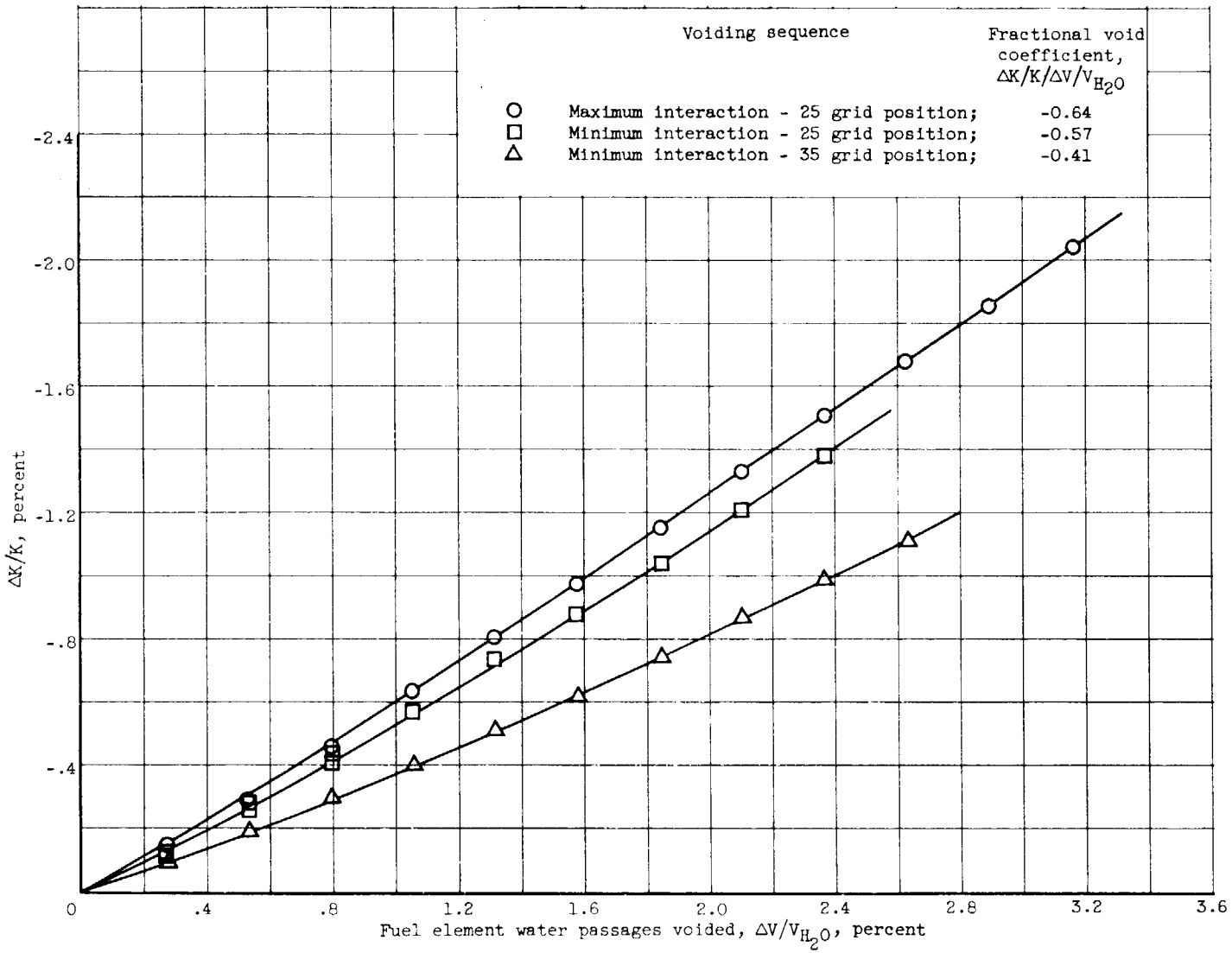

Figure 16. - Cumulative reactivity effects of voided fuel element water passages.

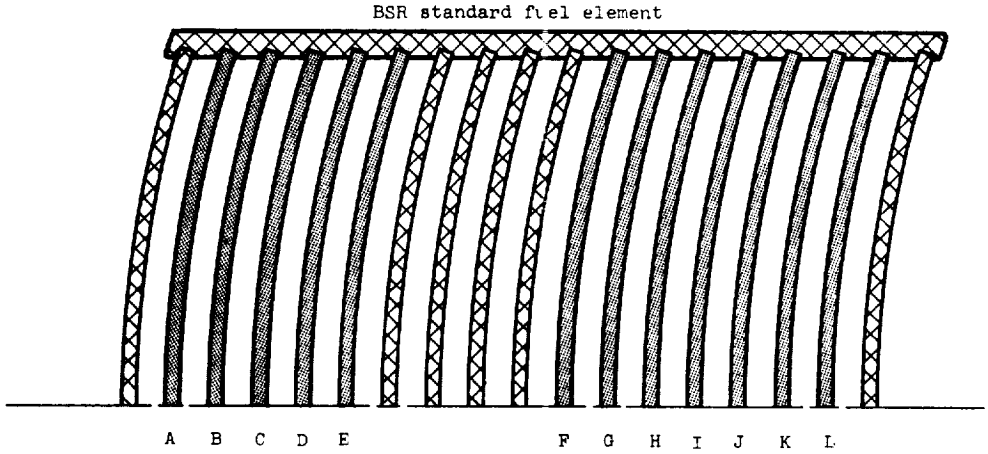

Maximum interaction Sequence I

1									J			
2									J	K		
3								I	J	K		
4							H	I	J	K		
5							H	I	J	K	L	
6						G	H	I	J	K	L	
7						F	G	H	I	J	K	L
8					A	F	G	H	I	J	K	L
9				A	B	F	G	H	I	J	K	L
10			A	B	C	F	G	H	I	J	K	L
11			A	B	C	F	G	H	I	J	K	L
12		A	B	C	D	F	G	H	I	J	K	L

Minimum interaction Sequence II

1					A							
2					A							L
3					A	F						L
4					A	F						L
5					A	F				J		L
6				C	A	F				J		L
7				C	A	F		H		J		L
8				C	A	F		H		J	K	L
9				C	A	F		H		J	K	L
10				C	A	F	G	H		J	K	L
11			A	B	C	F	G	H		J	K	L

Figure 17. - Sequences of removing fuel plates in standard fuel element.

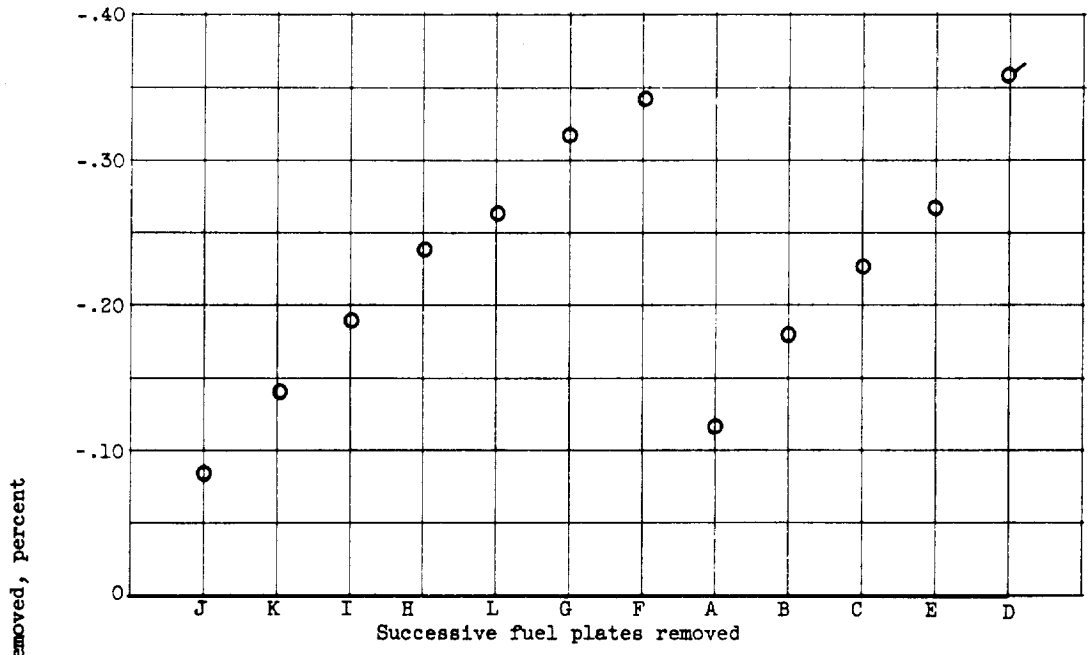

(a) Maximum interaction Sequence I.

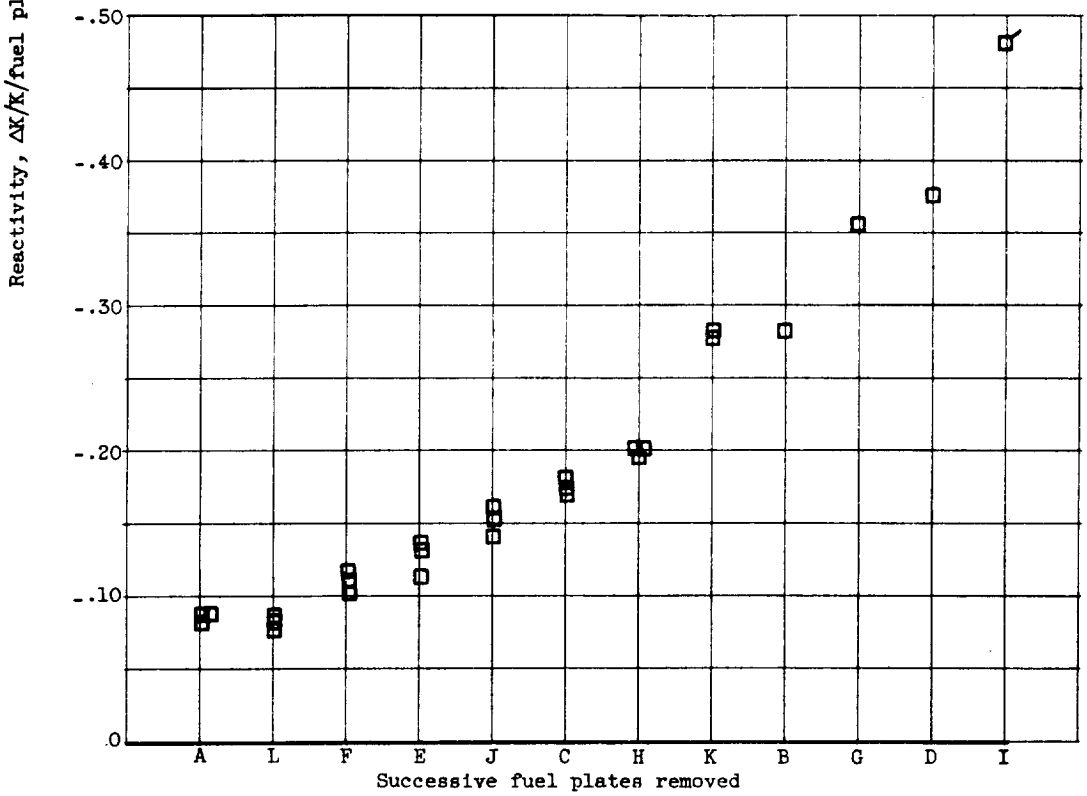

(b) Minimum interaction Sequence II.

Figure 18. - Reactivity per incremental fuel element plate removed.

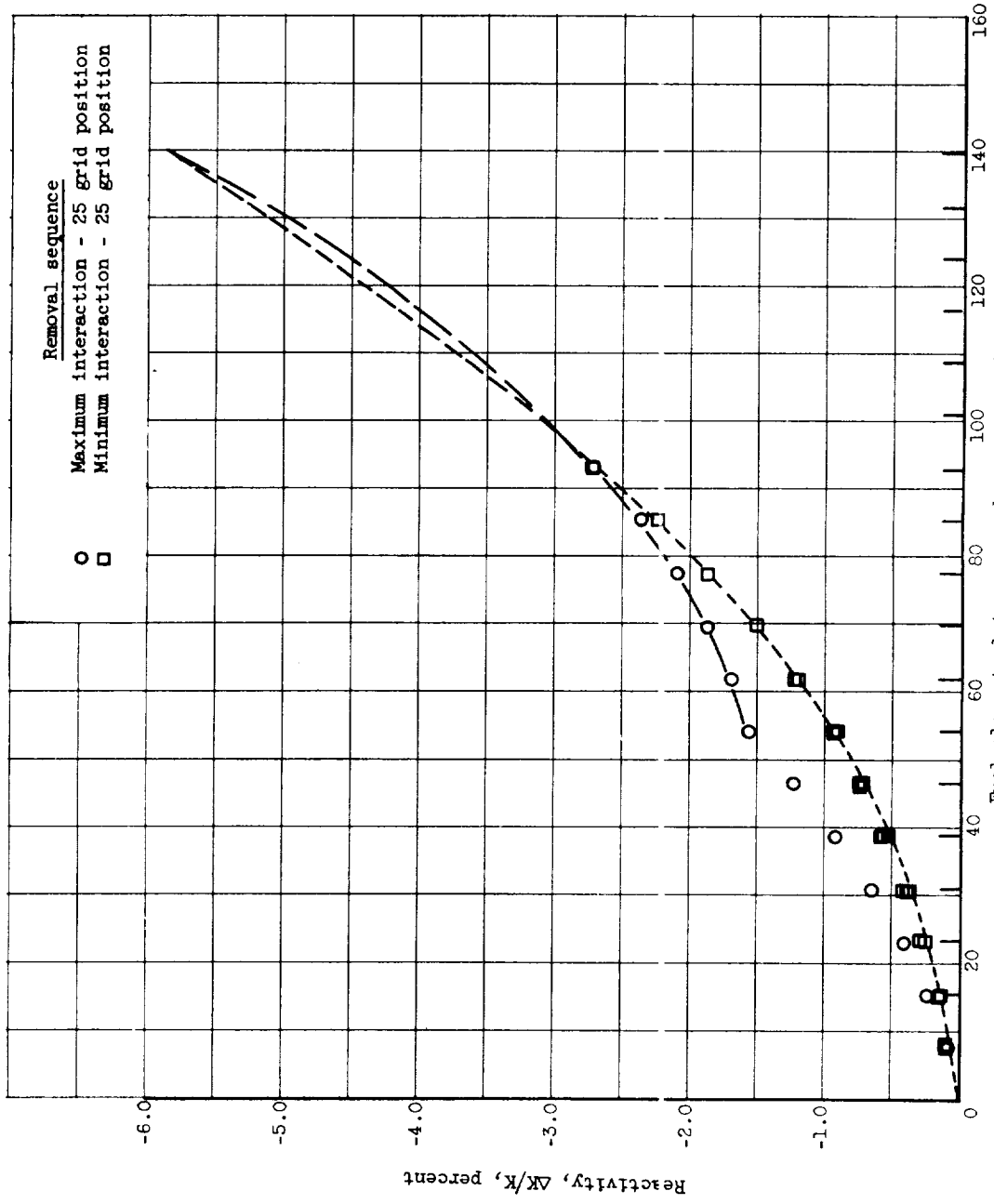

Figure 19. - Cumulative reactivity effects of removed fuel element plates.

IV. ANSWERS TO MISCELLANEOUS QUESTIONS RAISED BY THE ATOMIC ENERGY COMMISSION

March 26, 1957

In order to clarify certain points relative to the safety of the proposed NACA Reactor Facility, the Atomic Energy Commission, in a letter (ref. 1), has requested written answers to a number of miscellaneous questions. These questions had previously been discussed informally in conversation between representatives of the NACA and the AEC. The answers to the six questions of the AEC letter are given herein.

1. QUESTION 1

"As a consequence of malfunction or misoperation of experiment equipment, or in the remote possibility of catastrophic accident to the reactor itself, fission products may be released into the vapor shell. The probability of release of these radioactive materials from the outer vapor container in amounts which would be hazardous to adjacent public areas must be reduced to an acceptable minimum. In order to determine that this has been accomplished, it is necessary to know, among other things, the maximum rate at which it is expected fission products can escape from the vapor container together with an indication of how these rates were determined. This should include the releases expected from the operation of the airlocks as personnel escape from an accident."

The ability of the containment structure to withstand the effects of the worst conceivable accident, and to maintain the integrity of the containment tank (outer vapor container) has been discussed at length in the Hazards Summary report (ref. 2, section 6.4). The maximum rate at which it is expected that fission products could escape from the containment tank is determined by the leakage of air borne fission products out of the containment tank. The discussion of leakage of air borne fission products from the containment tank will be divided into two parts. First the maximum allowable leakage will be considered. Then the design of the containment tank and the methods of checking it so as to assure the maintenance of acceptable leakage rates will be discussed.

1.1 Allowable Leakage Rate

The order of consideration in the establishment of a maximum allowable leakage rate will be

1. Allowable radiation exposure for public in the event of the worst conceivable release of activity

2. Worst conceivable fission product concentration in the air of the containment tank

3. Meteorology as related to the dispersion of fission products

4. Establishment of allowable leakage rate

1.1.1 Allowable radiation exposure for public. - In areas open to the public, the allowable concentration of fission products in air, in the event of the worst conceivable fission product release, is taken to be such that the average exposure over 13 weeks shall not exceed the limits specified in Federal Register, Part 20 Title 10, CFR (ref. 3) for areas where people regularly reside. This is a reasonable criteria since the AEC will accept applications for licenses for the release of fission products in larger than normal amounts provided this above criteria is maintained and provided the half-life in the body of the fission products is less than 60 days (ref. 3). All the gaseous fission products of consequence have half-lives in the body of less than 60 days. The allowable concentration in air for areas where people regularly reside is used for all areas open to the public because, in the case of the NACA reactor, the distance from the reactor to the closest point open to the public, and to the closest residence are about the same.

1.1.2 Worst conceivable fission product concentration in the air of the containment tank. - The most serious conceivable release of fission products would be the result of a catastrophic accident to the reactor itself. The fission product inventory at the time of this accident depends on the operating history of the reactor. The reactor operation has been discussed in the Hazards Summary (ref. 2, section 2.2) and will be reviewed briefly. The reactor is designed to operate for a ten day operating cycle at a constant average power density of 600 watts/cc of active core.

This average power density will give a power of about 30 megawatts at startup when the control rods are about half-way in the reactor and the top half of the reactor is inactive. As time passes and the control rods are withdrawn, the power level will be increased to maintain the average power density of 600 watts/cc. The reactor will not actually generate 60 megawatts until perhaps the last day of the operating cycle. The total operating time would be 240 hours and the average power over the entire operation period would be 40 to 50 megawatts. The down time between operating cycles would be of the order of at least several days. Partially spent fuel elements from the corner of the loading would be moved to the center and new fuel elements would replace these, as described in the Hazards Summary (ref. 2, section 2.2.2). Then a new operating cycle would begin.

Because of the mode of operation at varying total power, the indeterminate length of down time between operating cycles, and the shifting

of fuel elements between operating cycles, the calculation of the exact fission product inventory is more complex than is warranted. Accordingly a conservative assumption was made that the maximum fission product inventory was that which corresponded to a reactor operating continuously at 60 megawatts for a period long enough to saturate all the gaseous fission products of significance. It was then further assumed that all the gaseous fission products in the inventory were released in the accident and mixed uniformly in the 451,000 cubic feet of air in the containment tank. The gaseous fission products considered were

E-103

Kr^{83}	Xe^{133}	Br^{83}	I^{131}
Kr^{85} (2 isomers)	Xe^{135} (2 isomers)	Br^{84}	I^{132}
Kr^{87}	Xe^{137}	Br^{85}	I^{133}
Kr^{88}	Xe^{138}	Br^{87}	I^{134}
Kr^{89}	Xe^{139}	Br^{88}	I^{135}
Kr^{90}	Xe^{140}		I^{136}

CO-18

All fission products were assumed saturated except the long lived isomer of Kr^{85}. Only a negligible amount of this fission product would be present.

It was further assumed that all of these fission products remained in the air of the containment tank for the entire length of time considered (13 weeks). This is a rather conservative assumption inasmuch as the boiling points of bromine and iodine are 138° F and 361° F, respectively, and it might be expected that a considerable amount of these products would condense out in a thirteen week period. The effect of this assumption on the allowable leakage rate will be discussed later.

Since very low leakage rates over long periods of time are being considered, it is expected that a large portion of the nongaseous airborne activity would be deposited on the walls and floors of the containment tank or "filtered out" at the leak locations. Therefore, the nongaseous fission products were not considered. It is felt that any optimism in this assumption is more than compensated for by the conservatism inherent in assuming that there are 60 megawatts of saturated fission products in the inventory and that none of the bromine or iodine is condensed out of the air during the entire period under consideration.

In summary, the worst conceivable fission product concentration in air in the containment tank will be taken to be that resulting from the uniform distribution in the air of the containment tank of all the gaseous fission products resulting from the operation of a 60 megawatt reactor

to fission product saturation. It will be assumed that none of the iodine or bromine will condense out of the air in the containment tank during the period in question (13 weeks).

1.1.3 Meteorology as related to fission product dispersion. - The meteorology of the NACA reactor site is discussed in appendix C of the Hazards Summary (ref. 2). All the site meteorology data used in this section come from this appendix.

In order to compute the 13-week average concentration of fission products per unit rate of activity release at any point of interest, it is necessary to compute the instantaneous concentrations at the point of interest for the various types of meteorological conditions encountered and then to sum this over the 13-week period, weighting each type of meteorological condition according to its relative frequency.

The instantaneous concentrations for various types of meteorological conditions were computed using figure 9.1, of Meteorology and Atomic Energy (ref. 4). The assumptions used in performing these calculations are discussed briefly below:

1. Type of source: Since leakage over a long period is being considered and since the points of interest are distant from the reactor, a continuous point source was assumed.

2. Height of release: Release at ground level was assumed, since this results in the maximum fission product concentrations at the points of interest.

3. Distance from the source: The closest areas open the the public are to the North and Northeast (see ref. 2, fig. J-16). In both of these directions the fence is 3000 feet from the reactor. Accordingly, a distance from the source of 3000 feet was used in the calculations.

4. Wind speeds: The wind speeds were broken into four groups and the average velocity of each group was used. These velocities were 1.5, 5.5, 10, and 16 mph.

5. Sutton diffusion parameters n and C^2: The Sutton stability parameter n is a function of lapse rate. C^2 is a function of n and wind velocity. In the site meteorology data, the Weather Bureau only distinguishes between "inversion" and no inversion. For average inversion conditions, n was taken as 0.40 and C^2 as 0.006 for all wind speeds. For average "no inversion conditions," n was taken as 0.22 and C^2 varied from 0.09 to 0.06 with increasing wind speed. These values were taken from table 4.3 and figure 9.4 of reference 4.

The items needed in order to determine the average concentration over 13 weeks at the points of interest are discussed below.

1. Season of the year: Because it combines a large percentage of inversions with a high frequency of unfavorable wind directions and speeds, summer is probably the worst season and it was used in the computations.

2. Frequency of general wind direction: As described in (2) above, the directions of the nearest areas open to the public are North and Northeast. The relative frequency of wind direction in the summer is 15 percent from the South and 21 percent from the Southwest. The chief point of interest is therefore in the Northeast direction (winds from the Southwest) and the frequency of this general wind direction is 21 percent.

3. Frequency of various wind speeds: These are taken from the site meteorology data.

4. Frequency of various lapse conditions: These are also taken from the site meteorology data.

5. Reduction in concentration with distance from centerline of radioactive cloud: The frequency of the general wind direction is given above as 21 percent in the direction of interest, Northeast. It is assumed that all wind directions in the Northeast sector are equally probable with respect to one another. That is, it is assumed that when the wind is blowing in the Northeast direction, the centerline of the radioactive cloud may be anywhere in the Northeast sector with equal probability. The reduction in concentration with distance from the radioactive cloud centerline is determined from figure 9.3 of reference 4 using a distance of 3000 feet and the Sutton diffusion parameter discussed above.

Using the assumptions indicated above, the 13-week average concentration at the critical point (at the fence in the Northeast direction) was calculated to be 2.8×10^{-6} μc/ml, per curie/sec released.

1.1.4 Allowable leakage rate. - The concentration of gaseous fission products per cubic foot of air in the containment tank was computed as described in 1.1.2 for each of the fission products tabulated in 1.1.2. The activity of each fission product as a function of time after the catastrophe was taken from reference 5. From this information, the rate of release of activity in curies/sec, per cubic foot/sec of leakage, was determined for each individual fission product as a function of time. This rate of activity release was then integrated mechanically to give the 13-week average rate of activity release for each individual fission product. Using this information, the 13-week average concentration per

unit rate of activity release at the point of interest given in 1.1.3, and the criteria for allowable concentration discussed in 1.1.1, an allowable leakage rate of 15 cubic feet per day was established.

As mentioned previously in 1.1.2, it is possible that some of the bromine and iodine would condense out of the air in the containment tank during the 13-week period under consideration. If any portion of the iodine does condense out, this would appreciably increase the allowable leakage rate, iodine being the worst offender of the gaseous fission products, e.g., if half the iodine condensed out, the leakage rate could be as high as 30 cu ft/day and still not result in excessive concentrations in the critical areas.

In the event that the fission product release in the containment tank is from an experiment rather than from the reactor itself, the fission product concentration would be much lower than assumed above since the largest experiments contemplated are about one megawatt. In this case, the allowable leakage rate could reach 900 cu ft/day and not result in excessive concentrations in the critical areas.

To aid in the cleanup of radioactive releases in the containment tank, a high efficiency silver nitrate packed tower, such as is presently in use at Hanford, will be installed to remove iodine from the fission gases. The tower will only be used in the event of a radioactive release. The flow capacity is such that the iodine concentration could be reduced about a factor of two each 24 hours. This loop can be operated from the fan house. The allowable leakage rate from the containment tank could be considerably increased, if account were taken of this iodine removal, but inasmuch as the problem of maintaining a leakage rate of 15 cu ft/day is not much different from the problem of maintaining a leakage rate of 100 cu ft/day, it was decided not to rely on the iodine removal. The iodine removal equipment, then, constitutes another safety factor.

1.2 Design and Testing of the Containment Tank

The requirement that the leakage rate not exceed 15 cubic feet per day at the maximum pressure likely to be encountered (2 psi, ref. 2, appendix H), determined much of the containment tank design and testing procedure. The design and testing of the following items will be discussed:

1. Containment tank welds

2. Pipe penetrations

3. Wire and cable penetrations

4. Ventilation system

5. Canal lift gate

6. Truck door

7. Air locks

E-105

1.2.1 Containment tank welds. - All containment tank welds are to be shielded arc, submerged arc, or equivalent welds. All seams in the tank bottom will be lapped and fillet welded with 3/8" fillet weld except seams in the spherically shaped part of the bottom which will be butt welded. Radial seams in the sole plate will be single-butt welds with back-up strips. All seams above the flat bottom plate will be full throat, complete penetration, butt welds.

Each procedure of welding will be in accordance with Section IX of the ASME Boiler and Pressure Vessel Code and the contractor will be required to keep a detailed record of this procedure. The contractor will be required to submit each welding procedure for approval before welding. All the contractors welders will be required to pass qualification tests prescribed in Section IX of the ASME code.

All welds which are accessible from both sides will be radiographed and tested with a Freon or ammonia leak detector, or equivalent. Those welds which are accessible from only one side (welds in the tank bottom) will be checked with a vacuum seam tester. These latter welds in the tank bottom are less critical inasmuch as the space between the tank and the earth will be pressure grouted and any leakage would have to come up through the grout.

1.2.2 Pipe penetrations. - The pipe penetrations will be fillet welded on both sides. The minimum depth of fillet will be 1/4 inch. The welds will be checked with a vacuum seam tester and with a Freon or ammonia leak detector, or equivalent.

All pipes penetrating the containment tank which might conceivably be in use during the operation of the reactor will have emergency shut off valves which will close in the event of overpressure in the containment tank.

1.2.3 Wire and cable penetrations. - Design of a typical wire or cable penetration and associated vacuum system is shown in figure 1. A standard pipe coupling, size as required, is welded into the containment tank. The welding procedure and check is the same as described in 1.2.2 for pipe penetrations. Each end of the pipe coupling is fitted with a seal adapter. Sealant retaining plates are cut to fit wire or cable and installed. Sealant is injected and allowed to cure. The

space between the two seals is maintained at vacuum during reactor operation. The seals are expected to be essentially leakproof and the vacuum system is used primarily to detect excessive leakage. If the pumping rate of the vacuum pump exceeds a predetermined amount, the reactor would be shut down immediately and the seals checked until the faulty ones were discovered and repaired.

The vacuum pump system discharges back into the containment tank and so even the small leakages which are permitted are not discharged to the atmosphere but returned to the containment tank.

1.2.4 Ventilation system. - The containment tank ventilating system has been described in the Hazards Summary (ref. 2, section 2.1). Some changes have been made and some additional detail is now available. The ventilation system for the 100 foot containment vessel are shown in figure 2. Ventilation air will be drawn into the shell at a rate of 400 cubic feet per minute through a filter, two check valves, and a spring-loaded solenoid valve in the 6 inch line. The pressure in the tank will be held at one inch of water below atmospheric. The discharge air passes through another spring-loaded solenoid valve and is compressed to 300 psi by two 200 cfm reciprocating compressors. Four accumulator bottles will be provided for the compressed air, each large enough to run the compressors for 2 and 1/2 minutes without discharging to atmosphere.

Monitors will be placed in the system as shown. The spring-loaded solenoid valves will close and the compressors stop if any of the following occurs:

1. Reactor power goes up to 1.5 times normal

2. High activity in the containment vessel

3. High activity in the outlet line

4. High activity in the accumulator bottles

5. High pressure in the containment vessel

Although the bottles will operate at 300 psi, they will be designed for a pressure of 600 psi with allowable design stresses one-quarter of the ultimate stress for the material used. Tanks three feet in diameter by approximately seven feet long have the required volume of 50 cubic feet per tank. Such tanks would be 0.75 inch thick if constructed of carbon steel.

1.2.5 Canal lift gate. - The location of the vertical lift gate between the containment tank and the canal may be seen in the Hazards Summary (ref. 2, fig. 2.12). Details of the lift gate seal are shown

in figure 3. Only a single seal is used here because, in operation, the outside of the lift gate will have a head of 11 feet of water above the top of the gate. The leakage, if any, would therefore be inward even in the event of the 2 psi pressure on the tank resulting from the worst conceivable accident (ref. 2, appendix H). The gasket in the seal will be of neoprene conforming to ASTM specification D-735-54T, type S. Leakage in the seal would be determined by damp spots on the inside of the seal.

The canal lift gate, and the truck door and air lock doors discussed in subsequent paragraphs (1.2.6 and 1.2.7), are all designed so that an increase in pressure in the containment tank would increase the force on the gaskets of the seal.

1.2.6 Truck door. - The location of the truck door in the containment tank is shown in the Hazards Summary (ref. 2, fig. 2.12). Details of the truck door seal are shown in figure 3. A double gasket is used here and a vacuum is maintained between the two gaskets by the same vacuum pump as is used for the wire and cable penetrations. As in the case of the wire and cable penetrations (1.2.2) excessive leakage would be determined by the pumping rate of the vacuum pump and would force a reactor shutdown. All leakage is pumped back into the containment tank. The gasket material is neoprene of the same specification as for the canal lift gate (1.2.5).

1.2.7 Air locks. - The location of the two air locks are shown in the Hazards Summary (ref. 2, fig. 2.12). Details of the air lock and the air-lock seals are shown in figure 4. The proper operation of the air locks is insured in two different ways. First, there is a mechanical interlock which prevents either air lock door from being opened unless the other is closed and dogged. Secondly, there is a pressure system which always maintains a 1/2 inch water differential pressure across both doors, the pressure being such that the air flow through the door when it is open is always inward.

A schematic diagram of the air lock pressure system is shown in figure 5, and its operation will be described briefly. Two different pressure controllers are used, one controlling the pressure across each door. Each controller is set to maintain 1/2 inch water differentials during normal operation. The control (output) pressure from each controller is fed through a selector valve, the position of which can be controlled from the three areas in question (the containment tank, the air lock, and the building).

In the event of an accident which raises the pressure inside the containment tank above that in the air lock the operation of the inside air lock door would be prevented because of pressure force on the inward-swinging door. Operation of the selector valve would reestablish

the original 1/2 inch differential pressure and the door could then be opened. Once inside the lock with the inner door closed behind, the selector valve is repositioned and the air pressure bleeds off to give proper differential across outside door. (Pressure will again prevent premature opening of the door). Air removed from air lock is pumped back into the containment tank.

The air lock pressure system insures that the pressure differential across the air lock doors is such that the air flow is always inward when either air lock door is open, both in normal operation and in the event of containment tank overpressure. An individual in entering the air lock would therefore bring very little if any containment tank air with him when he entered the lock. Inasmuch as the prevalent air flow is into the containment tank, a rough estimate of the amount of containment tank air that might be forced into the air lock by one individuals body motion is about 5 cubic feet. These 5 cubic feet would mix in the volume of the air lock which is about 500 cubic feet and be diluted. Since the prevalent air flow is again inward when the air lock outer door is opened, perhaps 5 cubic feet of the air lock mixture might be forced out by one individuals body motion. Thus, the passage of one individual through the air lock would release the equivalent of about 1/20 of a cubic foot of containment tank air.

The ventilating system of the containment tank provides, during reactor operation, only enough air for ten people. The number of personnel normally in the containment tank would be less than this. The exit of all personnel consecutively through one air lock would result in the emission of only about 3 cubic feet of containment tank air. This is not serious inasmuch as the allowable leakage rate is 15 cubic feet per day for thirteen weeks.

1.2.8 Summary. - With the design and testing methods described in 1.2.1 through 1.2.7, it is felt that a leakage rate from the containment tank lower than the allowable leakage rate of 15 cubic feet per day could be maintained. The operating policy relative to leakage rate maintenance will be that appreciable leaks would be located and repaired as soon as they became noticeable, even though the total leakage rate from the containment tank were less than allowable.

2. QUESTION 2

"It is the experience elsewhere that radioactivity releases from the experimental equipment around the reactor will occur. This may likely occur also in the NACA reactor. Since this reactor is to be located in an area of high population density, large amounts of radioactivity cannot be discharged to the atmosphere. Thus, if the reactor is to continue to operate after such radioactive releases, some feasible

method of decontaminating the building without release of hazardous amount of radioactivity to the surrounding area must be devised. To determine whether you have adequately provided for such contingencies, we need an outline of your general approach to this problem."

The discussion of this point will be divided into two parts. The approach to the problem of trying to prevent uncontrolled radioactive releases in the containment tank or in the hot lab will be considered first. Then the approach to the cleanup problem in the event that there are releases in spite of all precautions will be considered.

E-103

CO-19

2.1 Control of Radioactive Releases

2.1.1 The experiment container tank. - As observed in reference 1, radioactive releases from experimental equipment will occur. This point is well taken. It is proposed that the experimental loops will be designed as carefully as possible and their operation checked by running out of pile tests of the loops prior to their insertion in the reactor, but in spite of all precautions of this type it is anticipated that some radioactive releases from the experimental loops will occur. This is particularly true with respect to those loops in which fuel elements will be operated in damaged condition. In order to prevent these releases from unduly hampering reactor operation it will be normal procedure to complete "can" all hazardous experiments. An experiment container tank will enclose every pumped loop or other dangerous experiment. The primary coolant will always be recirculated entirely within the experiment container tank. Only secondary coolant lines, and instrument and power leads will penetrate the container. It is anticipated that the experiment container can will be of the order of 6-10 feet in diameter and 10-15 feet long with a snout about 8 feet long which goes into the test hole in the reactor.

The experiment container will be designed, constructed, and tested with all the care given the containment tank of the reactor itself. All penetrations of the experiment container will be of the same type as the similar penetrations of the reactor containment tank discussed in the previous section (section 1.2). The experiment container will be maintained at low levels of temperature and stress and its only function will be containment.

This high integrity experiment container is not as much "extra work" in the NACA reactor as it would be in other reactors, since it would be located in one of the quadrants of the shielding pool and some type of water tight container would be necessary in any event.

Brookhaven National Laboratory and the MTR were visited recently by NACA personnel and discussions took place with the operating personnel of

the proposed method of handling pumped loops, in particular the idea of the experiment container tank. A similar visit to ORNL is to be made within a week. The people at Brookhaven had run one in-pile pump loop experiment which approximated some of the conditions of relevance. The loop was canned in two different sections and though leaks were encountered in both sections of the loop, radioactive material never escaped from the container cans. Brookhaven is currently designing and building a larger version of this loop, which will be canned, and do not anticipate any great difficulties in restricting radioactive releases to the container cans.

A visit was made to the MTR for the special purpose of learning from MTR operating personnel the troubles that they have experienced with large pumped loops. In addition, the NACA method of handling pumped loops was described and discussed with them. It was learned that the releases which have caused building evacuations would have been prevented had the experiments been "canned" as is planned to be done in the NACA reactor. The project engineers who were talked to at the MTR were unanimous in their favorable opinion of the NACA method of handling experiments. Their only criticism of the method was that they believed that the maintenance work would be more inconvenient to do because the experiments must be removed from the reactor each time repairs are necessary.

2.1.2 Leak philosophy. - The philosophy with respect to leaks in the reactor containment tank or in the experiment container tank is as follows. If the leakage from the reactor containment tank exceeds the allowable leakage of 15 cu ft/day, the reactor will be shut down immediately and will remain down until the leakage is reduced to permissible values. In general, any appreciable leak would be repaired as soon as possible after it was detected, even though the total leakage rate from the containment tank was less than 15 cu ft/day. A leakage rate of 15 cu ft/day would shut the reactor down regardless of surrounding circumstances.

An allowable leakage rate will be established for each experiment container tank dependent on the experiment it contains. As in the case of the containment tank, any appreciable leak would be repaired as soon as possible even though the total leak from the experiment container was less than allowable. If the leakage rate from the experiment container exceeds the allowable value procedure will depend upon the status of the experiment. If the experiment has, prior to this time, released radioactivity into the experiment container, then the experiment and the reactor will both be shut down.

If the leakage rate from the experiment container exceeds the allowable and the experiment has not released radioactivity into the experiment container, the experiment alone will be shut down, with only a few exceptions. In the event of an experiment so important that it is deemed

worthwhile to risk contamination of the reactor containment tank to finish running the experiment, the experiment would be permitted to continue to operate. However, no experiment with a damaged fuel element would be permitted to continue in such a case.

If the leakage rate is not excessive in either the reactor containment tank or the experiment container tank, then it is proposed that operation be continued even though there are radioactive releases from the experiment to the experiment container tank.

E-103

CO-19 back

2.1.3 Operating procedure. - As stated previously, the experimental loop would be designed and fabricated as carefully as possible. It would be tested out of pile as completely as possible. It would then be placed in its container tank (which had been tested previously) and both experiment and container tank would be tested as completely as possible. The experiment and its container would then be moved to the reactor building as a unit and located in the shielding pool quadrant while the reactor is down and the quadrant dry. The snout would be inserted in the test hole. All the secondary coolant lines and instrument and power leads which possibly could, would be designed to come up above the level of the top of the shielding pool and the disconnects would be located in air at all times. All handling equipment necessary for the removal of the experiment would be ready and the removal procedure would be rehearsed before the experiment is irradiated. The quadrant would then be flooded prior to reactor start up.

When the experiment is completed, all lines leaving the experiment container would be closed off and disconnected, "afterheat system" coolant and power lines would be connected (these lines provide power and secondary coolant for the afterheat removal system), and the experiment would be removed entirely underwater to the wet storage area of the hot handling section where it will normally be allowed to cool for about 90 days to reduce the level of fission product activity. It is possible that this decay time could be cut down if it becomes desirable (and feasible from the standpoint of after-heat) to dismantle the experiment after a shorter time.

It is planned to bottle the experiment off-gases at moderate pressure. They will be drawn from the experimental container by a vacuum pump in cases where the entire container has been contaminated. In cases where the fuel element is still intact, the vacuum pump will be connected to an enclosure surrounding the machine used to penetrate into the fuel region. Discharge from the vacuum pump will be compressed by another pump which will discharge into one of a group of storage bottles. The second pump and the storage bottles will be located in a pressure vessel so that there will be effectively double containment for the off-gases. It is presently planned that a high efficiency silver nitrate packed tower, such as is now in use at Hanford, will be installed to

remove iodine from the off-gases. Discharge of the off-gases through the iodine remover and out the stack will be permitted only under favorable weather conditions.

The iodine removal equipment will afford several advantages. It will reduce appreciably the storage time for off-gases. In the event of leakage from the storage bottles, the bottle enclosing vessel can be purged of contamination through this equipment. In the event of contamination of the 100 foot containment vessel, downtime can be reduced by recirculating vessel air through the tower. If the high efficiency units become unfeasible for any reason, most of the same type of advantages can be secured with lower efficiency caustic scrubbers by recirculating until the required clean-up is attained.

2.2 Cleanup of Uncontrolled Radioactive Releases

If in spite of all precautions a radioactive release occurs, the principal hazard as far as off-site personnel are concerned are the fission gases. Once the fission gases have been safely disposed of and the contaminated shielding pool water stored in the hot retention basins, orderly cleanup operations such as scrubbing down of walls and floors, etc., can begin. Contaminated liquids and solids could be handled and treated in some of the ways discussed in the Hazards Summary (ref. 2, sections 5.2 and 6.2.3). The problem of fission gas cleanup and safe disposal is perhaps the major problem of the cleanup operation.

2.2.1 Release in the containment tank. - The worst conceivable problem will be considered, namely, the release of all the fission gases from a one megawatt experiment which has run to saturation of all fission products of significance.

If the release occurs in the containment tank, the reactor would be shut down, the containment tank ventilation would be shut off, and the tank would be evacuated. Nothing would be done to cleanup the fission gases until four days had elapsed. This would permit most of the shorter-lived gaseous fission products to decay to low levels, only the long-lived iodines and xenons would be significant. At this time, circulation of the containment tank air through filters and through the iodine removal system would begin. The iodine removal system can reduce the iodine concentration by a factor of about two in twenty-four hours. After about ten days of recirculating the containment tank air, the iodine concentration will have dropped to the point where with reasonably favorable weather conditions, the air in the containment tank could be discharged up the stack without the 13-week average concentrations in areas open to the public exceeding the limits specified in reference 3.

At this time contaminated quadrant water would be pumped to hot storage tanks, the containment tank could be entered after careful survey, and clean-up could proceed at a rate compatible with permissible working times.

An estimate of the total reactor downtime, providing no part of the facility was seriously damaged, would be about 30 days. This length of time is felt to be quite reasonable in view of the fact that any release of radioactivity from the experimental container tank would be an infrequent occurrence and that a release of this magnitude must be viewed as a rather unusual accident.

2.2.2 Release in the hot lab. - The worst conceivable release of activity in the hot lab would occur if one of the bottles (discussed previously in 2.1.3) in which experiment off-gases are stored were to fail. This failure is not serious, inasmuch as all of these bottles are contained in a second pressure vessel and the gases are therefore still contained. At such a time as the fission gases released into the outer pressure vessel had decayed for four days, they would be circulated through the iodine removal system and discharged up the stack as soon as weather conditions were favorable. The capacity of the iodine removal system is sufficient to accomplish this job in less than one day. The inner fission gas storage bottles will be sized so that the 13-week average concentrations in areas open to the public will not exceed the limits specified in reference 3, in the event of the sequence of events described above.

The failure of one of these fission gas storage bottles will be a relatively unusual occurrence and the associated cleanup time of about 5 days maximum, is not unreasonable.

3. QUESTION 3

"If you contemplate releases of radioactive material from the reactor building or hot cells in concentrations greater than permissible under 10 CFR, Part 20 of our regulations, it will be necessary for you to obtain specific approval in your license for such release. Before we can grant such approval, we will need to evaluate the details of your proposed procedure to assure that the health and safety of the public will not be endangered by such release. This we will do later. At the present stage, an outline of how you would approach this problem would be helpful."

Releases of radioactive material from the reactor building or hot cells in concentrations greater than permissible in 10 CFR, Part 20 (ref. 3) during normal or near normal operation are not contemplated. Releases of radioactive material in concentrations greater than in

10 CFR, Part 20 might occur only in the event of three relatively improbable accidents. These accidents have been described above and their cleanup discussed. They are:

1. Borax-type runaway which destroys the reactor (discussed in section 1)

2. Combined failure in an experiment of the fuel element, the experiment loop, and the experiment container tank (discussed in section 2)

3. Failure of one of the gaseous fission product storage bottles (discussed in section 2)

In all of these cases, the release would be only of gaseous fission products, and in all cases the allowable 13-week average exposure does not exceed the limits of 10 CFR, Part 20.

4. QUESTION 4

"With regard to your calculations concerning the effect of the maximum credible accident on the containment vessel, we would be interested in the results of your study in which you assumed the entire energy release to be focused on the shrapnel shield as a projectile."

4.1 Discussion

In order for all the energy release of the maximum credible accident to be focused on the shrapnel shield it is necessary for the top of the 9 foot diameter reactor tank to fail while the barrel of the tank does not fail. From figure 2.9 of the Hazards Summary (ref. 2) it can be seen that the top of the reactor tank is about three feet below the face of the shrapnel shield. The time required, after the failure of the reactor tank top, for the water to reach the face of the shrapnel shield will vary with the pressure level but is of the order of 30 to 100 milliseconds for pressure levels of interest in this case. The length of time required for a rarefaction wave from the reactor barrel to reach the top of the water is of the order of 4 milliseconds. Therefore, if the barrel of the reactor tank breaks either before or shortly after the top of the reactor tank, the rarefaction waves from the barrel will reach the top of the water column before the water column reaches the shrapnel shield and these rarefaction waves will stop the water or slow it to such a point that there will be no appreciable force on the shrapnel shield.

There are only two situations, therefore, in which the shrapnel shield could feel an appreciable force from the water column. One

situation is if the pressure levels were extremely high and the time required for the water to reach the shrapnel shield lower than the 30-100 milliseconds mentioned above. This is just the case in the explosion considered in the Hazards Summary. There the pressures were high and the time required for the water column to reach the shrapnel shield is short. To be completely conservative, it was assumed that the water reached the shrapnel shield "instantaneously." The result, as discussed in the Hazards Summary (ref. 2, appendix I), was that the shrapnel shield rose about 15 feet.

The only other way in which the shrapnel shield could feel an appreciable force from the water column would be if the head of the reactor tank failed, but the barrel did not. This is possible since it is estimated that the reactor tank head would fail at a steady pressure of about 700 psi while the barrel would fail at a steady pressure of about 1100 psi.

Consider pressure rises in the reactor of various periods.

1. If the period is less than 7 milliseconds, the reactor tank barrel will actually fail before the head because, being closer to the reactor, it sees the pressure which existed in the reactor about 1 millisecond previously while the reactor tank top sees pressures which occurred about 4 milliseconds previously.

2. If the period is between 7 and 16 milliseconds, the top will break first but the barrel will break before the rarefaction wave from the top can reach the barrel and reduce the pressure. The rarefaction wave from the barrel will reach the top of the water column before the water reaches the shrapnel shield.

3. If the period is between 16 and 26 milliseconds, the rarefaction wave from the tank top reaches the barrel and reduces the pressure so the barrel breaks at a later time. However, the rarefaction wave from the barrel still reaches the top of the water column before the water reaches the shrapnel shield.

Therefore, pressure periods of the order of 30 milliseconds or longer are required in order for the shrapnel shield to feel any appreciable force in this situation. But every method of analysis considered in appendix F of the Hazards Summary indicates that the maximum pressure excursion pressure would not exceed the 700 psi required to fail the tank head unless the power period were shorter than 10 milliseconds. It therefore appears that this very slow rate of pressure rise for an indefinite period could probably not occur because of the self-regulating features of the reactor and it was for this reason that the subsequent analysis was not included in the Hazards Summary.

Suppose it is assumed that somehow the pressure did rise very slowly and that the self-regulating mechanism was inadequate to shut down the reactor and that the reactor tank top failed. Four milliseconds later the rarefaction wave from the tank top would reach the reactor core and the volume of void in the core would be considerably increased due to the lowering of the pressure which would increase the volume of voids already present and would flash some water due to the lowering of the saturation temperature. At this point the reactor would probably shut down due to the self-regulating mechanism and the force of the water when it struck the shrapnel shield would not be very great.

However, if it is assumed that the reactor does not completely shut itself off, but continues to operate in the chugging fashion which has been observed in some reactors, then the formation of steam will drive the water column into the shrapnel shield like a piston and essentially all the energy of the excursion will be "focused on the shrapnel shield as a projectile." The shrapnel shield would be accelerated upward until the sides of the shrapnel shield cleared the concrete a sufficient distance for the pressure inside the reactor tank to be relieved and then would continue upwards, decelerating until it reached the peak of its travel.

4.2 Analysis

A computation was carried out of the above course of events. The equations used were

$$a_1 = \frac{(P_s - P_o)A_w - W_s}{M_w} \tag{1}$$

$$a_2 = \frac{(P_s - P_o)A_w - (W_s + W_{ss})}{M_w + M_s} \tag{2}$$

$$v_s = \frac{hA_w}{W_s} \tag{3}$$

where

a_1 acceleration of the water column before it contacts shrapnel shield

a_2 acceleration of the water column after it contacts shrapnel sheild

P_s steam pressure in the core

P_o ambient pressure in the containment tank

A_w cross-sectional area of the water column

W_s weight of steam generated

M_w mass of water column

W_{ss} weight of shrapnel shield

M_s mass of shrapnel shield

v_s specific volume of steam

h height of rise of water column

The steam pressure P_s and the specific volume v_s were related by assuming the steam to be saturated. The rate of steam generation was assumed constant at a value representing the average of the "chugs." A reasonably conservative value for computation purposes seemed to be a steam generation rate representing a power level of 10 megawatts (refs. 6, 7, and 8). The height at which relief occurred was estimated as follows. The pressure P_s at which the acceleration a_2 would be zero was determined from equation (2). The steam volume generation rate was computed at this pressure. The height of the shrapnel shield which would leave a gap large enough so that the water volume flow from the tank at this pressure would be equal to the steam volume generation rate was taken to be the height of complete relief. Equations (1), (2), and (3) were integrated numerically up to the height of complete relief. No relief was considered up to this point, a conservative assumption. For the remainder of its rise, the shrapnel shield was assumed to be only under the influence of gravity.

The height of rise of the shrapnel shield calculated by this method was 1.8 feet and the total energy generated in the chugging portion of the excursion up to the time the "height of complete relief" of the shrapnel shield was attained was about 23 megawatt seconds. To get some idea of the sensitivity of these results to the average power level assumed in the chugging phase (10 megawatts), a similar computation was carried out assuming an average power level of 20 megawatts. The corresponding values were found to be 2.3 feet rise and 27 megawatt seconds of energy in the chugging phase. Therefore, the results are not particularly sensitive to the assumed average power level. The height of rise is, in both cases, considerably less than the height of rise calculated in the Hazards Summary for the equivalent TNT explosion which was about 15 feet. The foregoing analysis is crude but the height of rise computed is sufficiently low that refined analysis is unwarranted.

5. QUESTION 5

"Your calculations of the effect of the maximum credible accident assumed that the energy release takes place at the rate of a TNT explosion. If such a study is at all feasible, we would be interested in similar calculations in which the energy release is equated to some explosive which burns slower than TNT."

In our calculations of the effect of the maximum credible accident, it was assumed that the energy release takes place at the rate of a TNT explosion because it was felt that the destructive effects would be greater than if a slower release rate were assumed. This was felt to be the case because of several reasons of which the following two are perhaps most significant.

1. A slower release of the energy would result in lower pressure levels and possibly longer durations. In many cases, the duration of the force is determined, not by the duration of the primary pressure wave, but rather by the time at which a rarefaction wave relieves the primary pressure wave. A typical example is the force on the 70 feet diameter shielding pool wall. The force on this wall would be greatly relieved when a rarefaction wave from the pool surface reaches the wall a short time later. This time interval is independent of the pressure level (ref. 2, appendix H). Thus, for situations of this type, a slower release of energy would result in lower pressure levels, but not in significantly longer durations and the fast energy release would be more destructive.

2. At the lower pressure levels of the slower energy release, the material may be able to resist the forces. A typical example of this is in the shielding pool floor. At distances from the reactor centerline of 25 feet or more, the peak pressures on the floor due to the equivalent TNT explosion are estimated as 6000 to 10,000 psi (ref. 2, fig. H.1). The dynamic crushing strength of concrete is between 5000 and 6000 psi (ref. 9) and therefore any appreciable reduction in pressure levels would result in the concrete not being crushed. Thus, for situations of this type, the fast energy release would be more destructive.

The recent model tests conducted by the Ballistics Research Laboratories of the Aberdeen Proving Grounds for the Wright Air Development Center (ref. 10) strongly substantiate our feeling that the fast energy release of a TNT explosion is more destructive than the slow energy release of a propellant. Ten charges of different sizes were exploded in a quarter scale model of the proposed WADC Nuclear Engineering Test Reactor. Six of these charges were explosives, four were propellants. The results indicated that the explosives did considerably more damage. A direct quote from reference 10 best describes the comparison.

"Comparison of the results from propellant and explosive show the strong dependence of damage on rate of energy release. Round 3, with a full-scale equivalent energy of 278 megawatt-seconds released relatively slowly by burning a propellant, produced about equivalent damage to Rounds 4 or 8, which rapidly released a full-scale energy equivalent of 21.5 megawatt-seconds by detonating an explosive."

In view of the qualitative theoretical discussion, the results of these model tests, and the length of the computations necessary to evaluate the effect of a slower rate of energy release, it does not seem worthwhile to carry out the computations.

E-103

An interesting point relative to the model tests, though not concerned with this particular question, is the fact that the measured pressures in those sections of the WADC reactor which resemble the NACA reactor are less than those calculated either by WADC or by methods similar to that used in appendix H of reference 2. This is a further indication that the pressure-time histories which were assumed in the analysis of the Hazards Summary were conservative, as they were intended to be.

CO-20 back

6. QUESTION 6

"We are also interested in whether you have considered, in the course of your hazards analysis, the possibility that the cadmium control sheets might melt and thus be removed as an effective control."

The Hazards Summary is not clear on this point, but it has never been intended that bare cadmium control sheets would be used. The cadmium will be clad or canned in a material whose melting point is at least as high as that of aluminum in such a manner that even though the cadmium should melt it would still be held in place by the cladding or can.

REFERENCES

1. Letter to NACA from H. L. Price of the AEC dated March 1, 1957.

2. Lewis Research Center: NASA Reactor Facility Hazards Summary. Vol. I. NASA MEMO

3. Radioisotope Distribution Regulation, Federal Register, Part 20, Title 10, CFR.

4. Meteorology and Atomic Energy. Weather Bureau, United States Department of Commerce, 1955.

5. Enlund, H. L. F.: Interoffice Memorandum, Oak Ridge National Laboratory, September 1952.

6. Dietrich, J. R.: Experimental Investigation of the Self-Limitation of Power During Reactivity Transients in a Subcooled Water-Moderated Reactor. AECD-3668.

7. Dietrich, J. R.: Experimental Determinations of the Self-Regulation and Safety of Operating Water-Moderated Reactors. International Conference on the Peaceful Uses of Atomic Energy (Geneva), vol. 13, paper 481, pp. 88-101.

8. Nyer, W. E., Forbes, S. G., Bentzen, F. L. Bright, G. O., Schroeder, F., and Wilson, T. R.: Experimental Investigation of Reactor Transients. IDO 16285.

9. Watstein, D.: Properties of Concrete at High Rates of Loading. ASTM preprint 93b, 1955.

10. Baker, E. W., and Patterson, J. D. II: Blast Effects Tests of a One-Quarter Scale Model of the Wright Air Development Center Nuclear Engineering Test Reactor (Preliminary Report) Ballistics Research Laboratories, Aberdeen Proving Grounds.

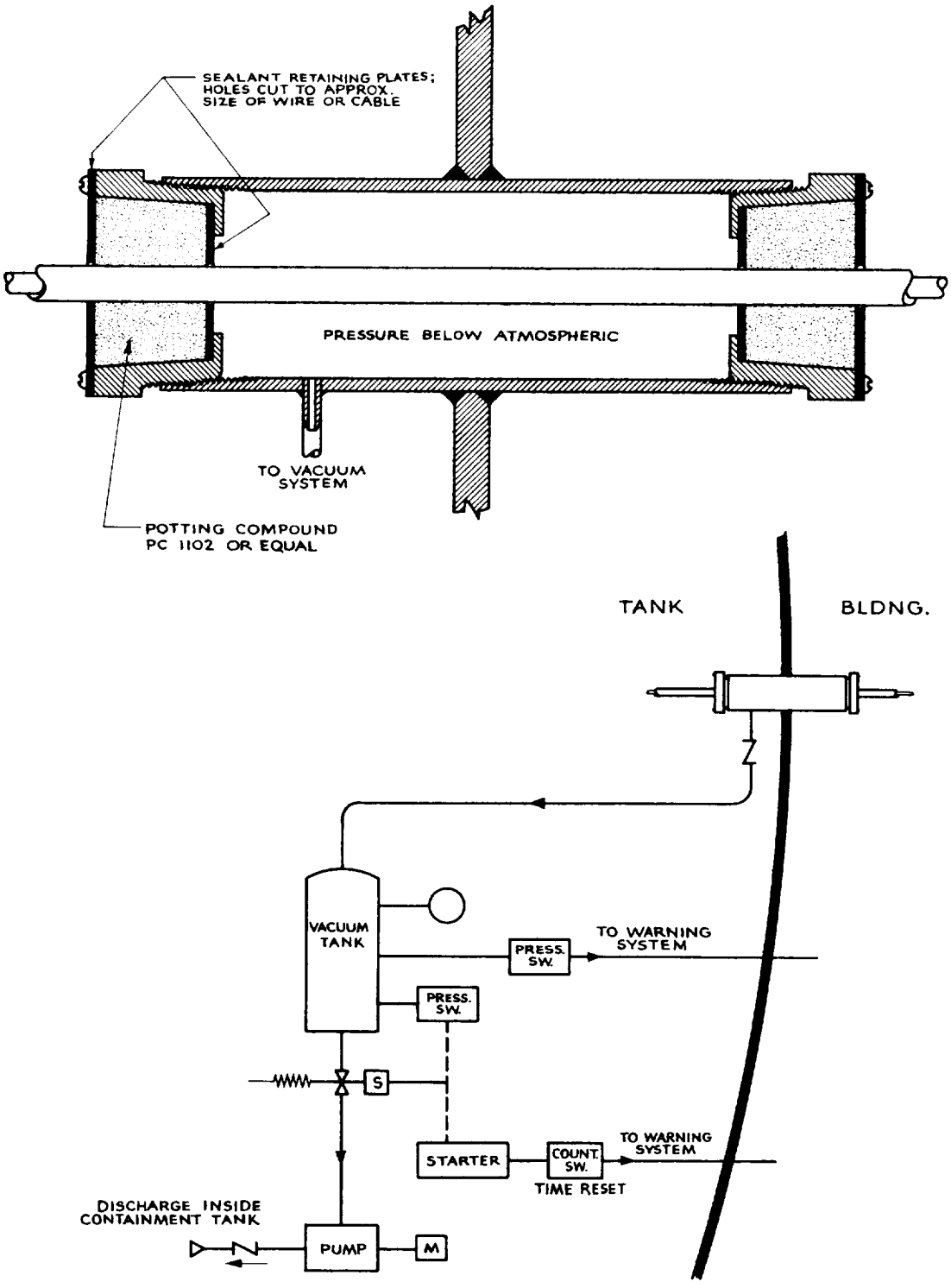

Figure 1. - Typical wire or cable penetration and vacuum system.

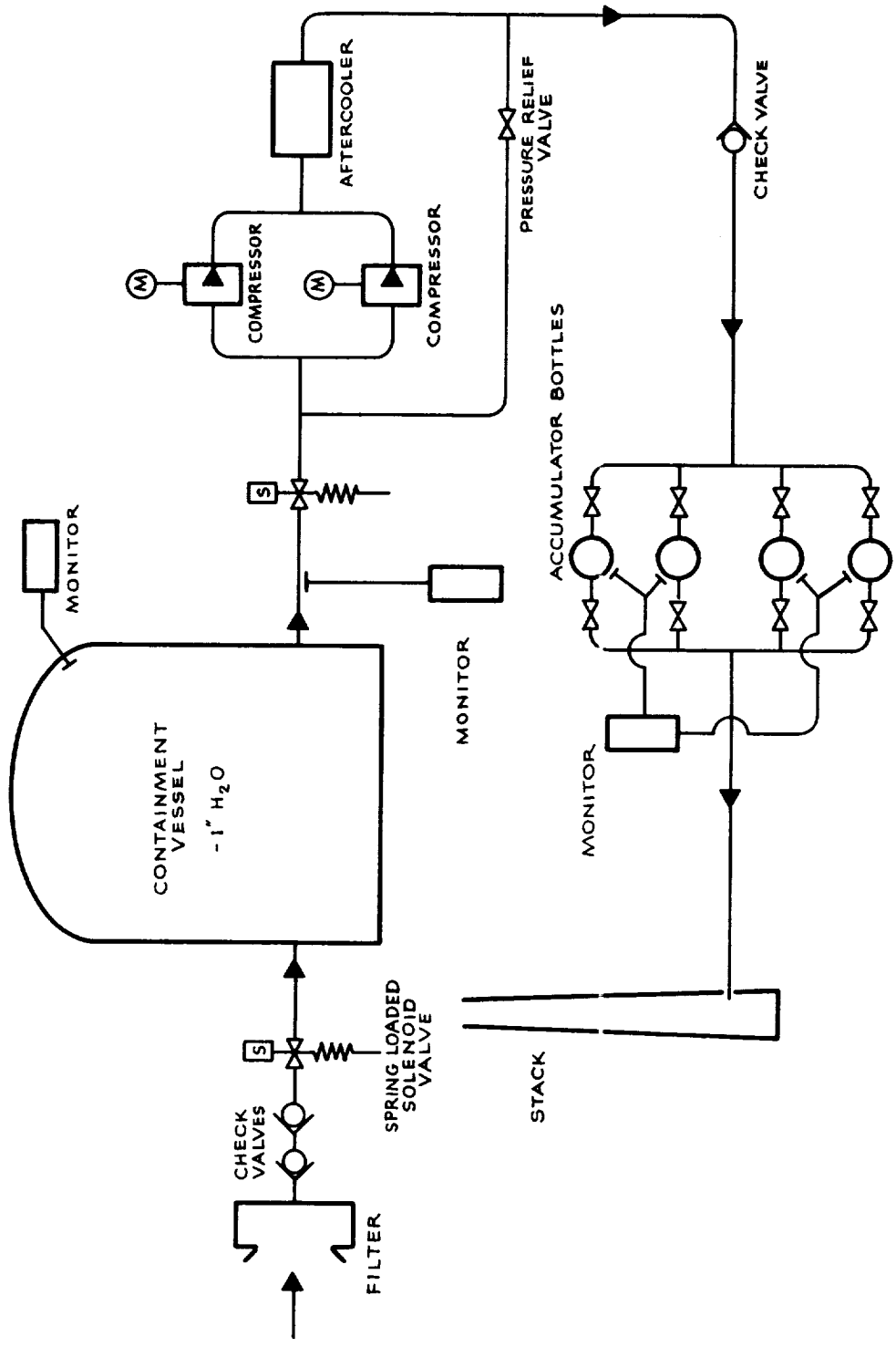

Figure 2. - Containment tank ventilation system.

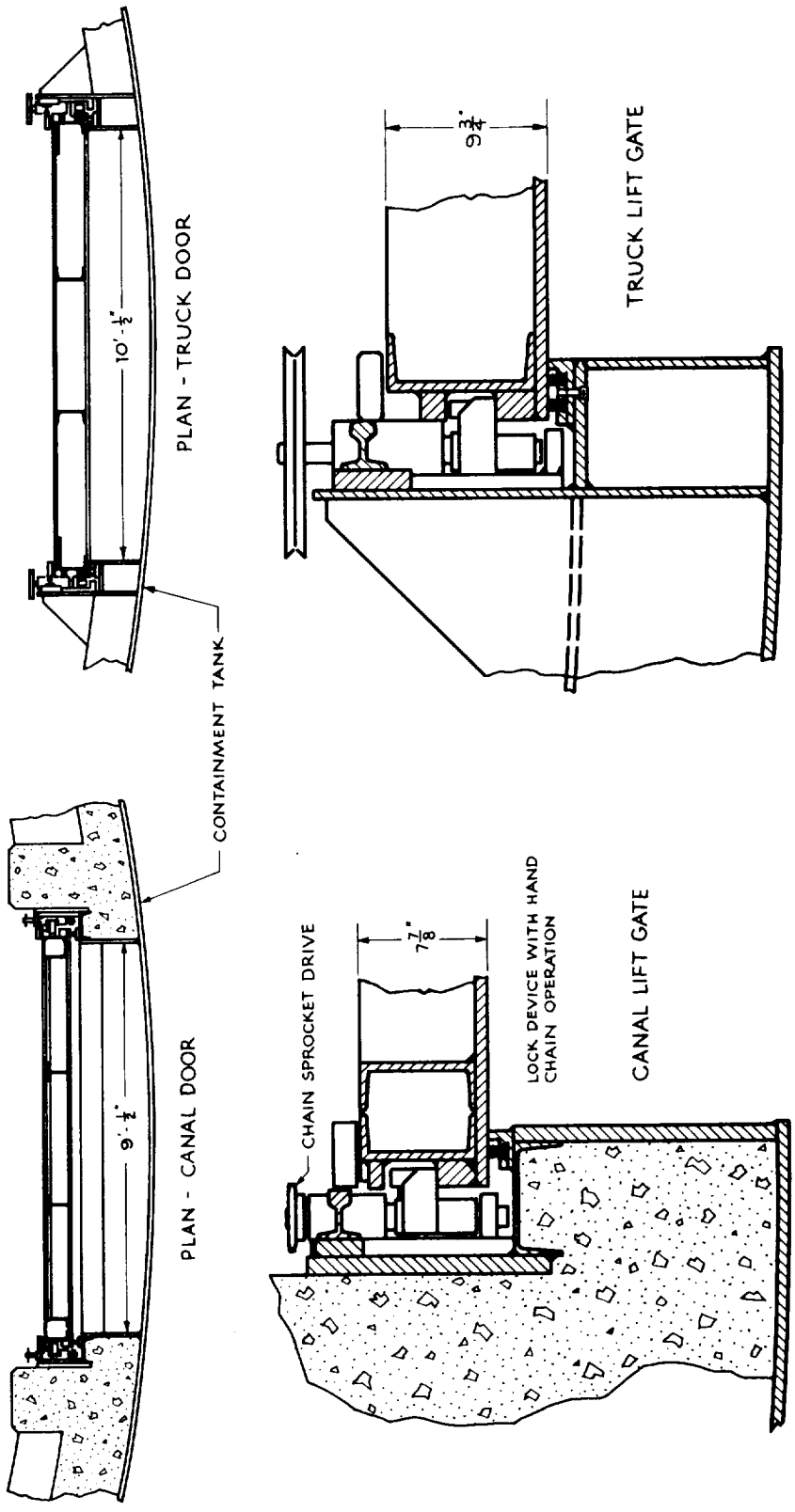

Figure 3. - Details of canal lift gate and truck door seals.

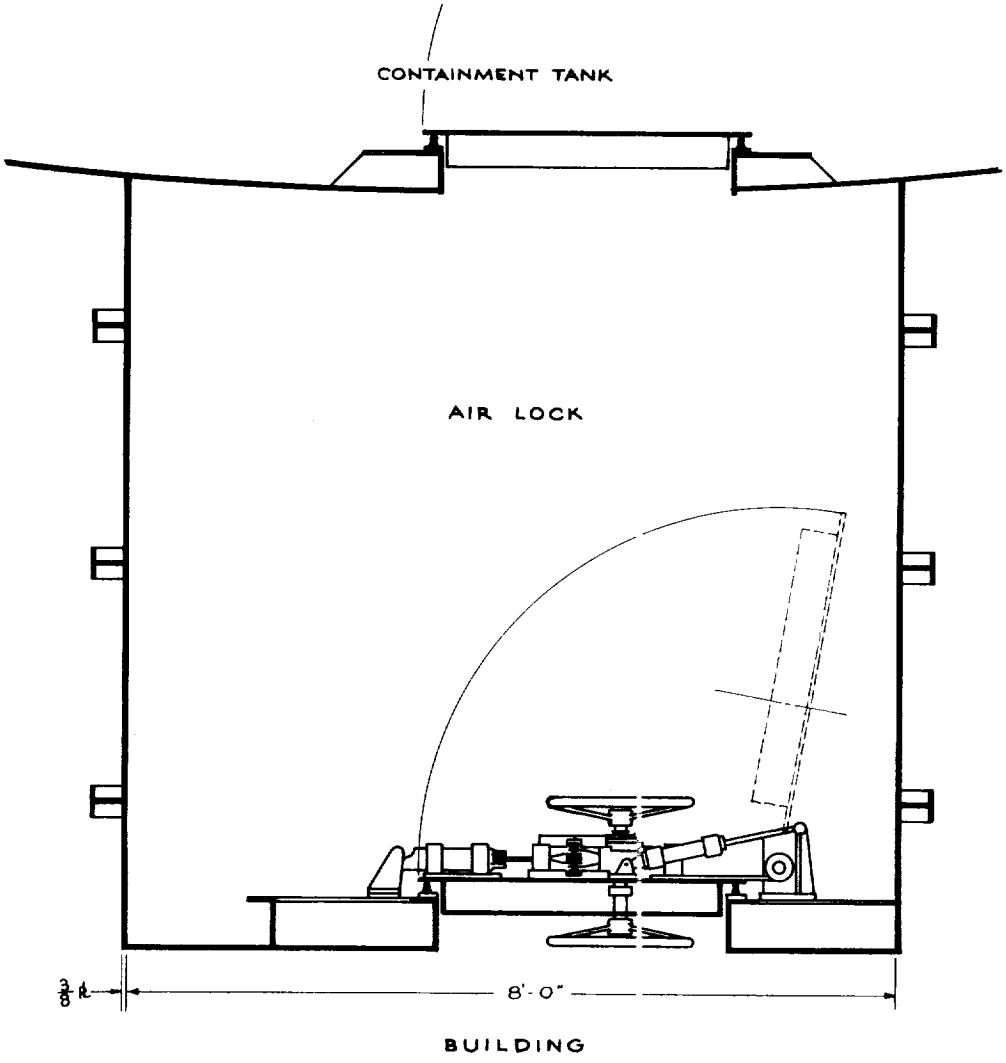

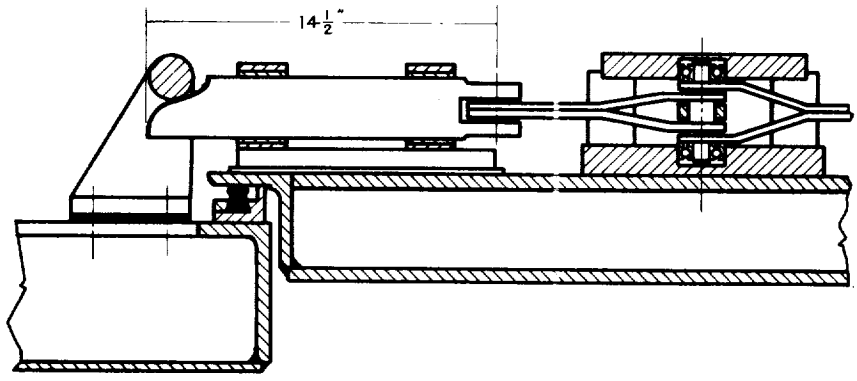

Figure 4. - Air lock and air lock seal details.

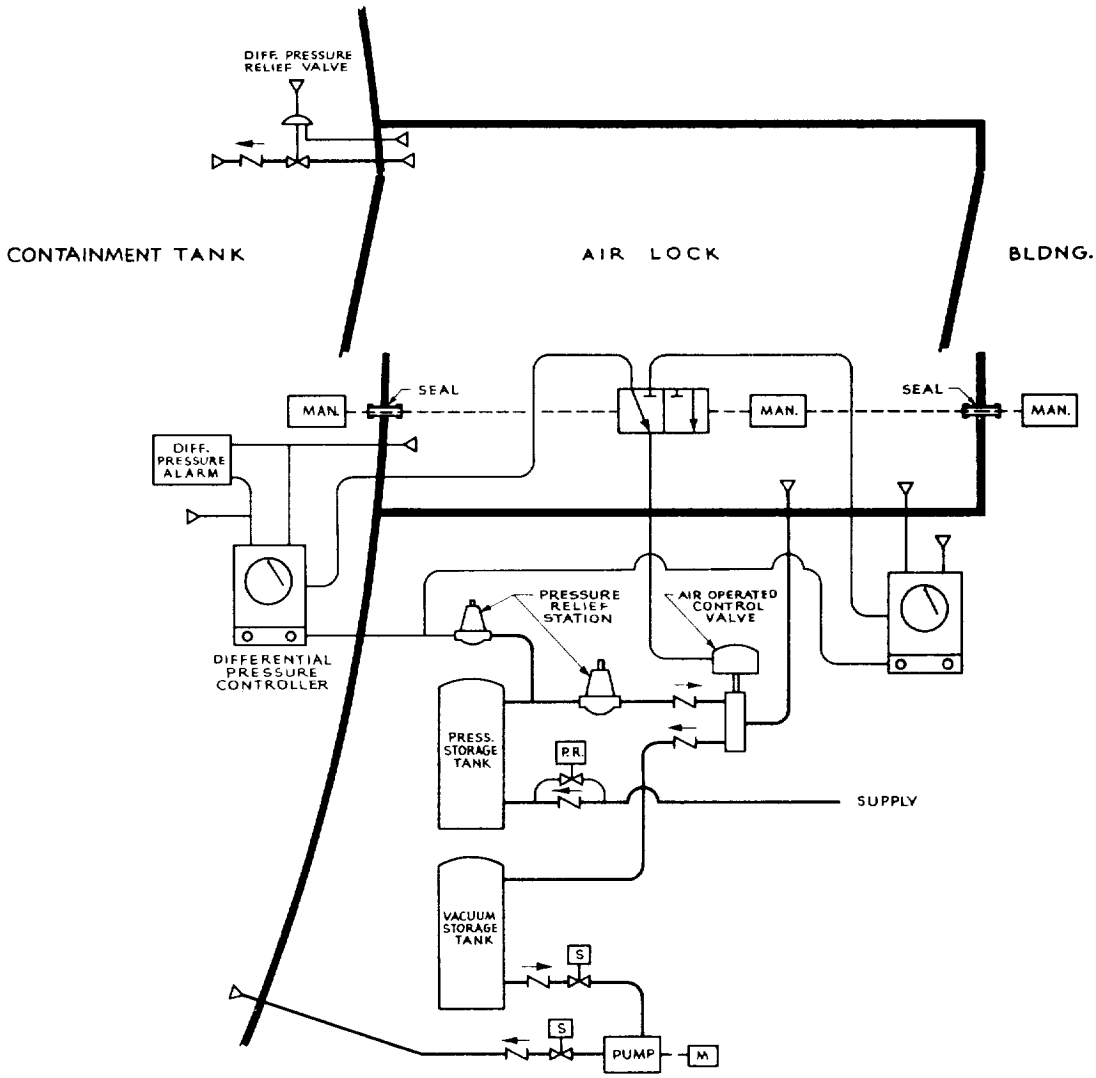

Figure 5. - Air lock pressure system.

V. LEAKAGE RATES FROM THE CONTAINMENT TANK OF THE NACA REACTOR FACILITY

June 10, 1957

In supplement IV to the Reactor Hazards report, an allowable leakage rate from the containment tank of the NACA Reactor Facility was determined which would insure that, in the event of a maximum credible accident, the average, thirteen-week concentration at the nearest point open to the public would not exceed the limits specified in Federal Register, Part 20, Title 10, CFR for areas where people regularly reside. This allowable leakage rate was 15 cubic feet/day. The design and testing of the containment tank to maintain this leakage rate was discussed.

E-103

CO-21 back

The NACA believes that this leakage rate can be maintained by the methods described in supplement IV, and all the design details and testing procedures described therein will be carried out with this aim. It is true, however, that there was perhaps an undue amount of conservatism in the assumptions that were used in arriving at the allowable leakage rate.

It is the purpose of this memorandum to discuss those assumptions which were felt to be too conservative and to arrive at a more realistic leakage rate, but one which would still insure that the average, thirteen-week concentration did not exceed the limits specified in the Federal Register. Testing procedures apropos to this leakage rate will also be discussed.

1. Allowable Leakage Rate

Four assumptions made in computing the allowable leakage rate will be discussed, as follows:

(a) The fission product inventory in the reactor

(b) The amount of radioactive iodine in the air of the containment tank after the accident

(c) The height of release of the fission products

(d) The equilibrium pressure after the accident

1.1 Fission product inventory. - The assumption was made (Supplement IV, section 1.1.2) that the inventory of fission products in the reactor was that which corresponded to a reactor operating continuously at 60 megawatts for a period long enough to saturate all the gaseous fission

products of significance. The operating cycle of the reactor is such, however, that the average power over the ten day operating period is 40-50 megawatts with a power of 60 megawatts occurring only for a short period at the end of the cycle. Therefore, for this leakage rate estimate, it will be assumed that the fission product inventory in the reactor is that which corresponds to a reactor operating continuously at 50 megawatts for a period long enough to saturate all the gaseous fission products of consequence.

1.2 Iodine release. - The assumption was made (Supplement IV, section 1.1.2) that all the radioactive iodine was distributed in the air of the containment tank. The reactor is located in a nine foot diameter tank with twenty feet of water over the core. This reactor tank is in the center of a seventy foot diameter, twenty five foot high water pool. Therefore, in the maximum credible accident, the nuclear excursion and the metal-water reaction occur primarily underwater. It would be reasonable to expect that a good deal of the radioactive iodine would be released in intimate contact with water. Iodine is quite water soluble; indeed, all of the radioactive iodine in the fission product inventory (about 14 gms) could be dissolved in about 1.5 cubic feet of water at room temperature, and the solubility increases with water temperature. It seems reasonable to assume that a large fraction of the radioactive iodine will remain in solution and not be present in the air of the containment tank. Therefore, it will be assumed that 25 percent of the radioactive iodine would be distributed in the air of the containment tank.

1.3 Height of release. - The assumption was made (Supplement IV, section 1.1.3) that the fission products would be leaking out of the containment tank at ground level. For the first 27 feet above grade, the containment tank is surrounded by the main reactor building (ref. 1, fig. 2.13). Any radioactive fission products issuing from the containment tank below the 27 foot level would be mixed in the air of the reactor building and blown out the reactor building ventilating system. The exhausts of the reactor ventilating system are a minimum of 30 feet above grade. Therefore, it will be assumed that the height of release of the fission products is 27 feet.

1.4 Equilibrium pressure. - The assumption was made in estimating the equilibrium pressure after the accident, that all the energy of the nuclear excursion, the metal-water reaction, and the hydrogen-air explosion went into increasing the temperature and humidity of the air (ref. 1, appendix H). It was also assumed that all the hydrogen generated by the metal-water reaction would combine with air. The nuclear excursion and the metal-water reaction both occur underwater and most of their energy will go to heating water. If the energy in the nuclear excursion and metal-water reaction were assumed to be distributed between the water and the air in the containment tank so as to produce an equal

rise in temperature, less than one percent of the energy would go into the air. A reasonably conservative estimate of the portion of the energy of the nuclear excursion and the metal-water reaction which would go into the air might be about ten percent and this assumption is made here. The assumption that all the hydrogen produced reacts is also too conservative. In the maximum credible accident, the greatest part of the hydrogen will be produced underwater and will be hurled into the air of the containment tank by the violence of the explosion. In order for it to react with air it would have to form a flammable mixture and there would have to be an ignition source present. Further, the equilibrium concentration is below the combustion limit by a factor of four (ref. 1, appendix G). Therefore, it does not seem likely that most or all of the hydrogen would react with air. It will be assumed that one-third of the hydrogen generated reacts with air and that all of this energy goes into the air. The equilibrium pressure after the accident computed by the use of these assumptions is about 0.3 psi as compared to the 1.9 psi computed in the Hazards Summary (ref. 1, appendix H).

1.5 Leakage rate. - The effect of the change in these four assumptions on the allowable leakage rate was computed, keeping all other assumptions identical to those used in Supplement IV. The allowable leakage rate is 115 cubic feet/day at an overpressure of 0.3 psi.

2. Leakage Rate Test Procedures

All the testing procedures described in Supplement IV will be performed as described. However, with the new leakage rate of 115 cubic feet/day at an overpressure of 0.3 psi it is possible to make an additional test which was not possible previously, that is an accelerated overpressure test. Since the containment tank is designed to withstand an internal overpressure of 5 psi with a safety factor of three, a leakage rate test could be run at an overpressure of 4 psi instead of the 0.3 psi overpressure expected as the result of the maximum credible accident. At the low flow rates being considered, the leaks would be small in size and the flow through them would be laminar. In laminar flow, the volumetric flow is directly proportional to the pressure difference. An overpressure of 4 psi would produce about 13 times the leakage rate which would occur at an overpressure of 0.3 psi. It is therefore possible to produce in one day of accelerated testing, the leakage which would occur in 13 days of testing at the expected overpressure. Therefore, in the accelerated test the leakage rate which one is called upon to detect would be about 1500 cubic feet/day.

The accelerated overpressure test would be conducted in the following manner. Resistance thermometers or thermopile junctions would be

placed at various locations in the air of the containment tank. These instruments would be of sufficient number and accuracy so that the average air temperature inside the containment tank could be determined to an accuracy of at least 1° F.

The containment tank would be pressurized to 4 psig and then closed off in precisely the manner it would be in the event of an accident. The reduction in pressure would be measured after a 24 to 48 hour period and corrected for air temperature variation. A leakage of 1500 cubic feet/day would result in a corrected pressure drop of about 2.8 inches of water in 48 hours. The uncertainty in pressure drop due to an uncertainty of 1° F in air temperature is about 0.8 inches of water. Accordingly, an excessive leakage rate could readily be determined after 48 hours. If the average air temperature were accurate to 1/2° F, this length of time could be cut to 24 hours. As part of the initial testing prior to the reactor going into service a series of tests of this type will be conducted. The number of temperature sensing devices in the air of the containment tank will be varied to determine the number required to give the desired accuracy of measurement of air temperature. This type of test would then be run periodically during the life of the reactor.

If an excessive leakage rate was detected, the source of the leak would be located by helium leak detector tests and repaired. The reactor would, of course, not be permitted to operate until the leakage rate had been brought down to permissible values.

3. Containment Tank Air Conditioning

An additional safety feature of the NACA Reactor Facility which has not been discussed previously is the containment tank air conditioning. The containment tank is air conditioned during normal reactor operation. There are four units which provide a total cooling capacity of 27 tons; their location may be seen in figure 2.13(b) of the Hazards Summary (ref. 1). The units are connected in pairs to two separate electric circuits. Therefore, in the event of the accident, it is unlikely that any more than two of these units would be inoperable. The air conditioners surviving the accident would continue to run and would after a time reduce the overpressure in the containment tank to the order of a few inches of water. The length of time required to do this would vary with such factors as the roof heating load, the number of units which survive the accident, etc., but even assuming unfavorable circumstances, the overpressure in the containment tank would be reduced to a few inches of water within 24 hours.

4. Summary

The contents of this supplement can be summarized as follows:

1. All design details and testing procedures described in Supplement IV will be carried out with the aim of maintaining a leakage rate below 15 cubic feet/day.

2. If some of the conservative assumptions in the previous analyses are changed to more realistic ones, an allowable leakage rate of 115 cubic feet/day would not exceed the limits for thirteen-week average concentration specified in the Federal Register for areas where people regularly reside. The equilibrium pressure after the maximum credible accident would be 0.3 psi.

3. An accelerated leakage rate test with the containment tank pressurized to 4 psi would require the detection of leakage rates of about 1500 cubic feet/day. This type of test can be conducted in 24 to 48 hours with suitable instrumentation for the determination of containment tank air temperature. Such tests will be run periodically throughout the life of the reactor.

4. An additional safety feature of the NACA Reactor Facility is the containment tank air conditioning which, even in unfavorable circumstances, would reduce the overpressure in the tank to a few inches of water within 24 hours.

REFERENCE

1. Lewis Research Center: NASA Reactor Facility Hazards Summary. Vol. I. NASA MEMO

VI. ANSWERS TO ADDITIONAL MISCELLANEOUS QUESTIONS

RAISED BY THE ATOMIC ENERGY COMMISSION

February 5, 1958

In order to clarify certain points relative to the safety of the proposed NACA Reactor Facility, the Atomic Energy Commission, in a letter (ref. 1) has requested written answers to a number of miscellaneous questions. This supplement to the NACA Reactor Facility Hazards Summary (ref. 2) consists of the answers to the ten questions of the AEC letter. In addition to these ten answers, this supplement contains answers to other questions raised by the AEC subsequent to the original questions.

1. QUESTION 1

"Estimates at this time of the quantity and nuclear characteristics of both 'cold' and 'hot' wastes."

The radioactive wastes from the reactor area are generally classified as liquid, solid, or gaseous wastes. An estimate of the quantity and the activity of these wastes along with information concerning the process handling is given in the following sections.

1.1 Liquids

1.1.1 Process system. - Contaminated water from the primary cooling water system will make up the largest volume of the liquid wastes. The operation of this system is discussed in section 2.1.12 of the Hazards Summary (ref. 2) and the radioactive waste disposal system has been outlined in section 5.2. Table 1.1 indicates an estimate of the quantity and the activity of the waste water from the primary system and the hot laboratory.

The volume of contaminated water to the hot retention tanks on a continuous basis is estimated at 14.65 gpm with an average activity during normal operation of 10^3 d/cm^{3}sec or 0.03 μc/cc. The volume of contaminated water on an intermediate basis will be between 12,000 and 36,000 gallons per operation cycle, with an average activity during normal operation of 10^3 d/cm^{3}sec.

The hot waste waters indicated in table 1.1 will be retained in separate 125,000 gallon tanks as follows:

Tank	Waste source	Initial activity, μc/cc	Type usage
A	Reactor loop	0.03	Intermittent
B	Reactor sump	.03	Continuous
C	Hot lab sump	.02	Intermittent and continuous
D	Pump and fan sump	.19	Intermittent and continuous

(Recent design information indicates that eight to ten 25,000 gallon tanks will give better flexibility for over-all hot water retention and waste transfer systems.)

If a fuel element leaks fission products into the primary water system, a continuously operating fission product monitoring unit in the line will detect the radioactive iodine from the leak and warn the reactor operator as described in section 2.3.14 of the Hazards Summary (ref. 2).

The triggering limit of iodine 131 in the anion chamber of the fission product monitoring unit is estimated to be 1.3×10^{-4} μc/cc or less depending on the purity of the primary water. This activity would be dispersed in the primary water such that the total activity due to fission products could be estimated at

$$\frac{1.3\times10^{-4}\ \mu c/cc\ (9.46\times10^{7}\ cc)}{0.028,\ \text{ratio}\ \ I^{131}\ \text{activity to total}} = 4.4\times10^{5}\ \mu c$$

$$\text{at a maximum concentration} \qquad = 5\times10^{-3}\ \mu c/cc$$

The bypass demineralizers (mixed bed and cation) will be capable of removing an estimated 99.5 percent of the active ions in the primary water system in case of a fission product leak. This will be accomplished by recycling the water through the beds on a once through basis with the reactor and the primary cooling water pumps shut down. Dumping to retention tanks will allow additional cleanup through the waste disposal demineralizers in the Fan House, and will give an estimated total decontamination factor of 2×10^{3}. After treatment, the radioactivity of the waste is estimated to be a maximum of 2.32×10^{-3} μc/cc and after being sampled to determine the concentration and nature of the activity, the waste will be stored or diluted to maximum permissible concentrations for area liquid effluents.

Shielding water in the quadrants and canal areas will have a continuous purge of 50 to 100 gpm for each divided area. This purge water will pass through a demineralizer mixed bed unit and return to the system, or be pumped to the 1,000,000 gallon storage tank. Table 1.2 indicates an estimate of the quantity and activity of cold and intermediate wastes from the process water system. The piping system for the quadrant and canal water is so arranged that the purge water may be sent to the hot retention tanks in the event that leakage from experiments or thimbles raise the water activity above 10^{-3} μc/cc, and fresh makeup water will replace the removal.

E-103

All waste water from the quadrant and canal areas or the storage tank will be cycled through the demineralizer until the concentration and nature of the activity indicates that it may be diluted to maximum permissible levels for area liquid effluents.

CO-22 back

1.1.2 Experimental systems. - Experiments that require water moderation or internal water flow systems that may become contaminated radioactively or materially will be required to have separate cleanup systems to operate such that the water activity to the waste retention tanks will be about 0.03 μc/cc.

1.2 Solids

1.2.1 Waste resins. - Spent resin from the primary water bypass loop demineralizer will be flushed from the demineralizer tank and discharged into an underground pit. The flushing operation will be completely remote by operating discharge valves and flush water valves from behind the room shield area. The resins will be allowed to settle and the liquid phase will drain to the pump house sump. Off gases from both units will be drawn to the stack gas system.

The resin pit will hold 480 cubic feet of resin with an initial estimated average activity of 0.3 μc/cc. Remote means will be used to transfer the resin into shielded or concrete mix shipping containers for transportation to a burial area such as Oak Ridge, when the activity has cooled sufficiently to be transported. The resin pit will have 36 inches of concrete plus the required earth shielding to place the surface activity at a value less than tolerance. A stainless steel lining inside the concrete pit will form a leakproof container for the liquid and the resins.

An overflow line to the sump and a liquid level indicating rod ensure containment of the slurry during discharge operations.

A similar system of resin transfer and burial will be used for the two demineralizers in the waste cleanup system if the residual activity of the resins exceeds 5×10^{-3} μc/cc.

1.2.2 Waste metals and debris. - Waste metal, machining scrap, and specimen samples as well as secondary scrap from the hot laboratory and other hot work areas, will be handled in the manner described in section 5.2.4 of the Hazards Summary (ref. 2). Some of this material will be stored in the dry storage area of the hot laboratory to await off-site disposal, and most of the rest will be baled or packaged for burial at an off-site location such as Oak Ridge. The combustible wastes which indicate extremely low activity (background conditions) and originate in uncontaminated areas, such as the Office Building or the Service Equipment Building, may be incinerated on the site.

1.3 Gases

1.3.1 Process system off gas. - The demineralized water to the primary cooling water system will be completely degassed in the Service Equipment Building prior to entering the reactor water system. With the high purity requirements of this water, maintained by the bypass demineralizers, it is estimated that little or no water decomposition products will be generated in the system to the point where continuous degassing will be required. It is expected that the few milliliters per day of these gases, dissolved in the water, can be removed by the demineralizers and their formation controlled by pH stabilization.

Radioactive off gases, which result from fuel element leakage of gaseous fission products, will be removed at the reactor pressure tank through a normally closed bleed valve. These gases, as well as gases formed from decomposition of the water, will be monitored and stored, or diluted and released in the effluent stack gas system in accordance with allowable concentrations for the stack. The estimated activity of these gases will be 0.02 μc/cc when bled from the process system and the estimated volume will be 0.15 cubic foot per operational cycle at S.T.P. conditions.

Other process system off gases will feed into the 10,000 cfm venting system described as the basement area fan in section 2.1.14.2 of the Hazards Summary (ref. 2). This vent system operates from the basement of the Reactor Building through the Utility Tunnel under the Hot Laboratory to the Fan House. Vent gases from the Reactor Sump and the Hot Laboratory Sump and Treatment Tank are collected into this system in the Utility Tunnel area. The activity of this ventilating system is expected to be negligible in the basement area but may rise to 10^{-13} μc/cc downstream in the Utility Tunnel. The sumps can be emptied and purged in the case that access to the Utility Tunnel is required and only then under Health Physics supervision.

Vent gases from the Pump House Building, Sump and Resin Pit are connected to an individual 500 cfm vent system in the Fan House. Under normal operation, the activity of this air is estimated to be negligible but may rise to a value of 10^{-12} μc/cc after a fuel element leak has been experienced. This system will operate at a negative pressure of 4 to 6 inches of water.

1.3.2 Fission gases out of experiments. - Fission gases accidentally released from experimental loops will accumulate in the experiment container tank (section 2.1.1 of Supplement IV). As was pointed out in Supplement IV, such gaseous fission products would be purged from the container and bottled at 250 psi in 10 to 30 cubic foot tanks of small diameter. This operation would be carried out in the hot handling section of the Hot Laboratory. These storage tanks would in turn be enclosed in a safety tank to afford double containment. The safety tank would also house the vacuum pumps, blowers, and compressors necessary for the off gas system.

The operation by which fuel bearing elements would be dissected into specimens will be carried out in a hood within cell number 2. Such hoods would be made as leakproof as possible, and a pressure differential maintained between hood and cell sufficiently high to ensure a 150 foot per minute velocity through unavoidable holes. Hood effluent will be filtered, compressed, and stored in the same manner outlined above for gaseous fission products from the container.

An iodine removal system will be installed through which stored air will be passed after an adequate storage time in the tanks. The required storage time will depend on the efficiencies attainable in the iodine removal system. Efficiencies of 99.9 percent have been reported on three different types of iodine removal equipment, silver nitrate coated packed towers, caustic bubble cap scrubbers, and synthetic zeolite adsorption beds. We are presently preparing tests on models of the latter to determine performance.

Initially installed storage capacity and iodine removal equipment will be sized to accommodate expected experiment operation, conservatively

estimated volumes of air involved and required storage time. Additional units can be fairly readily added if the need for them becomes apparent. Experiment operation would, of course, be limited to the off gas facilities available to handle gaseous fission products.

Present estimates are that approximately 120 cubic feet of tank storage would be required for each 1 MW experiment requiring purging of the experiment container. Of this, 20 cubic feet would be required for a double purge, the remainder would allow approximately 15 hours of dissecting time in the hood. Hood leakage is estimated at 2 cfm based on the Berkely experience of 0.02 cfm combined leakage and off gas in a 5 cubic foot glove box (ref. 3). Present plans call for the initial installation of approximately 500 cubic feet of compressed off gas storage capacity. There is space available for the installation of 3 times that amount if required.

Release of stored gases will be regulated so that concentrations permitted under 10 CFR, part 20 of Federal Register will not be exceeded. Factors affecting this release will be:

(a) Activity of effluent from iodine remover

(b) Storage time

(c) Normal ventilating air available for dilution

(d) Meteorological conditions.

2. QUESTION 2

"The criteria for determining the treatment capacity of proposed processing equipment, such as demineralizers, evaporators, and filters."

2.1 Primary Water Bypass Demineralizer

The mixed bed and the cation demineralizers, described in sections 2.1.12.1 and 5.2.1.3 of the Hazards Summary (ref. 2) will operate on 100 gpm of the primary water system. On the basis of the information in appendix E, the demineralizing system must maintain a water concentration in the primary water loop as given on page 178 (ref. 2) and have maximum total ion concentration of 0.1 ppm $CaCO_3$ equivalent. This system will require a cleanup capacity as calculated on the following page.

Na	- 0.03	ppm	- 0.0654 ppm as $CaCO_3$
K	- 0.005		- 0.0064
Ca	- 0.005		- 0.0125
Mg	- 0.002		- 0.0082
SiO_2	- 0.02		- 0.0334
Cl	- 0.06		- 0.0846
Stainless	- 0.10		- 0.2690
Al	- 0.07		- 0.3892
Be	- 0.002		- 0.0222
Input			= 0.8909 ppm as $CaCO_3$
Output			0.10
Difference			= 0.7909 ppm as $CaCO_3$
			= 0.0461 grains/gal as $CaCO_3$

Bed capacity requirement for 1/2 year operation at 100 gpm

$0.0461(100)(60)(340 \text{ hr/cycle})(12 \text{ cycles}) = 1.2\times10^6$ grains

One mixed bed exchanger and one cation exchanger with a total of 120 cubic feet of resin will have a combined capacity of 4.8×10^6 grains.

It is expected that the mixed bed and cation demineralizers will be capable of reducing the ion concentration to a value lower than the set effluent value of 0.1 ppm as $CaCO_3$. This value was chosen as a compromise to ensure that the resulting pH of the water would be about 6.6 to 6.8, an optimum for the lowest aluminum corrosion rate. If the cleanup efficiency of the designed demineralizers turns out to be more like 99.5 percent, as is indicated by industrial demineralizer manufacturers, the two units can be operated at a reduced flow rate.

In the case that fission products from a fuel element leak enter the primary water system, the demineralizers, operating at full flow rate for a period of 20 to 60 hours, will be capable of reducing the total ion concentration to less than 4×10^{-3} ppm and the total activity to less than 2.5×10^{-3} μc/cc.

2.2 Waste Disposal and Quadrant-Canal Water Cleanup Demineralizers

The demineralizers for waste disposal system and the quadrant and canal water cleanup system are mixed bed units with a maximum combined flow rate of 400 gpm. For the most part, these units will be operating on low ion concentration waste waters or recycle waters with activities unsuitable for direct disposal or re-entry into the system. These units will be of a design capacity and construction similar to the bypass demineralizer

mixed bed unit. Regeneration liquids, after neutralization, will be further concentrated, stored or diluted for plant liquid effluent in accordance with 10 CFR, part 20 of Federal Register. Information on the efficiency for removal of radioactive contaminants from liquids of this type and on a volume scale of this size is not available. However, laboratory scale studies indicate that long-lived active nuclides such as cesium-137, strontium-89, cerium-144, cobalt-60, and zirconium-95 can be removed from solutions containing 10^{-6} ppm or less in the presence of inactive ions such as calcium with a concentration of 10^{7} times greater. Indications also show that some trivalent ions such as cerium 144 can replace inactive calcium ions even after breakthrough or bed exhaustion conditions exist (ref. 4). For quadrant and the canal water, as an influent, it is estimated that decontamination factors of 20 (at 400 gpm) to 1000 (at 80 gpm) may be realized for the demineralizers.

2.3 Waste Disposal Evaporator

The evaporator discussed in section 5.2.5 (ref. 2) will not be installed in the initial operation. At this time, it is estimated that its purpose as a high activity material concentrator can be accomplished by the waste disposal demineralizer. If, however, the volume of waste liquid from the demineralizers and the hot laboratory sump concentrate becomes a hot storage problem, a 10 gallon per hour evaporator or a flash dryer will be added.

2.4 Air Filters

There are two types of air filters which will be used on the ventilation and off-gas systems of this installation. They are the standard roughing filter and the absolute filter.

No estimate has been made on the amount of airborne particulate material that could be expected in normal operation of the reactor system. Rather then, individual air velocities and air changes were set on the individual rooms and areas based on existing systems in good operation such as ANL, ORNL, and MTR. Modifications were made where the existing operation has had difficulties in the spread of airborne contamination.

Area	Changes/hr	In velocity through opening, ft/min
Hot Laboratory Cells	60	150
Hot Laboratory - Decontamination Area	3.5 - 4.5	10 - 40
Reactor Containment Tank	.053	Limited access
Pump House Building	1.5 - 2.0	Limited access

All of the Hot Laboratory cells will have roughing filters on the inlet and exit side of the venting system. All independent laboratory hoods will have roughing and absolute filters.

The four 10,000 cfm lines to the stack will have absolute filters of 99.9 percent efficiency and roughing filters on the upstream side. An additional 1000 cfm system for the Pump House and the off-gas system will have a similar system.

The roughing filters and the absolute filters will be canned in drums for off-site disposal when they become clogged, contaminated, or indicate leakage.

3. QUESTION 3

"An evaluation of the possibility of leaks in the liquid waste disposal system. If any such leak is credible, an evaluation of the consequencies of such a leak."

Two types of tank and plumbing installations are proposed for the liquid waste disposal system. Both types are designed as absolute containment systems for neutralized liquid wastes. Both types will have level indicators, vents, cooling water lines if required, and plumbing for inlets and outlets.

3.1 Type 1

This type construction will be composed of tanks and plumbing in a double wall of steel. The inner steel tank will hold the waste liquid and the outer steel tank will act as a barrier against the possibility of waste liquids leaking out of the containing area. This open area between the inner and outer steel tanks will have a low spot sump which will be monitored for water, either as ground water seeping in through outer steel surface or waste liquids leaking in through cracks, seam breaks, and so forth in the inner surface. After an indication of water in this drain sump, a liquid sample may be taken to determine which surface is leaking, and, after emptying the retention tank, repairs can be made. In the case of uncontrollable leakage from the inner tank, the liquid can be pumped immediately to another retention tank.

3.2 Type 2

This type construction will be composed of steel tanks and plumbing within a reinforced concrete structure. Between the tank base and the concrete basepad, there will be a secondary barrier in the form of a steel

dish. The size of this dish will be such as to extend beyond the vertical walls of the retention tank but inside the concrete structure, thereby collecting any waste liquid leakage. This dish will have a collection sump, an alarm indicator, and a sump pump.

The concrete structure will be waterproofed on the outside surface. Inside, on the basepad there will be a drainage collection sump, an alarm indicator, and a sump pump. Ground water which may seep through the concrete structure will be pumped out, monitored, and discarded. In the event that there is water in the dish, an increase in the ground water collection or activity in the ground water collection, the individual tank will be drained and the leak repaired.

3.3 Waste Liquid Transfer Pump Area

The waste disposal retention tanks will have interconnecting piping and a series of pumps and valves which will be housed in a steel-lined concrete drain pit. Leakage from the pipe, pump housing, or packing seals will be collected and pumped or drained into one of the waste disposal tanks.

4. QUESTION 4

"Basis for believing that NACA can attain the leakage rate specified for the containment vessel. In this regard, NACA has orally provided information as to their own experience with wind tunnels. However, this information does not appear in the record on which the Commission must act. There should be an indication of the validity of NACA's experience with wind tunnels in terms of the proposed test reactor, considering such matters as the number of penetrations, size, and accessibility of the various parts of the sphere for testing leakage rates."

4.1 Basis for Believing that NACA Can Attain the Leakage Rate Specified for the Containment Vessel

The allowable leakage rate from the containment tank is 1500 cubic feet per day at an overpressure of 4 pounds per square inch as described in section 2 of Supplement V. The total air volume in the containment tank is about 451,000 cubic feet. The leakage rate is, therefore, about 1/3 percent per day at 4 pounds per square inch overpressure.

Leakage rate tests on the containment tank of the Experimental Boiling Water Reactor are reported in ANL 5607. The final leakage rate test conducted after all construction was completed and the plant ready to operate

gave a leakage rate of 450 cubic feet per day at an overpressure of 15 pounds per square inch. The total air volume in the containment tank of the EBWR is about 500,000 cubic feet. The test leakage rate is, therefore, about 0.09 percent per day at an overpressure of 15 pounds per square inch.

The NACA containment tank is about the same size as the EBWR containment tank. The allowable leakage rate of the NACA containment tank is over 3.5 times the measured leakage rate of the EBWR containment tank, and this allowable leakage rate is at an overpressure of less than one-third the overpressure of the EBWR tests.

E-103

On this basis, it is felt that the leakage rate specified for the NACA containment tank can be achieved.

CO-23 back

4.2 NACA Experience with Wind Tunnels

Although the supersonic wind tunnel is a large welded vessel, it differs from the containment vessel in that it is a dynamic rather than a static air containment device. The problem to be handled in the wind tunnel is not that of containing the air within it, but preventing the contamination of such air with the moisture laden atmospheric air from without. The 10 by 10 Foot Supersonic Wind Tunnel, at its lowest pressure condition, contains about one-half pint of water vapor in a tunnel volume of approximately 675,000 cubic feet. This is equivalent to a specific humidity of 80 parts per million.

There are many places where outside (wet) air might leak in large quantity. The main ones are the compressor shaft seals, the flexible wall and second throat seals, the disc of the fifteen foot butterfly valve, and the peripheral seal of the twenty-four foot diameter swinging gate valve. Some of these are impossible to seal completely, and a system of buffer air has been provided so that any leaks into the tunnel will be the buffer or dry air. The compressor seals use the most air in this system because the compressor end play is large. The flexible wall and second throat seals have an aggregate length exceeding five hundred and fifty feet. These are sliding seals with a buffer air system. The twenty-four foot swinging gate valve has an inflatable seal. A buffer system was supplied here as well, but is not used. The buffer air system might have been replaced by a vacuum system such as is to be provided for the penetration seals of the reactor containment vessel, but a pressure air system using dry air was easier to handle for this specific problem.

There are many other penetrations in the tunnel that were sealed; each in a way adapted to the specific design problem, that is, the tunnel bottom door (over 30 ft long and 10 ft wide) used "O" ring type pressure seal.

The tunnel sealing problem is not specifically applicable to the reactor containment tank sealing problems, but the techniques and the degree of care are the same. A leak of wet air (100 plus grains per pound) can invalidate a test through the effects of a condensation shock. Under conditions of aerodynamic testing (the tunnel operating on a recirculating basis) the entire vessel is pumped to very low pressures. The test section simulated altitude can be higher than 100,000 feet. During this type of operation, the highest total pressure in the vessel is less than three inches of mercury absolute.

5. QUESTION 5

"Basis for believing that NACA can maintain the leakage rate specified. In particular, we would like you to direct your attention to the following matters that do not appear to be covered in your application."

5.1 Question 5(a)

"The existence of plugs or unused holes in the walls of the container and the system to be used for measuring the leak rate at these penetrations."

The unused penetrations, whether for electrical cables or piping connections, will be connected to the vacuum system shown in figure 1 of Supplement IV and also shown in figure 1 of this supplement. Unused electrical penetrations will have pipe plugs instead of sealant plug adapters. Unused pipe or other such penetrations will have the vacuum system connection in the pipe cap or plug or blind flange. In addition, a flow measuring system will be supplied in the line (s) from the penetrations to the vacuum tank. This will provide a faster response to any leaks. Other flow measuring points will be provided to aid in localizing the area of any leaks.

5.2 Question 5(b)

"How will the spring-loaded solenoid valves in the ventilation system be made leak tight? What kind of valves are these (i.e., butterfly or gate)?"

The spring-loaded solenoid valves will be of the globe or poppet type held open against the spring (closing) pressure by air pressure on a diaphragm. The valves will be Clayton or Annin valves. The air pressure will in turn be controlled by a solenoid pilot valve designed to release the air holding pressure upon electrical power cut-off. The valve will be placed in the line so that a positive pressure in the containment vessel

will tend to close the valve more tightly. Two such valves will be in series with a check valve and a hand operated valve in the inlet line as well as the outlet line. The containment tank test will include the solenoid valves as part of the test. Valves of this type have been used in very many places throughout this laboratory in widely varying applications. They have been found to be tight sealing under vacuum conditions as low as forty microns.

5.3 Question 5(c)

"Can the reactor be operated with the truck access door open?"

The truck door must be in the full closed position and the seal vacuum within normal limits in order to permit reactor startup. Moving the main reactor control switch to the "O.K. to Start" position will disconnect the door opening circuit on a "power-off, fail-safe" criterion. This electrical interlock will assure that the door is in a closed position and the seal is satisfactory before the reactor can be started and will assure that the door cannot be opened during operation.

5.4 Question 5(d)

"What size hole could exist in the containment shell without you necessarily knowing about it within a short period of time, and what leakage rate would result?"

There appear to be three ways in which leaks might occur in the containment tank during normal operation between regularly scheduled leak tests:

1. Failure of seals at wire and cable penetrations, air locks, canal opening, or truck door.

2. Unauthorized and unreported openings made in the tank wall by workmen during maintenance, modifications, or installation of new equipment.

3. Opening due to undetected failures in the tank structure (e.g., weld cracks).

The method of sealing and leak detection for the first type of penetration has been described in Supplement IV. A further discussion of these penetrations is given in sections 5(a) and 9 of this supplement. It is felt that leakage during operation at any of these points is highly improbable, but that if a significant leak should occur, it would be detected almost immediately (see section 9).

To minimize the possibility of leaks due to unauthorized and/or unreported openings being made in the tank walls, a rigid control will be used for all structural modifications at the facility. The proposed procedure is outlined in sections 7.3 and 7.4 of the Hazards Summary (ref. 2). Insofar as possible, all structural modifications involving the containment tank will be made just prior to a regularly scheduled leakage test. The leakage test will be performed immediately after the modifications are completed, and before the reactor is restarted. Should modifications to the containment shell be required at times between the regular leakage tests, a test will be made at the time the work is done. The foregoing procedure will be rigidly followed to minimize the possibility of unauthorized and/or unreported openings being made in the tank walls.

There is a small probability that leaks resulting from minor failures in the tank structure (e.g., weld cracks) might exist. Inasmuch as leak tests will be made with considerably higher overpressures in the shell than will exist in normal operation, or even after the maximum credible accident, it seems likely that such failures would develop during leak testing rather than during normal operation between leak checks.

There is, at present, no way to estimate with any degree of accuracy the size of opening which might occur (due to unauthorized penetrations or to structural failures) and be undetected between leak tests. It might be noted that this inability to detect, between leak tests, small leaks due to unauthorized penetrations or structural failure is common to most existing reactors with containment tanks.

Further, it is recalled that during operation the pressure within the containment tank will be at least one inch of water below atmospheric so that any leakage under normal condition would be into the tank. In the event of a radioactive release, short of the maximum credible accident, the tank ventilation system would be shut off and the tank pressure would slowly rise to atmospheric pressure. At this time all leakage would be due either to diffusion or changes in ambient pressure and would be considerably less than the leakage rate for 0.3 pounds per square inch overpressure of the maximum credible accident.

5.5 Question 5(e)

"How often is the container to be tested for leak tightness?"

The containment tank will be given a complete pressure check as outlined in Supplement V for the accelerated overpressure test each three months for the first year, and every six months thereafter. It is felt that any defects in the containment vessel would show up in the four overpressure tests of the first year.

6. QUESTION 6

"We would like some additional information concerning the general nature of the experimental program to be conducted in this facility, and clarification of certain information which you have already provided."

6.1 Question 6(a)

"Whether you expect to conduct fuel bearing experiments (1) in the core, (2) in loops outside of the core? What will be the maximum power level of fuel bearing experiments which you are likely to want to perform?"

(1) No fuel bearing experiments will be run in the core. (2) These experiments will be run in the through holes or beam holes outside the core. (3) The NACA proposes to run fuel bearing experiments of maximum power level of 1 megawatt.

6.2 Question 6(b)

"Could you be more explicit in your estimate of the possibility and probability of failure of experiments which are likely to be conducted in the facility? (Your attention is directed to statements made in the Hazards Summary at pages 1 to 2 and pages 6 to 20.)"

The general types of experiments carried out in the NACA facility will be similar to those carried out in the MTR or ORR. These types of experiments will include pumped loop tests of fuel elements, corrosion tests (both capsule and pumped loop), irradiation of materials, testing of small components (i.e., bearings, pumps, etc.) in a radiation field, shielding studies, basic nuclear physics experiments, and so forth.

The possibility and probability of failure of these experiments might be expected to be of the same order as the possibility or probability of failure of similar experiments in the MTR or ORR. (The accidents which resulted in radioactive releases at the MTR in 1955 and 1956 are discussed in the answer to 6(c) below.)

In reference to the statements made in the Hazards Summary at pages 1 to 2 it is presumed that the statement referred to is, "Under these conditions failures of experimental components can be expected on a routine basis."

The failures we are referring to here are not failures of the experimental loop, but failures of the item being tested. These failures can be divided into two categories: items whose failure under test involves no appreciable radioactive release such as bearing tests in a radiation field,

and items whose failure can involve appreciable radioactive release such as fuel element tests in pumped loops. In both of these types of experiments it is not expected that the experimental loop or structure will normally fail and the possibility and probability of their failure might be expected to be similar to MTR experience as discussed above.

In reference to the statements made in the Hazards Summary at pages 6 to 20 it is presumed that the statements referred to are in section 6.2.3.1.

Section 6.2.3.1 attempts to estimate the type and extent of failures which might occur in a fuel element test in a pumped loop. As stated on pages 6 to 20, the probability of fission products leaking from the fuel element into the experimental loop is large. The chance of leakage from the experimental loop into the experiment container can is much smaller and should parallel MTR experience. The chance of leakage from the experimental container can into the reactor containment tank is smaller still as discussed in section 6.3 below.

Section 6.2.3.1 goes on to consider the type of failure which might occur in the "maximum conceivable experiment accident". An accident of this magnitude is unlikely to occur in the life of the reactor as evidenced by the fact that, to the best of our knowledge, no accident of this magnitude has occurred to a fuel element pumped loop test in any reactor.

6.3 Question 6(c)

"Could you be more explicit as to the result of failure of experiments in terms of possibility and probability of release from the cans surrounding the experiment? What is your estimate of the volume and nuclear characteristics of radioactivity which could credibly be released from experiments into the container?"

As discussed above, the types of experiments which would be carried out in the NACA reactor are very similar to the types of experiments carried out in the MTR, and the possibility and probability of experiment failure should be about the same. The most important difference is the method in which these experiments would be carried out in the NACA reactor. Every fuel bearing experiment in the NACA reactor will be enclosed in an experiment container can. This can would be maintained at low temperature and its only function would be to contain radioactive releases from the experiment.

It is felt that the majority of the radioactive releases will be confined to the experimental container can. A rough estimate is that at least nine out of ten radioactive releases would be confined to the experimental container cans.

As discussed in the answer to 6(b), it is expected that the number of experiment failures will be about the same as the number of failures at MTR. These experiment failures at MTR in 1955 and 1956 which resulted in release of radioactivity are discussed in a letter to J. B. Philipson, Director, Division of Operations, Atomic Energy Commission, Idaho Operations Office from J. P. Lyon, Assistant Manager, Operations, Atomic Energy Commission (Ly-179-57A). During this two year period 25 releases were of sufficient importance to be noted individually. The releases range in size from a few hundred microcuries to several thousand curies. In addition, 54 minor releases occurred in 1955 with the total activity release from all of these releases of about 2 millicuries. Assuming that in the NACA reactor at least nine out of ten of these releases would be restricted to the experimental container cans, it is expected that releases to the containment tank would not exceed about 1 major release per year with an activity release of the order of several hundred curies, and about 5 minor releases per year with an activity release of the order of 100 microcuries or less.

E-103

CO-24

A rough estimate of the maximum credible release of activity from the experiment container can would be about 10 percent of the total activity of a 1 megawatt experiment. The probability of a "maximum credible release" is small, and it is not expected to occur during the life of the reactor.

6.4 Question 6(d)

"Will the reactivity effects of the experiments be determined in a critical assembly prior to insertion of the experiments in the reactor?"

All major fuel bearing experiments and any other experiments deemed necessary will be tested in a critical assembly before being run in the reactor.

7. QUESTION 7

"What would be the effect of credible releases (either from the maximum credible accident postulated or from lesser accidents) to employees on-site? What are the number of employees that may be affected by such release? What is your evaluation of your ability to move such employees with sufficient rapidity to avoid dangerous exposure to radiation?"

The effect of releases of radioactivity expected in normal operation will be negligible except to employees in the containment shell. For a release of 100 millicuries of unknown airborne activity in the containment shell and uniformly dispersed, the weekly occupational dose of 300 mrem would be exceeded in about one minute. A reasonable evacuation time for

the 10 or fewer employees in the containment shell is 2 or 3 minutes; therefore, no serious damage would result. As a comparison, the maximum amount of airborne activity released at any one time accidentally in the reactor building of the Materials Testing Reactor during 1955 and 1956 was estimated at 5 millicuries (ref. letter to J. B. Philipson, Director Division of Operations, Atomic Energy Commission (Ly-179-57A). Most of the releases at the MTR were 2 millicuries or less. It is felt that a 100 millicurie release is larger than that normally expected because of the similarity with the MTR operation.

It is pertinent to mention that 9 activity releases at the MTR during 1955 and 1956 required building evacuations. If these same incidents had occurred in the NACA reactor, 8 of them would have required at most only a containment shell evacuation. The one remaining release could have occurred either inside or outside of the containment shell. Several of the incidents confined to the containment shell also would probably have been confined to experiment containers, and in this case, no evacuation would have been necessary.

A considerably larger release would be required to affect employees outside of the containment shell. Assume a large pumped-loop fuel bearing experiment were to fail, and in addition, a rupture of the experiment container were to occur. Also, assume that 1 percent of the fission products in the experiment were to be released to the quadrant pool water and into the air of the containment shell. The estimated doses received by the employees outside of the containment shell is tabulated in the following table.

Dose, milliroentgens	Number of people affected	
	Day shift	Night shift
0	7	0
4	7	2
10	76	4
17	6	1
24	30	2
83	3	3
105	14	12

None of these doses are extreme in view of the very severe accident assumed. These results were obtained assuming a full staff of about 167 employees. Reasonable evacuation times were assumed based on experience in civil defense drills at the Lewis laboratory. Consideration was taken of the probable locations of personnel and shielding which would be available at their normal work locations and on their evacuation routes. For more severe accidents, these doses can be scaled up accordingly. For a 10 percent fission product release from a 1 megawatt experiment, the maximum credible experiment release, the dose rates would be greater by a

factor of 10. For the maximum credible accident to the reactor consisting of 100 percent release of the fission products in the reactor, the scaling factor would be 6000. Even for this extremely improbable situation, only 17 of the employees outside of the containment shell would receive 500 roentgens or more.

The number of employees present at any one time in the containment vessel will be about ten. The number normally present will be considerably less than this because most experiments will be operated remotely, and there will be only occasional necessity for entering while the reactor is operating. Shielding and beam hole experiments will require the most attention, and these will also be remotely operated whenever practicable.

E-103

It is assumed that the principal hazard to employees in the containment shell is that of inhalation of radioactive gases or airborne particulate matter. Respiratory protection will be provided for each person in the containment shell. This equipment will be used whenever monitor alarms indicate an excessive airborne activity.

CO-24 back

Public address equipment will sound evacuation alarms. Specific instructions can be voiced simultaneously. Evacuation will be periodically rehearsed.

8. QUESTION 8

"Is the containment vessel to be an ASME code vessel?"

The NACA containment tank meets the 1952 ASME Unfired Pressure Vessels Code requirements for an internal pressure of 7.5 pounds per square inch. This is 50 percent above the design pressure of 5 pounds per square inch, and many times greater than the 0.3 pounds per square inch overpressure which would result from the maximum credible accident (section 1.4, Supplement V).

9. QUESTION 9

"How do you know that the vacuums in penetrations to which the vacuum pump system is attached are being maintained? What size hole will cause the reactor to be automatically shut down? What size hole in the penetration is detectable by the measuring methods?"

Pressure switches in combination with a flow meter (s) will monitor the vacuum in the penetrations. A flow equivalent to the maximum leakage rate of the containment vessel will cause automatic shutdown of the reactor. A hole one-sixteenth of an inch in diameter is detectable. (This corresponds to approximately 1/3 of the allowable leakage rate.)

10. QUESTION 10

"What is your evaluation of the feasibility of operation of your proposed reactor at a site which would afford a higher degree of protection to the health and safety of the public?"

During the period when the site for the NACA reactor was selected, consideration was given to a more remote site such as the NRTS site in Idaho. The Plumbrook Ordnance Works offered a number of advantages compared to a site of this type:

1. Because of its proximity to the Lewis Laboratory of the NACA, the reactor and its operating crew would have, near at hand, a large pool of highly trained scientists and technicians who would be available to advise and assist on all problems which might arise. In particular, since most of the experiments will be conceived and constructed at the Lewis Laboratory, more of the people who designed and built the experiments could be present at the various stages of the insertion and operation of the experiment in the reactor with resulting improvements in efficiency and safety. Therefore, the first advantage of the Plumbrook site is the availability, near at hand, of a large pool of highly trained scientists and technicians, and in particular, of the people who designed and built the individual experiments.

2. The second advantage of the Plumbrook site is in decreased operating costs. Because of its proximity to Lewis laboratory, a number of services which would otherwise be required at the reactor site may be reduced or eliminated. For example, shop facilities, stock rooms, computational facilities and many administrative and service functions such as the payroll, time and leave, and purchase offices, can be reduced or eliminated. Also, since most of the experiments will be conceived and built at the Lewis laboratory, the transportation cost of experiments to and from the reactor will be considerably reduced.

3. The third advantage of the Plumbrook site is decreased initial costs. The Plumbrook site is already developed. It has available on it a copious water supply, more than ample electricity, area drainage, roads, and so forth. In addition, an unused building is available for use as an Administration Building. The increased costs of developing some remote site would have been substantial. To give some idea of the costs of site development, the water intake system from Lake Erie to the Plumbrook site, were it not available, would cost about four million dollars to install.

4. Because the Plumbrook site is already developed and because of the proximity to the Lewis laboratory, the reactor facility can be completed more rapidly and would be available for research considerably sooner than if it were located at a more remote site.

The chief disadvantage of the Plumbrook site compared to more remote sites is its location near populated areas which would prohibit the carrying out of the "most hazardous experiments." That is, there would be a few experiments whose potential hazard to the local population would be sufficiently great that they could not be carried out at the Plumbrook site. To put this disadvantage in proper perspective, it is important to note that the NACA reactor is not the only reactor of its type in the country. The MTR and ETR, both located at NRTS in Idaho, are reactors with similar facilities. Any experiment vital to the progress of scientific knowledge or aircraft nuclear propulsion which is deemed too hazardous for the Plumbrook site, could readily be carried out at MTR or ETR. This fact minimizes this disadvantage of the Plumbrook site.

In summary, the Plumbrook site offers the advantages of improved operation, lower operating costs, lower initial costs, and earlier availability for research as compared to a remote site. Its chief disadvantage, the inability to carry out a few "most hazardous experiments," is reduced to a minimum because of the availability of the MTR and ETR for these types of experiments. In view of these considerations, it is felt that the Plumbrook site is superior to a remote site.

11. QUESTION 11

The Atomic Energy Commission has added the following questions to those listed above.

"What system is proposed to measure leakage around the entrance of doors at the reactor where personnel would be entering and exiting? How will the leakage rate be maintained at the interlock doors when the pressure difference is slight? What will be done when the pressure is up to 0.3 pounds per square inch, the maximum credible accident pressure rate which has been postulated? How often and by what method will the gaskets around the interlock doors be tested? (Will this be a recurring test?)"

There is no system proposed to measure leakage, as such, around the personnel doors to the containment tank. Leakage tests, however, will include the scheduled overpressure leak tests of the entire containment vessel and either overpressure tests of the air-lock cavities individually or helium leak detection tests of the door gaskets and structure with the doors in a dogged down position.

Two air locks are proposed, each having a double set of mechanically interlocked doors, which prevent either door from being opened unless the other is closed and dogged tightly against its gaskets. A sufficient load is supplied by the locking mechanism to assure that the gasket is tightly sealed. A description of the proposed system is given in Supplement IV, section 1.2.7, Air Locks and figures 4 and 5. There is also a pressure

TABLE 1.1 - HOT WASTES FROM THE PROCESS WATER SYSTEM

Place	Unit volume, gal	Continuous flow, gal/min	Intermittent flow, gal/min	Intermittent flow, hr/cycle	Normal initial activity, $(d/cm^3)/sec$	Normal activity of waste to hot retention tanks after 30 hours, $(d/cm^3)/sec$		Abnormal activity of waste after 30 hours, $(d/cm^3)/sec$
Reactor loop	25,000							
Shutdown drain	1,000		200	0.085	10^3	5×10^2 without bypass demineralization	Na^{24} Cr^{51} Mn^{56} S^{35}	0.2% over normal due to fuel element leakage
Shutdown flush	1,200		200	.100	10^3			
Drainage, total	25,000		700	.595	10^3			
Drainage, flush	1,200		200	.100	7×10^2			
Reactor sump	300							
Monitoring tubes		7.5			10^3		Na^{24}	
Experimental loops		5.0	100	6.0	10^3		Mn^{56}	No significant change unless equipment alterations are required.
Equipment seals		.5			10^2	0.5	Fe^{55}	
Subpile sump	100		6	.080	10^2		Fe^{59} Cr^{51}	
Pump house sump	200							
Piping leaks		.003			10^4			
Other drains		.002			5×10^3		Na^{24}	
Valve flush	1,500		4.0	1.0	10^2		Cr^{51}	0.2% over normal due to fuel element leakage
Pump flush	2,000		3.0	3.0	10^2	10^2	Mn^{56}	
Pump priming	10		1.7	.1	10^2		S^{35}	
Deion resin change	1,200		20	.035	10^2			
Resin drain basin		0.040			10			
Hot laboratory sump	200							
Drainage and decontamination		1.555	10	1.5	5×10^2	10^2		No significant change unless a large decontamination problem occurs
Fan house sump	200							
Deion resin change			20	.070	10	0.5		Small rise due to change in hot retention tanks.
Resin and drain basin		.050			0.1			

TABLE 1.2 - COLD AND INTERMEDIATE WASTES FROM THE PROCESS WATER SYSTEM

Place	Unit volume, gal.	Continuous flow, gal/min	Intermittent flow, gal/min	Intermittent flow, hr/cycle	Normal activity, $(d/cm^3)/sec$	Type activity and remarks
Cold Wastes						
Water treatment building						
Precipitator - start up	90,000		300	1.0		No activity above background.
Process filters	5,000		1000	.75		This water, as a continuous purge, will be used to dilute wastes to MPC levels for disposal.
Deionizer units	800		30	15		
Rinse			100	6		
Cooling tower blowdown	180,000	170				
Cooling tower filters	2,000		350	6		
Domestic water supply			300			
Fire water supply			300			
Intermediate wastes						
Quadrant tanks (4)	200,000					Beta activity, with some associated gamma, from corrosion products, contamination and activation.
Complete drainage			1000(+3000)	4	20	
Overflow		Up to 400				
Canals (6)	200,000					
Complete drainage			1000(+3000)	4	20	
Overflow		Up to 400				

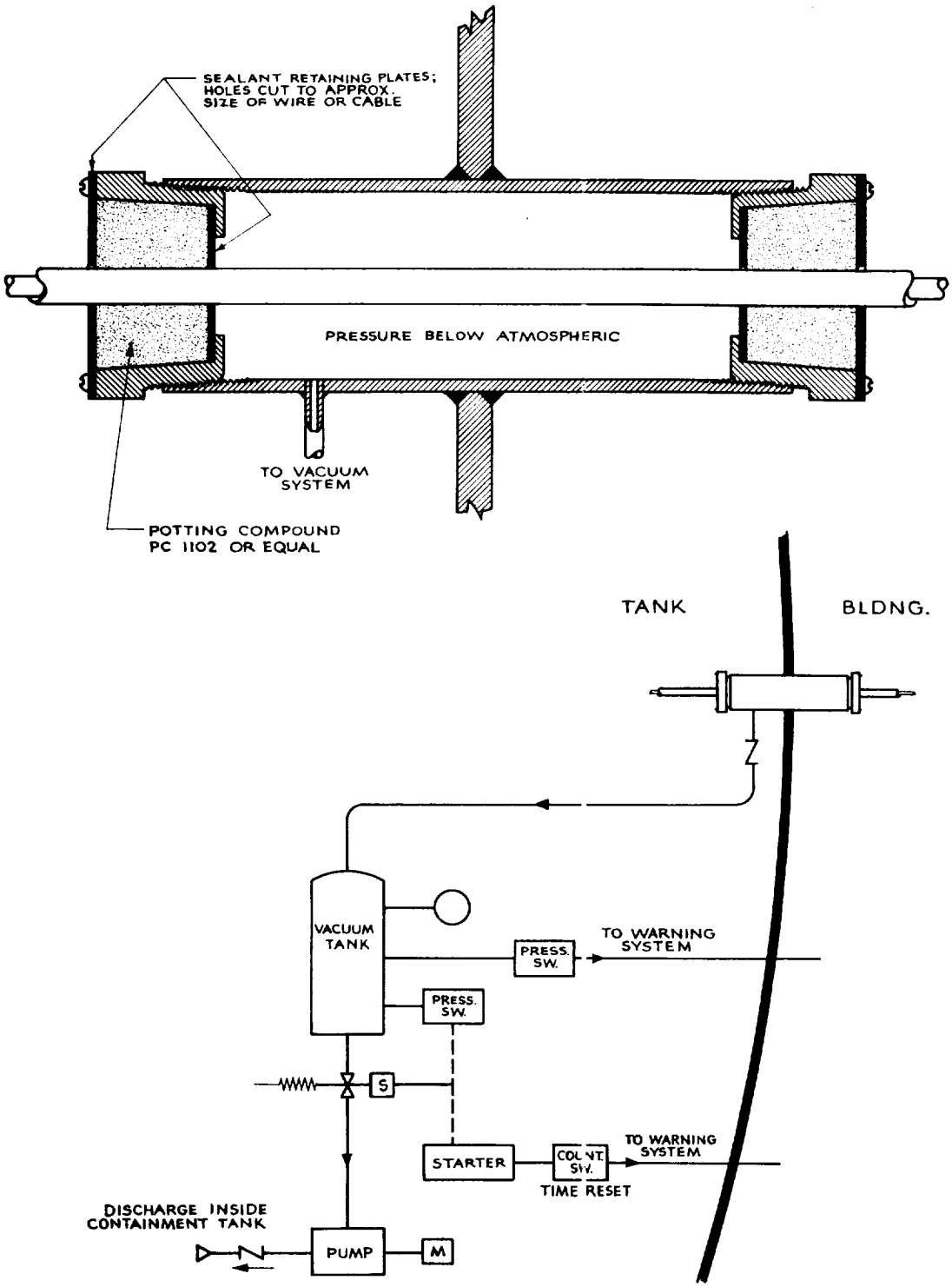

Figure 1. - Typical wire or cable penetration and vacuum system.